

# chapter 7

*electrodynamics—  
fields and waves*

The electromagnetic field laws, derived thus far from the empirically determined Coulomb–Lorentz forces, are correct on the time scales of our own physical experiences. However, just as Newton’s force law must be corrected for material speeds approaching that of light, the field laws must be corrected when fast time variations are on the order of the time it takes light to travel over the length of a system. Unlike the abstractness of relativistic mechanics, the complete electrodynamic equations describe a familiar phenomenon—propagation of electromagnetic waves. Throughout the rest of this text, we will examine when appropriate the low-frequency limits to justify the past quasi-static assumptions.

## 7-1 MAXWELL’S EQUATIONS

### 7-1-1 Displacement Current Correction to Ampere’s Law

In the historical development of electromagnetic field theory through the nineteenth century, charge and its electric field were studied separately from currents and their magnetic fields. Until Faraday showed that a time varying magnetic field generates an electric field, it was thought that the electric and magnetic fields were distinct and uncoupled. Faraday believed in the duality that a time varying electric field should also generate a magnetic field, but he was not able to prove this supposition.

It remained for James Clerk Maxwell to show that Faraday’s hypothesis was correct and that without this correction Ampere’s law and conservation of charge were inconsistent:

$$\nabla \times \mathbf{H} = \mathbf{J}_f \Rightarrow \nabla \cdot \mathbf{J}_f = 0 \quad (1)$$

$$\nabla \cdot \mathbf{J}_f + \frac{\partial \rho_f}{\partial t} = 0 \quad (2)$$

for if we take the divergence of Ampere’s law in (1), the current density must have zero divergence because the divergence of the curl of a vector is always zero. This result contradicts (2) if a time varying charge is present. Maxwell

realized that adding the displacement current on the right-hand side of Ampere's law would satisfy charge conservation, because of Gauss's law relating  $\mathbf{D}$  to  $\rho_f$  ( $\nabla \cdot \mathbf{D} = \rho_f$ ).

This simple correction has far-reaching consequences, because we will be able to show the existence of electromagnetic waves that travel at the speed of light  $c$ , thus proving that light is an electromagnetic wave. Because of the significance of Maxwell's correction, the complete set of coupled electromagnetic field laws are called Maxwell's equations:

Faraday's Law

$$\nabla \times \mathbf{E} = -\frac{\partial \mathbf{B}}{\partial t} \Rightarrow \oint_L \mathbf{E} \cdot d\mathbf{l} = -\frac{d}{dt} \int_S \mathbf{B} \cdot d\mathbf{S} \quad (3)$$

Ampere's law with Maxwell's displacement current correction

$$\nabla \times \mathbf{H} = \mathbf{J}_f + \frac{\partial \mathbf{D}}{\partial t} \Rightarrow \oint_L \mathbf{H} \cdot d\mathbf{l} = \int_S \mathbf{J}_f \cdot d\mathbf{S} + \frac{d}{dt} \int_S \mathbf{D} \cdot d\mathbf{S} \quad (4)$$

Gauss's laws

$$\nabla \cdot \mathbf{D} = \rho_f \Rightarrow \oint_S \mathbf{D} \cdot d\mathbf{S} = \int_V \rho_f dV \quad (5)$$

$$\nabla \cdot \mathbf{B} = 0 \Rightarrow \oint_S \mathbf{B} \cdot d\mathbf{S} = 0 \quad (6)$$

Conservation of charge

$$\nabla \cdot \mathbf{J}_f + \frac{\partial \rho_f}{\partial t} = 0 \Rightarrow \oint_S \mathbf{J}_f \cdot d\mathbf{S} + \frac{d}{dt} \int_V \rho_f dV = 0 \quad (7)$$

As we have justified, (7) is derived from the divergence of (4) using (5).

Note that (6) is not independent of (3) for if we take the divergence of Faraday's law,  $\nabla \cdot \mathbf{B}$  could at most be a time-independent function. Since we assume that at some point in time  $\mathbf{B} = 0$ , this function must be zero.

The symmetry in Maxwell's equations would be complete if a magnetic charge density appeared on the right-hand side of Gauss's law in (6) with an associated magnetic current due to the flow of magnetic charge appearing on the right-hand side of (3). Thus far, no one has found a magnetic charge or current, although many people are actively looking. Throughout this text we accept (3)–(7) keeping in mind that if magnetic charge is discovered, we must modify (3) and (6) and add an equation like (7) for conservation of magnetic charge.

### 7-1-2 Circuit Theory as a Quasi-static Approximation

Circuit theory assumes that the electric and magnetic fields are highly localized within the circuit elements. Although the displacement current is dominant within a capacitor, it is negligible outside so that Ampere's law can neglect time variations of  $\mathbf{D}$  making the current divergence-free. Then we obtain Kirchoff's current law that the algebraic sum of all currents flowing into (or out of) a node is zero:

$$\nabla \cdot \mathbf{J} = 0 \Rightarrow \oint_S \mathbf{J} \cdot d\mathbf{S} = 0 \Rightarrow \sum i_k = 0 \quad (8)$$

Similarly, time varying magnetic flux that is dominant within inductors and transformers is assumed negligible outside so that the electric field is curl free. We then have Kirchoff's voltage law that the algebraic sum of voltage drops (or rises) around any closed loop in a circuit is zero:

$$\nabla \times \mathbf{E} = 0 \Rightarrow \mathbf{E} = -\nabla V \Rightarrow \oint_L \mathbf{E} \cdot d\mathbf{l} = 0 \Rightarrow \sum v_k = 0 \quad (9)$$

## 7-2 CONSERVATION OF ENERGY

### 7-2-1 Poynting's Theorem

We expand the vector quantity

$$\begin{aligned} \nabla \cdot (\mathbf{E} \times \mathbf{H}) &= \mathbf{H} \cdot (\nabla \times \mathbf{E}) - \mathbf{E} \cdot (\nabla \times \mathbf{H}) \\ &= -\mathbf{H} \cdot \frac{\partial \mathbf{B}}{\partial t} - \mathbf{E} \cdot \frac{\partial \mathbf{D}}{\partial t} - \mathbf{E} \cdot \mathbf{J}_f \end{aligned} \quad (1)$$

where we change the curl terms using Faraday's and Ampere's laws.

For linear homogeneous media, including free space, the constitutive laws are

$$\mathbf{D} = \epsilon \mathbf{E}, \quad \mathbf{B} = \mu \mathbf{H} \quad (2)$$

so that (1) can be rewritten as

$$\nabla \cdot (\mathbf{E} \times \mathbf{H}) + \frac{\partial}{\partial t} \left( \frac{1}{2} \epsilon E^2 + \frac{1}{2} \mu H^2 \right) = -\mathbf{E} \cdot \mathbf{J}_f \quad (3)$$

which is known as Poynting's theorem. We integrate (3) over a closed volume, using the divergence theorem to convert the

first term to a surface integral:

$$\underbrace{\oint_S (\mathbf{E} \times \mathbf{H}) \cdot d\mathbf{S}}_{\int_V \nabla \cdot (\mathbf{E} \times \mathbf{H}) dV} + \frac{d}{dt} \int_V \left( \frac{1}{2} \epsilon E^2 + \frac{1}{2} \mu H^2 \right) dV = - \int_V \mathbf{E} \cdot \mathbf{J}_f dV \quad (4)$$

We recognize the time derivative in (4) as operating on the electric and magnetic energy densities, which suggests the interpretation of (4) as

$$P_{\text{out}} + \frac{dW}{dt} = -P_d \quad (5)$$

where  $P_{\text{out}}$  is the total electromagnetic power flowing out of the volume with density

$$\mathbf{S} = \mathbf{E} \times \mathbf{H} \text{ watts/m}^2 \text{ [kg}\cdot\text{s}^{-3}] \quad (6)$$

where  $\mathbf{S}$  is called the Poynting vector,  $W$  is the electromagnetic stored energy, and  $P_d$  is the power dissipated or generated:

$$\begin{aligned} P_{\text{out}} &= \oint_S (\mathbf{E} \times \mathbf{H}) \cdot d\mathbf{S} = \oint_S \mathbf{S} \cdot d\mathbf{S} \\ W &= \int_V \left[ \frac{1}{2} \epsilon E^2 + \frac{1}{2} \mu H^2 \right] dV \\ P_d &= \int_V \mathbf{E} \cdot \mathbf{J}_f dV \end{aligned} \quad (7)$$

If  $\mathbf{E}$  and  $\mathbf{J}_f$  are in the same direction as in an Ohmic conductor ( $\mathbf{E} \cdot \mathbf{J}_f = \sigma E^2$ ), then  $P_d$  is positive, representing power dissipation since the right-hand side of (5) is negative. A source that supplies power to the volume has  $\mathbf{E}$  and  $\mathbf{J}_f$  in opposite directions so that  $P_d$  is negative.

### 7-2-2 A Lossy Capacitor

Poynting's theorem offers a different and to some a paradoxical explanation of power flow to circuit elements. Consider the cylindrical lossy capacitor excited by a time varying voltage source in Figure 7-1. The terminal current has both Ohmic and displacement current contributions:

$$i = \frac{\epsilon A}{l} \frac{dv}{dt} + \frac{\sigma A v}{l} = C \frac{dv}{dt} + \frac{v}{R}, \quad C = \frac{\epsilon A}{l}, \quad R = \frac{l}{\sigma A} \quad (8)$$

From a circuit theory point of view we would say that the power flows from the terminal wires, being dissipated in the

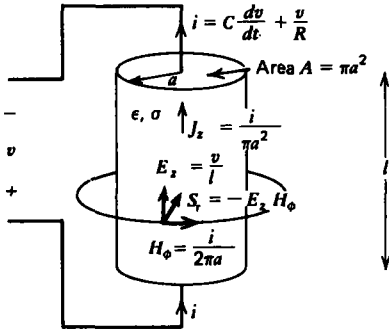


Figure 7-1 The power delivered to a lossy cylindrical capacitor  $vi$  is partly dissipated by the Ohmic conduction and partly stored in the electric field. This power can also be thought to flow in radially from the surrounding electric and magnetic fields via the Poynting vector  $\mathbf{S} = \mathbf{E} \times \mathbf{H}$ .

resistance and stored as electrical energy in the capacitor:

$$P = vi = \frac{v^2}{R} + \frac{d}{dt} \left( \frac{1}{2} C v^2 \right) \quad (9)$$

We obtain the same results from a field's viewpoint using Poynting's theorem. Neglecting fringing, the electric field is simply

$$E_z = v/l \quad (10)$$

while the magnetic field at the outside surface of the resistor is generated by the conduction and displacement currents:

$$\oint_L \mathbf{H} \cdot d\mathbf{l} = \int_S \left( J_z + \epsilon \frac{\partial E_z}{\partial t} \right) dS \Rightarrow H_\phi 2\pi a = \frac{\sigma A v}{l} + \frac{\epsilon}{l} A \frac{dv}{dt} = i \quad (11)$$

where we recognize the right-hand side as the terminal current in (8),

$$H_\phi = i/(2\pi a) \quad (12)$$

The power flow through the surface at  $r = a$  surrounding the resistor is then radially inward,

$$\oint_S (\mathbf{E} \times \mathbf{H}) \cdot d\mathbf{S} = - \int_S \frac{v}{l} \frac{i}{2\pi a} a d\phi dz = -vi \quad (13)$$

and equals the familiar circuit power formula. The minus sign arises because the left-hand side of (13) is the power out of the volume as the surface area element  $d\mathbf{S}$  points radially outwards. From the field point of view, power flows into the lossy capacitor from the electric and magnetic fields outside

the resistor via the Poynting vector. Whether the power is thought to flow along the terminal wires or from the surrounding fields is a matter of convenience as the results are identical. The presence of the electric and magnetic fields are directly due to the voltage and current. It is impossible to have the fields without the related circuit variables.

**7-2-3 Power in Electric Circuits**

We saw in (13) that the flux of  $\mathbf{S}$  entering the surface surrounding a circuit element just equals  $vi$ . We can show this for the general network with  $N$  terminals in Figure 7-2 using the quasi-static field laws that describe networks outside the circuit elements:

$$\begin{aligned} \nabla \times \mathbf{E} = 0 &\Rightarrow \mathbf{E} = -\nabla V \\ \nabla \times \mathbf{H} = \mathbf{J}_f &\Rightarrow \nabla \cdot \mathbf{J}_f = 0 \end{aligned} \tag{14}$$

We then can rewrite the electromagnetic power into a surface as

$$\begin{aligned} P_{in} &= -\oint_S \mathbf{E} \times \mathbf{H} \cdot d\mathbf{S} \\ &= -\int_V \nabla \cdot (\mathbf{E} \times \mathbf{H}) dV \\ &= \int_V \nabla \cdot (\nabla V \times \mathbf{H}) dV \end{aligned} \tag{15}$$

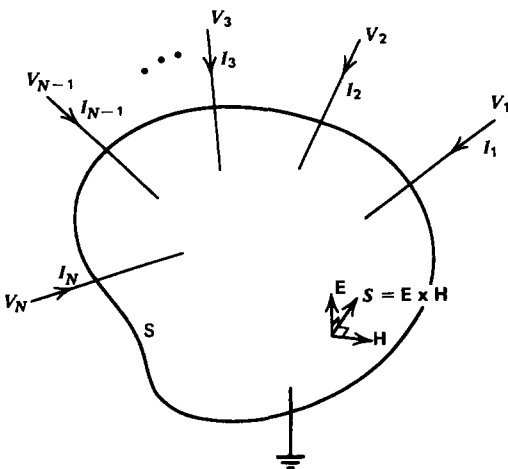


Figure 7-2 The circuit power into an  $N$  terminal network  $\sum_{k=1}^N V_k I_k$  equals the electromagnetic power flow into the surface surrounding the network,  $-\oint_S \mathbf{E} \times \mathbf{H} \cdot d\mathbf{S}$ .

where the minus is introduced because we want the power in and we use the divergence theorem to convert the surface integral to a volume integral. We expand the divergence term as

$$\begin{aligned}\nabla \cdot (\nabla V \times \mathbf{H}) &= \mathbf{H} \cdot (\nabla \times \nabla V) - \nabla V \cdot (\nabla \times \mathbf{H}) \\ &= -\mathbf{J}_f \cdot \nabla V = -\nabla \cdot (\mathbf{J}_f V)\end{aligned}\quad (16)$$

where we use (14).

Substituting (16) into (15) yields

$$\begin{aligned}P_{\text{in}} &= -\int_V \nabla \cdot (\mathbf{J}_f V) dV \\ &= -\oint_S \mathbf{J}_f V \cdot d\mathbf{S}\end{aligned}\quad (17)$$

where we again use the divergence theorem. On the surface  $S$ , the potential just equals the voltages on each terminal wire allowing  $V$  to be brought outside the surface integral:

$$\begin{aligned}P_{\text{in}} &= \sum_{k=1}^N -V_k \oint_S \mathbf{J}_f \cdot d\mathbf{S} \\ &= \sum_{k=1}^N V_k I_k\end{aligned}\quad (18)$$

where we recognize the remaining surface integral as just being the negative (remember  $d\mathbf{S}$  points outward) of each terminal current flowing into the volume. This formula is usually given as a postulate along with Kirchoff's laws in most circuit theory courses. Their correctness follows from the quasi-static field laws that are only an approximation to more general phenomena which we continue to explore.

#### 7-2-4 The Complex Poynting's Theorem

For many situations the electric and magnetic fields vary sinusoidally with time:

$$\begin{aligned}\mathbf{E}(\mathbf{r}, t) &= \text{Re} [\hat{\mathbf{E}}(\mathbf{r}) e^{j\omega t}] \\ \mathbf{H}(\mathbf{r}, t) &= \text{Re} [\hat{\mathbf{H}}(\mathbf{r}) e^{j\omega t}]\end{aligned}\quad (19)$$

where the caret is used to indicate a complex amplitude that can vary with position  $\mathbf{r}$ . The instantaneous power density is obtained by taking the cross product of  $\mathbf{E}$  and  $\mathbf{H}$ . However, it is often useful to calculate the time-average power density  $\langle \mathbf{S} \rangle$ , where we can avoid the lengthy algebraic and trigonometric manipulations in expanding the real parts in (19).

A simple rule for the time average of products is obtained by realizing that the real part of a complex number is equal to one half the sum of the complex number and its conjugate (denoted by a superscript asterisk). The power density is then

$$\begin{aligned}
 \mathbf{S}(\mathbf{r}, t) &= \mathbf{E}(\mathbf{r}, t) \times \mathbf{H}(\mathbf{r}, t) \\
 &= \frac{1}{4}[\hat{\mathbf{E}}(\mathbf{r}) e^{j\omega t} + \hat{\mathbf{E}}^*(\mathbf{r}) e^{-j\omega t}] \times [\hat{\mathbf{H}}(\mathbf{r}) e^{j\omega t} + \hat{\mathbf{H}}^*(\mathbf{r}) e^{-j\omega t}] \\
 &= \frac{1}{4}[\hat{\mathbf{E}}(\mathbf{r}) \times \hat{\mathbf{H}}(\mathbf{r}) e^{2j\omega t} + \hat{\mathbf{E}}^*(\mathbf{r}) \times \hat{\mathbf{H}}(\mathbf{r}) + \hat{\mathbf{E}}(\mathbf{r}) \times \hat{\mathbf{H}}^*(\mathbf{r}) \\
 &\quad + \hat{\mathbf{E}}^*(\mathbf{r}) \times \hat{\mathbf{H}}^*(\mathbf{r}) e^{-2j\omega t}] \tag{20}
 \end{aligned}$$

The time average of (20) is then

$$\begin{aligned}
 \langle \mathbf{S} \rangle &= \frac{1}{4}[\hat{\mathbf{E}}^*(\mathbf{r}) \times \hat{\mathbf{H}}(\mathbf{r}) + \hat{\mathbf{E}}(\mathbf{r}) \times \hat{\mathbf{H}}^*(\mathbf{r})] \\
 &= \frac{1}{2} \text{Re} [\hat{\mathbf{E}}(\mathbf{r}) \times \hat{\mathbf{H}}^*(\mathbf{r})] \\
 &= \frac{1}{2} \text{Re} [\hat{\mathbf{E}}^*(\mathbf{r}) \times \hat{\mathbf{H}}(\mathbf{r})] \tag{21}
 \end{aligned}$$

as the complex exponential terms  $e^{\pm 2j\omega t}$  average to zero over a period  $T = 2\pi/\omega$  and we again realized that the first bracketed term on the right-hand side of (21) was the sum of a complex function and its conjugate.

Motivated by (21) we define the complex Poynting vector as

$$\hat{\mathbf{S}} = \frac{1}{2} \hat{\mathbf{E}}(\mathbf{r}) \times \hat{\mathbf{H}}^*(\mathbf{r}) \tag{22}$$

whose real part is just the time-average power density.

We can now derive a complex form of Poynting's theorem by rewriting Maxwell's equations for sinusoidal time variations as

$$\begin{aligned}
 \nabla \times \hat{\mathbf{E}}(\mathbf{r}) &= -j\omega\mu \hat{\mathbf{H}}(\mathbf{r}) \\
 \nabla \times \hat{\mathbf{H}}(\mathbf{r}) &= \hat{\mathbf{J}}_f(\mathbf{r}) + j\omega\varepsilon \hat{\mathbf{E}}(\mathbf{r}) \\
 \nabla \cdot \hat{\mathbf{E}}(\mathbf{r}) &= \hat{\rho}_f(\mathbf{r})/\varepsilon \\
 \nabla \cdot \hat{\mathbf{B}}(\mathbf{r}) &= 0
 \end{aligned} \tag{23}$$

and expanding the product

$$\begin{aligned}
 \nabla \cdot \hat{\mathbf{S}} &= \nabla \cdot [\frac{1}{2} \hat{\mathbf{E}}(\mathbf{r}) \times \hat{\mathbf{H}}^*(\mathbf{r})] = \frac{1}{2}[\hat{\mathbf{H}}^*(\mathbf{r}) \cdot \nabla \times \hat{\mathbf{E}}(\mathbf{r}) - \hat{\mathbf{E}}(\mathbf{r}) \cdot \nabla \times \hat{\mathbf{H}}^*(\mathbf{r})] \\
 &= \frac{1}{2}[-j\omega\mu |\hat{\mathbf{H}}(\mathbf{r})|^2 + j\omega\varepsilon |\hat{\mathbf{E}}(\mathbf{r})|^2] - \frac{1}{2} \hat{\mathbf{E}}(\mathbf{r}) \cdot \hat{\mathbf{J}}_f^*(\mathbf{r}) \tag{24}
 \end{aligned}$$

which can be rewritten as

$$\nabla \cdot \hat{\mathbf{S}} + 2j\omega[\langle w_m \rangle - \langle w_e \rangle] = -\hat{P}_d \tag{25}$$

where

$$\begin{aligned}
 \langle w_m \rangle &= \frac{1}{4}\mu |\hat{\mathbf{H}}(\mathbf{r})|^2 \\
 \langle w_e \rangle &= \frac{1}{4}\varepsilon |\hat{\mathbf{E}}(\mathbf{r})|^2 \\
 \hat{P}_d &= \frac{1}{2} \hat{\mathbf{E}}(\mathbf{r}) \cdot \hat{\mathbf{J}}_f^*(\mathbf{r})
 \end{aligned} \tag{26}$$

We note that  $\langle w_m \rangle$  and  $\langle w_e \rangle$  are the time-average magnetic and electric energy densities and that the complex Poynting's theorem depends on their difference rather than their sum.

## 7-3 TRANSVERSE ELECTROMAGNETIC WAVES

### 7-3-1 Plane Waves

Let us try to find solutions to Maxwell's equations that only depend on the  $z$  coordinate and time in linear media with permittivity  $\epsilon$  and permeability  $\mu$ . In regions where there are no sources so that  $\rho_f = 0$ ,  $\mathbf{J}_f = 0$ , Maxwell's equations then reduce to

$$-\frac{\partial E_y}{\partial z} \mathbf{i}_x + \frac{\partial E_x}{\partial z} \mathbf{i}_y = -\mu \frac{\partial \mathbf{H}}{\partial t} \quad (1)$$

$$-\frac{\partial H_y}{\partial z} \mathbf{i}_x + \frac{\partial H_x}{\partial z} \mathbf{i}_y = \epsilon \frac{\partial \mathbf{E}}{\partial t} \quad (2)$$

$$\epsilon \frac{\partial E_z}{\partial z} = 0 \quad (3)$$

$$\mu \frac{\partial H_z}{\partial z} = 0 \quad (4)$$

These relations tell us that at best  $E_z$  and  $H_z$  are constant in time and space. Because they are uncoupled, in the absence of sources we take them to be zero. By separating vector components in (1) and (2) we see that  $E_x$  is coupled to  $H_y$ , and  $E_y$  is coupled to  $H_x$ :

$$\begin{aligned} \frac{\partial E_x}{\partial z} &= -\mu \frac{\partial H_y}{\partial t}, & \frac{\partial E_y}{\partial z} &= \mu \frac{\partial H_x}{\partial t} \\ \frac{\partial H_y}{\partial z} &= -\epsilon \frac{\partial E_x}{\partial t}, & \frac{\partial H_x}{\partial z} &= \epsilon \frac{\partial E_y}{\partial t} \end{aligned} \quad (5)$$

forming two sets of independent equations. Each solution has perpendicular electric and magnetic fields. The power flow  $\mathbf{S} = \mathbf{E} \times \mathbf{H}$  for each solution is  $z$  directed also being perpendicular to  $\mathbf{E}$  and  $\mathbf{H}$ . Since the fields and power flow are mutually perpendicular, such solutions are called transverse electromagnetic waves (TEM). They are waves because if we take  $\partial/\partial z$  of the upper equations and  $\partial/\partial t$  of the lower equations and solve for the electric fields, we obtain one-dimensional wave equations:

$$\frac{\partial^2 E_x}{\partial z^2} = \frac{1}{c^2} \frac{\partial^2 E_x}{\partial t^2}, \quad \frac{\partial^2 E_y}{\partial z^2} = \frac{1}{c^2} \frac{\partial^2 E_y}{\partial t^2} \quad (6)$$

where  $c$  is the speed of the wave,

$$c = \frac{1}{\sqrt{\epsilon\mu}} = \frac{1}{\sqrt{\epsilon_0\mu_0}\sqrt{\epsilon_r\mu_r}} \approx \frac{3 \times 10^8}{\sqrt{\epsilon_r\mu_r}} \text{ m/sec} \quad (7)$$

In free space, where  $\epsilon_r = 1$  and  $\mu_r = 1$ , this quantity equals the speed of light in vacuum which demonstrated that light is a transverse electromagnetic wave. If we similarly take  $\partial/\partial t$  of the upper and  $\partial/\partial z$  of the lower equations in (5), we obtain wave equations in the magnetic fields:

$$\frac{\partial^2 H_y}{\partial z^2} = \frac{1}{c^2} \frac{\partial^2 H_y}{\partial t^2}, \quad \frac{\partial^2 H_x}{\partial z^2} = \frac{1}{c^2} \frac{\partial^2 H_x}{\partial t^2} \quad (8)$$

### 7-3-2 The Wave Equation

#### (a) Solutions

These equations arise in many physical systems, so their solutions are well known. Working with the  $E_x$  and  $H_y$  equations, the solutions are

$$\begin{aligned} E_x(z, t) &= E_+(t - z/c) + E_-(t + z/c) \\ H_y(z, t) &= H_+(t - z/c) + H_-(t + z/c) \end{aligned} \quad (9)$$

where the functions  $E_+$ ,  $E_-$ ,  $H_+$ , and  $H_-$  depend on initial conditions in time and boundary conditions in space. These solutions can be easily verified by defining the arguments  $\alpha$  and  $\beta$  with their resulting partial derivatives as

$$\begin{aligned} \alpha = t - \frac{z}{c} \Rightarrow \frac{\partial \alpha}{\partial t} &= 1, & \frac{\partial \alpha}{\partial z} &= -\frac{1}{c} \\ \beta = t + \frac{z}{c} \Rightarrow \frac{\partial \beta}{\partial t} &= 1, & \frac{\partial \beta}{\partial z} &= \frac{1}{c} \end{aligned} \quad (10)$$

and realizing that the first partial derivatives of  $E_x(z, t)$  are

$$\begin{aligned} \frac{\partial E_x}{\partial t} &= \frac{dE_+}{d\alpha} \frac{\partial \alpha}{\partial t} + \frac{dE_-}{d\beta} \frac{\partial \beta}{\partial t} \\ &= \frac{dE_+}{d\alpha} + \frac{dE_-}{d\beta} \\ \frac{\partial E_x}{\partial z} &= \frac{dE_+}{d\alpha} \frac{\partial \alpha}{\partial z} + \frac{dE_-}{d\beta} \frac{\partial \beta}{\partial z} \\ &= \frac{1}{c} \left( -\frac{dE_+}{d\alpha} + \frac{dE_-}{d\beta} \right) \end{aligned} \quad (11)$$

The second derivatives are then

$$\begin{aligned}\frac{\partial^2 E_x}{\partial t^2} &= \frac{d^2 E_+}{d\alpha^2} \frac{\partial \alpha}{\partial t} + \frac{d^2 E_-}{d\beta^2} \frac{\partial \beta}{\partial t} \\ &= \frac{d^2 E_+}{d\alpha^2} + \frac{d^2 E_-}{d\beta^2} \\ \frac{\partial^2 E_x}{\partial z^2} &= \frac{1}{c} \left( -\frac{d^2 E_+}{d\alpha^2} \frac{\partial \alpha}{\partial z} + \frac{d^2 E_-}{d\beta^2} \frac{\partial \beta}{\partial z} \right) \\ &= \frac{1}{c^2} \left( \frac{d^2 E_+}{d\alpha^2} + \frac{d^2 E_-}{d\beta^2} \right) = \frac{1}{c^2} \frac{\partial^2 E_x}{\partial t^2}\end{aligned}\quad (12)$$

which satisfies the wave equation of (6). Similar operations apply for  $H_y$ ,  $E_y$ , and  $H_x$ .

In (9), the pair  $H_+$  and  $E_+$  as well as the pair  $H_-$  and  $E_-$  are not independent, as can be seen by substituting the solutions of (9) back into (5) and using (11):

$$\frac{\partial E_x}{\partial z} = -\mu \frac{\partial H_y}{\partial t} \Rightarrow \frac{1}{c} \left( -\frac{dE_+}{d\alpha} + \frac{dE_-}{d\beta} \right) = -\mu \left( \frac{dH_+}{d\alpha} + \frac{dH_-}{d\beta} \right) \quad (13)$$

The functions of  $\alpha$  and  $\beta$  must separately be equal,

$$\frac{d}{d\alpha} (E_+ - \mu c H_+) = 0, \quad \frac{d}{d\beta} (E_- + \mu c H_-) = 0 \quad (14)$$

which requires that

$$E_+ = \mu c H_+ = \sqrt{\frac{\mu}{\epsilon}} H_+, \quad E_- = -\mu c H_- = -\sqrt{\frac{\mu}{\epsilon}} H_- \quad (15)$$

where we use (7). Since  $\sqrt{\mu/\epsilon}$  has units of Ohms, this quantity is known as the wave impedance  $\eta$ ,

$$\eta = \sqrt{\frac{\mu}{\epsilon}} \approx 120\pi \sqrt{\frac{\mu_r}{\epsilon_r}} \quad (16)$$

and has value  $120\pi \approx 377$  ohm in free space ( $\mu_r = 1$ ,  $\epsilon_r = 1$ ).

The power flux density in TEM waves is

$$\begin{aligned}\mathbf{S} = \mathbf{E} \times \mathbf{H} &= [E_+(t-z/c) + E_-(t+z/c)] \mathbf{i}_x \\ &\quad \times [H_+(t-z/c) + H_-(t+z/c)] \mathbf{i}_y \\ &= (E_+ H_+ + E_- H_- + E_- H_+ + E_+ H_-) \mathbf{i}_z\end{aligned}\quad (17)$$

Using (15) and (16) this result can be written as

$$S_z = \frac{1}{\eta} (E_+^2 - E_-^2) \quad (18)$$

where the last two cross terms in (17) cancel because of the minus sign relating  $E_-$  to  $H_-$  in (15). For TEM waves the total power flux density is due to the difference in power densities between the squares of the positively  $z$ -directed and negatively  $z$ -directed waves.

### (b) Properties

The solutions of (9) are propagating waves at speed  $c$ . To see this, let us examine  $E_+(t - z/c)$  and consider the case where at  $z = 0$ ,  $E_+(t)$  is the staircase pulse shown in Figure 7-3a. In Figure 7-3b we replace the argument  $t$  by  $t - z/c$ . As long as the function  $E_+$  is plotted versus its argument, no matter what its argument is, the plot remains unchanged. However, in Figure 7-3c the function  $E_+(t - z/c)$  is plotted versus  $t$  resulting in the pulse being translated in time by an amount  $z/c$ . To help in plotting this translated function, we use the following logic:

- (i) The pulse jumps to amplitude  $E_0$  when the argument is zero. When the argument is  $t - z/c$ , this occurs for  $t = z/c$ .
- (ii) The pulse jumps to amplitude  $2E_0$  when the argument is  $T$ . When the argument is  $t - z/c$ , this occurs for  $t = T + z/c$ .
- (iii) The pulse returns to zero when the argument is  $2T$ . For the argument  $t - z/c$ , we have  $t = 2T + z/c$ .

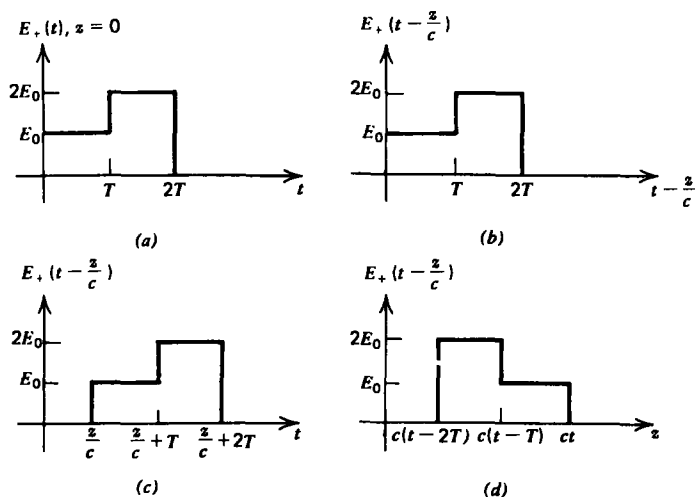


Figure 7-3 (a)  $E_+(t)$  at  $z = 0$  is a staircase pulse. (b)  $E_+(\phi)$  always has the same shape as (a) when plotted versus  $\phi$ , no matter what  $\phi$  is. Here  $\phi = t - z/c$ . (c) When plotted versus  $t$ , the pulse is translated in time where  $z$  must be positive to keep  $t$  positive. (d) When plotted versus  $z$ , it is translated and inverted. The pulse propagates at speed  $c$  in the positive  $z$  direction.

Note that  $z$  can only be positive as causality imposes the condition that time can only be increasing. The response at any positive position  $z$  to an initial  $E_+$  pulse imposed at  $z = 0$  has the same shape in time but occurs at a time  $z/c$  later. The pulse travels the distance  $z$  at the speed  $c$ . This is why the function  $E_+(t - z/c)$  is called a positively traveling wave.

In Figure 7-3*d* we plot the same function versus  $z$ . Its appearance is inverted as that part of the pulse generated first (step of amplitude  $E_0$ ) will reach any positive position  $z$  first. The second step of amplitude  $2E_0$  has not traveled as far since it was generated a time  $T$  later. To help in plotting, we use the same criterion on the argument as used in the plot versus time, only we solve for  $z$ . The important rule we use is that as long as the argument of a function remains constant, the value of the function is unchanged, no matter how the individual terms in the argument change.

Thus, as long as

$$t - z/c = \text{const} \quad (19)$$

$E_+(t - z/c)$  is unchanged. As time increases, so must  $z$  to satisfy (19) at the rate

$$t - \frac{z}{c} = \text{const} \Rightarrow \frac{dz}{dt} = c \quad (20)$$

to keep the  $E_+$  function constant.

For similar reasons  $E_-(t + z/c)$  represents a traveling wave at the speed  $c$  in the negative  $z$  direction as an observer must move to keep the argument  $t + z/c$  constant at speed:

$$t + \frac{z}{c} = \text{const} \Rightarrow \frac{dz}{dt} = -c \quad (21)$$

as demonstrated for the same staircase pulse in Figure 7-4. Note in Figure 7-4*d* that the pulse is not inverted when plotted versus  $z$  as it was for the positively traveling wave, because that part of the pulse generated first (step of amplitude  $E_0$ ) reaches the maximum distance but in the negative  $z$  direction. These differences between the positively and negatively traveling waves are functionally due to the difference in signs in the arguments ( $t - z/c$ ) and ( $t + z/c$ ).

### 7-3-3 Sources of Plane Waves

These solutions are called plane waves because at any constant  $z$  plane the fields are constant and do not vary with the  $x$  and  $y$  coordinates.

The idealized source of a plane wave is a time varying current sheet of infinite extent that we take to be  $x$  directed,

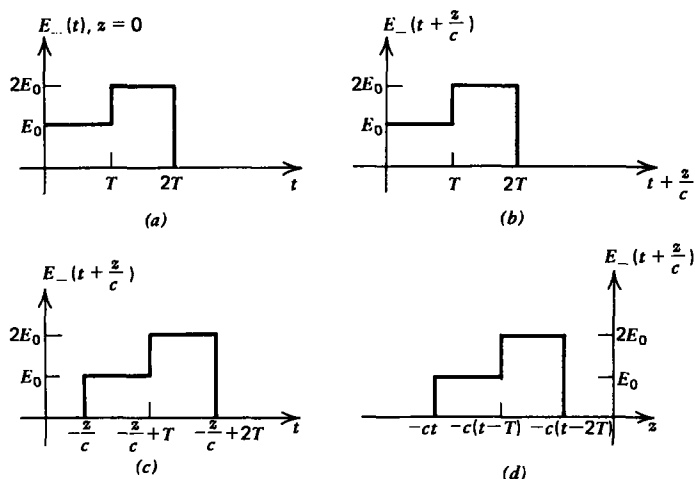


Figure 7-4 (a)  $E_-(t)$  at  $z = 0$  is a staircase pulse. (b)  $E_-(\phi)$  always has the same form of (a) when plotted versus  $\phi$ . Here  $\phi = t + z/c$ . (c) When plotted versus  $t$ , the pulse is translated in time where  $z$  must be negative to keep  $t$  positive. (d) When plotted versus  $z$ , it is translated but not inverted.

as shown in Figure 7-5. From the boundary condition on the discontinuity of tangential  $\mathbf{H}$ , we find that the  $x$ -directed current sheet gives rise to a  $y$ -directed magnetic field:

$$H_y(z = 0_+) - H_y(z = 0_-) = -K_x(t) \tag{22}$$

In general, a uniform current sheet gives rise to a magnetic field perpendicular to the direction of current flow but in the plane of the sheet. Thus to generate an  $x$ -directed magnetic field, a  $y$ -directed surface current is required.

Since there are no other sources, the waves must travel away from the sheet so that the solutions on each side of the sheet are of the form

$$H_y(z, t) = \begin{cases} H_+(t - z/c) \\ H_-(t + z/c) \end{cases} \quad E_x(z, t) = \begin{cases} \eta H_+(t - z/c), & z > 0 \\ -\eta H_-(t + z/c), & z < 0 \end{cases} \tag{23}$$

For  $z > 0$ , the waves propagate only in the positive  $z$  direction. In the absence of any other sources or boundaries, there can be no negatively traveling waves in this region. Similarly for  $z < 0$ , we only have waves propagating in the  $-z$  direction. In addition to the boundary condition of (22), the tangential component of  $\mathbf{E}$  must be continuous across the sheet at  $z = 0$

$$\left. \begin{aligned} H_+(t) - H_-(t) &= -K_x(t) \\ \eta[H_+(t) + H_-(t)] &= 0 \end{aligned} \right\} \Rightarrow H_+(t) = -H_-(t) = \frac{-K_x(t)}{2} \tag{24}$$

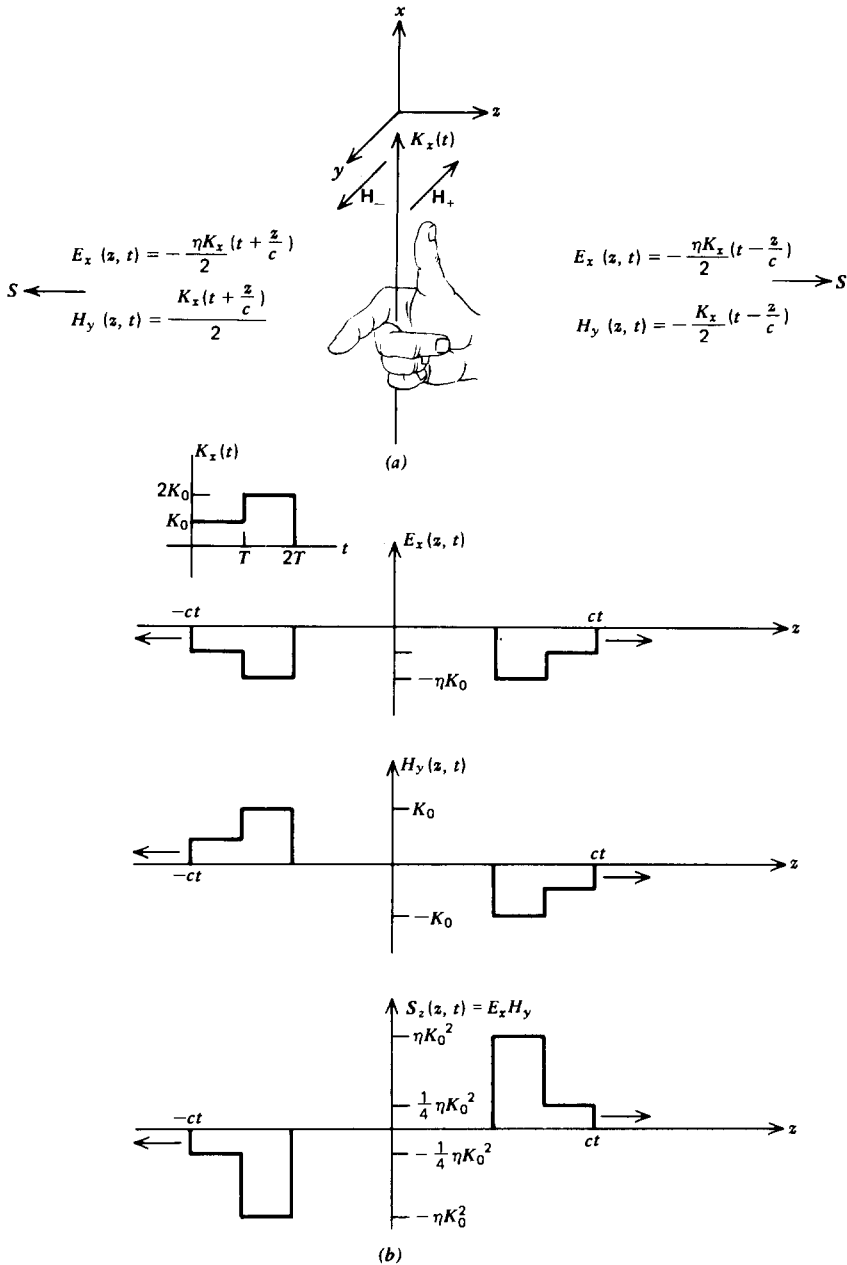


Figure 7-5 (a) A linearly polarized plane wave is generated by an infinite current sheet. The electric field is in the direction opposite to the current on either side of the sheet. The magnetic field is perpendicular to the current but in the plane of the current sheet and in opposite directions as given by the right-hand rule on either side of the sheet. The power flow  $S$  is thus perpendicular to the current and to the sheet. (b) The field solutions for  $t > 2T$  if the current source is a staircase pulse in time.

so that the electric and magnetic fields have the same shape as the current. Because the time and space shape of the fields remains unchanged as the waves propagate, linear dielectric media are said to be nondispersive.

Note that the electric field at  $z = 0$  is in the opposite direction as the current, so the power per unit area delivered by the current sheet,

$$-\mathbf{E}(z=0, t) \cdot \mathbf{K}_x(t) = \frac{\eta K_x^2(t)}{2} \quad (25)$$

is equally carried away by the Poynting vector on each side of the sheet:

$$\mathbf{S}(z=0) = \mathbf{E} \times \mathbf{H} = \begin{cases} \frac{\eta K_x^2(t)}{4} \mathbf{i}_z, & z > 0 \\ -\frac{\eta K_x^2(t)}{4} \mathbf{i}_z, & z < 0 \end{cases} \quad (26)$$

### 7-3-4 A Brief Introduction to the Theory of Relativity

Maxwell's equations show that electromagnetic waves propagate at the speed  $c_0 = 1/\sqrt{\epsilon_0 \mu_0}$  in vacuum. Our natural intuition would tell us that if we moved at a speed  $v$  we would measure a wave speed of  $c_0 - v$  when moving in the same direction as the wave, and a speed  $c_0 + v$  when moving in the opposite direction. However, our intuition would be wrong, for nowhere in the free space, source-free Maxwell's equations does the speed of the observer appear. Maxwell's equations predict that the speed of electromagnetic waves is  $c_0$  for all observers no matter their relative velocity. This assumption is a fundamental postulate of the theory of relativity and has been verified by all experiments. The most notable experiment was performed by A. A. Michelson and E. W. Morley in the late nineteenth century, where they showed that the speed of light reflected between mirrors is the same whether it propagated in the direction parallel or perpendicular to the velocity of the earth. This postulate required a revision of the usual notions of time and distance.

If the surface current sheet of Section 7-3-3 is first turned on at  $t = 0$ , the position of the wave front on either side of the sheet at time  $t$  later obeys the equality

$$z^2 - c_0^2 t^2 = 0 \quad (27)$$

Similarly, an observer in a coordinate system moving with constant velocity  $u\mathbf{i}_x$ , which is aligned with the current sheet at

$t = 0$  finds the wavefront position to obey the equality

$$z'^2 - c_0^2 t'^2 = 0 \quad (28)$$

The two coordinate systems must be related by a linear transformation of the form

$$z' = a_1 z + a_2 t, \quad t' = b_1 z + b_2 t \quad (29)$$

The position of the origin of the moving frame ( $z' = 0$ ) as measured in the stationary frame is  $z = vt$ , as shown in Figure 7-6, so that  $a_1$  and  $a_2$  are related as

$$0 = a_1 vt + a_2 t \Rightarrow a_1 v + a_2 = 0 \quad (30)$$

We can also equate the two equalities of (27) and (28),

$$z^2 - c_0^2 t^2 = z'^2 - c_0^2 t'^2 = (a_1 z + a_2 t)^2 - c_0^2 (b_1 z + b_2 t)^2 \quad (31)$$

so that combining terms yields

$$z^2(1 - a_1^2 + c_0^2 b_1^2) - c_0^2 t^2 \left(1 + \frac{a_2^2}{c_0^2} - b_2^2\right) - 2(a_1 a_2 - c_0^2 b_1 b_2) z t = 0 \quad (32)$$

Since (32) must be true for all  $z$  and  $t$ , each of the coefficients must be zero, which with (30) gives solutions

$$\begin{aligned} a_1 &= \frac{1}{\sqrt{1 - (v/c_0)^2}}, & b_1 &= \frac{-v/c_0^2}{\sqrt{1 - (v/c_0)^2}} \\ a_2 &= \frac{-v}{\sqrt{1 - (v/c_0)^2}}, & b_2 &= \frac{1}{\sqrt{1 - (v/c_0)^2}} \end{aligned} \quad (33)$$

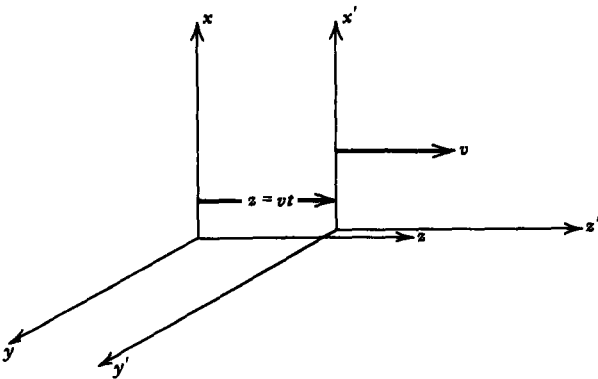


Figure 7-6 The primed coordinate system moves at constant velocity  $v\mathbf{i}_1$  with respect to a stationary coordinate system. The free space speed of an electromagnetic wave is  $c_0$  as measured by observers in either coordinate system no matter the velocity  $v$ .

The transformations of (29) are then

$$z' = \frac{z - vt}{\sqrt{1 - (v/c_0)^2}}, \quad t' = \frac{t - vz/c_0^2}{\sqrt{1 - (v/c_0)^2}} \quad (34)$$

and are known as the Lorentz transformations. Measured lengths and time intervals are different for observers moving at different speeds. If the velocity  $v$  is much less than the speed of light, (34) reduces to the Galilean transformations,

$$\lim_{v/c \ll 1} z' \approx z - vt, \quad t' \approx t \quad (35)$$

which describe our usual experiences at nonrelativistic speeds.

The coordinates perpendicular to the motion are unaffected by the relative velocity between reference frames

$$x' = x, \quad y' = y \quad (36)$$

Continued development of the theory of relativity is beyond the scope of this text and is worth a course unto itself. Applying the Lorentz transformation to Newton's law and Maxwell's equations yield new results that at first appearance seem contrary to our experiences because we live in a world where most material velocities are much less than  $c_0$ . However, continued experiments on such disparate time and space scales as between atomic physics and astronomy verify the predictions of relativity theory, in part spawned by Maxwell's equations.

## 7-4 SINUSOIDAL TIME VARIATIONS

### 7-4-1 Frequency and Wavenumber

If the current sheet of Section 7-3-3 varies sinusoidally with time as  $\text{Re}(K_0 e^{j\omega t})$ , the wave solutions require the fields to vary as  $e^{j\omega(t-z/c)}$  and  $e^{j\omega(t+z/c)}$ :

$$\begin{aligned} H_y(z, t) &= \begin{cases} \text{Re}\left(-\frac{K_0}{2} e^{j\omega(t-z/c)}\right), & z > 0 \\ \text{Re}\left(+\frac{K_0}{2} e^{j\omega(t+z/c)}\right), & z < 0 \end{cases} \\ E_x(z, t) &= \begin{cases} \text{Re}\left(-\frac{\eta K_0}{2} e^{j\omega(t-z/c)}\right), & z > 0 \\ \text{Re}\left(-\frac{\eta K_0}{2} e^{j\omega(t+z/c)}\right), & z < 0 \end{cases} \end{aligned} \quad (1)$$

At a fixed time the fields then also vary sinusoidally with position so that it is convenient to define the wavenumber as

$$k = \frac{2\pi}{\lambda} = \frac{\omega}{c} = \omega\sqrt{\mu\epsilon} \tag{2}$$

where  $\lambda$  is the fundamental spatial period of the wave. At a fixed position the waveform is also periodic in time with period  $T$ :

$$T = \frac{1}{f} = \frac{2\pi}{\omega} \tag{3}$$

where  $f$  is the frequency of the source. Using (3) with (2) gives us the familiar frequency-wavelength formula:

$$\omega = kc \Rightarrow f\lambda = c \tag{4}$$

Throughout the electromagnetic spectrum, summarized in Figure 7-7, time varying phenomena differ only in the scaling of time and size. No matter the frequency or wavelength, although easily encompassing 20 orders of magnitude, electromagnetic phenomena are all described by Maxwell's equations. Note that visible light only takes up a tiny fraction of the spectrum.

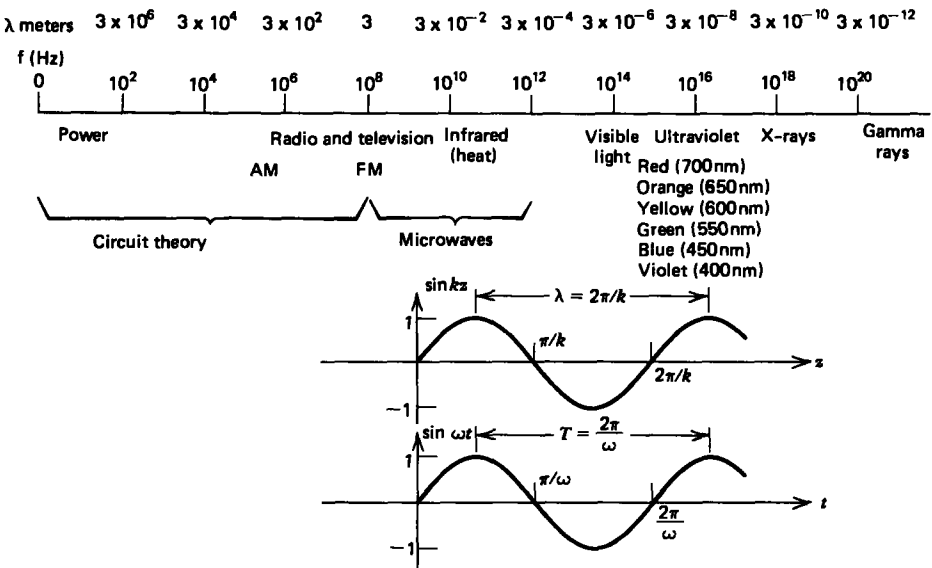


Figure 7-7 Time varying electromagnetic phenomena differ only in the scaling of time (frequency) and size (wavelength). In linear dielectric media the frequency and wavelength are related as  $f\lambda = c$  ( $\omega = kc$ ), where  $c = 1/\sqrt{\epsilon\mu}$  is the speed of light in the medium.

For a single sinusoidally varying plane wave, the time-average electric and magnetic energy densities are equal because the electric and magnetic field amplitudes are related through the wave impedance  $\eta$ :

$$\langle w_m \rangle = \langle w_e \rangle = \frac{1}{4}\mu |\mathbf{H}|^2 = \frac{1}{4}\epsilon |\mathbf{E}|^2 = \frac{1}{16}\mu K_0^2 \quad (5)$$

From the complex Poynting theorem derived in Section 7-2-4, we then see that in a lossless region with no sources for  $|z| > 0$  that  $\hat{P}_d = 0$  so that the complex Poynting vector has zero divergence. With only one-dimensional variations with  $z$ , this requires the time-average power density to be a constant throughout space on each side of the current sheet:

$$\begin{aligned} \langle \mathbf{S} \rangle &= \frac{1}{2} \operatorname{Re} [\hat{\mathbf{E}}(\mathbf{r}) \times \hat{\mathbf{H}}^*(\mathbf{r})] \\ &= \begin{cases} \frac{1}{8}\eta K_0^2 \mathbf{i}_z, & z > 0 \\ -\frac{1}{8}\eta K_0^2 \mathbf{i}_z, & z < 0 \end{cases} \end{aligned} \quad (6)$$

The discontinuity in  $\langle \mathbf{S} \rangle$  at  $z = 0$  is due to the power output of the source.

#### 7-4-2 Doppler Frequency Shifts

If the sinusoidally varying current sheet  $\operatorname{Re}(K_0 e^{j\omega t})$  moves with constant velocity  $v\mathbf{i}_z$ , as in Figure 7-8, the boundary conditions are no longer at  $z = 0$  but at  $z = vt$ . The general form of field solutions are then:

$$\begin{aligned} H_y(z, t) &= \begin{cases} \operatorname{Re}(\hat{H}_+ e^{j\omega_+(t-z/c)}), & z > vt \\ \operatorname{Re}(\hat{H}_- e^{j\omega_-(t+z/c)}), & z < vt \end{cases} \\ E_x(z, t) &= \begin{cases} \operatorname{Re}(\eta \hat{H}_+ e^{j\omega_+(t-z/c)}), & z > vt \\ \operatorname{Re}(-\eta \hat{H}_- e^{j\omega_-(t+z/c)}), & z < vt \end{cases} \end{aligned} \quad (7)$$

where the frequencies of the fields  $\omega_+$  and  $\omega_-$  on each side of the sheet will be different from each other as well as differing from the frequency of the current source  $\omega$ . We assume  $v/c \ll 1$  so that we can neglect relativistic effects discussed in Section 7-3-4. The boundary conditions

$$\begin{aligned} E_{x_+}(z = vt) = E_{x_-}(z = vt) &\Rightarrow \hat{H}_+ e^{j\omega_+ t(1-v/c)} = -\hat{H}_- e^{j\omega_- t(1+v/c)} \\ H_{y_+}(z = vt) - H_{y_-}(z = vt) &= -K_x \\ &\Rightarrow \hat{H}_+ e^{j\omega_+ t(1-v/c)} - \hat{H}_- e^{j\omega_- t(1+v/c)} = -K_0 e^{j\omega t} \end{aligned} \quad (8)$$

must be satisfied for all values of  $t$  so that the exponential time factors in (8) must all be equal, which gives the shifted

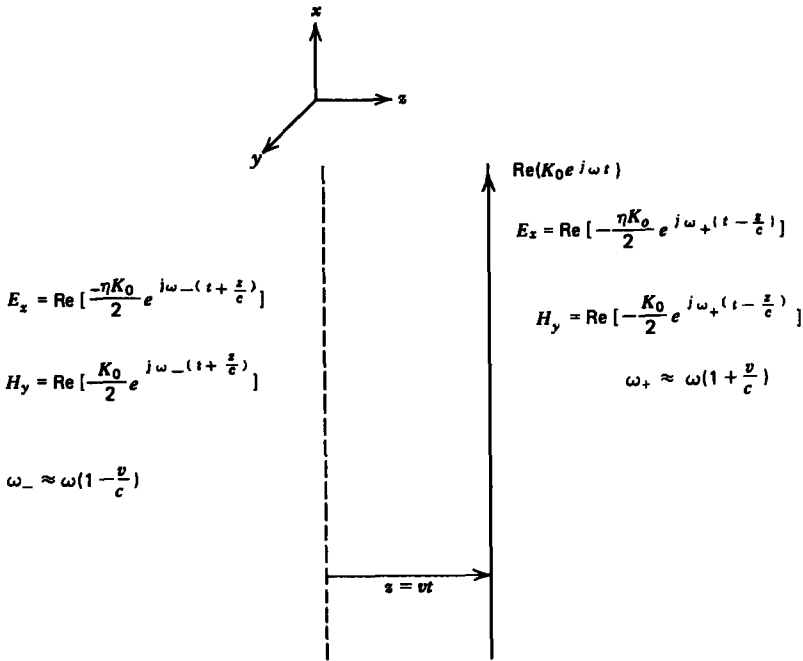


Figure 7-8 When a source of electromagnetic waves moves towards an observer, the frequency is raised while it is lowered when it moves away from an observer.

frequencies on each side of the sheet as

$$\omega_+ = \frac{\omega}{1 - v/c} \approx \omega \left( 1 + \frac{v}{c} \right), \tag{9}$$

$$\omega_- = \frac{\omega}{1 + v/c} \approx \omega \left( 1 - \frac{v}{c} \right) \Rightarrow \hat{H}_+ = -\hat{H}_- = -\frac{K_0}{2}$$

where  $v/c \ll 1$ . When the source is moving towards an observer, the frequency is raised while it is lowered when it moves away. Such frequency changes due to the motion of a source or observer are called Doppler shifts and are used to measure the velocities of moving bodies in radar systems. For  $v/c \ll 1$ , the frequency shifts are a small percentage of the driving frequency, but in absolute terms can be large enough to be easily measured. At a velocity  $v = 300$  m/sec with a driving frequency of  $f = 10^{10}$  Hz, the frequency is raised and lowered on each side of the sheet by  $\Delta f = \pm f(v/c) = \pm 10^4$  Hz.

### 7-4-3 Ohmic Losses

Thus far we have only considered lossless materials. If the medium also has an Ohmic conductivity  $\sigma$ , the electric field

will cause a current flow that must be included in Ampere's law:

$$\begin{aligned} \frac{\partial E_x}{\partial z} &= -\mu \frac{\partial H_y}{\partial t} \\ \frac{\partial H_y}{\partial z} &= -J_x - \epsilon \frac{\partial E_x}{\partial t} = -\sigma E_x - \epsilon \frac{\partial E_x}{\partial t} \end{aligned} \tag{10}$$

where for conciseness we only consider the  $x$ -directed electric field solution as the same results hold for the  $E_y$ ,  $H_x$  solution. Our wave solutions of Section 7-3-2 no longer hold with this additional term, but because Maxwell's equations are linear with constant coefficients, for sinusoidal time variations the solutions in space must also be exponential functions, which we write as

$$\begin{aligned} E_x(z, t) &= \text{Re} (\hat{E}_0 e^{j(\omega t - kz)}) \\ H_y(z, t) &= \text{Re} (\hat{H}_0 e^{j(\omega t - kz)}) \end{aligned} \tag{11}$$

where  $\hat{E}_0$  and  $\hat{H}_0$  are complex amplitudes and the wavenumber  $k$  is no longer simply related to  $\omega$  as in (4) but is found by substituting (11) back into (10):

$$\begin{aligned} -jk\hat{E}_0 &= -j\omega\mu\hat{H}_0 \\ -jk\hat{H}_0 &= -j\omega\epsilon(1 + \sigma/j\omega\epsilon)\hat{E}_0 \end{aligned} \tag{12}$$

This last relation was written in a way that shows that the conductivity enters in the same way as the permittivity so that we can define a complex permittivity  $\hat{\epsilon}$  as

$$\hat{\epsilon} = \epsilon(1 + \sigma/j\omega\epsilon) \tag{13}$$

Then the solutions to (12) are

$$\frac{\hat{E}_0}{\hat{H}_0} = \frac{\omega\mu}{k} = \frac{k}{\omega\hat{\epsilon}} \Rightarrow k^2 = \omega^2\mu\hat{\epsilon} = \omega^2\mu\epsilon\left(1 + \frac{\sigma}{j\omega\epsilon}\right) \tag{14}$$

which is similar in form to (2) with a complex permittivity.

There are two interesting limits of (14):

**(a) Low Loss Limit**

If the conductivity is small so that  $\sigma/\omega\epsilon \ll 1$ , then the solution of (14) reduces to

$$\lim_{\sigma/\omega\epsilon \ll 1} k = \pm\omega\sqrt{\mu\epsilon}\left(1 + \frac{\sigma}{2j\omega\epsilon}\right) = \pm\left(\frac{\omega}{c} - \frac{j\sigma}{2}\sqrt{\frac{\mu}{\epsilon}}\right) \tag{15}$$

where  $c$  is the speed of the light in the medium if there were no losses,  $c = 1/\sqrt{\mu\epsilon}$ . Because of the spatial exponential dependence in (11), the real part of  $k$  is the same as for the

lossless case and represents the sinusoidal spatial distribution of the fields. The imaginary part of  $k$  represents the exponential decay of the fields due to the Ohmic losses with exponential decay length  $\frac{1}{2}\sigma\eta$ , where  $\eta = \sqrt{\mu/\epsilon}$  is the wave impedance. Note that for waves traveling in the positive  $z$  direction we take the upper positive sign in (15) using the lower negative sign for negatively traveling waves so that the solutions all decay and do not grow for distances far from the source. This solution is only valid for small  $\sigma$  so that the wave is only slightly damped as it propagates, as illustrated in Figure 7-9a.

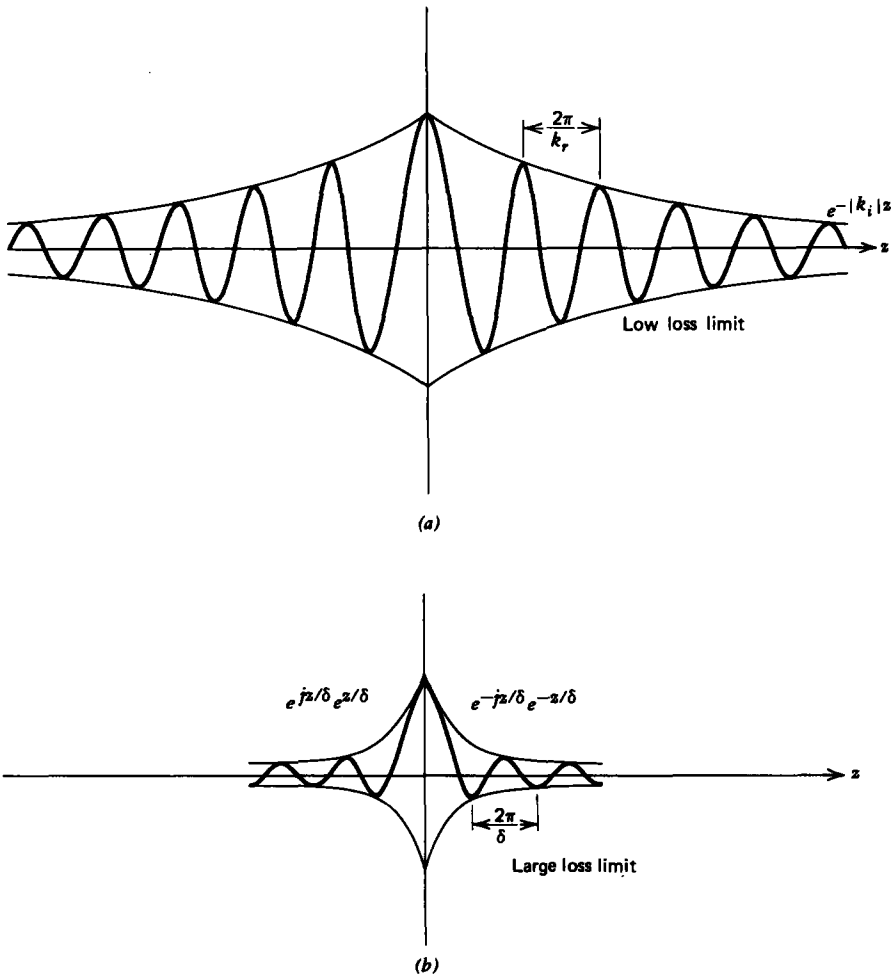


Figure 7-9 (a) In a slightly lossy dielectric, the fields decay away from a source at a slow rate while the wavelength is essentially unchanged. (b) In the large loss limit the spatial decay rate is equal to the skin depth. The wavelength also equals the skin depth.

**(b) Large Loss Limit**

In the other extreme of a highly conducting material so that  $\sigma/\omega\epsilon \gg 1$ , (14) reduces to

$$\lim_{\sigma/\omega\epsilon \gg 1} k^2 \approx -j\omega\mu\sigma \Rightarrow k = \pm \frac{(1-j)}{\delta}, \quad \delta = \sqrt{\frac{2}{\omega\mu\sigma}} \quad (16)$$

where  $\delta$  is just the skin depth found in Section 6-4-3 for magneto-quasi-static fields within a conductor. The skin-depth term also arises for electrodynamic fields because the large loss limit has negligible displacement current compared to the conduction currents.

Because the real and imaginary part of  $k$  have equal magnitudes, the spatial decay rate is large so that within a few oscillation intervals the fields are negligibly small, as illustrated in Figure 7-9b. For a metal like copper with  $\mu = \mu_0 = 4\pi \times 10^{-7}$  henry/m and  $\sigma \approx 6 \times 10^7$  siemens/m at a frequency of 1 MHz, the skin depth is  $\delta \approx 6.5 \times 10^{-5}$  m.

**7-4-4 High-Frequency Wave Propagation in Media**

Ohm's law is only valid for frequencies much below the collision frequencies of the charge carriers, which is typically on the order of  $10^{13}$  Hz. In this low-frequency regime the inertia of the particles is negligible. For frequencies much higher than the collision frequency the inertia dominates and the current constitutive law for a single species of charge carrier  $q$  with mass  $m$  and number density  $n$  is as found in Section 3-2-2d:

$$\partial \mathbf{J}_f / \partial t = \omega_p^2 \epsilon \mathbf{E} \quad (17)$$

where  $\omega_p = \sqrt{q^2 n / m \epsilon}$  is the plasma frequency. This constitutive law is accurate for radio waves propagating in the ionosphere, for light waves propagating in many dielectrics, and is also valid for superconductors where the collision frequency is zero.

Using (17) rather than Ohm's law in (10) for sinusoidal time and space variations as given in (11), Maxwell's equations are

$$\begin{aligned} \frac{\partial E_x}{\partial z} &= -\mu \frac{\partial H_y}{\partial t} \Rightarrow -jk \hat{E}_0 = -j\omega\mu \hat{H}_0 \\ \frac{\partial H_y}{\partial z} &= -J_x - \epsilon \frac{\partial E_x}{\partial t} \Rightarrow -jk \hat{H}_0 = -j\omega\epsilon \left(1 - \frac{\omega_p^2}{\omega^2}\right) \hat{E}_0 \end{aligned} \quad (18)$$

The effective permittivity is now frequency dependent:

$$\hat{\epsilon} = \epsilon \left(1 - \frac{\omega_p^2}{\omega^2}\right) \quad (19)$$

The solutions to (18) are

$$\frac{\hat{E}_0}{\hat{H}_0} = \frac{\omega\mu}{k} = \frac{k}{\omega\hat{\epsilon}} \Rightarrow k^2 = \omega^2\mu\hat{\epsilon} = \frac{\omega^2 - \omega_p^2}{c^2} \quad (20)$$

For  $\omega > \omega_p$ ,  $k$  is real and we have pure propagation where the wavenumber depends on the frequency. For  $\omega < \omega_p$ ,  $k$  is imaginary representing pure exponential decay.

Poynting's theorem for this medium is

$$\begin{aligned} \nabla \cdot \mathbf{S} + \frac{\partial}{\partial t} \left( \frac{1}{2}\epsilon |\mathbf{E}|^2 + \frac{1}{2}\mu |\mathbf{H}|^2 \right) &= -\mathbf{E} \cdot \mathbf{J}_f = -\frac{1}{\omega_p^2 \epsilon} \mathbf{J}_f \cdot \frac{\partial \mathbf{J}_f}{\partial t} \\ &= -\frac{\partial}{\partial t} \left( \frac{1}{\omega_p^2 \epsilon} \frac{|\mathbf{J}_f|^2}{2} \right) \end{aligned} \quad (21)$$

Because this system is lossless, the right-hand side of (21) can be brought to the left-hand side and lumped with the energy densities:

$$\nabla \cdot \mathbf{S} + \frac{\partial}{\partial t} \left[ \frac{1}{2}\epsilon |\mathbf{E}|^2 + \frac{1}{2}\mu |\mathbf{H}|^2 + \frac{1}{2} \frac{1}{\omega_p^2 \epsilon} |\mathbf{J}_f|^2 \right] = 0 \quad (22)$$

This new energy term just represents the kinetic energy density of the charge carriers since their velocity is related to the current density as

$$\mathbf{J}_f = qn\mathbf{v} \Rightarrow \frac{1}{2} \frac{1}{\omega_p^2 \epsilon} |\mathbf{J}_f|^2 = \frac{1}{2} mn |\mathbf{v}|^2 \quad (23)$$

### 7-4-5 Dispersive Media

When the wavenumber is not proportional to the frequency of the wave, the medium is said to be dispersive. A nonsinusoidal time signal (such as a square wave) will change shape and become distorted as the wave propagates because each Fourier component of the signal travels at a different speed.

To be specific, consider a stationary current sheet source at  $z = 0$  composed of two signals with slightly different frequencies:

$$\begin{aligned} K(t) &= K_0[\cos(\omega_0 + \Delta\omega)t + \cos(\omega_0 - \Delta\omega)t] \\ &= 2K_0 \cos \Delta\omega t \cos \omega_0 t \end{aligned} \quad (24)$$

With  $\Delta\omega \ll \omega$  the fast oscillations at frequency  $\omega_0$  are modulated by the slow envelope function at frequency  $\Delta\omega$ . In a linear dielectric medium this wave packet would propagate away from the current sheet at the speed of light,  $c = 1/\sqrt{\epsilon\mu}$ .

If the medium is dispersive, with the wavenumber  $k(\omega)$  being a function of  $\omega$ , each frequency component in (24) travels at a slightly different speed. Since each frequency is very close to  $\omega_0$  we expand  $k(\omega)$  as

$$\begin{aligned} k(\omega_0 + \Delta\omega) &\approx k(\omega_0) + \left. \frac{dk}{d\omega} \right|_{\omega_0} \Delta\omega \\ k(\omega_0 - \Delta\omega) &\approx k(\omega_0) - \left. \frac{dk}{d\omega} \right|_{\omega_0} \Delta\omega \end{aligned} \quad (25)$$

where for propagation  $k(\omega_0)$  must be real.

The fields for waves propagating in the  $+z$  direction are then of the following form:

$$\begin{aligned} E_x(z, t) &= \text{Re } \hat{E}_0 \left( \exp \left\{ j \left[ (\omega_0 + \Delta\omega)t - \left( k(\omega_0) + \left. \frac{dk}{d\omega} \right|_{\omega_0} \Delta\omega \right) z \right] \right\} \right. \\ &\quad \left. + \exp \left\{ j \left[ (\omega_0 - \Delta\omega)t - \left( k(\omega_0) - \left. \frac{dk}{d\omega} \right|_{\omega_0} \Delta\omega \right) z \right] \right\} \right) \\ &= \text{Re} \left( \hat{E}_0 \exp \{ j[\omega_0 t - k(\omega_0)z] \} \left\{ \exp \left[ j \Delta\omega \left( t - \left. \frac{dk}{d\omega} \right|_{\omega_0} z \right) \right] \right. \right. \\ &\quad \left. \left. + \exp \left[ -j \Delta\omega \left( t - \left. \frac{dk}{d\omega} \right|_{\omega_0} z \right) \right] \right\} \right) \\ &= 2E_0 \cos(\omega_0 t - k(\omega_0)z) \cos \Delta\omega \left( t - \left. \frac{dk}{d\omega} \right|_{\omega_0} z \right) \end{aligned} \quad (26)$$

where without loss of generality we assume in the last relation that  $\hat{E}_0 = E_0$  is real. This result is plotted in Figure 7-10 as a function of  $z$  for fixed time. The fast waves with argument  $\omega_0 t - k(\omega_0)z$  travel at the phase speed  $v_p = \omega_0/k(\omega_0)$  through the modulating envelope with argument  $\Delta\omega(t - dk/d\omega|_{\omega_0} z)$ . This envelope itself travels at the slow speed

$$t - \left. \frac{dk}{d\omega} \right|_{\omega_0} z = \text{const} \Rightarrow \frac{dz}{dt} = v_g = \left. \frac{d\omega}{dk} \right|_{\omega_0} \quad (27)$$

known as the group velocity, for it is the velocity at which a packet of waves within a narrow frequency band around  $\omega_0$  will travel.

For linear media the group and phase velocities are equal:

$$\begin{aligned} \omega = kc \Rightarrow v_p = \frac{\omega}{k} = c \\ v_g = \frac{d\omega}{dk} = c \end{aligned} \quad (28)$$

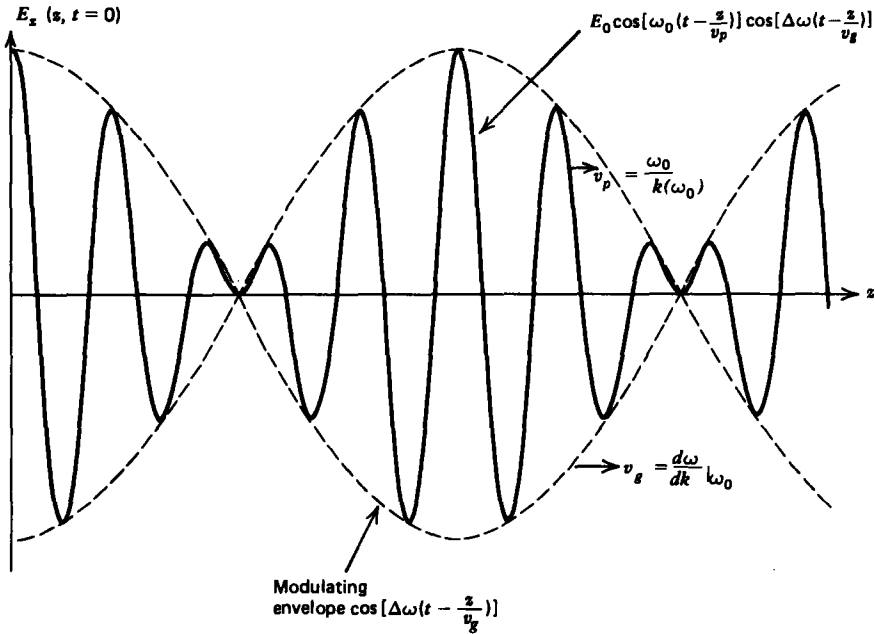


Figure 7-10 In a dispersive medium the shape of the waves becomes distorted so the velocity of a wave is not uniquely defined. For a group of signals within a narrow frequency band the modulating envelope travels at the group velocity  $v_g$ . The signal within the envelope propagates through at the phase velocity  $v_p$ .

while from Section 7-4-4 in the high-frequency limit for conductors, we see that

$$\omega^2 = k^2 c^2 + \omega_p^2 \Rightarrow v_p = \frac{\omega}{k} \tag{29}$$

$$v_g = \frac{d\omega}{dk} = \frac{k}{\omega} c^2$$

where the velocities only make sense when  $k$  is real so that  $\omega > \omega_p$ . Note that in this limit

$$v_g v_p = c^2 \tag{30}$$

Group velocity only has meaning in a dispersive medium when the signals of interest are clustered over a narrow frequency range so that the slope defined by (27), is approximately constant and real.

### 7-4-6 Polarization

The two independent sets of solutions of Section 7-3-1 both have their power flow  $\mathbf{S} = \mathbf{E} \times \mathbf{H}$  in the  $z$  direction. One solution is said to have its electric field polarized in the  $x$  direction

while the second has its electric field polarized in the  $y$  direction. Each solution alone is said to be linearly polarized because the electric field always points in the same direction for all time. If both field solutions are present, the direction of net electric field varies with time. In particular, let us say that the  $x$  and  $y$  components of electric field at any value of  $z$  differ in phase by angle  $\phi$ :

$$\mathbf{E} = \text{Re} [E_{x_0} \mathbf{i}_x + E_{y_0} e^{j\phi} \mathbf{i}_y] e^{j\omega t} = E_{x_0} \cos \omega t \mathbf{i}_x + E_{y_0} \cos(\omega t + \phi) \mathbf{i}_y \quad (31)$$

We can eliminate time as a parameter, realizing from (31) that

$$\cos \omega t = E_x / E_{x_0} \quad (32)$$

$$\sin \omega t = \frac{\cos \omega t \cos \phi - E_y / E_{y_0}}{\sin \phi} = \frac{(E_x / E_{x_0}) \cos \phi - E_y / E_{y_0}}{\sin \phi}$$

and using the identity that

$$\begin{aligned} \sin^2 \omega t + \cos^2 \omega t \\ = 1 = \left( \frac{E_x}{E_{x_0}} \right)^2 + \frac{(E_x / E_{x_0})^2 \cos^2 \phi + (E_y / E_{y_0})^2 - (2E_x E_y / E_{x_0} E_{y_0}) \cos \phi}{\sin^2 \phi} \end{aligned} \quad (33)$$

to give us the equation of an ellipse relating  $E_x$  to  $E_y$ :

$$\left( \frac{E_x}{E_{x_0}} \right)^2 + \left( \frac{E_y}{E_{y_0}} \right)^2 - \frac{2E_x E_y}{E_{x_0} E_{y_0}} \cos \phi = \sin^2 \phi \quad (34)$$

as plotted in Figure 7-11a. As time increases the electric field vector traces out an ellipse each period so this general case of the superposition of two linear polarizations with arbitrary phase  $\phi$  is known as elliptical polarization. There are two important special cases:

#### (a) Linear Polarization

If  $E_x$  and  $E_y$  are in phase so that  $\phi = 0$ , (34) reduces to

$$\left( \frac{E_x}{E_{x_0}} - \frac{E_y}{E_{y_0}} \right)^2 = 0 \Rightarrow \tan \theta = \frac{E_y}{E_x} = \frac{E_{y_0}}{E_{x_0}} \quad (35)$$

The electric field at all times is at a constant angle  $\theta$  to the  $x$  axis. The electric field amplitude oscillates with time along this line, as in Figure 7-11b. Because its direction is always along the same line, the electric field is linearly polarized.

#### (b) Circular Polarization

If both components have equal amplitudes but are  $90^\circ$  out of phase,

$$E_{x_0} = E_{y_0} = E_0, \quad \phi = \pm \pi/2 \quad (36)$$

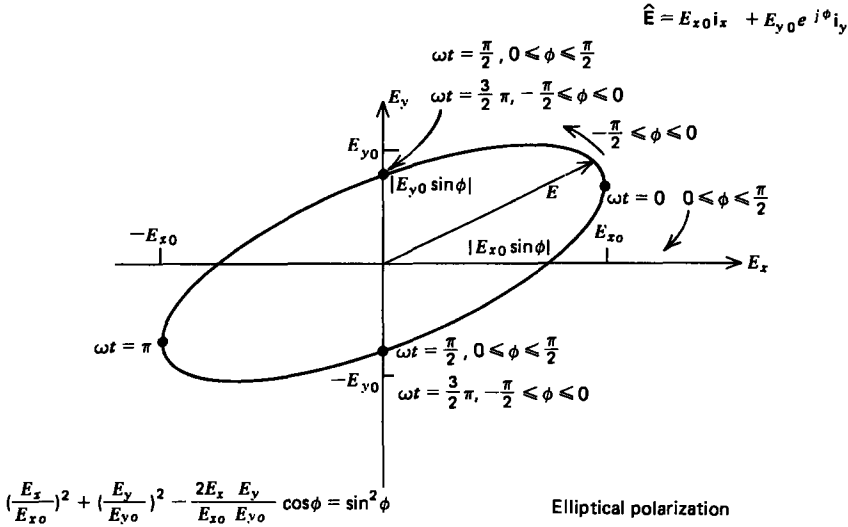


Figure 7-11 (a) Two perpendicular field components with phase difference  $\phi$  have the tip of the net electric field vector tracing out an ellipse each period. (b) If both field components are in phase, the ellipse reduces to a straight line. (c) If the field components have the same magnitude but are  $90^\circ$  out of phase, the ellipse becomes a circle. The polarization is left circularly polarized to  $z$ -directed power flow if the electric field rotates clockwise and is (d) right circularly polarized if it rotates counterclockwise.

(34) reduces to the equation of a circle:

$$E_x^2 + E_y^2 = E_0^2 \tag{37}$$

The tip of the electric field vector traces out a circle as time evolves over a period, as in Figure 7-11c. For the upper (+) sign for  $\phi$  in (36), the electric field rotates clockwise while the negative sign has the electric field rotating counterclockwise. These cases are, respectively, called left and right circular polarization for waves propagating in the  $+z$  direction as found by placing the thumb of either hand in the direction of power flow. The fingers on the left hand curl in the direction of the rotating field for left circular polarization, while the fingers of the right hand curl in the direction of the rotating field for right circular polarization. Left and right circular polarizations reverse for waves traveling in the  $-z$  direction.

### 7-4-7 Wave Propagation in Anisotropic Media

Many properties of plane waves have particular applications to optics. Because visible light has a wavelength on the order of 500 nm, even a pencil beam of light 1 mm wide is 2000 wavelengths wide and thus approximates a plane wave.

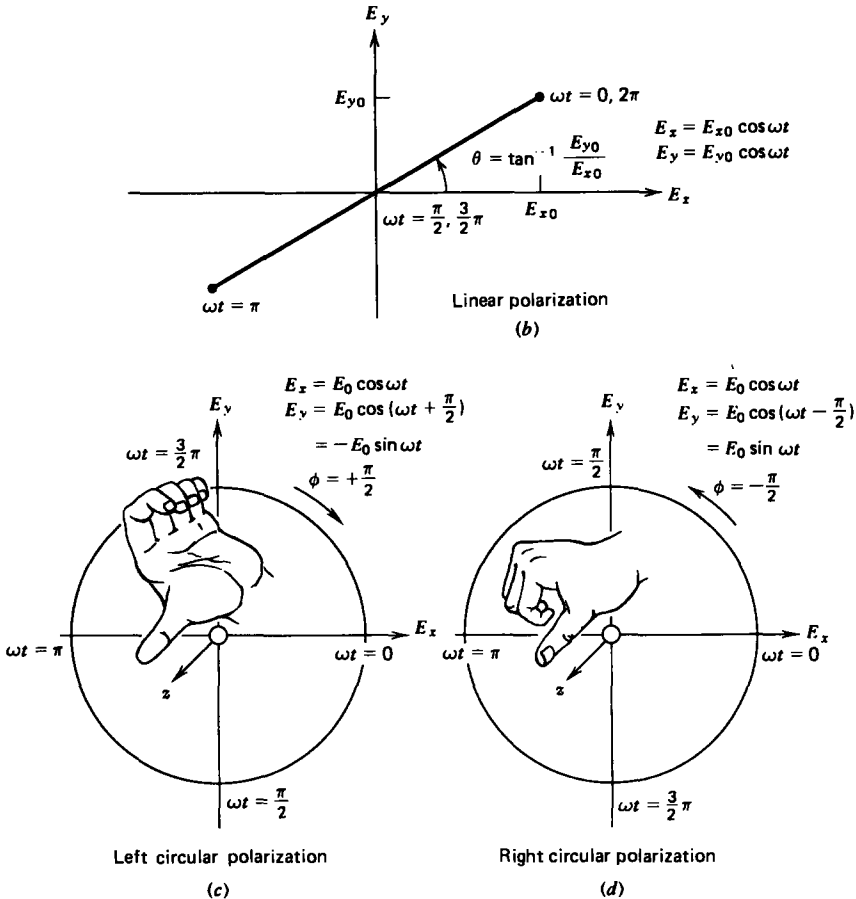


Figure 7-11

**(a) Polarizers**

Light is produced by oscillating molecules whether in a light bulb or by the sun. This natural light is usually unpolarized as each molecule oscillates in time and direction independent of its neighbors so that even though the power flow may be in a single direction the electric field phase changes randomly with time and the source is said to be incoherent. Lasers, an acronym for "light amplification by stimulated emission of radiation," emits coherent light by having all the oscillating molecules emit in time phase.

A polarizer will only pass those electric field components aligned with the polarizer's transmission axis so that the transmitted light is linearly polarized. Polarizers are made of such crystals as tourmaline, which exhibit dichroism—the selective absorption of the polarization along a crystal axis.

The polarization perpendicular to this axis is transmitted.

Because tourmaline polarizers are expensive, fragile, and of small size, improved low cost and sturdy sheet polarizers were developed by embedding long needlelike crystals or chainlike molecules in a plastic sheet. The electric field component in the long direction of the molecules or crystals is strongly absorbed while the perpendicular component of the electric field is passed.

For an electric field of magnitude  $E_0$  at angle  $\phi$  to the transmission axis of a polarizer, the magnitude of the transmitted field is

$$E_t = E_0 \cos \phi \quad (38)$$

so that the time-average power flux density is

$$\begin{aligned} \langle S \rangle &= \left| \frac{1}{2} \operatorname{Re} [\hat{\mathbf{E}}(\mathbf{r}) \times \hat{\mathbf{H}}^*(\mathbf{r})] \right| \\ &= \frac{1}{2} \frac{E_0^2}{\eta} \cos^2 \phi \end{aligned} \quad (39)$$

which is known as the law of Malus.

### (b) Double Refraction (Birefringence)

If a second polarizer, now called the analyzer, is placed parallel to the first but with its transmission axis at right angles, as in Figure 7-12, no light is transmitted. The combination is called a polariscope. However, if an anisotropic crystal is inserted between the polarizer and analyzer, light is transmitted through the analyzer. In these doubly refracting crystals, light polarized along the optic axis travels at speed  $c_{\parallel}$  while light polarized perpendicular to the axis travels at a slightly different speed  $c_{\perp}$ . The crystal is said to be birefringent. If linearly polarized light is incident at  $45^\circ$  to the axis,

$$\mathbf{E}(z=0, t) = E_0(\mathbf{i}_x + \mathbf{i}_y) \operatorname{Re}(e^{j\omega t}) \quad (40)$$

the components of electric field along and perpendicular to the axis travel at different speeds:

$$\begin{aligned} E_x(z, t) &= E_0 \operatorname{Re}(e^{j(\omega t - k_{\parallel} z)}), & k_{\parallel} &= \omega/c_{\parallel} \\ E_y(z, t) &= E_0 \operatorname{Re}(e^{j(\omega t - k_{\perp} z)}), & k_{\perp} &= \omega/c_{\perp} \end{aligned} \quad (41)$$

After exiting the crystal at  $z = l$ , the total electric field is

$$\begin{aligned} \mathbf{E}(z=l, t) &= E_0 \operatorname{Re} [e^{j\omega t} (e^{-jk_{\parallel} l} \mathbf{i}_x + e^{-jk_{\perp} l} \mathbf{i}_y)] \\ &= E_0 \operatorname{Re} [e^{j(\omega t - k_{\parallel} l)} (\mathbf{i}_x + e^{j(k_{\parallel} - k_{\perp}) l} \mathbf{i}_y)] \end{aligned} \quad (42)$$

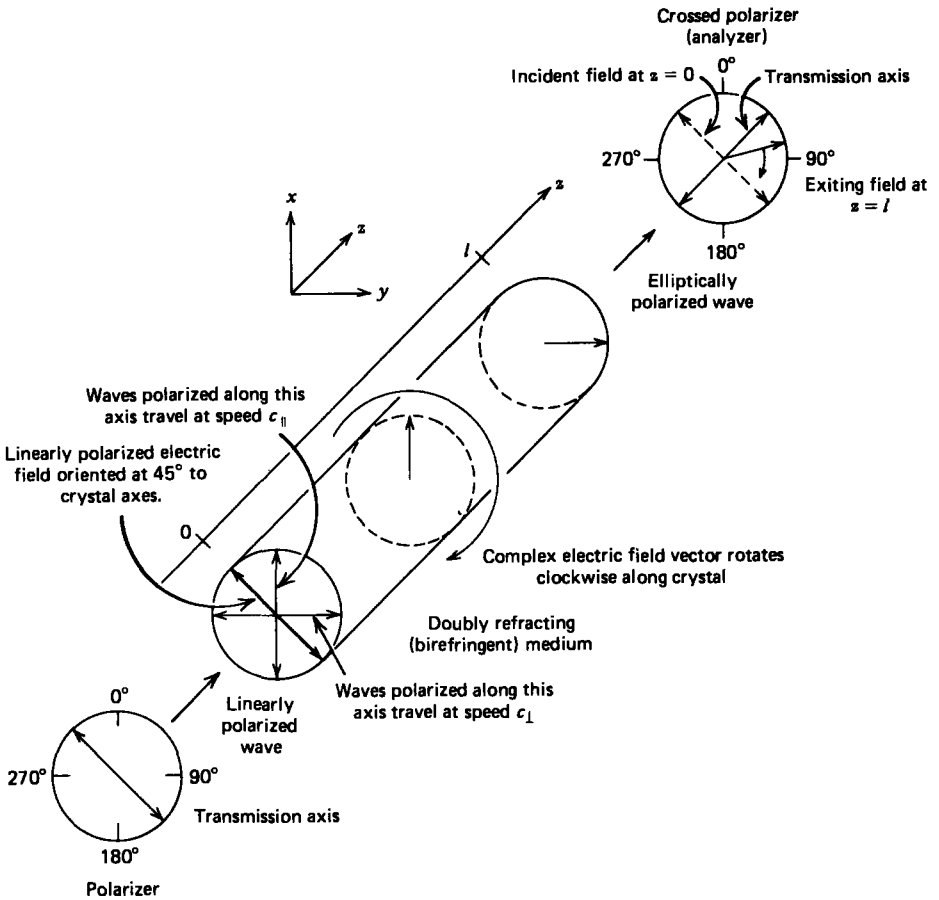


Figure 7-12 When a linearly polarized wave passes through a doubly refracting (birefringent) medium at an angle to the crystal axes, the transmitted light is elliptically polarized.

which is of the form of (31) for an elliptically polarized wave where the phase difference is

$$\phi = (k_{\parallel} - k_{\perp})l = \omega l \left( \frac{1}{c_{\parallel}} - \frac{1}{c_{\perp}} \right) \quad (43)$$

When  $\phi$  is an integer multiple of  $2\pi$ , the light exiting the crystal is the same as if the crystal were not there so that it is not transmitted through the analyzer. If  $\phi$  is an odd integer multiple of  $\pi$ , the exiting light is also linearly polarized but perpendicularly to the incident light so that it is polarized in the same direction as the transmission axis of the analyzer, and thus is transmitted. Such elements are called half-wave plates at the frequency of operation. When  $\phi$  is an odd integer multiple of  $\pi/2$ , the exiting light is circularly

polarized and the crystal serves as a quarter-wave plate. However, only that polarization of light along the transmission axis of the analyzer is transmitted.

Double refraction occurs naturally in many crystals due to their anisotropic molecular structure. Many plastics and glasses that are generally isotropic have induced birefringence when mechanically stressed. When placed within a polariscope the photoelastic stress patterns can be seen. Some liquids, notably nitrobenzene, also become birefringent when stressed by large electric fields. This phenomena is called the Kerr effect. Electro-optical measurements allow electric field mapping in the dielectric between high voltage stressed electrodes, useful in the study of high voltage conduction and breakdown phenomena. The Kerr effect is also used as a light switch in high-speed shutters. A parallel plate capacitor is placed within a polariscope so that in the absence of voltage no light is transmitted. When the voltage is increased the light is transmitted, being a maximum when  $\phi = \pi$ . (See problem 17.)

## 7-5 NORMAL INCIDENCE ONTO A PERFECT CONDUCTOR

A uniform plane wave with  $x$ -directed electric field is normally incident upon a perfectly conducting plane at  $z = 0$ , as shown in Figure 7-13. The presence of the boundary gives rise to a reflected wave that propagates in the  $-z$  direction. There are no fields within the perfect conductor. The known incident fields traveling in the  $+z$  direction can be written as

$$\begin{aligned} \mathbf{E}_i(z, t) &= \text{Re} (\hat{\mathbf{E}}_i e^{j(\omega t - kz)} \mathbf{i}_x) \\ \mathbf{H}_i(z, t) &= \text{Re} \left( \frac{\hat{\mathbf{E}}_i}{\eta_0} e^{j(\omega t - kz)} \mathbf{i}_y \right) \end{aligned} \quad (1)$$

while the reflected fields propagating in the  $-z$  direction are similarly

$$\begin{aligned} \mathbf{E}_r(z, t) &= \text{Re} (\hat{\mathbf{E}}_r e^{j(\omega t + kz)} \mathbf{i}_x) \\ \mathbf{H}_r(z, t) &= \text{Re} \left( \frac{-\hat{\mathbf{E}}_r}{\eta_0} e^{j(\omega t + kz)} \mathbf{i}_y \right) \end{aligned} \quad (2)$$

where in the lossless free space

$$\eta_0 = \sqrt{\mu_0 / \epsilon_0}, \quad k = \omega \sqrt{\epsilon_0 \mu_0} \quad (3)$$

Note the minus sign difference in the spatial exponential phase factors of (1) and (2) as the waves are traveling in opposite directions. The amplitude of incident and reflected magnetic fields are given by the ratio of electric field amplitude to the wave impedance, as derived in Eq. (15) of Section

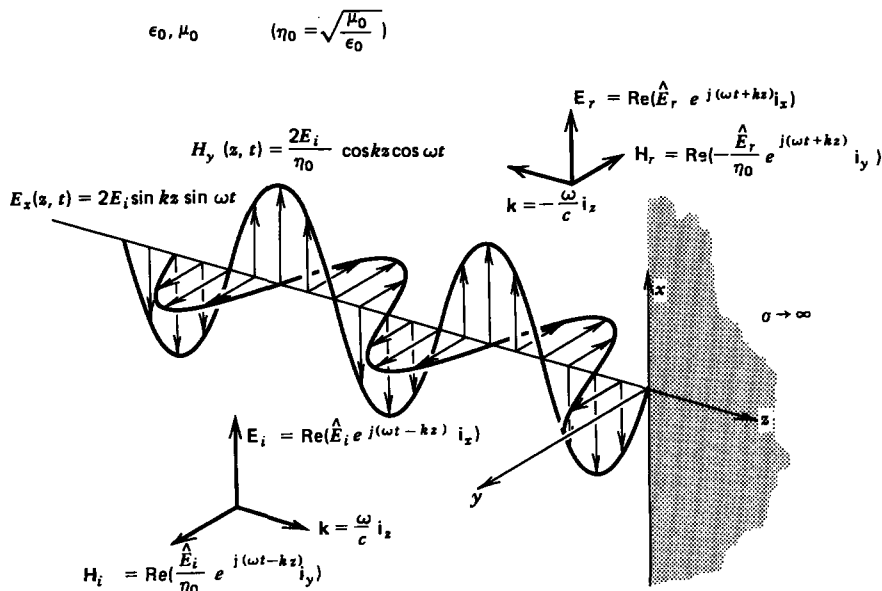


Figure 7-13 A uniform plane wave normally incident upon a perfect conductor has zero electric field at the conducting surface thus requiring a reflected wave. The source of this reflected wave is the surface current at  $z = 0$ , which equals the magnetic field there. The total electric and magnetic fields are  $90^\circ$  out of phase in time and space.

7-3-2. The negative sign in front of the reflected magnetic field for the wave in the  $-z$  direction arises because the power flow  $\mathbf{S}_r = \mathbf{E}_r \times \mathbf{H}_r$  in the reflected wave must also be in the  $-z$  direction.

The total electric and magnetic fields are just the sum of the incident and reflected fields. The only unknown parameter  $E_r$  can be evaluated from the boundary condition at  $z = 0$  where the tangential component of  $\mathbf{E}$  must be continuous and thus zero along the perfect conductor:

$$\hat{E}_i + \hat{E}_r = 0 \Rightarrow \hat{E}_r = -\hat{E}_i \quad (4)$$

The total fields are then the sum of the incident and reflected fields

$$\begin{aligned} \mathbf{E}_x(z, t) &= \mathbf{E}_i(z, t) + \mathbf{E}_r(z, t) \\ &= \text{Re} [\hat{E}_i (e^{-jkz} - e^{+jkz}) e^{j\omega t}] \\ &= 2E_i \sin kz \sin \omega t \\ \mathbf{H}_y(z, t) &= \mathbf{H}_i(z, t) + \mathbf{H}_r(z, t) \\ &= \text{Re} \left( \frac{\hat{E}_i}{\eta_0} (e^{-jkz} + e^{+jkz}) e^{j\omega t} \right) \\ &= \frac{2E_i}{\eta_0} \cos kz \cos \omega t \end{aligned} \quad (5)$$

where we take  $\hat{E}_i = E_i$  to be real. The electric and magnetic fields are  $90^\circ$  out of phase with each other both in time and space. We note that the two oppositely traveling wave solutions combined for a standing wave solution. The total solution does not propagate but is a standing sinusoidal solution in space whose amplitude varies sinusoidally in time.

A surface current flows on the perfect conductor at  $z = 0$  due to the discontinuity in tangential component of  $\mathbf{H}$ ,

$$K_x = H_y(z = 0) = \frac{2E_i}{\eta_0} \cos \omega t \quad (6)$$

giving rise to a force per unit area on the conductor,

$$\mathbf{F} = \frac{1}{2} \mathbf{K} \times \mu_0 \mathbf{H} = \frac{1}{2} \mu_0 H_y^2(z = 0) \mathbf{i}_z = 2\epsilon_0 E_i^2 \cos^2 \omega t \mathbf{i}_z \quad (7)$$

known as the radiation pressure. The factor of  $\frac{1}{2}$  arises in (7) because the force on a surface current is proportional to the average value of magnetic field on each side of the interface, here being zero for  $z = 0_+$ .

## 7-6 NORMAL INCIDENCE ONTO A DIELECTRIC

### 7-6-1 Lossless Dielectric

We replace the perfect conductor with a lossless dielectric of permittivity  $\epsilon_2$  and permeability  $\mu_2$ , as in Figure 7-14, with a uniform plane wave normally incident from a medium with permittivity  $\epsilon_1$  and permeability  $\mu_1$ . In addition to the incident and reflected fields for  $z < 0$ , there are transmitted fields which propagate in the  $+z$  direction within the medium for  $z > 0$ :

$$\left. \begin{aligned} \mathbf{E}_i(z, t) &= \text{Re} [\hat{E}_i e^{j(\omega t - k_1 z)} \mathbf{i}_x], & k_1 &= \omega \sqrt{\epsilon_1 \mu_1} \\ \mathbf{H}_i(z, t) &= \text{Re} \left[ \frac{\hat{E}_i}{\eta_1} e^{j(\omega t - k_1 z)} \mathbf{i}_y \right], & \eta_1 &= \sqrt{\frac{\mu_1}{\epsilon_1}} \\ \mathbf{E}_r(z, t) &= \text{Re} [\hat{E}_r e^{j(\omega t + k_1 z)} \mathbf{i}_x] \\ \mathbf{H}_r(z, t) &= \text{Re} \left[ -\frac{\hat{E}_r}{\eta_1} e^{j(\omega t + k_1 z)} \mathbf{i}_y \right] \end{aligned} \right\} z < 0 \quad (1)$$

$$\left. \begin{aligned} \mathbf{E}_t(z, t) &= \text{Re} [\hat{E}_t e^{j(\omega t - k_2 z)} \mathbf{i}_x], & k_2 &= \omega \sqrt{\epsilon_2 \mu_2} \\ \mathbf{H}_t(z, t) &= \text{Re} \left[ \frac{\hat{E}_t}{\eta_2} e^{j(\omega t - k_2 z)} \mathbf{i}_y \right], & \eta_2 &= \sqrt{\frac{\mu_2}{\epsilon_2}} \end{aligned} \right\} z > 0$$

It is necessary in (1) to use the appropriate wavenumber and impedance within each region. There is no wave traveling in the  $-z$  direction in the second region as we assume no boundaries or sources for  $z > 0$ .

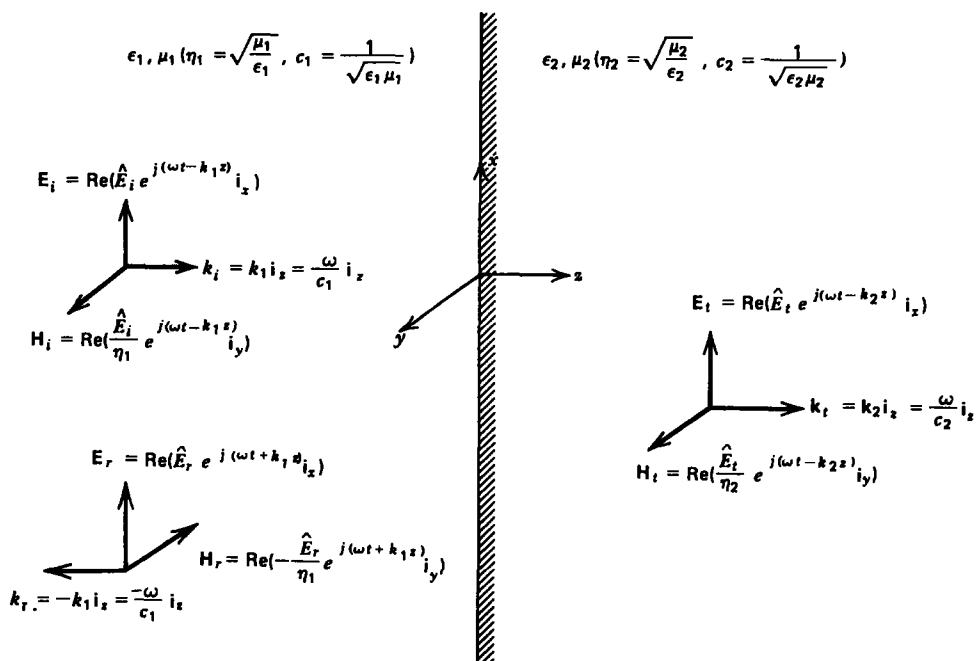


Figure 7-14 A uniform plane wave normally incident upon a dielectric interface separating two different materials has part of its power reflected and part transmitted.

The unknown quantities  $\hat{E}_r$  and  $\hat{E}_t$  can be found from the boundary conditions of continuity of tangential  $\mathbf{E}$  and  $\mathbf{H}$  at  $z = 0$ ,

$$\begin{aligned} \hat{E}_i + \hat{E}_r &= \hat{E}_t \\ \frac{\hat{E}_i - \hat{E}_r}{\eta_1} &= \frac{\hat{E}_t}{\eta_2} \end{aligned} \tag{2}$$

from which we find the reflection  $R$  and transmission  $T$  field coefficients as

$$\begin{aligned} R = \frac{\hat{E}_r}{\hat{E}_i} &= \frac{\eta_2 - \eta_1}{\eta_2 + \eta_1} \\ T = \frac{\hat{E}_t}{\hat{E}_i} &= \frac{2\eta_2}{\eta_2 + \eta_1} \end{aligned} \tag{3}$$

where from (2)

$$1 + R = T \tag{4}$$

If both mediums have the same wave impedance,  $\eta_1 = \eta_2$ , there is no reflected wave.

## 7-6-2 Time-Average Power Flow

The time-average power flow in the region  $z < 0$  is

$$\begin{aligned}
 \langle S_{zi} \rangle &= \frac{1}{2} \operatorname{Re} [\hat{E}_z(z) \hat{H}_y^*(z)] \\
 &= \frac{1}{2\eta_1} \operatorname{Re} [\hat{E}_i e^{-jk_1 z} + \hat{E}_r e^{+jk_1 z}] [\hat{E}_i^* e^{+jk_1 z} - \hat{E}_r^* e^{-jk_1 z}] \\
 &= \frac{1}{2\eta_1} [|\hat{E}_i|^2 - |\hat{E}_r|^2] \\
 &\quad + \frac{1}{2\eta_1} \underbrace{\operatorname{Re} [\hat{E}_r \hat{E}_i^* e^{+2jk_1 z} - \hat{E}_r^* \hat{E}_i e^{-2jk_1 z}]}_0
 \end{aligned} \tag{5}$$

The last term on the right-hand side of (5) is zero as it is the difference between a number and its complex conjugate, which is pure imaginary and equals  $2j$  times its imaginary part. Being pure imaginary, its real part is zero. Thus the time-average power flow just equals the difference in the power flows in the incident and reflected waves as found more generally in Section 7-3-2. The coupling terms between oppositely traveling waves have no time-average yielding the simple superposition of time-average powers:

$$\begin{aligned}
 \langle S_{zi} \rangle &= \frac{1}{2\eta_1} [|\hat{E}_i|^2 - |\hat{E}_r|^2] \\
 &= \frac{|\hat{E}_i|^2}{2\eta_1} [1 - R^2]
 \end{aligned} \tag{6}$$

This net time-average power flows into the dielectric medium, as it also equals the transmitted power;

$$\langle S_{zi} \rangle = \frac{1}{2\eta_2} |\hat{E}_t|^2 = \frac{|\hat{E}_i|^2 T^2}{2\eta_2} = \frac{|\hat{E}_i|^2}{2\eta_1} [1 - R^2] \tag{7}$$

## 7-6-3 Lossy Dielectric

If medium 2 is lossy with Ohmic conductivity  $\sigma$ , the solutions of (3) are still correct if we replace the permittivity  $\epsilon_2$  by the complex permittivity  $\hat{\epsilon}_2$ ,

$$\hat{\epsilon}_2 = \epsilon_2 \left( 1 + \frac{\sigma}{j\omega\epsilon_2} \right) \tag{8}$$

so that the wave impedance in region 2 is complex:

$$\eta_2 = \sqrt{\mu_2 / \hat{\epsilon}_2} \tag{9}$$

We can easily explore the effect of losses in the low and large loss limits.

**(a) Low Losses**

If the Ohmic conductivity is small, we can neglect it in all terms except in the wavenumber  $k_2$ :

$$\lim_{\sigma/\omega\epsilon_2 \ll 1} k_2 \approx \omega \sqrt{\epsilon_2 \mu_2} - \frac{j}{2} \sigma \sqrt{\frac{\mu_2}{\epsilon_2}} \quad (10)$$

The imaginary part of  $k_2$  gives rise to a small rate of exponential decay in medium 2 as the wave propagates away from the  $z = 0$  boundary.

**(b) Large Losses**

For large conductivities so that the displacement current is negligible in medium 2, the wavenumber and impedance in region 2 are complex:

$$\lim_{\sigma/\omega\epsilon_2 \gg 1} \begin{cases} k_2 = \frac{1-j}{\delta}, & \delta = \sqrt{\frac{2}{\omega\mu_2\sigma}} \\ \eta_2 = \sqrt{\frac{j\omega\mu_2}{\sigma}} = \frac{1+j}{\sigma\delta} \end{cases} \quad (11)$$

The fields decay within a characteristic distance equal to the skin depth  $\delta$ . This is why communications to submerged submarines are difficult. For seawater,  $\mu_2 = \mu_0 = 4\pi \times 10^{-7}$  henry/m and  $\sigma \approx 4$  siemens/m so that for 1 MHz signals,  $\delta \approx 0.25$  m. However, at 100 Hz the skin depth increases to 25 meters. If a submarine is within this distance from the surface, it can receive the signals. However, it is difficult to transmit these low frequencies because of the large free space wavelength,  $\lambda \approx 3 \times 10^6$  m. Note that as the conductivity approaches infinity,

$$\lim_{\sigma \rightarrow \infty} \begin{cases} k_2 = \infty \\ \eta_2 = 0 \end{cases} \Rightarrow \begin{cases} R = -1 \\ T = 0 \end{cases} \quad (12)$$

so that the field solution approaches that of normal incidence upon a perfect conductor found in Section 7-5.

### EXAMPLE 7-1 DIELECTRIC COATING

A thin lossless dielectric with permittivity  $\epsilon$  and permeability  $\mu$  is coated onto the interface between two infinite half-spaces of lossless media with respective properties  $(\epsilon_1, \mu_1)$  and  $(\epsilon_2, \mu_2)$ , as shown in Figure 7-15. What coating parameters  $\epsilon$  and  $\mu$  and thickness  $d$  will allow all the time-average power

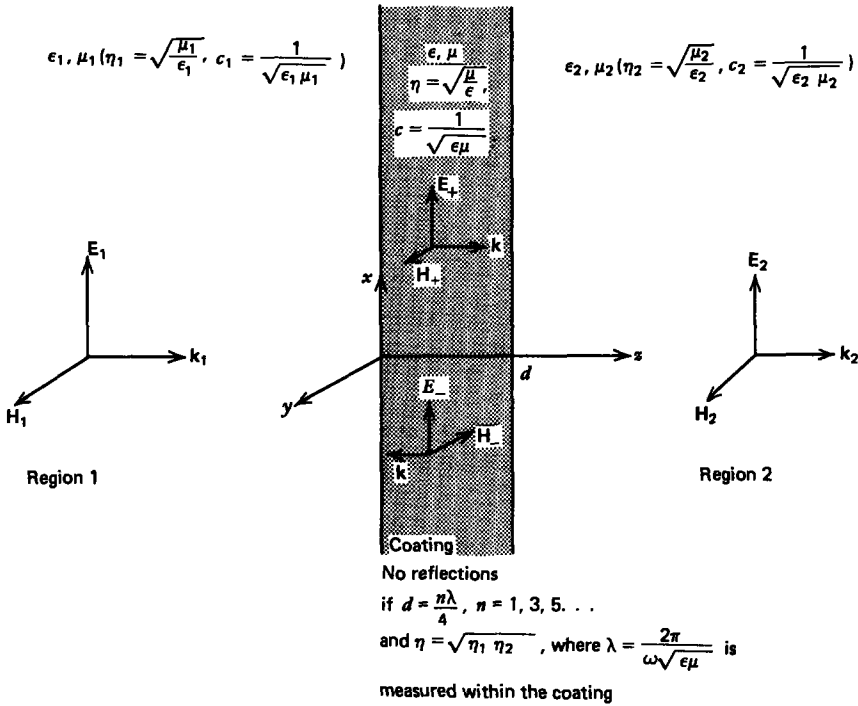


Figure 7-15 A suitable dielectric coating applied on the interface of discontinuity between differing media can eliminate reflections at a given frequency.

from region 1 to be transmitted through the coating to region 2? Such coatings are applied to optical components such as lenses to minimize unwanted reflections and to maximize the transmitted light intensity.

**SOLUTION**

For all the incident power to be transmitted into region 2, there can be no reflected field in region 1, although we do have oppositely traveling waves in the coating due to the reflection at the second interface. Region 2 only has positively z-directed power flow. The fields in each region are thus of the following form:

*Region 1*

$$\begin{aligned}
 \mathbf{E}_1 &= \text{Re} \left[ \hat{E}_1 e^{j(\omega t - k_1 z)} \mathbf{i}_x \right], & k_1 &= \omega/c_1 = \omega \sqrt{\epsilon_1 \mu_1} \\
 \mathbf{H}_1 &= \text{Re} \left[ \frac{\hat{E}_1}{\eta_1} e^{j(\omega t - k_1 z)} \mathbf{i}_y \right], & \eta_1 &= \sqrt{\frac{\mu_1}{\epsilon_1}}
 \end{aligned}$$

## Coating

$$\mathbf{E}_+ = \text{Re} [\hat{E}_+ e^{j(\omega t - kz)} \mathbf{i}_z], \quad k = \omega/c = \omega \sqrt{\epsilon \mu}$$

$$\mathbf{H}_+ = \text{Re} \left[ \frac{\hat{E}_+}{\eta} e^{j(\omega t - kz)} \mathbf{i}_y \right], \quad \eta = \sqrt{\frac{\mu}{\epsilon}}$$

$$\mathbf{E}_- = \text{Re} [\hat{E}_- e^{j(\omega t + kz)} \mathbf{i}_z]$$

$$\mathbf{H}_- = \text{Re} \left[ -\frac{\hat{E}_-}{\eta} e^{j(\omega t + kz)} \mathbf{i}_y \right]$$

## Region 2

$$\mathbf{E}_2 = \text{Re} [\hat{E}_2 e^{j(\omega t - k_2 z)} \mathbf{i}_z], \quad k_2 = \omega/c_2 = \omega \sqrt{\epsilon_2 \mu_2}$$

$$\mathbf{H}_2 = \text{Re} \left[ \frac{\hat{E}_2}{\eta_2} e^{j(\omega t - k_2 z)} \mathbf{i}_y \right], \quad \eta_2 = \sqrt{\frac{\mu_2}{\epsilon_2}}$$

Continuity of tangential  $\mathbf{E}$  and  $\mathbf{H}$  at  $z = 0$  and  $z = d$  requires

$$\begin{aligned} \hat{E}_1 &= \hat{E}_+ + \hat{E}_-, & \frac{\hat{E}_1}{\eta_1} &= \frac{\hat{E}_+ - \hat{E}_-}{\eta} \\ \hat{E}_+ e^{-jkd} + \hat{E}_- e^{+jkd} &= \hat{E}_2 e^{-jk_2 d} \\ \frac{\hat{E}_+ e^{-jkd} - \hat{E}_- e^{+jkd}}{\eta} &= \frac{\hat{E}_2 e^{-jk_2 d}}{\eta_2} \end{aligned}$$

Each of these amplitudes in terms of  $\hat{E}_1$  is then

$$\begin{aligned} \hat{E}_+ &= \frac{1}{2} \left( 1 + \frac{\eta}{\eta_1} \right) \hat{E}_1 \\ \hat{E}_- &= \frac{1}{2} \left( 1 - \frac{\eta}{\eta_1} \right) \hat{E}_1 \\ \hat{E}_2 &= e^{jk_2 d} [\hat{E}_+ e^{-jkd} + \hat{E}_- e^{+jkd}] \\ &= \frac{\eta_2}{\eta} e^{jk_2 d} [\hat{E}_+ e^{-jkd} - \hat{E}_- e^{+jkd}] \end{aligned}$$

Solving this last relation self-consistently requires that

$$\hat{E}_+ e^{-jkd} \left( 1 - \frac{\eta_2}{\eta} \right) + \hat{E}_- e^{jkd} \left( 1 + \frac{\eta_2}{\eta} \right) = 0$$

Writing  $\hat{E}_+$  and  $\hat{E}_-$  in terms of  $\hat{E}_1$  yields

$$\left( 1 + \frac{\eta}{\eta_1} \right) \left( 1 - \frac{\eta_2}{\eta} \right) + e^{2jkd} \left( 1 + \frac{\eta_2}{\eta} \right) \left( 1 - \frac{\eta}{\eta_1} \right) = 0$$

Since this relation is complex, the real and imaginary parts must separately be satisfied. For the imaginary part to be zero requires that the coating thickness  $d$  be an integral number of

quarter wavelengths as measured within the coating,

$$2kd = n\pi \Rightarrow d = n\lambda/4, \quad n = 1, 2, 3, \dots$$

The real part then requires

$$\left(1 + \frac{\eta}{\eta_1}\right)\left(1 - \frac{\eta_2}{\eta}\right) \pm \left(1 + \frac{\eta_2}{\eta}\right)\left(1 - \frac{\eta}{\eta_1}\right) = 0 \begin{cases} n \text{ even} \\ n \text{ odd} \end{cases}$$

For the upper sign where  $d$  is a multiple of half-wavelengths the only solution is

$$\eta_2 = \eta_1 \quad (d = n\lambda/4, \quad n = 2, 4, 6, \dots)$$

which requires that media 1 and 2 be the same so that the coating serves no purpose. If regions 1 and 2 have differing wave impedances, we must use the lower sign where  $d$  is an odd integer number of quarter wavelengths so that

$$\eta^2 = \eta_1\eta_2 \Rightarrow \eta = \sqrt{\eta_1\eta_2} \quad (d = n\lambda/4, \quad n = 1, 3, 5, \dots)$$

Thus, if the coating is a quarter wavelength thick as measured within the coating, or any odd integer multiple of this thickness with its wave impedance equal to the geometrical average of the impedances in each adjacent region, all the time-average power flow in region 1 passes through the coating into region 2:

$$\begin{aligned} \langle S_z \rangle &= \frac{1}{2} \frac{|\hat{E}_1|^2}{\eta_1} = \frac{1}{2} \frac{|\hat{E}_2|^2}{\eta_2} \\ &= \frac{1}{2} \operatorname{Re} \left[ (\hat{E}_+ e^{-jkz} + \hat{E}_- e^{+jkz}) \frac{(\hat{E}_+^* e^{+jkz} - \hat{E}_-^* e^{-jkz})}{\eta} \right] \\ &= \frac{1}{2\eta} (|\hat{E}_+|^2 - |\hat{E}_-|^2) \end{aligned}$$

Note that for a given coating thickness  $d$ , there is no reflection only at select frequencies corresponding to wavelengths  $d = n\lambda/4$ ,  $n = 1, 3, 5, \dots$ . For a narrow band of wavelengths about these select wavelengths, reflections are small. The magnetic permeability of coatings and of the glass used in optical components are usually that of free space while the permittivities differ. The permittivity of the coating  $\epsilon$  is then picked so that

$$\epsilon = \sqrt{\epsilon_2 \epsilon_0}$$

and with a thickness corresponding to the central range of the wavelengths of interest (often in the visible).

7-7 UNIFORM AND NONUNIFORM PLANE WAVES

Our analysis thus far has been limited to waves propagating in the  $z$  direction normally incident upon plane interfaces. Although our examples had the electric field polarized in the  $x$  direction, the solution procedure is the same for the  $y$ -directed electric field polarization as both polarizations are parallel to the interfaces of discontinuity.

7-7-1 Propagation at an Arbitrary Angle

We now consider a uniform plane wave with power flow at an angle  $\theta$  to the  $z$  axis, as shown in Figure 7-16. The electric field is assumed to be  $y$  directed, but the magnetic field that is perpendicular to both  $\mathbf{E}$  and  $\mathbf{S}$  now has components in the  $x$  and  $z$  directions.

The direction of the power flow, which we can call  $z'$ , is related to the Cartesian coordinates as

$$z' = x \sin \theta + z \cos \theta \tag{1}$$

so that the phase factor  $kz'$  can be written as

$$\begin{aligned} kz' &= k_x x + k_z z, & k_x &= k \sin \theta \\ & & k_z &= k \cos \theta \end{aligned} \tag{2}$$

where the wavenumber magnitude is

$$k = \omega \sqrt{\epsilon \mu} \tag{3}$$

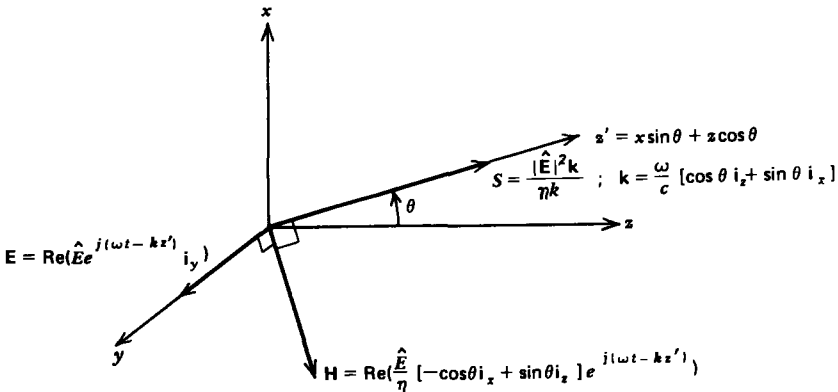


Figure 7-16 The spatial dependence of a uniform plane wave at an arbitrary angle  $\theta$  can be expressed in terms of a vector wavenumber  $\mathbf{k}$  as  $e^{-j\mathbf{k}\cdot\mathbf{r}}$ , where  $\mathbf{k}$  is in the direction of power flow and has magnitude  $\omega/c$ .

This allows us to write the fields as

$$\begin{aligned}\mathbf{E} &= \text{Re} [\hat{\mathbf{E}} e^{j(\omega t - k_x x - k_z z)} \mathbf{i}_y] \\ \mathbf{H} &= \text{Re} \left[ \frac{\hat{\mathbf{E}}}{\eta} (-\cos \theta \mathbf{i}_x + \sin \theta \mathbf{i}_z) e^{j(\omega t - k_x x - k_z z)} \right]\end{aligned}\quad (4)$$

We note that the spatial dependence of the fields can be written as  $e^{-j\mathbf{k}\cdot\mathbf{r}}$ , where the wavenumber is treated as a vector:

$$\mathbf{k} = k_x \mathbf{i}_x + k_y \mathbf{i}_y + k_z \mathbf{i}_z \quad (5)$$

with

$$\mathbf{r} = x \mathbf{i}_x + y \mathbf{i}_y + z \mathbf{i}_z \quad (6)$$

so that

$$\mathbf{k} \cdot \mathbf{r} = k_x x + k_y y + k_z z \quad (7)$$

The magnitude of  $\mathbf{k}$  is as given in (3) and its direction is the same as the power flow  $\mathbf{S}$ :

$$\begin{aligned}\mathbf{S} = \mathbf{E} \times \mathbf{H} &= \frac{|\hat{\mathbf{E}}|^2}{\eta} (\cos \theta \mathbf{i}_z + \sin \theta \mathbf{i}_x) \cos^2 (\omega t - \mathbf{k} \cdot \mathbf{r}) \\ &= \frac{|\hat{\mathbf{E}}|^2 \mathbf{k}}{\omega \mu} \cos^2 (\omega t - \mathbf{k} \cdot \mathbf{r})\end{aligned}\quad (8)$$

where without loss of generality we picked the phase of  $\hat{\mathbf{E}}$  to be zero so that it is real.

### 7-7-2 The Complex Propagation Constant

Let us generalize further by considering fields of the form

$$\begin{aligned}\mathbf{E} &= \text{Re} [\hat{\mathbf{E}} e^{j\omega t} e^{-\boldsymbol{\gamma} \cdot \mathbf{r}}] = \text{Re} [\hat{\mathbf{E}} e^{j(\omega t - \mathbf{k} \cdot \mathbf{r})} e^{-\boldsymbol{\alpha} \cdot \mathbf{r}}] \\ \mathbf{H} &= \text{Re} [\hat{\mathbf{H}} e^{j\omega t} e^{-\boldsymbol{\gamma} \cdot \mathbf{r}}] = \text{Re} [\hat{\mathbf{H}} e^{j(\omega t - \mathbf{k} \cdot \mathbf{r})} e^{-\boldsymbol{\alpha} \cdot \mathbf{r}}]\end{aligned}\quad (9)$$

where  $\boldsymbol{\gamma}$  is the complex propagation vector and  $\mathbf{r}$  is the position vector of (6):

$$\begin{aligned}\boldsymbol{\gamma} &= \boldsymbol{\alpha} + j\mathbf{k} = \gamma_x \mathbf{i}_x + \gamma_y \mathbf{i}_y + \gamma_z \mathbf{i}_z \\ \boldsymbol{\gamma} \cdot \mathbf{r} &= \gamma_x x + \gamma_y y + \gamma_z z\end{aligned}\quad (10)$$

We have previously considered uniform plane waves in lossless media where the wavenumber  $\mathbf{k}$  is pure real and  $z$  directed with  $\boldsymbol{\alpha} = 0$  so that  $\boldsymbol{\gamma}$  is pure imaginary. The parameter  $\boldsymbol{\alpha}$  represents the decay rate of the fields even though the medium is lossless. If  $\boldsymbol{\alpha}$  is nonzero, the solutions are called nonuniform plane waves. We saw this decay in our quasi-static solutions of Laplace's equation where solutions had oscillations in one direction but decay in the perpendicular direction. We would expect this evanescence to remain at low frequencies.

The value of the assumed form of solutions in (9) is that the  $\text{del}$  ( $\nabla$ ) operator in Maxwell's equations can be replaced by the vector operator  $-\boldsymbol{\gamma}$ :

$$\begin{aligned}\nabla &= \frac{\partial}{\partial x} \mathbf{i}_x + \frac{\partial}{\partial y} \mathbf{i}_y + \frac{\partial}{\partial z} \mathbf{i}_z \\ &= -\gamma_x \mathbf{i}_x - \gamma_y \mathbf{i}_y - \gamma_z \mathbf{i}_z \\ &= -\boldsymbol{\gamma}\end{aligned}\quad (11)$$

This is true because any spatial derivatives only operate on the exponential term in (9). Then the source free Maxwell's equations can be written in terms of the complex amplitudes as

$$\begin{aligned}-\boldsymbol{\gamma} \times \hat{\mathbf{E}} &= -j\omega\mu \hat{\mathbf{H}} \\ -\boldsymbol{\gamma} \times \hat{\mathbf{H}} &= j\omega\varepsilon \hat{\mathbf{E}} \\ -\boldsymbol{\gamma} \cdot \varepsilon \hat{\mathbf{E}} &= 0 \\ -\boldsymbol{\gamma} \cdot \mu \hat{\mathbf{H}} &= 0\end{aligned}\quad (12)$$

The last two relations tell us that  $\boldsymbol{\gamma}$  is perpendicular to both  $\mathbf{E}$  and  $\mathbf{H}$ . If we take  $\boldsymbol{\gamma} \times$  the top equation and use the second equation, we have

$$\begin{aligned}-\boldsymbol{\gamma} \times (\boldsymbol{\gamma} \times \hat{\mathbf{E}}) &= -j\omega\mu (\boldsymbol{\gamma} \times \hat{\mathbf{H}}) = -j\omega\mu (-j\omega\varepsilon \hat{\mathbf{E}}) \\ &= -\omega^2 \mu\varepsilon \hat{\mathbf{E}}\end{aligned}\quad (13)$$

The double cross product can be expanded as

$$\begin{aligned}-\boldsymbol{\gamma} \times (\boldsymbol{\gamma} \times \hat{\mathbf{E}}) &= -\boldsymbol{\gamma}(\boldsymbol{\gamma} \cdot \hat{\mathbf{E}}) + (\boldsymbol{\gamma} \cdot \boldsymbol{\gamma})\hat{\mathbf{E}} \\ &= (\boldsymbol{\gamma} \cdot \boldsymbol{\gamma})\hat{\mathbf{E}} = -\omega^2 \mu\varepsilon \hat{\mathbf{E}}\end{aligned}\quad (14)$$

The  $\boldsymbol{\gamma} \cdot \hat{\mathbf{E}}$  term is zero from the third relation in (12). The dispersion relation is then

$$\boldsymbol{\gamma} \cdot \boldsymbol{\gamma} = (\alpha^2 - k^2 + 2j\boldsymbol{\alpha} \cdot \mathbf{k}) = -\omega^2 \mu\varepsilon \quad (15)$$

For solution, the real and imaginary parts of (15) must be separately equal:

$$\begin{aligned}\alpha^2 - k^2 &= -\omega^2 \mu\varepsilon \\ \boldsymbol{\alpha} \cdot \mathbf{k} &= 0\end{aligned}\quad (16)$$

When  $\boldsymbol{\alpha} = 0$ , (16) reduces to the familiar frequency-wavenumber relation of Section 7-3.4.

The last relation now tells us that evanescence (decay) in space as represented by  $\boldsymbol{\alpha}$  is allowed by Maxwell's equations, but must be perpendicular to propagation represented by  $\mathbf{k}$ .

We can compute the time-average power flow for fields of the form of (9) using (12) in terms of either  $\hat{\mathbf{E}}$  or  $\hat{\mathbf{H}}$  as follows:

$$\begin{aligned}
 \langle \mathbf{S} \rangle &= \frac{1}{2} \operatorname{Re} (\hat{\mathbf{E}} \times \hat{\mathbf{H}}^*), \\
 &= -\frac{1}{2} \operatorname{Re} \left( \hat{\mathbf{E}} \times \frac{(\boldsymbol{\gamma}^* \times \hat{\mathbf{E}}^*)}{j\omega\mu} \right), \\
 &= -\frac{1}{2} \operatorname{Re} \left( \frac{\boldsymbol{\gamma}^* |\hat{\mathbf{E}}|^2 - \hat{\mathbf{E}}^* (\boldsymbol{\gamma}^* \cdot \hat{\mathbf{E}})}{j\omega\mu} \right), \\
 &= \frac{1}{2} \frac{\mathbf{k}}{\omega\mu} |\hat{\mathbf{E}}|^2 + \frac{1}{2} \operatorname{Re} \left( \frac{\hat{\mathbf{E}}^* (\boldsymbol{\gamma}^* \cdot \hat{\mathbf{E}})}{j\omega\mu} \right), \\
 \langle \mathbf{S} \rangle &= \frac{1}{2} \operatorname{Re} (\hat{\mathbf{E}} \times \hat{\mathbf{H}}^*) \\
 &= -\frac{1}{2} \operatorname{Re} \left( \frac{(\boldsymbol{\gamma} \times \hat{\mathbf{H}})}{j\omega\epsilon} \times \hat{\mathbf{H}}^* \right) \\
 &= \frac{1}{2} \operatorname{Re} \left( \frac{\boldsymbol{\gamma} |\hat{\mathbf{H}}|^2 - \hat{\mathbf{H}} (\boldsymbol{\gamma} \cdot \hat{\mathbf{H}}^*)}{j\omega\epsilon} \right) \\
 &= \frac{1}{2} \frac{\mathbf{k}}{\omega\epsilon} |\hat{\mathbf{H}}|^2 - \frac{1}{2} \operatorname{Re} \left( \frac{\hat{\mathbf{H}} (\boldsymbol{\gamma} \cdot \hat{\mathbf{H}}^*)}{j\omega\epsilon} \right)
 \end{aligned} \tag{17}$$

Although both final expressions in (17) are equivalent, it is convenient to write the power flow in terms of either  $\hat{\mathbf{E}}$  or  $\hat{\mathbf{H}}$ . When  $\hat{\mathbf{E}}$  is perpendicular to both the real vectors  $\boldsymbol{\alpha}$  and  $\boldsymbol{\beta}$ , defined in (10) and (16), the dot product  $\boldsymbol{\gamma}^* \cdot \hat{\mathbf{E}}$  is zero. Such a mode is called transverse electric (TE), and we see in (17) that the time-average power flow is still in the direction of the wavenumber  $\mathbf{k}$ . Similarly, when  $\hat{\mathbf{H}}$  is perpendicular to  $\boldsymbol{\alpha}$  and  $\boldsymbol{\beta}$ , the dot product  $\boldsymbol{\gamma} \cdot \hat{\mathbf{H}}^*$  is zero and we have a transverse magnetic (TM) mode. Again, the time-average power flow in (17) is in the direction of  $\mathbf{k}$ . The magnitude of  $\mathbf{k}$  is related to  $\omega$  in (16).

Note that our discussion has been limited to lossless systems. We can include Ohmic losses if we replace  $\epsilon$  by the complex permittivity  $\hat{\epsilon}$  of Section 7-4-3 in (15) and (17). Then, there is always decay ( $\alpha \neq 0$ ) because of Ohmic dissipation (see Problem 22).

### 7-7-3 Nonuniform Plane Waves

We can examine nonuniform plane wave solutions with nonzero  $\alpha$  by considering a current sheet in the  $z = 0$  plane, which is a traveling wave in the  $x$  direction:

$$K_x(z = 0) = K_0 \cos(\omega t - k_x x) = \operatorname{Re} (K_0 e^{j(\omega t - k_x x)}) \tag{18}$$

The  $x$ -directed surface current gives rise to a  $y$ -directed magnetic field. Because the system does not depend on the  $y$  coordinate, solutions are thus of the following form:

$$H_y = \begin{cases} \operatorname{Re} (\hat{H}_1 e^{j\omega t} e^{-\gamma_1 \cdot r}), & z > 0 \\ \operatorname{Re} (\hat{H}_2 e^{j\omega t} e^{-\gamma_2 \cdot r}), & z < 0 \end{cases} \quad (19)$$

$$\mathbf{E} = \begin{cases} \operatorname{Re} \left[ -\frac{\boldsymbol{\gamma}_1 \times \hat{H}_1}{j\omega\epsilon} \mathbf{i}_y e^{j\omega t} e^{-\gamma_1 \cdot r} \right], & z > 0 \\ \operatorname{Re} \left[ -\frac{\boldsymbol{\gamma}_2 \times \hat{H}_2}{j\omega\epsilon} \mathbf{i}_y e^{j\omega t} e^{-\gamma_2 \cdot r} \right], & z < 0 \end{cases}$$

where  $\boldsymbol{\gamma}_1$  and  $\boldsymbol{\gamma}_2$  are the complex propagation vectors on each side of the current sheet:

$$\begin{aligned} \boldsymbol{\gamma}_1 &= \gamma_{1x} \mathbf{i}_x + \gamma_{1z} \mathbf{i}_z \\ \boldsymbol{\gamma}_2 &= \gamma_{2x} \mathbf{i}_x + \gamma_{2z} \mathbf{i}_z \end{aligned} \quad (20)$$

The boundary condition of the discontinuity of tangential  $\mathbf{H}$  at  $z = 0$  equaling the surface current yields

$$-\hat{H}_1 e^{-\gamma_{1x} x} + \hat{H}_2 e^{-\gamma_{2x} x} = K_0 e^{-jk_x x} \quad (21)$$

which tells us that the  $x$  components of the complex propagation vectors equal the trigonometric spatial dependence of the surface current:

$$\gamma_{1x} = \gamma_{2x} = jk_x \quad (22)$$

The  $z$  components of  $\boldsymbol{\gamma}_1$  and  $\boldsymbol{\gamma}_2$  are then determined from (15) as

$$\gamma_x^2 + \gamma_z^2 = -\omega^2 \epsilon \mu \Rightarrow \gamma_z = \pm (k_x^2 - \omega^2 \epsilon \mu)^{1/2} \quad (23)$$

If  $k_x^2 < \omega^2 \epsilon \mu$ ,  $\gamma_z$  is pure imaginary representing propagation and we have uniform plane waves. If  $k_x^2 > \omega^2 \epsilon \mu$ , then  $\gamma_z$  is pure real representing evanescence in the  $z$  direction so that we generate nonuniform plane waves. When  $\omega = 0$ , (23) corresponds to Laplacian solutions that oscillate in the  $x$  direction but decay in the  $z$  direction.

The  $z$  component of  $\boldsymbol{\gamma}$  is of opposite sign in each region,

$$\gamma_{1z} = -\gamma_{2z} = +(k_x^2 - \omega^2 \epsilon \mu)^{1/2} \quad (24)$$

as the waves propagate or decay away from the sheet. Continuity of the tangential component of  $\mathbf{E}$  requires

$$\gamma_{1z} \hat{H}_1 = \gamma_{2z} \hat{H}_2 \Rightarrow \hat{H}_2 = -\hat{H}_1 = K_0/2 \quad (25)$$

If  $k_x = 0$ , we re-obtain the solution of Section 7-4-1. Increasing  $k_x$  generates propagating waves with power flow in the  $k_x \mathbf{i}_x \pm k_z \mathbf{i}_z$  directions. At  $k_x^2 = \omega^2 \epsilon \mu$ ,  $k_z = 0$  so that the power flow is purely  $x$  directed with no spatial dependence on  $z$ . Further increasing  $k_x$  converts  $k_z$  to  $\alpha_z$  as  $\gamma_z$  becomes real and the fields decay with  $z$ .

**7-8 OBLIQUE INCIDENCE ONTO A PERFECT CONDUCTOR**

**7-8-1 E Field Parallel to the Interface**

In Figure 7-17a we show a uniform plane wave incident upon a perfect conductor with power flow at an angle  $\theta_i$  to the normal. The electric field is parallel to the surface with the magnetic field having both  $x$  and  $z$  components:

$$\mathbf{E}_i = \text{Re} [\hat{\mathbf{E}}_i e^{j(\omega t - k_{xi}x - k_{zi}z)} \mathbf{i}_y] \tag{1}$$

$$\mathbf{H}_i = \text{Re} \left[ \frac{\hat{\mathbf{E}}_i}{\eta} (-\cos \theta_i \mathbf{i}_x + \sin \theta_i \mathbf{i}_z) e^{j(\omega t - k_{xi}x - k_{zi}z)} \right]$$

where

$$\left. \begin{aligned} k_{xi} &= k \sin \theta_i \\ k_{zi} &= k \cos \theta_i \end{aligned} \right\} \quad k = \omega \sqrt{\epsilon \mu}, \quad \eta = \sqrt{\frac{\mu}{\epsilon}} \tag{2}$$

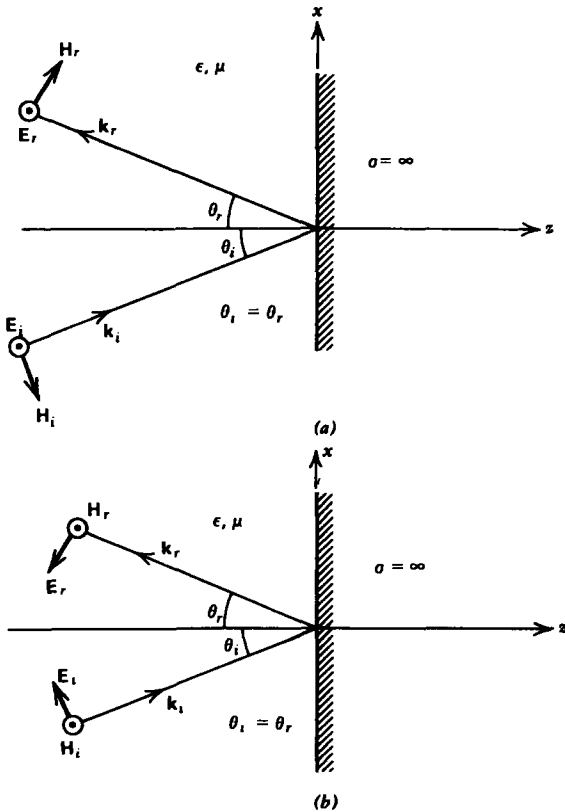


Figure 7-17 A uniform plane wave obliquely incident upon a perfect conductor has its angle of incidence equal to the angle of reflection. (a) Electric field polarized parallel to the interface. (b) Magnetic field parallel to the interface.

There are no transmitted fields within the perfect conductor, but there is a reflected field with power flow at angle  $\theta_r$  from the interface normal. The reflected electric field is also in the  $y$  direction so the magnetic field, which must be perpendicular to both  $\mathbf{E}$  and  $\mathbf{S} = \mathbf{E} \times \mathbf{H}$ , is in the direction shown in Figure 7-17a:

$$\begin{aligned} \mathbf{E}_r &= \text{Re} [\hat{E}_r e^{j(\omega t - k_{rx}x + k_{rz}z)} \mathbf{i}_y] \\ \mathbf{H}_r &= \text{Re} \left[ \frac{\hat{E}_r}{\eta} (\cos \theta_r \mathbf{i}_x + \sin \theta_r \mathbf{i}_z) e^{j(\omega t - k_{rx}x + k_{rz}z)} \right] \end{aligned} \quad (3)$$

where the reflected wavenumbers are

$$\begin{aligned} k_{rx} &= k \sin \theta_r \\ k_{rz} &= k \cos \theta_r \end{aligned} \quad (4)$$

At this point we do not know the angle of reflection  $\theta_r$  or the reflected amplitude  $\hat{E}_r$ . They will be determined from the boundary conditions at  $z = 0$  of continuity of tangential  $\mathbf{E}$  and normal  $\mathbf{B}$ . Because there are no fields within the perfect conductor these boundary conditions at  $z = 0$  are

$$\begin{aligned} \hat{E}_i e^{-jk_{xi}x} + \hat{E}_r e^{-jk_{rx}x} &= 0 \\ \frac{\mu}{\eta} (\hat{E}_i \sin \theta_i e^{-jk_{xi}x} + \hat{E}_r \sin \theta_r e^{-jk_{rx}x}) &= 0 \end{aligned} \quad (5)$$

These conditions must be true for every value of  $x$  along  $z = 0$  so that the phase factors given in (2) and (4) must be equal,

$$k_{xi} = k_{rx} \Rightarrow \theta_i = \theta_r \equiv \theta \quad (6)$$

giving the well-known rule that the angle of incidence equals the angle of reflection. The reflected field amplitude is then

$$\hat{E}_r = -\hat{E}_i \quad (7)$$

with the boundary conditions in (5) being redundant as they both yield (7). The total fields are then:

$$\begin{aligned} E_y &= \text{Re} [\hat{E}_i (e^{-jk_{xi}z} - e^{+jk_{iz}z}) e^{j(\omega t - k_x x)}] \\ &= 2E_i \sin k_z z \sin (\omega t - k_x x) \\ \mathbf{H} &= \text{Re} \left[ \frac{\hat{E}_i}{\eta} [\cos \theta (-e^{-jk_{xi}z} - e^{+jk_{iz}z}) \mathbf{i}_x + \sin \theta (e^{-jk_{xi}z} \right. \\ &\quad \left. - e^{+jk_{iz}z}) \mathbf{i}_z] e^{j(\omega t - k_x x)} \right] \\ &= \frac{2E_i}{\eta} [-\cos \theta \cos k_z z \cos (\omega t - k_x x) \mathbf{i}_x \\ &\quad + \sin \theta \sin k_z z \sin (\omega t - k_x x) \mathbf{i}_z] \end{aligned} \quad (8)$$

where without loss of generality we take  $\hat{E}_i$  to be real.

We drop the  $i$  and  $r$  subscripts on the wavenumbers and angles because they are equal. The fields travel in the  $x$  direction parallel to the interface, but are stationary in the  $z$  direction. Note that another perfectly conducting plane can be placed at distances  $d$  to the left of the interface at

$$k_z d = n\pi \quad (9)$$

where the electric field is already zero without disturbing the solutions of (8). The boundary conditions at the second conductor are automatically satisfied. Such a structure is called a waveguide and is discussed in Section 8-6.

Because the tangential component of  $\mathbf{H}$  is discontinuous at  $z=0$ , a traveling wave surface current flows along the interface,

$$K_y = -H_x(z=0) = \frac{2E_i}{\eta} \cos \theta \cos(\omega t - k_x x) \quad (10)$$

From (8) we compute the time-average power flow as

$$\begin{aligned} \langle S \rangle &= \frac{1}{2} \text{Re} [\hat{\mathbf{E}}(\mathbf{x}, z) \times \hat{\mathbf{H}}^*(\mathbf{x}, z)] \\ &= \frac{2E_i^2}{\eta} \sin \theta \sin^2 k_z z \mathbf{i}_x \end{aligned} \quad (11)$$

We see that the only nonzero power flow is in the direction parallel to the interfacial boundary and it varies as a function of  $z$ .

### 7-8-2 H Field Parallel to the Interface

If the  $\mathbf{H}$  field is parallel to the conducting boundary, as in Figure 7-17b, the incident and reflected fields are as follows:

$$\begin{aligned} \mathbf{E}_i &= \text{Re} [\hat{E}_i (\cos \theta_i \mathbf{i}_x - \sin \theta_i \mathbf{i}_z) e^{j(\omega t - k_{xi}x - k_{zi}z)}] \\ \mathbf{H}_i &= \text{Re} \left[ \frac{\hat{E}_i}{\eta} e^{j(\omega t - k_{xi}x - k_{zi}z)} \mathbf{i}_y \right] \\ \mathbf{E}_r &= \text{Re} [\hat{E}_r (-\cos \theta_r \mathbf{i}_x - \sin \theta_r \mathbf{i}_z) e^{j(\omega t - k_{xr}x + k_{zr}z)}] \\ \mathbf{H}_r &= \text{Re} \left[ \frac{\hat{E}_r}{\eta} e^{j(\omega t - k_{xr}x + k_{zr}z)} \mathbf{i}_y \right] \end{aligned} \quad (12)$$

The tangential component of  $\mathbf{E}$  is continuous and thus zero at  $z=0$ :

$$\hat{E}_i \cos \theta_i e^{-jk_{xi}x} - \hat{E}_r \cos \theta_r e^{-jk_{xr}x} = 0 \quad (13)$$

There is no normal component of  $\mathbf{B}$ . This boundary condition must be satisfied for all values of  $x$  so again the angle of

incidence must equal the angle of reflection ( $\theta_i = \theta_r$ ) so that

$$\hat{E}_i = \hat{E}_r \tag{14}$$

The total  $\mathbf{E}$  and  $\mathbf{H}$  fields can be obtained from (12) by adding the incident and reflected fields and taking the real part;

$$\begin{aligned} \mathbf{E} &= \text{Re} \{ \hat{E}_i [\cos \theta (e^{-jk_z z} - e^{+jk_z z}) \mathbf{i}_x \\ &\quad - \sin \theta (e^{-jk_z z} + e^{+jk_z z}) \mathbf{i}_z] e^{j(\omega t - k_x x)} \} \\ &= 2E_i \{ \cos \theta \sin k_z z \sin (\omega t - k_x x) \mathbf{i}_x \\ &\quad - \sin \theta \cos k_z z \cos (\omega t - k_x x) \mathbf{i}_z \} \\ \mathbf{H} &= \text{Re} \left[ \frac{\hat{E}_i}{\eta} (e^{-jk_z z} + e^{+jk_z z}) e^{j(\omega t - k_x x)} \mathbf{i}_y \right] \\ &= \frac{2E_i}{\eta} \cos k_z z \cos (\omega t - k_x x) \mathbf{i}_y \end{aligned} \tag{15}$$

The surface current on the conducting surface at  $z = 0$  is given by the tangential component of  $\mathbf{H}$

$$K_x(z = 0) = H_y(z = 0) = \frac{2E_i}{\eta} \cos (\omega t - k_x x) \tag{16}$$

while the surface charge at  $z = 0$  is proportional to the normal component of electric field,

$$\sigma_f(z = 0) = -\epsilon E_z(z = 0) = 2\epsilon E_i \sin \theta \cos (\omega t - k_x x) \tag{17}$$

Note that (16) and (17) satisfy conservation of current on the conducting surface,

$$\nabla_{\Sigma} \cdot \mathbf{K} + \frac{\partial \sigma_f}{\partial t} = 0 \Rightarrow \frac{\partial K_x}{\partial x} + \frac{\partial \sigma_f}{\partial t} = 0 \tag{18}$$

where

$$\nabla_{\Sigma} = \frac{\partial}{\partial x} \mathbf{i}_x + \frac{\partial}{\partial y} \mathbf{i}_y$$

is the surface divergence operator. The time-average power flow for this polarization is also  $x$  directed:

$$\begin{aligned} \langle S \rangle &= \frac{1}{2} \text{Re} (\hat{\mathbf{E}} \times \hat{\mathbf{H}}^*) \\ &= \frac{2E_i^2}{\eta} \sin \theta \cos^2 k_z z \mathbf{i}_x \end{aligned} \tag{19}$$

## 7-9 OBLIQUE INCIDENCE ONTO A DIELECTRIC

## 7-9-1 E Parallel to the Interface

A plane wave incident upon a dielectric interface, as in Figure 7-18a, now has transmitted fields as well as reflected fields. For the electric field polarized parallel to the interface, the fields in each region can be expressed as

$$\begin{aligned}
 \mathbf{E}_i &= \text{Re} [\hat{\mathbf{E}}_i e^{j(\omega t - k_{xi}x - k_{zi}z)} \mathbf{i}_y] \\
 \mathbf{H}_i &= \text{Re} \left[ \frac{\hat{\mathbf{E}}_i}{\eta_1} (-\cos \theta_i \mathbf{i}_x + \sin \theta_i \mathbf{i}_z) e^{j(\omega t - k_{xi}x - k_{zi}z)} \right] \\
 \mathbf{E}_r &= \text{Re} [\hat{\mathbf{E}}_r e^{j(\omega t - k_{xr}x + k_{zr}z)} \mathbf{i}_y] \\
 \mathbf{H}_r &= \text{Re} \left[ \frac{\hat{\mathbf{E}}_r}{\eta_1} (\cos \theta_r \mathbf{i}_x + \sin \theta_r \mathbf{i}_z) e^{j(\omega t - k_{xr}x + k_{zr}z)} \right] \\
 \mathbf{E}_t &= \text{Re} [\hat{\mathbf{E}}_t e^{j(\omega t - k_{xt}x - k_{zt}z)} \mathbf{i}_y] \\
 \mathbf{H}_t &= \text{Re} \left[ \frac{\hat{\mathbf{E}}_t}{\eta_2} (-\cos \theta_t \mathbf{i}_x + \sin \theta_t \mathbf{i}_z) e^{j(\omega t - k_{xt}x - k_{zt}z)} \right]
 \end{aligned} \tag{1}$$

where  $\theta_i$ ,  $\theta_r$ , and  $\theta_t$  are the angles from the normal of the incident, reflected, and transmitted power flows. The wavenumbers in each region are

$$\begin{aligned}
 k_{xi} &= k_1 \sin \theta_i, & k_{xr} &= k_1 \sin \theta_r, & k_{xt} &= k_2 \sin \theta_t \\
 k_{zi} &= k_1 \cos \theta_i, & k_{zr} &= k_1 \cos \theta_r, & k_{zt} &= k_2 \cos \theta_t
 \end{aligned} \tag{2}$$

where the wavenumber magnitudes, wave speeds, and wave impedances are

$$\begin{aligned}
 k_1 &= \frac{\omega}{c_1}, & k_2 &= \frac{\omega}{c_2}, & c_1 &= \frac{1}{\sqrt{\epsilon_1 \mu_1}} \\
 \eta_1 &= \sqrt{\frac{\mu_1}{\epsilon_1}}, & \eta_2 &= \sqrt{\frac{\mu_2}{\epsilon_2}}, & c_2 &= \frac{1}{\sqrt{\epsilon_2 \mu_2}}
 \end{aligned} \tag{3}$$

The unknown angles and amplitudes in (1) are found from the boundary conditions of continuity of tangential  $\mathbf{E}$  and  $\mathbf{H}$  at the  $z = 0$  interface.

$$\begin{aligned}
 \hat{\mathbf{E}}_i e^{-jk_{xi}x} + \hat{\mathbf{E}}_r e^{-jk_{xr}x} &= \hat{\mathbf{E}}_t e^{-jk_{xt}x} \\
 -\frac{\hat{\mathbf{E}}_i \cos \theta_i e^{-jk_{xi}x} + \hat{\mathbf{E}}_r \cos \theta_r e^{-jk_{xr}x}}{\eta_1} &= -\frac{\hat{\mathbf{E}}_t \cos \theta_t e^{-jk_{xt}x}}{\eta_2}
 \end{aligned} \tag{4}$$

These boundary conditions must be satisfied point by point for all  $x$ . This requires that the exponential factors also be

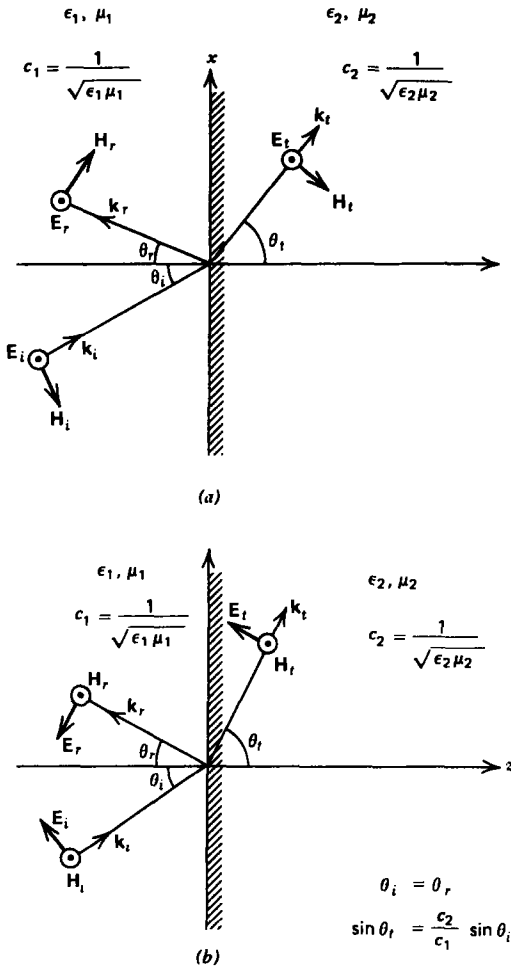


Figure 7-18 A uniform plane wave obliquely incident upon a dielectric interface also has its angle of incidence equal to the angle of reflection while the transmitted angle is given by Snell's law. (a) Electric field polarized parallel to the interface. (b) Magnetic field parallel to the interface.

equal so that the  $x$  components of all wavenumbers must be equal,

$$k_{xi} = k_{xr} = k_{xt} \Rightarrow k_1 \sin \theta_i = k_1 \sin \theta_r = k_2 \sin \theta_t \tag{5}$$

which relates the angles as

$$\theta_r = \theta_i \tag{6}$$

$$\sin \theta_t = (c_2/c_1) \sin \theta_i \tag{7}$$

As before, the angle of incidence equals the angle of reflection. The transmission angle obeys a more complicated relation called Snell's law relating the sines of the angles. The angle from the normal is largest in that region which has the faster speed of electromagnetic waves.

In optics, the ratio of the speed of light in vacuum,  $c_0 = 1/\sqrt{\epsilon_0\mu_0}$ , to the speed of light in the medium is defined as the index of refraction,

$$n_1 = c_0/c_1, \quad n_2 = c_0/c_2 \quad (8)$$

which is never less than unity. Then Snell's law is written as

$$\sin \theta_t = (n_1/n_2) \sin \theta_i \quad (9)$$

With the angles related as in (6), the reflected and transmitted field amplitudes can be expressed in the same way as for normal incidence (see Section 7-6-1) if we replace the wave impedances by  $\eta \rightarrow \eta/\cos \theta$  to yield

$$R = \frac{\hat{E}_r}{\hat{E}_i} = \frac{\frac{\eta_2}{\cos \theta_t} - \frac{\eta_1}{\cos \theta_i}}{\frac{\eta_2}{\cos \theta_t} + \frac{\eta_1}{\cos \theta_i}} = \frac{\eta_2 \cos \theta_i - \eta_1 \cos \theta_t}{\eta_2 \cos \theta_i + \eta_1 \cos \theta_t}$$

$$T = \frac{\hat{E}_t}{\hat{E}_i} = \frac{2\eta_2}{\cos \theta_i \left( \frac{\eta_2}{\cos \theta_t} + \frac{\eta_1}{\cos \theta_i} \right)} = \frac{2\eta_2 \cos \theta_i}{\eta_2 \cos \theta_i + \eta_1 \cos \theta_t} \quad (10)$$

In (4) we did not consider the boundary condition of continuity of normal  $\mathbf{B}$  at  $z = 0$ . This boundary condition is redundant as it is the same condition as the upper equation in (4):

$$\frac{\mu_1}{\eta_1} (\hat{E}_i + \hat{E}_r) \sin \theta_i = \frac{\mu_2}{\eta_2} \hat{E}_t \sin \theta_t \Rightarrow (\hat{E}_i + \hat{E}_r) = \hat{E}_t \quad (11)$$

where we use the relation between angles in (6). Since

$$\frac{\mu_1}{\eta_1} = \sqrt{\mu_1 \epsilon_1} = \frac{1}{c_1}, \quad \frac{\mu_2}{\eta_2} = \sqrt{\mu_2 \epsilon_2} = \frac{1}{c_2} \quad (12)$$

the trigonometric terms in (11) cancel due to Snell's law. There is no normal component of  $\mathbf{D}$  so it is automatically continuous across the interface.

### 7-9-2 Brewster's Angle of No Reflection

We see from (10) that at a certain angle of incidence, there is no reflected field as  $R = 0$ . This angle is called Brewster's angle:

$$R = 0 \Rightarrow \eta_2 \cos \theta_t = \eta_1 \cos \theta_i \quad (13)$$

By squaring (13), replacing the cosine terms with sine terms ( $\cos^2 \theta = 1 - \sin^2 \theta$ ), and using Snell's law of (6), the Brewster angle  $\theta_B$  is found as

$$\sin^2 \theta_B = \frac{1 - \varepsilon_2 \mu_1 / (\varepsilon_1 \mu_2)}{1 - (\mu_1 / \mu_2)^2} \quad (14)$$

There is not always a real solution to (14) as it depends on the material constants. The common dielectric case, where  $\mu_1 = \mu_2 \equiv \mu$  but  $\varepsilon_1 \neq \varepsilon_2$ , does not have a solution as the right-hand side of (14) becomes infinite. Real solutions to (14) require the right-hand side to be between zero and one. A Brewster's angle does exist for the uncommon situation where  $\varepsilon_1 = \varepsilon_2$  and  $\mu_1 \neq \mu_2$ :

$$\sin^2 \theta_B = \frac{1}{1 + \mu_1 / \mu_2} \Rightarrow \tan \theta_B = \sqrt{\frac{\mu_2}{\mu_1}} \quad (15)$$

At this Brewster's angle, the reflected and transmitted power flows are at right angles ( $\theta_B + \theta_t = \pi/2$ ) as can be seen by using (6), (13), and (14):

$$\begin{aligned} \cos(\theta_B + \theta_t) &= \cos \theta_B \cos \theta_t - \sin \theta_B \sin \theta_t \\ &= \cos^2 \theta_B \sqrt{\frac{\mu_2}{\mu_1}} - \sin^2 \theta_B \sqrt{\frac{\mu_1}{\mu_2}} \\ &= \sqrt{\frac{\mu_2}{\mu_1}} - \sin^2 \theta_B \left( \sqrt{\frac{\mu_1}{\mu_2}} + \sqrt{\frac{\mu_2}{\mu_1}} \right) = 0 \end{aligned} \quad (16)$$

### 7-9-3 Critical Angle of Transmission

Snell's law in (6) shows us that if  $c_2 > c_1$ , large angles of incident angle  $\theta_i$  could result in  $\sin \theta_t$  being greater than unity. There is no real angle  $\theta_t$  that satisfies this condition. The critical incident angle  $\theta_c$  is defined as that value of  $\theta_i$  that makes  $\theta_t = \pi/2$ ,

$$\sin \theta_c = c_1 / c_2 \quad (17)$$

which has a real solution only if  $c_1 < c_2$ . At the critical angle, the wavenumber  $k_{zt}$  is zero. Lesser incident angles have real values of  $k_{zt}$ . For larger incident angles there is no real angle  $\theta_t$  that satisfies (6). Snell's law must always be obeyed in order to satisfy the boundary conditions at  $z=0$  for all  $x$ . What happens is that  $\theta_t$  becomes a complex number that satisfies (6). Although  $\sin \theta_t$  is still real,  $\cos \theta_t$  is imaginary when  $\sin \theta_t$  exceeds unity:

$$\cos \theta_t = \sqrt{1 - \sin^2 \theta_t} \quad (18)$$

This then makes  $k_{z2}$  imaginary, which we can write as

$$k_{z2} = k_2 \cos \theta_t = -j\alpha \quad (19)$$

The negative sign of the square root is taken so that waves now decay with  $z$ :

$$\begin{aligned} \mathbf{E}_t &= \text{Re} [\hat{\mathbf{E}}_t e^{j(\omega t - k_{xz}x)} e^{-\alpha z} \mathbf{i}_y] \\ \mathbf{H}_t &= \text{Re} \left[ \frac{\hat{\mathbf{E}}_t}{\eta_2} (-\cos \theta_t \mathbf{i}_x + \sin \theta_t \mathbf{i}_z) e^{j(\omega t - k_{xz}x)} e^{-\alpha z} \right] \end{aligned} \quad (20)$$

The solutions are now nonuniform plane waves, as discussed in Section 7-7.

Complex angles of transmission are a valid mathematical concept. What has happened is that in (1) we wrote our assumed solutions for the transmitted fields in terms of pure propagating waves. Maxwell's equations for an incident angle greater than the critical angle require spatially decaying waves with  $z$  in region 2 so that the mathematics forced  $k_{z2}$  to be imaginary.

There is no power dissipation since the  $z$ -directed time-average power flow is zero,

$$\begin{aligned} \langle S_z \rangle &= -\frac{1}{2} \text{Re} [E_z H_x^*] \\ &= -\frac{1}{2} \text{Re} \left[ \frac{\hat{\mathbf{E}}_t \hat{\mathbf{E}}_t^*}{\eta_2} (-\cos \theta_t)^* e^{-2\alpha z} \right] = 0 \end{aligned} \quad (21)$$

because  $\cos \theta_t$  is pure imaginary so that the bracketed term in (21) is pure imaginary. The incident  $z$ -directed time-average power is totally reflected. Even though the time-averaged  $z$ -directed transmitted power is zero, there are nonzero but exponentially decaying fields in region 2.

### 7-9-4 H Field Parallel to the Boundary

For this polarization, illustrated in Figure 7-18*b*, the fields are

$$\begin{aligned} \mathbf{E}_i &= \text{Re} [\hat{\mathbf{E}}_i (\cos \theta_i \mathbf{i}_x - \sin \theta_i \mathbf{i}_z) e^{j(\omega t - k_{ix}x - k_{iz}z)}] \\ \mathbf{H}_i &= \text{Re} \left[ \frac{\hat{\mathbf{E}}_i}{\eta_1} e^{j(\omega t - k_{ix}x - k_{iz}z)} \mathbf{i}_y \right] \\ \mathbf{E}_r &= \text{Re} [\hat{\mathbf{E}}_r (-\cos \theta_r \mathbf{i}_x - \sin \theta_r \mathbf{i}_z) e^{j(\omega t - k_{rx}x + k_{rz}z)}] \\ \mathbf{H}_r &= \text{Re} \left[ \frac{\hat{\mathbf{E}}_r}{\eta_1} e^{j(\omega t - k_{rx}x + k_{rz}z)} \mathbf{i}_y \right] \\ \mathbf{E}_t &= \text{Re} [\hat{\mathbf{E}}_t (\cos \theta_t \mathbf{i}_x - \sin \theta_t \mathbf{i}_z) e^{j(\omega t - k_{tx}x - k_{tz}z)}] \\ \mathbf{H}_t &= \text{Re} \left[ \frac{\hat{\mathbf{E}}_t}{\eta_2} e^{j(\omega t - k_{tx}x - k_{tz}z)} \mathbf{i}_y \right] \end{aligned} \quad (22)$$

where the wavenumbers and impedances are the same as in (2) and (3).

Continuity of tangential  $\mathbf{E}$  and  $\mathbf{H}$  at  $z = 0$  requires

$$\hat{E}_i \cos \theta_i e^{-jk_{ix}} - \hat{E}_r \cos \theta_r e^{-jk_{rx}} = \hat{E}_t \cos \theta_t e^{-jk_{tx}} \quad (23)$$

$$\frac{\hat{E}_i e^{-jk_{ix}} + \hat{E}_r e^{-jk_{rx}}}{\eta_1} = \frac{\hat{E}_t e^{-jk_{tx}}}{\eta_2}$$

Again the phase factors must be equal so that (5) and (6) are again true. Snell's law and the angle of incidence equalling the angle of reflection are independent of polarization.

We solve (23) for the field reflection and transmission coefficients as

$$R = \frac{\hat{E}_r}{\hat{E}_i} = \frac{\eta_1 \cos \theta_i - \eta_2 \cos \theta_t}{\eta_2 \cos \theta_t + \eta_1 \cos \theta_i} \quad (24)$$

$$T = \frac{\hat{E}_t}{\hat{E}_i} = \frac{2\eta_2 \cos \theta_i}{\eta_2 \cos \theta_t + \eta_1 \cos \theta_i} \quad (25)$$

Now we note that the boundary condition of continuity of normal  $\mathbf{D}$  at  $z = 0$  is redundant to the lower relation in (23),

$$\epsilon_1 \hat{E}_i \sin \theta_i + \epsilon_1 \hat{E}_r \sin \theta_r = \epsilon_2 \hat{E}_t \sin \theta_t \quad (26)$$

using Snell's law to relate the angles.

For this polarization the condition for no reflected waves is

$$R = 0 \Rightarrow \eta_2 \cos \theta_t = \eta_1 \cos \theta_i \quad (27)$$

which from Snell's law gives the Brewster angle:

$$\sin^2 \theta_B = \frac{1 - \epsilon_1 \mu_2 / (\epsilon_2 \mu_1)}{1 - (\epsilon_1 / \epsilon_2)^2} \quad (28)$$

There is now a solution for the usual case where  $\mu_1 = \mu_2$  but  $\epsilon_1 \neq \epsilon_2$ :

$$\sin^2 \theta_B = \frac{1}{1 + \epsilon_1 / \epsilon_2} \Rightarrow \tan \theta_B = \sqrt{\frac{\epsilon_2}{\epsilon_1}} \quad (29)$$

At this Brewster's angle the reflected and transmitted power flows are at right angles  $(\theta_B + \theta_t) = \pi/2$  as can be seen by using (6), (27), and (29)

$$\begin{aligned} \cos(\theta_B + \theta_t) &= \cos \theta_B \cos \theta_t - \sin \theta_B \sin \theta_t \\ &= \cos^2 \theta_B \sqrt{\frac{\epsilon_2}{\epsilon_1}} - \sin^2 \theta_B \sqrt{\frac{\epsilon_1}{\epsilon_2}} \\ &= \sqrt{\frac{\epsilon_2}{\epsilon_1}} - \sin^2 \theta_B \left( \sqrt{\frac{\epsilon_1}{\epsilon_2}} + \sqrt{\frac{\epsilon_2}{\epsilon_1}} \right) = 0 \end{aligned} \quad (30)$$

Because Snell's law is independent of polarization, the critical angle of (17) is the same for both polarizations. Note that the Brewster's angle for either polarization, if it exists, is always less than the critical angle of (17), as can be particularly seen when  $\mu_1 = \mu_2$  for the magnetic field polarized parallel to the interface or when  $\epsilon_1 = \epsilon_2$  for the electric field polarized parallel to the interface, as then

$$\frac{1}{\sin^2 \theta_B} = \frac{1}{\sin^2 \theta_c} + 1 \quad (31)$$

## 7-10 APPLICATIONS TO OPTICS

Reflection and refraction of electromagnetic waves obliquely incident upon the interface between dissimilar linear lossless media are governed by the two rules illustrated in Figure 7-19:

- (i) The angle of incidence equals the angle of reflection.
- (ii) Waves incident from a medium of high light velocity (low index of refraction) to one of low velocity (high index of refraction) are bent towards the normal. If the wave is incident from a low velocity (high index) to high velocity (low index) medium, the light is bent away from the normal. The incident and refracted angles are related by Snell's law.

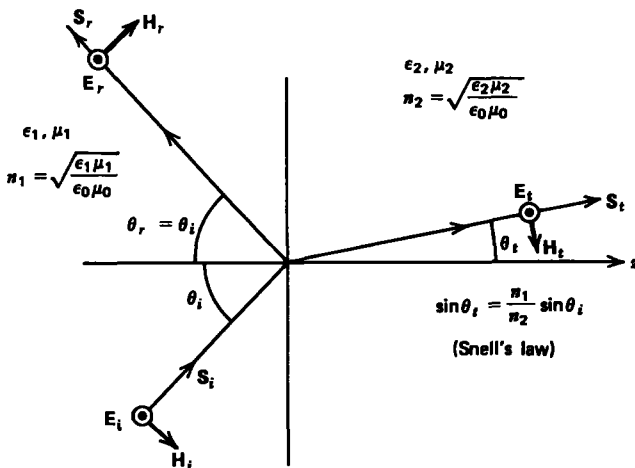


Figure 7-19 A summary of reflection and refraction phenomena across the interface separating two linear media. When  $\theta_i = \theta_B$  (Brewster's angle), there is no reflected ray. When  $\theta_i > \theta_c$  (critical angle), the transmitted fields decay with  $z$ .

Most optical materials, like glass, have a permeability of free space  $\mu_0$ . Therefore, a Brewster's angle of no reflection only exists if the  $\mathbf{H}$  field is parallel to the boundary.

At the critical angle, which can only exist if light travels from a high index of refraction material (low light velocity) to one of low index (high light velocity), there is a transmitted field that decays with distance as a nonuniform plane wave. However, there is no time-average power carried by this evanescent wave so that all the time-average power is reflected. This section briefly describes various applications of these special angles and the rules governing reflection and refraction.

### 7-10-1 Reflections from a Mirror

A person has their eyes at height  $h$  above their feet and a height  $\Delta h$  below the top of their head, as in Figure 7-20. A mirror in front extends a distance  $\Delta y$  above the eyes and a distance  $y$  below. How large must  $y$  and  $\Delta y$  be so that the person sees their entire image? The light reflected off the person into the mirror must be reflected again into the person's eyes. Since the angle of incidence equals the angle of reflection, Figure 7-20 shows that  $\Delta y = \Delta h/2$  and  $y = h/2$ .

### 7-10-2 Lateral Displacement of a Light Ray

A light ray is incident from free space upon a transparent medium with index of refraction  $n$  at angle  $\theta_i$ , as shown in Figure 7-21. The angle of the transmitted light is given by Snell's law:

$$\sin \theta_t = (1/n) \sin \theta_i \quad (1)$$

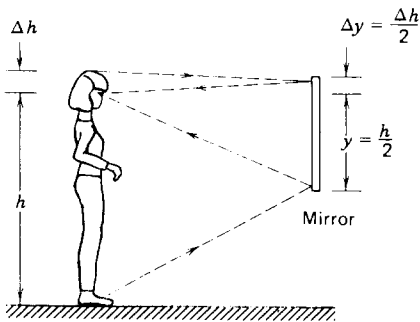


Figure 7-20 Because the angle of incidence equals the angle of reflection, a person can see their entire image if the mirror extends half the distance of extent above and below the eyes.

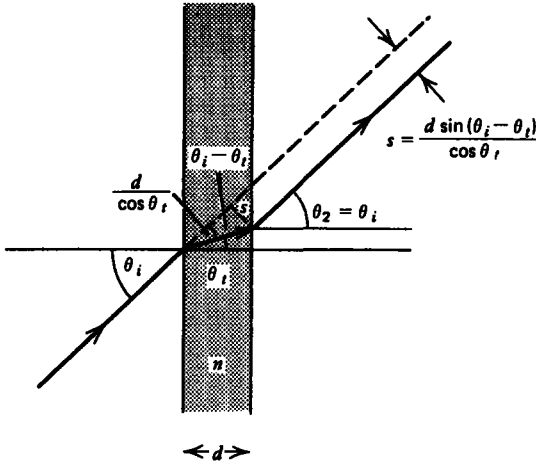


Figure 7-21 A light ray incident upon a glass plate exits the plate into the original medium parallel to its original trajectory but laterally displaced.

When this light hits the second interface, the angle  $\theta_i$  is now the incident angle so that the transmitted angle  $\theta_2$  is again given by Snell's law:

$$\sin \theta_2 = n \sin \theta_i = \sin \theta_i \tag{2}$$

so that the light exits at the original incident angle  $\theta_i$ . However, it is now shifted by the amount:

$$s = \frac{d \sin (\theta_i - \theta_r)}{\cos \theta_r} \tag{3}$$

If the plate is glass with refractive index  $n = 1.5$  and thickness  $d = 1 \text{ mm}$  with incident angle  $\theta_i = 30^\circ$ , the angle  $\theta_r$  in the glass is

$$\sin \theta_r = 0.33 \Rightarrow \theta_r = 19.5^\circ \tag{4}$$

so that the lateral displacement is  $s = 0.19 \text{ mm}$ .

### 7-10-3 Polarization By Reflection

Unpolarized light is incident upon the piece of glass in Section 7-10-2 with index of refraction  $n = 1.5$ . Unpolarized light has both  $\mathbf{E}$  and  $\mathbf{H}$  parallel to the interface. We assume that the permeability of the glass equals that of free space and that the light is incident at the Brewster's angle  $\theta_B$  for light polarized with  $\mathbf{H}$  parallel to the interface. The incident and

transmitted angles are then

$$\begin{aligned} \tan \theta_B &= \sqrt{\epsilon/\epsilon_0} = n \Rightarrow \theta_B = 56.3^\circ \\ \tan \theta_t &= \sqrt{\epsilon_0/\epsilon} = 1/n \Rightarrow \theta_t = 33.7^\circ \end{aligned} \tag{5}$$

The Brewster's angle is also called the polarizing angle because it can be used to separate the two orthogonal polarizations. The polarization, whose  $\mathbf{H}$  field is parallel to the interface, is entirely transmitted at the first interface with no reflection. The other polarization with electric field parallel to the interface is partially transmitted and reflected. At the second (glass-free space) interface the light is incident at angle  $\theta_t$ . From (5) we see that this angle is the Brewster's angle with  $\mathbf{H}$  parallel to the interface for light incident from the glass side onto the glass-free space interface. Then again, the  $\mathbf{H}$  parallel to the interface polarization is entirely transmitted while the  $\mathbf{E}$  parallel to the interface polarization is partially reflected and partially transmitted. Thus, the reflected wave is entirely polarized with electric field parallel to the interface. The transmitted waves, although composed of both polarizations, have the larger amplitude with  $\mathbf{H}$

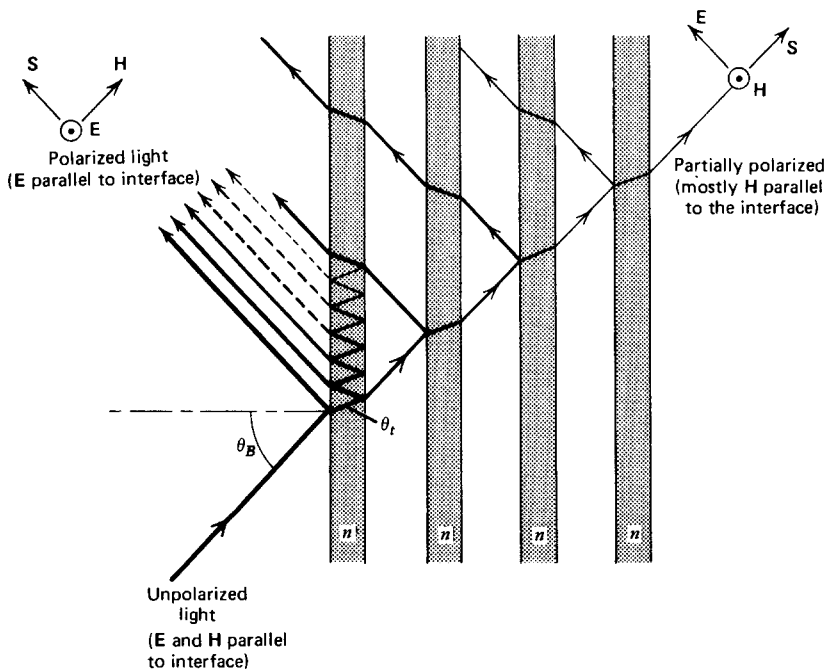


Figure 7-22 Unpolarized light incident upon glass with  $\mu = \mu_0$  can be polarized by reflection if it is incident at the Brewster's angle for the polarization with  $\mathbf{H}$  parallel to the interface. The transmitted light becomes more polarized with  $\mathbf{H}$  parallel to the interface by adding more parallel glass plates.

parallel to the interface because it was entirely transmitted with no reflection at both interfaces.

By passing the transmitted light through another parallel piece of glass, the polarization with electric field parallel to the interface becomes further diminished because it is partially reflected, while the other polarization is completely transmitted. With more glass elements, as in Figure 7-22, the transmitted light can be made essentially completely polarized with  $\mathbf{H}$  field parallel to the interface.

#### 7-10-4 Light Propagation In Water

##### (a) Submerged Source

A light source is a distance  $d$  below the surface of water with refractive index  $n = 1.33$ , as in Figure 7-23. The rays emanate from the source as a cone. Those rays at an angle from the normal greater than the critical angle,

$$\sin \theta_c = 1/n \Rightarrow \theta_c = 48.8^\circ \quad (6)$$

are not transmitted into the air but undergo total internal reflection. A circle of light with diameter

$$D = 2d \tan \theta_c \approx 2.28d \quad (7)$$

then forms on the water's surface due to the exiting light.

##### (b) Fish Below a Boat

A fish swims below a circular boat of diameter  $D$ , as in Figure 7-24. As we try to view the fish from the air above, the incident light ray is bent towards the normal. The region below the boat that we view from above is demarcated by the light rays at grazing incidence to the surface ( $\theta_i = \pi/2$ ) just entering the water ( $n = 1.33$ ) at the sides of the boat. The transmitted angle of these light rays is given from Snell's law as

$$\sin \theta_t = \frac{\sin \theta_i}{n} = \frac{1}{n} \Rightarrow \theta_t = 48.8^\circ \quad (8)$$

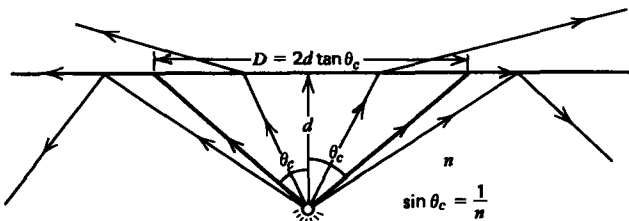


Figure 7-23 Light rays emanating from a source within a high index of refraction medium are totally internally reflected from the surface for angles greater than the critical angle. Lesser angles of incidence are transmitted.

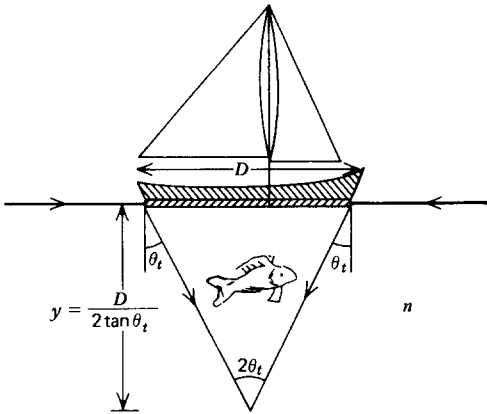


Figure 7-24 A fish cannot be seen from above if it swims below a circular boat within the cone bounded by light rays at grazing incidence entering the water at the side of the boat.

These rays from all sides of the boat intersect at the point a distance  $y$  below the boat, where

$$\tan \theta_t = \frac{D}{2y} \Rightarrow y = \frac{D}{2 \tan \theta_t} \approx 0.44D \tag{9}$$

If the fish swims within the cone, with vertex at the point  $y$  below the boat, it cannot be viewed from above.

### 7-10-5 Totally Reflecting Prisms

The glass isosceles right triangle in Figure 7-25 has an index of refraction of  $n = 1.5$  so that the critical angle for total

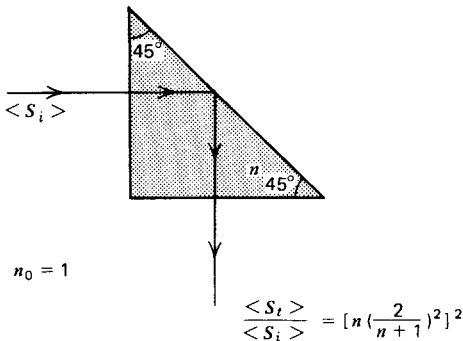


Figure 7-25 A totally reflecting prism. The index of refraction  $n$  must exceed  $\sqrt{2}$  so that the light incident on the hypotenuse at  $45^\circ$  exceeds the critical angle.

internal reflection is

$$\sin \theta_c = \frac{1}{n} = \frac{1}{1.5} \Rightarrow \theta_c = 41.8^\circ \quad (10)$$

The light is normally incident on the vertical face of the prism. The transmission coefficient is then given in Section 7-6-1 as

$$T_1 = \frac{\hat{E}_t}{\hat{E}_i} = \frac{2\eta}{\eta + \eta_0} = \frac{2/n}{1 + 1/n} = \frac{2}{n + 1} = 0.8 \quad (11)$$

where because the permeability of the prism equals that of free space  $n = \sqrt{\epsilon/\epsilon_0}$  while  $\eta/\eta_0 = \sqrt{\epsilon_0/\epsilon} = 1/n$ . The transmitted light is then incident upon the hypotenuse of the prism at an angle of  $45^\circ$ , which exceeds the critical angle so that no power is transmitted and the light is totally reflected being turned through a right angle. The light is then normally incident upon the horizontal face with transmission coefficient:

$$T_2 = \frac{\hat{E}_2}{0.8\hat{E}_i} = \frac{2\eta_0}{\eta + \eta_0} = \frac{2}{1/n + 1} = \frac{2n}{n + 1} = 1.2 \quad (12)$$

The resulting electric field amplitude is then

$$\hat{E}_2 = T_1 T_2 \hat{E}_i = 0.96 \hat{E}_i \quad (13)$$

The ratio of transmitted to incident power density is

$$\frac{\langle S \rangle}{\langle S_i \rangle} = \frac{\frac{1}{2} |\hat{E}_2|^2 / \eta_0}{\frac{1}{2} |\hat{E}_i|^2 / \eta_0} = \frac{|\hat{E}_2|^2}{|\hat{E}_i|^2} = \left(\frac{24}{25}\right)^2 \approx 0.92 \quad (14)$$

This ratio can be increased to unity by applying a quarter-wavelength-thick dielectric coating with index of refraction  $n_{\text{coating}} = \sqrt{n}$ , as developed in Example 7-1. This is not usually done because the ratio in (14) is already large without the expense of a coating.

## 7-10-6 Fiber Optics

### (a) Straight Light Pipe

Long thin fibers of transparent material can guide light along a straight path if the light within the pipe is incident upon the wall at an angle greater than the critical angle ( $\sin \theta_c = 1/n$ ):

$$\sin \theta_2 = \cos \theta_1 \geq \sin \theta_c \quad (15)$$

The light rays are then totally internally reflected being confined to the pipe until they exit, as in Figure 7-26. The

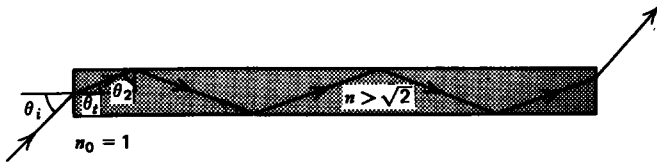


Figure 7-26 The index of refraction of a straight light pipe must be greater than  $\sqrt{2}$  for total internal reflections of incident light at any angle.

incident angle is related to the transmitted angle from Snell's law,

$$\sin \theta_t = (1/n) \sin \theta_i \quad (16)$$

so that (15) becomes

$$\cos \theta_i = \sqrt{1 - \sin^2 \theta_t} = \sqrt{1 - (1/n^2) \sin^2 \theta_i} \geq 1/n \quad (17)$$

which when solved for  $n$  yields

$$n^2 \geq 1 + \sin^2 \theta_i \quad (18)$$

If this condition is met for grazing incidence ( $\theta_i = \pi/2$ ), all incident light will be passed by the pipe, which requires that

$$n^2 \geq 2 \Rightarrow n \geq \sqrt{2} \quad (19)$$

Most types of glass have  $n \approx 1.5$  so that this condition is easily met.

### (b) Bent Fibers

Light can also be guided along a tortuous path if the fiber is bent, as in the semi-circular pipe shown in Figure 7-27. The minimum angle to the radial normal for the incident light shown is at the point  $A$ . This angle in terms of the radius of the bend and the light pipe width must exceed the critical angle

$$\sin \theta_A = \frac{R}{R+d} \geq \sin \theta_c \quad (20)$$

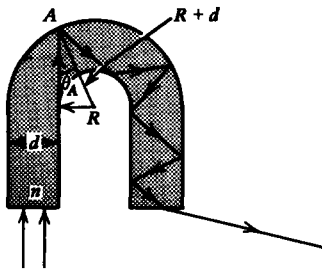


Figure 7-27 Light can be guided along a circularly bent fiber if  $R/d > 1/(n-1)$  as then there is always total internal reflection each time the light is incident on the walls.

so that

$$\frac{R/d}{R/d+1} \geq \frac{1}{n} \quad (21)$$

which when solved for  $R/d$  requires

$$\frac{R}{d} \geq \frac{1}{n-1} \quad (22)$$

## PROBLEMS

### Section 7-1

1. For the following electric fields in a linear media of permittivity  $\epsilon$  and permeability  $\mu$  find the charge density, magnetic field, and current density.

(a)  $\mathbf{E} = E_0(x\mathbf{i}_x + y\mathbf{i}_y) \sin \omega t$

(b)  $\mathbf{E} = E_0(y\mathbf{i}_x - x\mathbf{i}_y) \cos \omega t$

(c)  $\mathbf{E} = \text{Re} [E_0 e^{i(\omega t - k_x x - k_y y)} \mathbf{i}_y]$ . How must  $k_x$ ,  $k_y$ , and  $\omega$  be related so that  $\mathbf{J} = 0$ ?

2. An Ohmic conductor of arbitrary shape has an initial charge distribution  $\rho_0(\mathbf{r})$  at  $t = 0$ .

(a) What is the charge distribution for all time?

(b) The initial charge distribution is uniform and is confined between parallel plate electrodes of spacing  $d$ . What are the electric and magnetic fields when the electrodes are opened or short circuited?

(c) Repeat (b) for coaxial cylindrical electrodes of inner radius  $a$  and outer radius  $b$ .

(d) When does a time varying electric field not generate a magnetic field?

3. (a) For linear media of permittivity  $\epsilon$  and permeability  $\mu$ , use the magnetic vector potential  $\mathbf{A}$  to rewrite Faraday's law as the curl of a function.

(b) Can a scalar potential function  $V$  be defined? What is the electric field in terms of  $V$  and  $\mathbf{A}$ ? The choice of  $V$  is not unique so pick  $V$  so that under static conditions  $\mathbf{E} = -\nabla V$ .

(c) Use the results of (a) and (b) in Ampere's law with Maxwell's displacement current correction to obtain a single equation in  $\mathbf{A}$  and  $V$ . (**Hint:**  $\nabla \times (\nabla \times \mathbf{A}) = \nabla(\nabla \cdot \mathbf{A}) - \nabla^2 \mathbf{A}$ .)

(d) Since we are free to specify  $\nabla \cdot \mathbf{A}$ , what value should we pick to make (c) an equation just in  $\mathbf{A}$ ? This is called setting the gauge.

(e) Use the results of (a)–(d) in Gauss's law for  $\mathbf{D}$  to obtain a single equation in  $V$ .

(f) Consider a sinusoidally varying point charge at  $r=0$ ,  $\hat{Q} e^{j\omega t}$ . Solve (e) for  $r > 0$ .

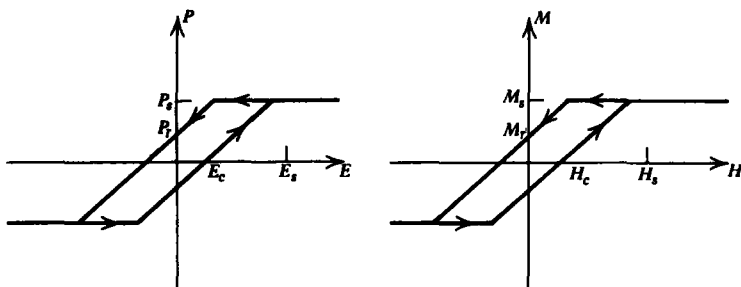
Hint:

$$\frac{1}{r} \frac{\partial}{\partial r} \left( r^2 \frac{\partial V}{\partial r} \right) = \frac{\partial^2}{\partial r^2} (rV)$$

Define a new variable  $(rV)$ . By symmetry,  $V$  only depends on  $r$  and waves can only propagate away from the charge and not towards it. As  $r \rightarrow 0$ , the potential approaches the quasi-static Coulomb potential.

Section 7-2

4. Poynting's theorem must be modified if we have a hysteretic material with a nonlinear and double-valued relationship between the polarization  $\mathbf{P}$  and electric field  $\mathbf{E}$  and the magnetization  $\mathbf{M}$  and magnetic field  $\mathbf{H}$ .



(a) For these nonlinear constitutive laws put Poynting's theorem in the form

$$\nabla \cdot \mathbf{S} + \frac{\partial w}{\partial t} = -P_d - P_P - P_M$$

where  $P_P$  and  $P_M$  are the power densities necessary to polarize and magnetize the material.

(b) Sinusoidal electric and magnetic fields  $\mathbf{E} = \mathbf{E}_s \cos \omega t$  and  $\mathbf{H} = \mathbf{H}_s \cos \omega t$  are applied. How much energy density is dissipated per cycle?

5. An electromagnetic field is present within a superconductor with constituent relation

$$\frac{\partial \mathbf{J}_f}{\partial t} = \omega_p^2 \epsilon \mathbf{E}$$

(a) Show that Poynting's theorem can be written in the form

$$\nabla \cdot \mathbf{S} + \frac{\partial w}{\partial t} = 0$$

What is  $w$ ?

(b) What is the velocity of the charge carriers each with charge  $q$  in terms of the current density  $\mathbf{J}_f$ ? The number density of charge carriers is  $n$ .

(c) What kind of energy does the superconductor add?

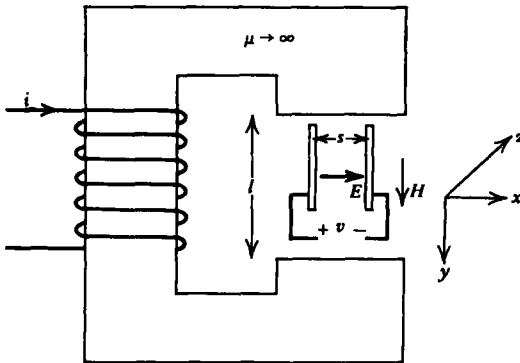
(d) Rewrite Maxwell's equations with this constitutive law for fields that vary sinusoidally with time.

(e) Derive the complex Poynting theorem in the form

$$\nabla \cdot [\frac{1}{2}\hat{\mathbf{E}}(\mathbf{r}) \times \hat{\mathbf{H}}^*(\mathbf{r})] + 2j\omega \langle w \rangle = 0$$

What is  $\langle w \rangle$ ?

6. A paradoxical case of Poynting's theorem occurs when a static electric field is applied perpendicularly to a static magnetic field, as in the case of a pair of electrodes placed within a magnetic circuit.



(a) What are  $\mathbf{E}$ ,  $\mathbf{H}$ , and  $\mathbf{S}$ ?

(b) What is the energy density stored in the system?

(c) Verify Poynting's theorem.

7. The complex electric field amplitude has real and imaginary parts

$$\hat{\mathbf{E}}(\mathbf{r}) = \mathbf{E}_r + j\mathbf{E}_i$$

Under what conditions are the following scalar and vector products zero:

(a)  $\hat{\mathbf{E}} \cdot \hat{\mathbf{E}} \stackrel{?}{=} 0$

(b)  $\hat{\mathbf{E}} \cdot \hat{\mathbf{E}}^* \stackrel{?}{=} 0$

(c)  $\hat{\mathbf{E}} \times \hat{\mathbf{E}} \stackrel{?}{=} 0$

(d)  $\hat{\mathbf{E}} \times \hat{\mathbf{E}}^* \stackrel{?}{=} 0$

Section 7.3

8. Consider a lossy medium of permittivity  $\epsilon$ , permeability  $\mu$ , and Ohmic conductivity  $\sigma$ .

(a) Write down the field equations for an  $x$ -directed electric field.

- (b) Obtain a single equation in  $E_x$ .
- (c) If the fields vary sinusoidally with time,

$$E_x = \text{Re} [\hat{E}_x(z) e^{j\omega t}]$$

what are the spatial dependences of the fields?

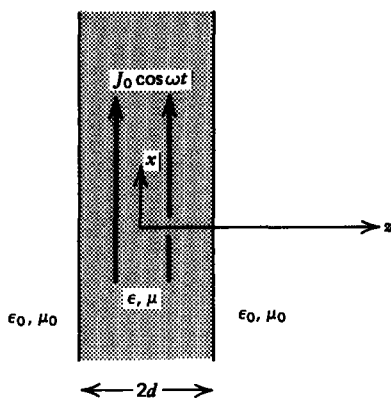
- (d) Specialize (c) to the (i) low loss limit ( $\sigma/\omega\epsilon \ll 1$ ) and (ii) large loss limit ( $\sigma/\omega\epsilon \gg 1$ ).

- (e) Repeat (a)–(c) if the medium is a plasma with constitutive law

$$\frac{\partial \mathbf{J}}{\partial t} = \omega_p^2 \epsilon \mathbf{E}$$

- (f) A current sheet  $K_0 \cos \omega t \mathbf{i}_x$  is placed at  $z = 0$ . Find the electric and magnetic fields if the sheet is placed within an Ohmic conductor or within a plasma.

9. A uniformly distributed volume current of thickness  $2d$ ,  $J_0 \cos \omega t \mathbf{i}_x$ , is a source of plane waves.



- (a) From Maxwell's equations obtain a single differential equation relating  $E_x$  to  $J_x$ .

- (b) Find the electric and magnetic fields within and outside the current distribution.

- (c) How much time-average power per unit area is delivered by the current?

- (d) How does this generated power compare to the electromagnetic time-average power per unit area leaving the volume current at  $z = \pm d$ ?

10. A TEM wave ( $E_x, H_y$ ) propagates in a medium whose permittivity and permeability are functions of  $z$ ,  $\epsilon(z)$ , and  $\mu(z)$ .

- (a) Write down Maxwell's equations and obtain single partial differential equations in  $E_x$  and  $H_y$ .

- (b) Consider the idealized case where  $\epsilon(z) = \epsilon e^{\alpha|z|}$  and  $\mu(z) = \mu e^{-\alpha|z|}$ . A current sheet  $K_0 e^{j\omega t} \mathbf{i}_x$  is at  $z = 0$ . What are

the resulting electric and magnetic fields on each side of the sheet?

(c) For what values of  $\alpha$  are the solutions spatially evanescent or oscillatory?

11. We wish to compare various measurements between two observers, the second moving at a constant velocity  $v\mathbf{i}_z$  with respect to the first.

(a) The first observer measures simultaneous events at two positions  $z_1$  and  $z_2$  so that  $t_1 = t_2$ . What is the time interval between the two events  $t'_1 - t'_2$  as measured by the second observer?

(b) The first observer measures a time interval  $\Delta t = t_1 - t_2$  between two events at the same position  $z$ . What is the time interval as measured by the second observer?

(c) The first observer measures the length of a stick as  $L = z_2 - z_1$ . What is the length of the stick as measured by the second observer?

12. A stationary observer measures the velocity of a particle as  $\mathbf{u} = u_x\mathbf{i}_x + u_y\mathbf{i}_y + u_z\mathbf{i}_z$ .

(a) What velocity,  $\mathbf{u}' = u'_x\mathbf{i}_x + u'_y\mathbf{i}_y + u'_z\mathbf{i}_z$ , does another observer moving at constant speed  $v\mathbf{i}_z$  measure?

(b) Find  $\mathbf{u}'$  for the following values of  $\mathbf{u}$  where  $c_0$  is the free space speed of light:

(i)  $\mathbf{u} = c_0\mathbf{i}_x$

(ii)  $\mathbf{u} = c_0\mathbf{i}_y$

(iii)  $\mathbf{u} = c_0\mathbf{i}_z$

(iv)  $\mathbf{u} = (c_0/\sqrt{3})(\mathbf{i}_x + \mathbf{i}_y + \mathbf{i}_z)$

(c) Do the results of (a) and (b) agree with the postulate that the speed of light for all observers is  $c_0$ ?

#### Section 7.4

13. An electric field is of the form

$$\mathbf{E} = 100 e^{j(2\pi \times 10^8 t - 2\pi \times 10^{-2} z)} \mathbf{i}_x \text{ volts/m}$$

(a) What is the frequency, wavelength, and speed of light in the medium?

(b) If the medium has permeability  $\mu_0 = 4\pi \times 10^{-7}$  henry/m, what is the permittivity  $\epsilon$ , wave impedance  $\eta$ , and the magnetic field?

(c) How much time-average power per unit area is carried by the wave?

14. The electric field of an elliptically polarized plane wave in a medium with wave impedance  $\eta$  is

$$\mathbf{E} = \text{Re} (E_{x0}\mathbf{i}_x + E_{y0} e^{j\phi}\mathbf{i}_y) e^{j(\omega t - kx)}$$

where  $E_{x0}$  and  $E_{y0}$  are real.

- (a) What is the magnetic field?
- (b) What is the instantaneous and time-average power flux densities?

15. In Section 3-1-4 we found that the force on one of the charges  $Q$  of a spherical atomic electric dipole of radius  $R_0$  is

$$\mathbf{F} = Q \left[ \mathbf{E} - \frac{Q\mathbf{d}}{4\pi\epsilon_0 R_0^3} \right]$$

where  $\mathbf{d}$  is the dipole spacing.

(a) Write Newton's law for this moveable charge with mass  $M$  assuming that the electric field varies sinusoidally with time as  $E_0 \cos \omega t$  and solve for  $\mathbf{d}$ . (Hint: Let  $\omega_0^2 = Q^2 / (M4\pi\epsilon_0 R_0^3)$ .)

(b) What is the polarization  $\mathbf{P}$  as a function of  $\mathbf{E}$  if there are  $N$  dipoles per unit volume? What is the frequency dependent permittivity function  $\epsilon(\omega)$ , where

$$\mathbf{D}(\mathbf{r}) = \epsilon(\omega)\mathbf{E}(\mathbf{r})$$

This model is often appropriate for light propagating in dielectric media.

(c) Use the results of (b) in Maxwell's equations to find the relation between the wavenumber  $k$  and frequency  $\omega$ .

(d) For what frequency ranges do we have propagation or evanescence?

(e) What are the phase and group velocities of the waves?

(f) Derive the complex Poynting's theorem for this dispersive dielectric.

16. High-frequency wave propagation in the ionosphere is partially described by the development in Section 7-4-4 except that we must include the earth's dc magnetic field, which we take to be  $H_0 \mathbf{i}_z$ .

(a) The charge carriers have charge  $q$  and mass  $m$ . Write the three components of Newton's force law neglecting collisions but including inertia and the Coulomb-Lorentz force law. Neglect the magnetic field amplitudes of the propagating waves compared to  $H_0$  in the Lorentz force law.

(b) Solve for each component of the current density  $\mathbf{J}$  in terms of the charge velocity components assuming that the propagating waves vary sinusoidally with time as  $e^{j\omega t}$ .

Hint: Define

$$\omega_p^2 = \frac{q^2 n}{m\epsilon}, \quad \omega_0 = \frac{q\mu_0 H_0}{m}$$

(c) Use the results of (b) in Maxwell's equations for fields of the form  $e^{j(\omega t - kz)}$  to solve for the wavenumber  $k$  in terms of  $\omega$ .

(d) At what frequencies is the wavenumber zero or infinite? Over what frequency range do we have evanescence or propagation?

(e) For each of the two modes found in (c), what is the polarization of the electric field?

(f) What is the phase velocity of each wave? Since each mode travels at a different speed, the atmosphere acts like an anisotropic birefringent crystal. A linearly polarized wave  $E_0 e^{j(\omega t - k_0 z)} \mathbf{i}_x$  is incident upon such a medium. Write this field as the sum of right and left circularly polarized waves.

**Hint:**

$$E_0 \mathbf{i}_x = \frac{E_0}{2} (\mathbf{i}_x + j\mathbf{i}_y) + \frac{E_0}{2} (\mathbf{i}_x - j\mathbf{i}_y)$$

(g) If the transmitted field at  $z = 0$  just inside the medium has amplitude  $E_t e^{j\omega t} \mathbf{i}_x$ , what are the electric and magnetic fields throughout the medium?

17. Nitrobenzene with  $\mu = \mu_0$  and  $\epsilon = 35\epsilon_0$  is placed between parallel plate electrodes of spacing  $s$  and length  $l$  stressed by a dc voltage  $V_0$ . Measurements have shown that light polarized parallel to the dc electric field travels at the speed  $c_{\parallel}$ , while light polarized perpendicular to the dc electric field travels slightly faster at the speed  $c_{\perp}$ , being related to the dc electric field  $E_0$  and free space light wavelength as

$$\frac{1}{c_{\parallel}} - \frac{1}{c_{\perp}} = \lambda B E_0^2$$

where  $B$  is called the Kerr constant which for nitrobenzene is  $B \approx 4.3 \times 10^{-12} \text{ sec/V}^2$  at  $\lambda = 500 \text{ nm}$ .

(a) Linearly polarized light with free space wavelength  $\lambda = 500 \text{ nm}$  is incident at  $45^\circ$  to the dc electric field. After exiting the Kerr cell, what is the phase difference between the field components of the light parallel and perpendicular to the dc electric field?

(b) What are all the values of electric field strengths that allow the Kerr cell to act as a quarter- or half-wave plate?

(c) The Kerr cell is placed between crossed polarizers (polariscope). What values of electric field allow maximum light transmission? No light transmission?

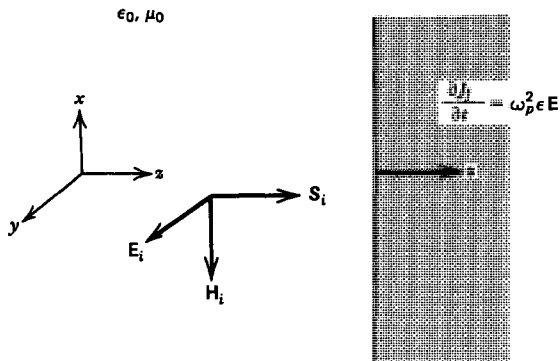
### Section 7.5

18. A uniform plane wave with  $y$ -directed electric field is normally incident upon a plasma medium at  $z = 0$  with constitutive law  $\partial \mathbf{J}_f / \partial t = \omega_p^2 \epsilon \mathbf{E}$ . The fields vary sinusoidally in time as  $e^{j\omega t}$ .

(a) What is the general form of the incident, reflected, and transmitted fields?

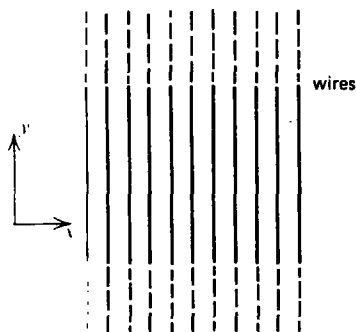
(b) Applying the boundary conditions, find the field amplitudes.

(c) What is the time-average electromagnetic power density in each region for  $\omega > \omega_p$  and for  $\omega < \omega_p$ ?



19. A polarizing filter to microwaves is essentially formed by many highly conducting parallel wires whose spacing is much smaller than a wavelength. That polarization whose electric field is transverse to the wires passes through. The incident electric field is

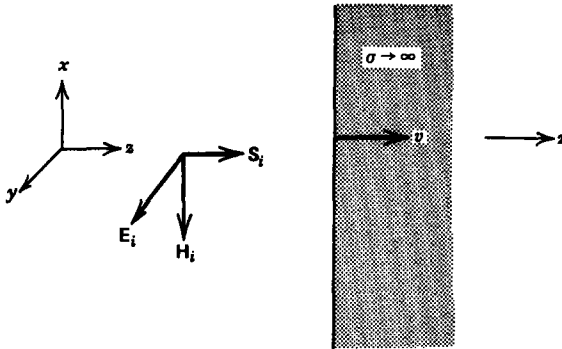
$$\mathbf{E} = E_x \cos(\omega t - kz)\mathbf{i}_x + E_y \sin(\omega t - kz)\mathbf{i}_y$$



- (a) What is the incident magnetic field and incident power density?
- (b) What are the transmitted fields and power density?
- (c) Another set of polarizing wires are placed parallel but a distance  $d$  and orientated at an angle  $\phi$  to the first. What are the transmitted fields?

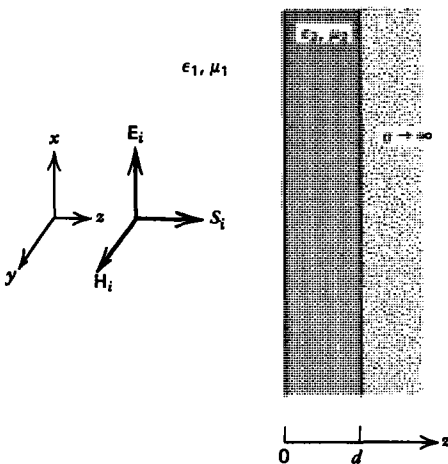
20. A uniform plane wave with  $y$ -directed electric field  $E_y = E_0 \cos \omega(t - z/c)$  is normally incident upon a perfectly conducting plane that is moving with constant velocity  $v\mathbf{i}_z$ , where  $v \ll c$ .

- (a) What are the total electric and magnetic fields in each region?
- (b) What is the frequency of the reflected wave?
- (c) What is the power flow density? Why can't we use the complex Poynting vector to find the time-average power?



## Section 7.6

21. A dielectric ( $\epsilon_2, \mu_2$ ) of thickness  $d$  coats a perfect conductor. A uniform plane wave is normally incident onto the coating from the surrounding medium with properties ( $\epsilon_1, \mu_1$ ).



(a) What is the general form of the fields in the two dielectric media? (**Hint:** Why can the transmitted electric field be written as  $\mathbf{E}_t = \text{Re} [\hat{\mathbf{E}}_t \sin k_2(z-d) e^{j\omega t} \mathbf{i}_z]$ ?)

(b) Applying the boundary conditions, what are the field amplitudes?

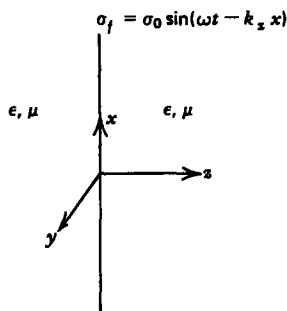
(c) What is the time-average power flow in each region?

(d) What is the time-average radiation pressure on the conductor?

## Section 7.7

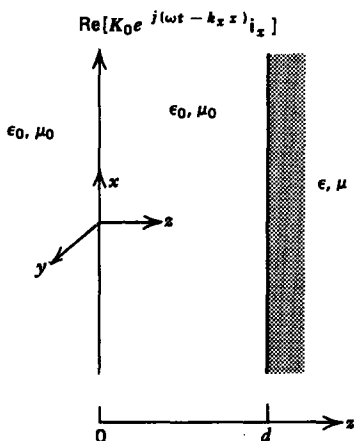
22. An electric field of the form  $\text{Re} [\hat{\mathbf{E}} e^{j\omega t} e^{-\boldsymbol{\gamma} \cdot \mathbf{r}}]$  propagates in a lossy conductor with permittivity  $\epsilon$ , permeability  $\mu$ , and conductivity  $\sigma$ . If  $\boldsymbol{\gamma} = \boldsymbol{\alpha} + j\mathbf{k}$ , what equalities must  $\boldsymbol{\alpha}$  and  $\mathbf{k}$  obey?

23. A sheet of surface charge with charge density  $\sigma_0 \sin(\omega t - k_x x)$  is placed at  $z = 0$  within a linear medium with properties  $(\epsilon, \mu)$ .



- (a) What are the electric and magnetic fields?
- (b) What surface current flows on the sheet?

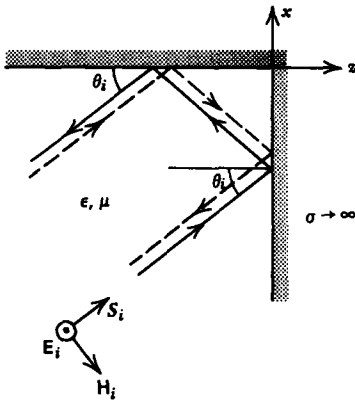
24. A current sheet of the form  $\text{Re}(K_0 e^{j(\omega t - k_x x)} \mathbf{i}_x)$  is located in free space at  $z = 0$ . A dielectric medium  $(\epsilon, \mu)$  of semi-infinite extent is placed at  $z = d$ .



- (a) For what range of frequency can we have a nonuniform plane wave in free space and a uniform plane wave in the dielectric? Nonuniform plane wave in each region? Uniform plane wave in each region?
- (b) What are the electric and magnetic fields everywhere?
- (c) What is the time-average  $z$ -directed power flow density in each region if we have a nonuniform plane wave in free space but a uniform plane wave in the dielectric?

Section 7.8

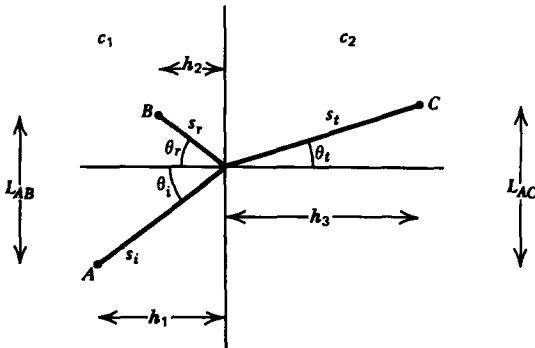
25. A uniform plane wave  $\text{Re}(E_0 e^{j(\omega t - k_x x - k_y y)} \mathbf{i}_y)$  is obliquely incident upon a right-angled perfectly conducting corner. The wave is incident at angle  $\theta_i$  to the  $z = 0$  wall.



- (a) Try a solution composed of the incident and reflected waves off each surface of the conductor. What is the general form of solution? (Hint: There are four different waves.)
- (b) Applying the boundary conditions, what are the electric and magnetic fields?
- (c) What are the surface charge and current distributions on the conducting walls?
- (d) What is the force per unit area on each wall?
- (e) What is the power flow density?

Section 7.9

26. Fermat's principle of least time states that light, when reflected or refracted off an interface, will pick the path of least time to propagate between two points.



- (a) A beam of light from point  $A$  is incident upon a dielectric interface at angle  $\theta_i$  from the normal and is reflected through the point  $B$  at angle  $\theta_r$ . In terms of  $\theta_i$ ,  $\theta_r$ ,  $h_1$  and  $h_2$ , and the speed of light  $c_1$ , how long does it take light to travel from  $A$  to  $B$  along this path? What other relation is there between  $\theta_i$ ,  $\theta_r$ ,  $L_{AB}$ ,  $h_1$  and  $h_2$ ?
- (b) Find the angle  $\theta_i$  that satisfies Fermat's principle. What is  $\theta_r$ ?

(c) In terms of  $\theta_i$ ,  $\theta_t$ ,  $h_1$ ,  $h_2$ , and the light speeds  $c_1$  and  $c_2$  in each medium, how long does it take light to travel from  $A$  to  $C$ ?

(d) Find the relationship between  $\theta_t$  and  $\theta_i$  that satisfies Fermat's principle.

27. In many cases the permeability of dielectric media equals that of free space. In this limit show that the reflection and transmission coefficients for waves obliquely incident upon dielectric media are:  $\mathbf{E}$  parallel to the interface

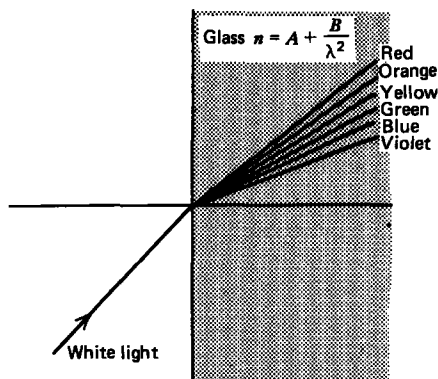
$$R = -\frac{\sin(\theta_i - \theta_t)}{\sin(\theta_i + \theta_t)}, \quad T = \frac{2 \cos \theta_i \sin \theta_t}{\sin(\theta_i + \theta_t)}$$

$\mathbf{H}$  parallel to the interface

$$R = \frac{\tan(\theta_i - \theta_t)}{\tan(\theta_i + \theta_t)}, \quad T = \frac{2 \cos \theta_i \sin \theta_t}{\sin(\theta_i + \theta_t) \cos(\theta_i - \theta_t)}$$

28. White light is composed of the entire visible spectrum. The index of refraction  $n$  for most materials is a weak function of wavelength  $\lambda$ , often described by Cauchy's equation

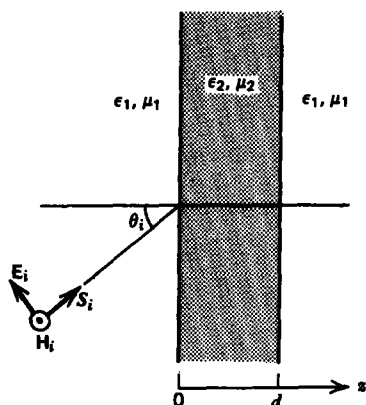
$$n = A + B/\lambda^2$$



A beam of white light is incident at  $30^\circ$  to a piece of glass with  $A = 1.5$  and  $B = 5 \times 10^{-15} \text{ m}^2$ . What are the transmitted angles for the colors violet (400 nm), blue (450 nm), green (550 nm), yellow (600 nm), orange (650 nm), and red (700 nm)? This separation of colors is called dispersion.

29. A dielectric slab of thickness  $d$  with speed of light  $c_2$  is placed within another dielectric medium of infinite extent with speed of light  $c_1$ , where  $c_1 < c_2$ . An electromagnetic wave with  $\mathbf{H}$  parallel to the interface is incident onto the slab at angle  $\theta_i$ .

(a) Find the electric and magnetic fields in each region. (**Hint:** Use Cramer's rule to find the four unknown field amplitudes in terms of  $E_i$ .)

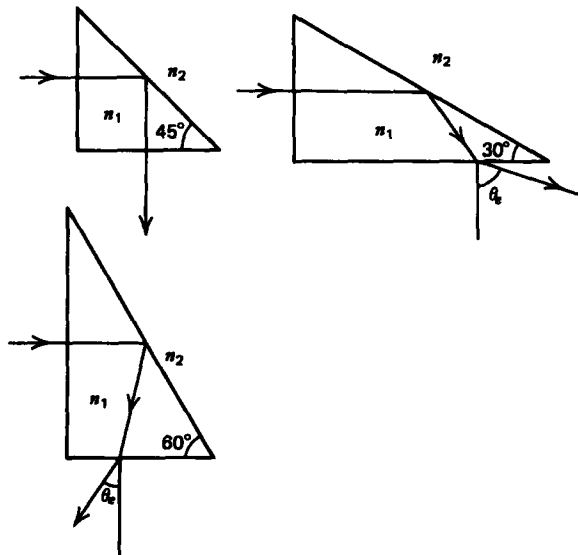


(b) For what range of incident angle do we have uniform or nonuniform plane waves through the middle region?

(c) What is the transmitted time-average power density with uniform or nonuniform plane waves through the middle region. How can we have power flow through the middle region with nonuniform plane waves?

### Section 7.10

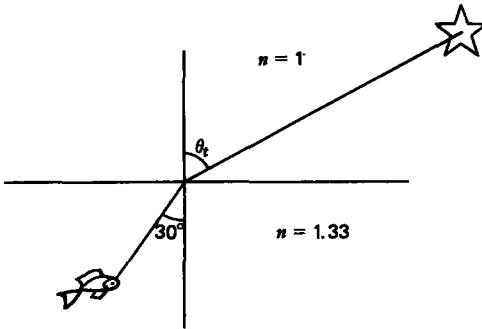
30. Consider the various prisms shown.



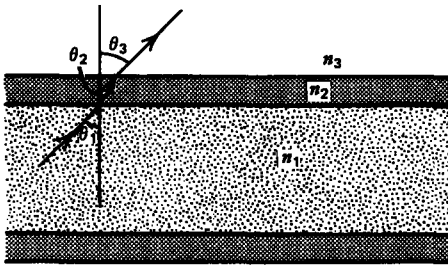
(a) What is the minimum index of refraction  $n_1$  necessary for no time-average power to be transmitted across the hypotenuse when the prisms are in free space,  $n_2 = 1$ , or water,  $n_2 = 1.33$ ?

(b) At these values of refractive index, what are the exiting angles  $\theta_e$ ?

31. A fish below the surface of water with index of refraction  $n = 1.33$  sees a star that he measures to be at  $30^\circ$  from the normal. What is the star's actual angle from the normal?



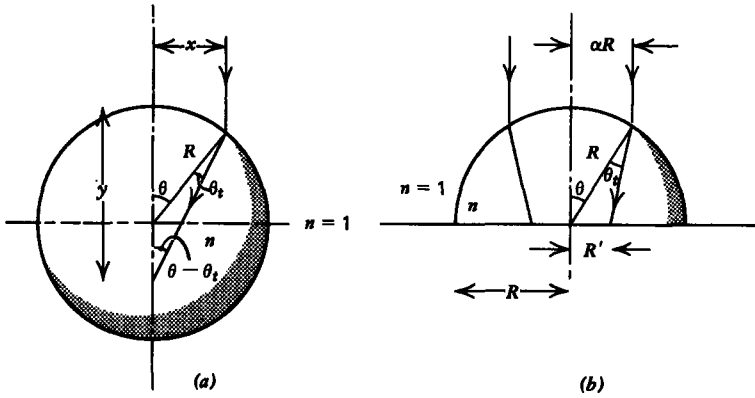
32. A straight light pipe with refractive index  $n_1$  has a dielectric coating with index  $n_2$  added for protection. The light pipe is usually within free space so that  $n_3$  is typically unity.



- Light within the pipe is incident upon the first interface at angle  $\theta_1$ . What are the angles  $\theta_2$  and  $\theta_3$ ?
- What value of  $\theta_1$  will make  $\theta_3$  just equal the critical angle for total internal reflection at the second interface?
- How does this value differ from the critical angle if the coating was not present so that  $n_1$  was directly in contact with  $n_3$ ?
- If we require that total reflection occur at the first interface, what is the allowed range of incident angle  $\theta_1$ . Must the coating have a larger or smaller index of refraction than the light pipe?

33. A spherical piece of glass of radius  $R$  has refractive index  $n$ .

- A vertical light ray is incident at the distance  $x$  ( $x < R$ ) from the vertical diameter. At what distance  $y$  from the top of the sphere will the light ray intersect the vertical diameter? For what range of  $n$  and  $x$  will the refracted light intersect the vertical diameter within the sphere?



(b) A vertical light beam of radius  $\alpha R$  ( $\alpha < 1$ ) is incident upon a hemisphere of this glass that rests on a table top. What is the radius  $R'$  of the light on the table?

# chapter 8

*guided electromagnetic  
waves*

The uniform plane wave solutions developed in Chapter 7 cannot in actuality exist throughout all space, as an infinite amount of energy would be required from the sources. However, TEM waves can also propagate in the region of finite volume between electrodes. Such electrode structures, known as transmission lines, are used for electromagnetic energy flow from power (60 Hz) to microwave frequencies, as delay lines due to the finite speed  $c$  of electromagnetic waves, and in pulse forming networks due to reflections at the end of the line. Because of the electrode boundaries, more general wave solutions are also permitted where the electric and magnetic fields are no longer perpendicular. These new solutions also allow electromagnetic power flow in closed single conductor structures known as waveguides.

## 8-1 THE TRANSMISSION LINE EQUATIONS

### 8-1-1 The Parallel Plate Transmission Line

The general properties of transmission lines are illustrated in Figure 8-1 by the parallel plate electrodes a small distance  $d$  apart enclosing linear media with permittivity  $\epsilon$  and permeability  $\mu$ . Because this spacing  $d$  is much less than the width  $w$  or length  $l$ , we neglect fringing field effects and assume that the fields only depend on the  $z$  coordinate.

The perfectly conducting electrodes impose the boundary conditions:

- (i) The tangential component of  $\mathbf{E}$  is zero.
- (ii) The normal component of  $\mathbf{B}$  (and thus  $\mathbf{H}$  in the linear media) is zero.

With these constraints and the neglect of fringing near the electrode edges, the fields cannot depend on  $x$  or  $y$  and thus are of the following form:

$$\begin{aligned}\mathbf{E} &= E_x(z, t)\mathbf{i}_x \\ \mathbf{H} &= H_y(z, t)\mathbf{i}_y\end{aligned}\tag{1}$$

which when substituted into Maxwell's equations yield

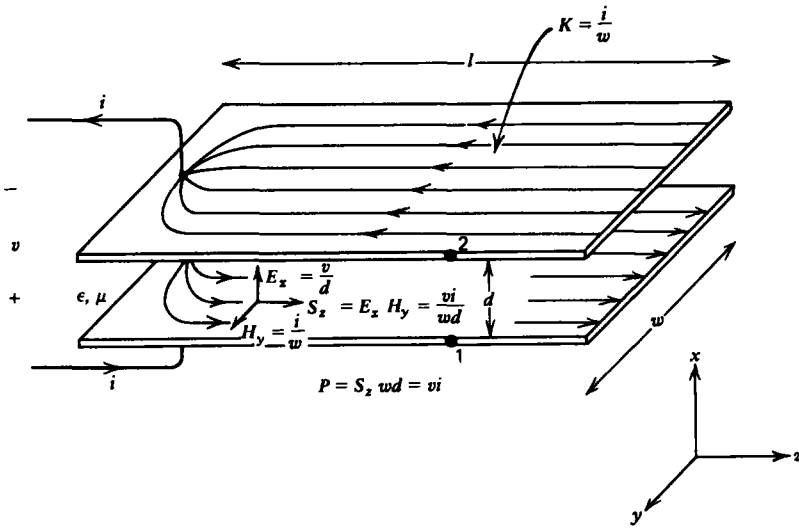


Figure 8-1 The simplest transmission line consists of two parallel perfectly conducting plates a small distance  $d$  apart.

$$\begin{aligned} \nabla \times \mathbf{E} &= -\mu \frac{\partial \mathbf{H}}{\partial t} \Rightarrow \frac{\partial E_x}{\partial z} = -\mu \frac{\partial H_y}{\partial t} \\ \nabla \times \mathbf{H} &= \epsilon \frac{\partial \mathbf{E}}{\partial t} \Rightarrow \frac{\partial H_y}{\partial z} = -\epsilon \frac{\partial E_x}{\partial t} \end{aligned} \tag{2}$$

We recognize these equations as the same ones developed for plane waves in Section 7-3-1. The wave solutions found there are also valid here. However, now it is more convenient to introduce the circuit variables of voltage and current along the transmission line, which will depend on  $z$  and  $t$ .

Kirchoff's voltage and current laws will not hold along the transmission line as the electric field in (2) has nonzero curl and the current along the electrodes will have a divergence due to the time varying surface charge distribution,  $\sigma_f = \pm \epsilon E_x(z, t)$ . Because  $\mathbf{E}$  has a curl, the voltage difference measured between any two points is not unique, as illustrated in Figure 8-2, where we see time varying magnetic flux passing through the contour  $L_1$ . However, no magnetic flux passes through the path  $L_2$ , where the potential difference is measured between the two electrodes at the same value of  $z$ , as the magnetic flux is parallel to the surface. Thus, the voltage can be uniquely defined between the two electrodes at the same value of  $z$ :

$$v(z, t) = \int_{z=\text{const}}^2 \mathbf{E} \cdot d\mathbf{l} = E_x(z, t)d \tag{3}$$

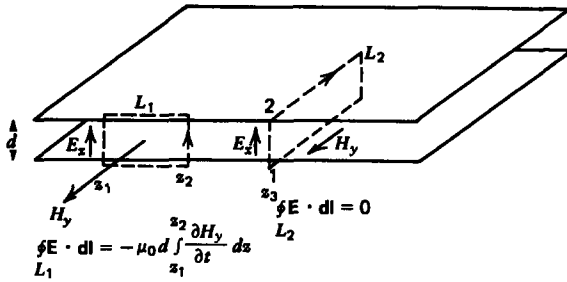


Figure 8-2 The potential difference measured between any two arbitrary points at different positions  $z_1$  and  $z_2$  on the transmission line is not unique—the line integral  $L_1$  of the electric field is nonzero since the contour has magnetic flux passing through it. If the contour  $L_2$  lies within a plane of constant  $z$  such as at  $z_3$ , no magnetic flux passes through it so that the voltage difference between the two electrodes at the same value of  $z$  is unique.

Similarly, the tangential component of  $\mathbf{H}$  is discontinuous at each plate by a surface current  $\pm \mathbf{K}$ . Thus, the total current  $i(z, t)$  flowing in the  $z$  direction on the lower plate is

$$i(z, t) = K_z w = H_y w \tag{4}$$

Substituting (3) and (4) back into (2) results in the transmission line equations:

$$\begin{aligned} \frac{\partial v}{\partial z} &= -L \frac{\partial i}{\partial t} \\ \frac{\partial i}{\partial z} &= -C \frac{\partial v}{\partial t} \end{aligned} \tag{5}$$

where  $L$  and  $C$  are the inductance and capacitance per unit length of the parallel plate structure:

$$L = \frac{\mu d}{w} \text{ henry/m}, \quad C = \frac{\epsilon w}{d} \text{ farad/m} \tag{6}$$

If both quantities are multiplied by the length of the line  $l$ , we obtain the inductance of a single turn plane loop if the line were short circuited, and the capacitance of a parallel plate capacitor if the line were open circuited.

It is no accident that the  $LC$  product

$$LC = \epsilon \mu = 1/c^2 \tag{7}$$

is related to the speed of light in the medium.

### 8-1-2 General Transmission Line Structures

The transmission line equations of (5) are valid for any two-conductor structure of arbitrary shape in the transverse

$xy$  plane but whose cross-sectional area does not change along its axis in the  $z$  direction.  $L$  and  $C$  are the inductance and capacitance per unit length as would be calculated in the quasi-static limits. Various simple types of transmission lines are shown in Figure 8-3. Note that, in general, the field equations of (2) must be extended to allow for  $x$  and  $y$  components but still no  $z$  components:

$$\begin{aligned} \mathbf{E} &= \mathbf{E}_T(x, y, z, t) = E_x \mathbf{i}_x + E_y \mathbf{i}_y, & E_z &= 0 \\ \mathbf{H} &= \mathbf{H}_T(x, y, z, t) = H_x \mathbf{i}_x + H_y \mathbf{i}_y, & H_z &= 0 \end{aligned} \tag{8}$$

We use the subscript  $T$  in (8) to remind ourselves that the fields lie purely in the transverse  $xy$  plane. We can then also distinguish between spatial derivatives along the  $z$  axis ( $\partial/\partial z$ ) from those in the transverse plane ( $\partial/\partial x, \partial/\partial y$ ):

$$\nabla = \underbrace{\nabla_T}_{\mathbf{i}_x \frac{\partial}{\partial x} + \mathbf{i}_y \frac{\partial}{\partial y}} + \mathbf{i}_z \frac{\partial}{\partial z} \tag{9}$$

We may then write Maxwell's equations as

$$\begin{aligned} \nabla_T \times \mathbf{E}_T + \frac{\partial}{\partial z} (\mathbf{i}_z \times \mathbf{E}_T) &= -\mu \frac{\partial \mathbf{H}_T}{\partial t} \\ \nabla_T \times \mathbf{H}_T + \frac{\partial}{\partial z} (\mathbf{i}_z \times \mathbf{H}_T) &= \epsilon \frac{\partial \mathbf{E}_T}{\partial t} \\ \nabla_T \cdot \mathbf{E}_T &= 0 \\ \nabla_T \cdot \mathbf{H}_T &= 0 \end{aligned} \tag{10}$$

The following vector properties for the terms in (10) apply:

- (i)  $\nabla_T \times \mathbf{H}_T$  and  $\nabla_T \times \mathbf{E}_T$  lie purely in the  $z$  direction.
- (ii)  $\mathbf{i}_z \times \mathbf{E}_T$  and  $\mathbf{i}_z \times \mathbf{H}_T$  lie purely in the  $xy$  plane.

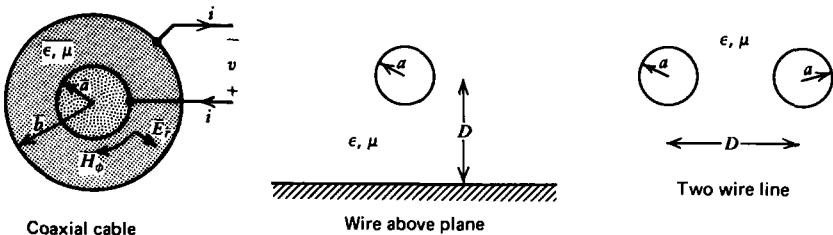


Figure 8-3 Various types of simple transmission lines.

Thus, the equations in (10) may be separated by equating vector components:

$$\begin{aligned}\nabla_T \times \mathbf{E}_T &= 0, & \nabla_T \times \mathbf{H}_T &= 0 \\ \nabla_T \cdot \mathbf{E}_T &= 0, & \nabla_T \cdot \mathbf{H}_T &= 0\end{aligned}\quad (11)$$

$$\begin{aligned}\frac{\partial}{\partial z}(\mathbf{i}_z \times \mathbf{E}_T) &= -\mu \frac{\partial \mathbf{H}_T}{\partial t} \Rightarrow \frac{\partial \mathbf{E}_T}{\partial z} = \mu \frac{\partial}{\partial t}(\mathbf{i}_z \times \mathbf{H}_T) \\ \frac{\partial}{\partial z}(\mathbf{i}_z \times \mathbf{H}_T) &= \epsilon \frac{\partial \mathbf{E}_T}{\partial t}\end{aligned}\quad (12)$$

where the Faraday's law equalities are obtained by crossing with  $\mathbf{i}_z$  and expanding the double cross product

$$\mathbf{i}_z \times (\mathbf{i}_z \times \mathbf{E}_T) = \mathbf{i}_z (\mathbf{i}_z \cdot \mathbf{E}_T) - \mathbf{E}_T (\mathbf{i}_z \cdot \mathbf{i}_z) = -\mathbf{E}_T \quad (13)$$

and remembering that  $\mathbf{i}_z \cdot \mathbf{E}_T = 0$ .

The set of equations in (11) tell us that the field dependences on the transverse coordinates are the same as if the system were static and source free. Thus, all the tools developed for solving static field solutions, including the two-dimensional Laplace's equations and the method of images, can be used to solve for  $\mathbf{E}_T$  and  $\mathbf{H}_T$  in the transverse  $xy$  plane.

We need to relate the fields to the voltage and current defined as a function of  $z$  and  $t$  for the transmission line of arbitrary shape shown in Figure 8-4 as

$$\begin{aligned}v(z, t) &= \int_{z=\text{const}}^2 \mathbf{E}_T \cdot d\mathbf{l} \\ i(z, t) &= \oint_{\text{contour } L \text{ at constant } z \text{ enclosing the inner conductor}} \mathbf{H}_T \cdot d\mathbf{s}\end{aligned}\quad (14)$$

The related quantities of charge per unit length  $q$  and flux per unit length  $\lambda$  along the transmission line are

$$\begin{aligned}q(z, t) &= \epsilon \oint_{z=\text{const}} \mathbf{E}_T \cdot \mathbf{n} \, ds \\ \lambda(z, t) &= \mu \int_{z=\text{const}}^2 \mathbf{H}_T \cdot (\mathbf{i}_z \times d\mathbf{l})\end{aligned}\quad (15)$$

The capacitance and inductance per unit length are then defined as the ratios:

$$\begin{aligned}C &= \frac{q(z, t)}{v(z, t)} = \frac{\epsilon \oint_L \mathbf{E}_T \cdot d\mathbf{s}}{\int_1^2 \mathbf{E}_T \cdot d\mathbf{l}} \Big|_{z=\text{const}} \\ L &= \frac{\lambda(z, t)}{i(z, t)} = \frac{\mu \int_1^2 \mathbf{H}_T \cdot (\mathbf{i}_z \times d\mathbf{l})}{\oint_L \mathbf{H}_T \cdot d\mathbf{s}} \Big|_{z=\text{const}}\end{aligned}\quad (16)$$

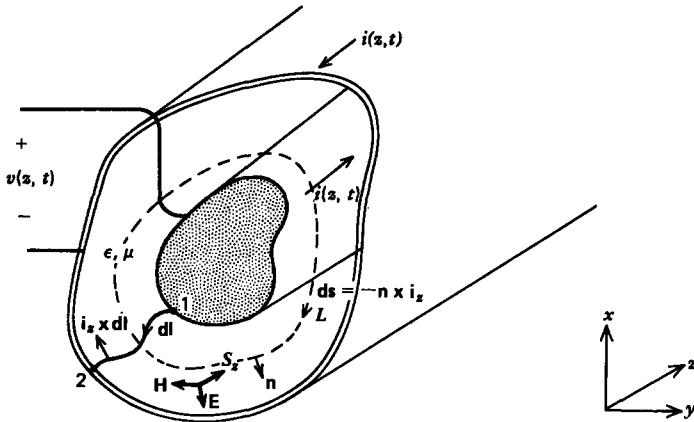


Figure 8-4 A general transmission line has two perfect conductors whose cross-sectional area does not change in the direction along its  $z$  axis, but whose shape in the transverse  $xy$  plane is arbitrary. The electric and magnetic fields are perpendicular, lie in the transverse  $xy$  plane, and have the same dependence on  $x$  and  $y$  as if the fields were static.

which are constants as the geometry of the transmission line does not vary with  $z$ . Even though the fields change with  $z$ , the ratios in (16) do not depend on the field amplitudes.

To obtain the general transmission line equations, we dot the upper equation in (12) with  $d\mathbf{l}$ , which can be brought inside the derivatives since  $d\mathbf{l}$  only varies with  $x$  and  $y$  and not  $z$  or  $t$ . We then integrate the resulting equation over a line at constant  $z$  joining the two electrodes:

$$\begin{aligned} \frac{\partial}{\partial z} \left( \int_1^2 \mathbf{E}_T \cdot d\mathbf{l} \right) &= \frac{\partial}{\partial t} \left( \mu \int_1^2 (\mathbf{i}_z \times \mathbf{H}_T) \cdot d\mathbf{l} \right) \\ &= -\frac{\partial}{\partial t} \left( \mu \int_1^2 \mathbf{H}_T \cdot (\mathbf{i}_z \times d\mathbf{l}) \right) \end{aligned} \quad (17)$$

where the last equality is obtained using the scalar triple product allowing the interchange of the dot and the cross:

$$(\mathbf{i}_z \times \mathbf{H}_T) \cdot d\mathbf{l} = -(\mathbf{H}_T \times \mathbf{i}_z) \cdot d\mathbf{l} = -\mathbf{H}_T \cdot (\mathbf{i}_z \times d\mathbf{l}) \quad (18)$$

We recognize the left-hand side of (17) as the  $z$  derivative of the voltage defined in (14), while the right-hand side is the negative time derivative of the flux per unit length defined in (15):

$$\frac{\partial v}{\partial z} = -\frac{\partial \lambda}{\partial t} = -L \frac{\partial i}{\partial t} \quad (19)$$

We could also have derived this last relation by dotting the upper equation in (12) with the normal  $\mathbf{n}$  to the inner

conductor and then integrating over the contour  $L$  surrounding the inner conductor:

$$\frac{\partial}{\partial z} \left( \oint_L \mathbf{n} \cdot \mathbf{E}_T ds \right) = \frac{\partial}{\partial t} \left( \mu \oint_L \mathbf{n} \cdot (\mathbf{i}_z \times \mathbf{H}_T) ds \right) = - \frac{\partial}{\partial t} \left( \mu \oint_L \mathbf{H}_T \cdot d\mathbf{s} \right) \quad (20)$$

where the last equality was again obtained by interchanging the dot and the cross in the scalar triple product identity:

$$\mathbf{n} \cdot (\mathbf{i}_z \times \mathbf{H}_T) = (\mathbf{n} \times \mathbf{i}_z) \cdot \mathbf{H}_T = -\mathbf{H}_T \cdot d\mathbf{s} \quad (21)$$

The left-hand side of (20) is proportional to the charge per unit length defined in (15), while the right-hand side is proportional to the current defined in (14):

$$\frac{1}{\epsilon} \frac{\partial q}{\partial z} = -\mu \frac{\partial i}{\partial t} \Rightarrow C \frac{\partial v}{\partial z} = -\epsilon \mu \frac{\partial i}{\partial t} \quad (22)$$

Since (19) and (22) must be identical, we obtain the general result previously obtained in Section 6-5-6 that the inductance and capacitance per unit length of any arbitrarily shaped transmission line are related as

$$LC = \epsilon \mu \quad (23)$$

We obtain the second transmission line equation by dotting the lower equation in (12) with  $d\mathbf{l}$  and integrating between electrodes:

$$\frac{\partial}{\partial t} \left( \epsilon \int_1^2 \mathbf{E}_T \cdot d\mathbf{l} \right) = \frac{\partial}{\partial z} \left( \int_1^2 (\mathbf{i}_z \times \mathbf{H}_T) \cdot d\mathbf{l} \right) = - \frac{\partial}{\partial z} \left( \int_1^2 \mathbf{H}_T \cdot (\mathbf{i}_z \times d\mathbf{l}) \right) \quad (24)$$

to yield from (14)–(16) and (23)

$$\epsilon \frac{\partial v}{\partial t} = - \frac{1}{\mu} \frac{\partial \lambda}{\partial z} = - \frac{L}{\mu} \frac{\partial i}{\partial z} \Rightarrow \frac{\partial i}{\partial z} = -C \frac{\partial v}{\partial t} \quad (25)$$

### EXAMPLE 8-1 THE COAXIAL TRANSMISSION LINE

Consider the coaxial transmission line shown in Figure 8-3 composed of two perfectly conducting concentric cylinders of radii  $a$  and  $b$  enclosing a linear medium with permittivity  $\epsilon$  and permeability  $\mu$ . We solve for the transverse dependence of the fields as if the problem were static, independent of time. If the voltage difference between cylinders is  $v$  with the inner cylinder carrying a total current  $i$  the static fields are

$$\mathbf{E}_r = \frac{v}{r \ln(b/a)}, \quad \mathbf{H}_\phi = \frac{i}{2\pi r}$$

The surface charge per unit length  $q$  and magnetic flux per unit length  $\lambda$  are

$$q = \epsilon E_r(r=a)2\pi a = \frac{2\pi\epsilon v}{\ln(b/a)}$$

$$\lambda = \int_a^b \mu H_\phi dr = \frac{\mu i}{2\pi} \ln \frac{b}{a}$$

so that the capacitance and inductance per unit length of this structure are

$$C = \frac{q}{v} = \frac{2\pi\epsilon}{\ln(b/a)}, \quad L = \frac{\lambda}{i} = \frac{\mu}{2\pi} \ln \frac{b}{a}$$

where we note that as required

$$LC = \epsilon\mu$$

Substituting  $E_r$  and  $H_\phi$  into (12) yields the following transmission line equations:

$$\frac{\partial E_r}{\partial z} = -\mu \frac{\partial H_\phi}{\partial t} \Rightarrow \frac{\partial v}{\partial z} = -L \frac{\partial i}{\partial t}$$

$$\frac{\partial H_\phi}{\partial z} = -\epsilon \frac{\partial E_r}{\partial t} \Rightarrow \frac{\partial i}{\partial z} = -C \frac{\partial v}{\partial t}$$

### 8-1-3 Distributed Circuit Representation

Thus far we have emphasized the field theory point of view from which we have derived relations for the voltage and current. However, we can also easily derive the transmission line equations using a distributed equivalent circuit derived from the following criteria:

- (i) The flow of current through a lossless medium between two conductors is entirely by displacement current, in exactly the same way as a capacitor.
- (ii) The flow of current along lossless electrodes generates a magnetic field as in an inductor.

Thus, we may discretize the transmission line into many small incremental sections of length  $\Delta z$  with series inductance  $L \Delta z$  and shunt capacitance  $C \Delta z$ , where  $L$  and  $C$  are the inductance and capacitance per unit lengths. We can also take into account the small series resistance of the electrodes  $R \Delta z$ , where  $R$  is the resistance per unit length (ohms per meter) and the shunt conductance loss in the dielectric  $G \Delta z$ , where  $G$  is the conductance per unit length (siemens per meter). If the transmission line and dielectric are lossless,  $R = 0$ ,  $G = 0$ .

The resulting equivalent circuit for a lossy transmission line shown in Figure 8-5 shows that the current at  $z + \Delta z$  and  $z$  differ by the amount flowing through the shunt capacitance and conductance:

$$i(z, t) - i(z + \Delta z, t) = C \Delta z \frac{\partial v(z, t)}{\partial t} + G \Delta z v(z, t) \quad (26)$$

Similarly, the voltage difference at  $z + \Delta z$  from  $z$  is due to the drop across the series inductor and resistor:

$$v(z, t) - v(z + \Delta z, t) = L \Delta z \frac{\partial i(z + \Delta z, t)}{\partial t} + i(z + \Delta z, t) R \Delta z \quad (27)$$

By dividing (26) and (27) through by  $\Delta z$  and taking the limit as  $\Delta z \rightarrow 0$ , we obtain the lossy transmission line equations:

$$\lim_{\Delta z \rightarrow 0} \frac{i(z + \Delta z, t) - i(z, t)}{\Delta z} = \frac{\partial i}{\partial z} = -C \frac{\partial v}{\partial t} - Gv \quad (28)$$

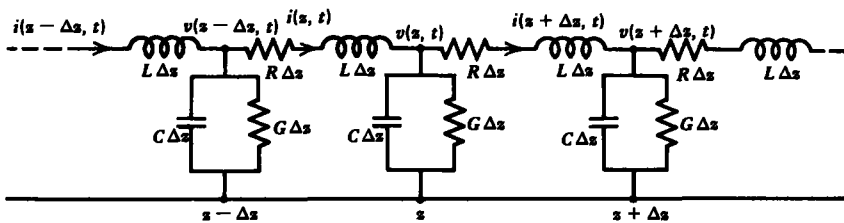
$$\lim_{\Delta z \rightarrow 0} \frac{v(z + \Delta z, t) - v(z, t)}{\Delta z} = \frac{\partial v}{\partial z} = -L \frac{\partial i}{\partial t} - iR$$

which reduce to (19) and (25) when  $R$  and  $G$  are zero.

### 8-1-4 Power Flow

Multiplying the upper equation in (28) by  $v$  and the lower by  $i$  and then adding yields the circuit equivalent form of Poynting's theorem:

$$\frac{\partial}{\partial z} (vi) = -\frac{\partial}{\partial t} (\frac{1}{2} C v^2 + \frac{1}{2} L i^2) - G v^2 - i^2 R \quad (29)$$



$$v(z, t) - v(z + \Delta z, t) = L \Delta z \frac{\partial}{\partial t} i(z + \Delta z, t) + i(z + \Delta z, t) R \Delta z$$

$$i(z, t) - i(z + \Delta z, t) = C \Delta z \frac{\partial}{\partial t} v(z, t) + G \Delta z v(z, t)$$

Figure 8-5 Distributed circuit model of a transmission line including small series and shunt resistive losses.

The power flow  $vi$  is converted into energy storage ( $\frac{1}{2}Cv^2 + \frac{1}{2}Li^2$ ) or is dissipated in the resistance and conductance per unit lengths.

From the fields point of view the total electromagnetic power flowing down the transmission line at any position  $z$  is

$$P(z, t) = \int_S (\mathbf{E}_T \times \mathbf{H}_T) \cdot \mathbf{i}_z dS = \int_S \mathbf{E}_T \cdot (\mathbf{H}_T \times \mathbf{i}_z) dS \quad (30)$$

where  $S$  is the region between electrodes in Figure 8-4. Because the transverse electric field is curl free, we can define the scalar potential

$$\nabla \times \mathbf{E}_T = 0 \Rightarrow \mathbf{E}_T = -\nabla_T V \quad (31)$$

so that (30) can be rewritten as

$$P(z, t) = \int_S (\mathbf{i}_z \times \mathbf{H}_T) \cdot \nabla_T V dS \quad (32)$$

It is useful to examine the vector expansion

$$\nabla_T \cdot [V(\mathbf{i}_z \times \mathbf{H}_T)] = (\mathbf{i}_z \times \mathbf{H}_T) \cdot \nabla_T V + V \nabla_T \cdot (\mathbf{i}_z \times \overset{0}{\mathbf{H}_T}) \quad (33)$$

where the last term is zero because  $\mathbf{i}_z$  is a constant vector and  $\mathbf{H}_T$  is also curl free:

$$\nabla_T \cdot (\mathbf{i}_z \times \mathbf{H}_T) = \mathbf{H}_T \cdot (\nabla_T \times \mathbf{i}_z) - \mathbf{i}_z \cdot (\nabla_T \times \mathbf{H}_T) = 0 \quad (34)$$

Then (32) can be converted to a line integral using the two-dimensional form of the divergence theorem:

$$\begin{aligned} P(z, t) &= \int_S \nabla_T \cdot [V(\mathbf{i}_z \times \mathbf{H}_T)] dS \\ &= - \int_{\substack{\text{contours on} \\ \text{the surfaces of} \\ \text{both electrodes}}} V(\mathbf{i}_z \times \mathbf{H}_T) \cdot \mathbf{n} ds \end{aligned} \quad (35)$$

where the line integral is evaluated at constant  $z$  along the surface of both electrodes. The minus sign arises in (35) because  $\mathbf{n}$  is defined inwards in Figure 8-4 rather than outwards as is usual in the divergence theorem. Since we are free to pick our zero potential reference anywhere, we take the outer conductor to be at zero voltage. Then the line integral in (35) is only nonzero over the inner conductor,

where  $V = v$ :

$$\begin{aligned}
 P(z, t) &= -v \oint_{\text{inner conductor}} (\mathbf{i}_z \times \mathbf{H}_T) \cdot \mathbf{n} \, ds \\
 &= v \oint_{\text{inner conductor}} (\mathbf{H}_T \times \mathbf{i}_z) \cdot \mathbf{n} \, ds \\
 &= v \oint_{\text{inner conductor}} \mathbf{H}_T \cdot (\mathbf{i}_z \times \mathbf{n}) \, ds \\
 &= v \oint_{\text{inner conductor}} \mathbf{H}_T \cdot \mathbf{d}\mathbf{s} \\
 &= vi
 \end{aligned} \tag{36}$$

where we realized that  $(\mathbf{i}_z \times \mathbf{n}) \, ds = \mathbf{d}\mathbf{s}$ , defined in Figure 8-4 if  $L$  lies along the surface of the inner conductor. The electromagnetic power flowing down a transmission line just equals the circuit power.

### 8-1-5 The Wave Equation

Restricting ourselves now to lossless transmission lines so that  $R = G = 0$  in (28), the two coupled equations in voltage and current can be reduced to two single wave equations in  $v$  and  $i$ :

$$\begin{aligned}
 \frac{\partial^2 v}{\partial t^2} &= c^2 \frac{\partial^2 v}{\partial z^2} \\
 \frac{\partial^2 i}{\partial t^2} &= c^2 \frac{\partial^2 i}{\partial z^2}
 \end{aligned} \tag{37}$$

where the speed of the waves is

$$c = \frac{1}{\sqrt{LC}} = \frac{1}{\sqrt{\epsilon\mu}} \text{ m/sec} \tag{38}$$

As we found in Section 7-3-2 the solutions to (37) are propagating waves in the  $\pm z$  directions at the speed  $c$ :

$$\begin{aligned}
 v(z, t) &= V_+(t - z/c) + V_-(t + z/c) \\
 i(z, t) &= I_+(t - z/c) + I_-(t + z/c)
 \end{aligned} \tag{39}$$

where the functions  $V_+$ ,  $V_-$ ,  $I_+$ , and  $I_-$  are determined by boundary conditions imposed by sources and transmission

line terminations. By substituting these solutions back into (28) with  $R = G = 0$ , we find the voltage and current functions related as

$$\begin{aligned} V_+ &= I_+ Z_0 \\ V_- &= -I_- Z_0 \end{aligned} \quad (40)$$

where

$$Z_0 = \sqrt{L/C} \text{ ohm} \quad (41)$$

is known as the characteristic impedance of the transmission line, analogous to the wave impedance  $\eta$  in Chapter 7. Its inverse  $Y_0 = 1/Z_0$  is also used and is termed the characteristic admittance. In practice, it is difficult to measure  $L$  and  $C$  of a transmission line directly. It is easier to measure the wave speed  $c$  and characteristic impedance  $Z_0$  and then calculate  $L$  and  $C$  from (38) and (41).

The most useful form of the transmission line solutions of (39) that we will use is

$$\begin{aligned} v(z, t) &= V_+(t - z/c) + V_-(t + z/c) \\ i(z, t) &= Y_0[V_+(t - z/c) - V_-(t + z/c)] \end{aligned} \quad (42)$$

Note the complete duality between these voltage-current solutions and the plane wave solutions in Section 7-3-2 for the electric and magnetic fields.

## 8-2 TRANSMISSION LINE TRANSIENT WAVES

The easiest way to solve for transient waves on transmission lines is through use of physical reasoning as opposed to mathematical rigor. Since the waves travel at a speed  $c$ , once generated they cannot reach any position  $z$  until a time  $z/c$  later. Waves traveling in the positive  $z$  direction are described by the function  $V_+(t - z/c)$  and waves traveling in the  $-z$  direction by  $V_-(t + z/c)$ . However, at any time  $t$  and position  $z$ , the voltage is equal to the sum of both solutions while the current is proportional to their difference.

### 8-2-1 Transients on Infinitely Long Transmission Lines

The transmission line shown in Figure 8-6a extends to infinity in the positive  $z$  direction. A time varying voltage source  $V(t)$  that is turned on at  $t = 0$  is applied at  $z = 0$  to the line which is initially unexcited. A positively traveling wave  $V_+(t - z/c)$  propagates away from the source. There is no negatively traveling wave,  $V_-(t + z/c) = 0$ . These physical

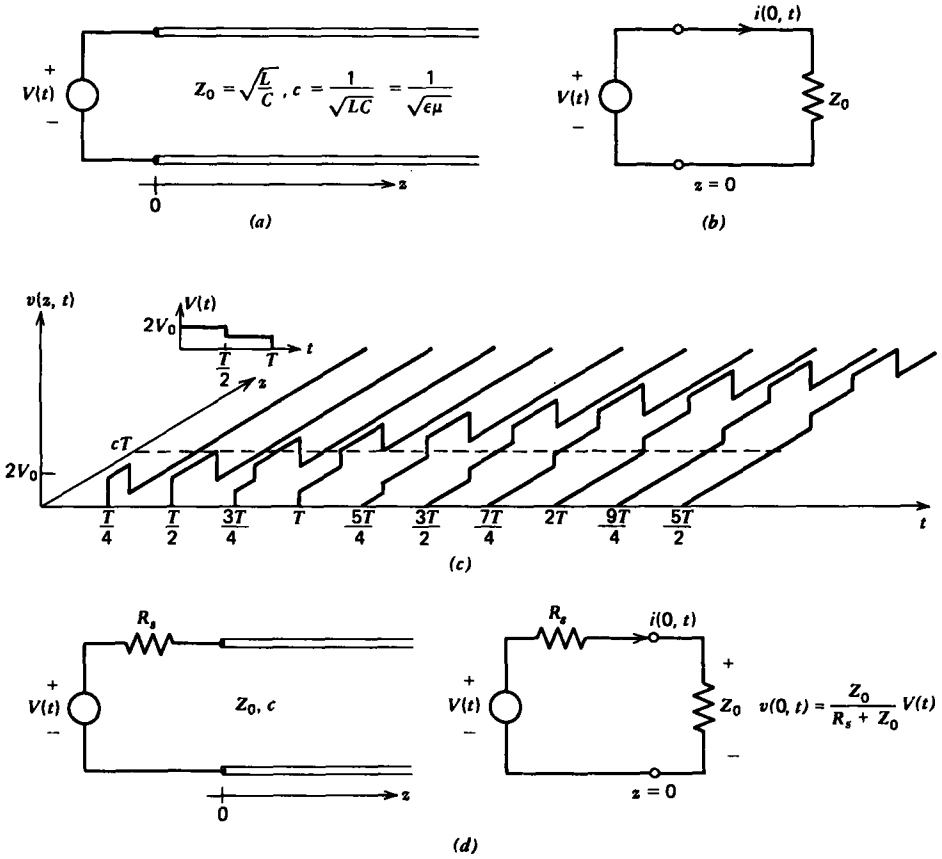


Figure 8-6 (a) A semi-infinite transmission line excited by a voltage source at  $z = 0$ . (b) To the source, the transmission line looks like a resistor  $Z_0$  equal to the characteristic impedance. (c) The spatial distribution of the voltage  $v(z, t)$  at various times for a staircase pulse of  $V(t)$ . (d) If the voltage source is applied to the transmission line through a series resistance  $R_s$ , the voltage across the line at  $z = 0$  is given by the voltage divider relation.

arguments are verified mathematically by realizing that at  $t = 0$  the voltage and current are zero for  $z > 0$ ,

$$v(z, t = 0) = V_+(-z/c) + V_-(-z/c) = 0 \tag{1}$$

$$i(z, t = 0) = Y_0[V_+(-z/c) - V_-(-z/c)] = 0$$

which only allows the trivial solutions

$$V_+(-z/c) = 0, \quad V_-(-z/c) = 0 \tag{2}$$

Since  $z$  can only be positive, whenever the argument of  $V_+$  is negative and of  $V_-$  positive, the functions are zero. Since  $t$  can only be positive, the argument of  $V_-(t + z/c)$  is always positive

so that the function is always zero. The argument of  $V_+(t - z/c)$  can be positive, allowing a nonzero solution if  $t > z/c$  agreeing with our conclusions reached by physical arguments.

With  $V_-(t + z/c) = 0$ , the voltage and current are related as

$$\begin{aligned} v(z, t) &= V_+(t - z/c) \\ i(z, t) &= Y_0 V_+(t - z/c) \end{aligned} \tag{3}$$

The line voltage and current have the same shape as the source, delayed in time for any  $z$  by  $z/c$  with the current scaled in amplitude by  $Y_0$ . Thus as far as the source is concerned, the transmission line looks like a resistor of value  $Z_0$  yielding the equivalent circuit at  $z = 0$  shown in Figure 8-6*b*. At  $z = 0$ , the voltage equals that of the source

$$v(0, t) = V(t) = V_+(t) \tag{4}$$

If  $V(t)$  is the staircase pulse of total duration  $T$  shown in Figure 8-6*c*, the pulse extends in space over the spatial interval:

$$\begin{aligned} 0 \leq z \leq ct, & \quad 0 \leq t \leq T \\ c(t - T) \leq z \leq ct, & \quad t > T \end{aligned} \tag{5}$$

The analysis is the same even if the voltage source is in series with a source resistance  $R_s$ , as in Figure 8-6*d*. At  $z = 0$  the transmission line still looks like a resistor of value  $Z_0$  so that the transmission line voltage divides in the ratio given by the equivalent circuit shown:

$$\begin{aligned} v(z = 0, t) &= \frac{Z_0}{R_s + Z_0} V(t) = V_+(t) \\ i(z = 0, t) &= Y_0 V_+(t) = \frac{V(t)}{R_s + Z_0} \end{aligned} \tag{6}$$

The total solution is then identical to that of (3) and (4) with the voltage and current amplitudes reduced by the voltage divider ratio  $Z_0/(R_s + Z_0)$ .

### 8-2-2 Reflections from Resistive Terminations

#### (a) Reflection Coefficient

All transmission lines must have an end. In Figure 8-7 we see a positively traveling wave incident upon a load resistor  $R_L$  at  $z = l$ . The reflected wave will travel back towards the source at  $z = 0$  as a  $V_-$  wave. At the  $z = l$  end the following circuit

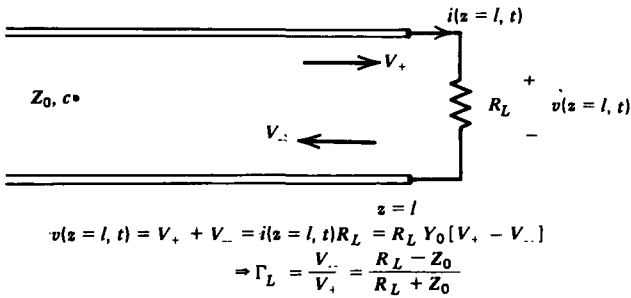


Figure 8-7 A  $V_+$  wave incident upon the end of a transmission line with a load resistor  $R_L$  is reflected as a  $V_-$  wave.

relations hold:

$$\begin{aligned} v(l, t) &= V_+(t - l/c) + V_-(t + l/c) \\ &= i(l, t)R_L \\ &= Y_0 R_L [V_+(t - l/c) - V_-(t + l/c)] \end{aligned} \quad (7)$$

We then find the amplitude of the negatively traveling wave in terms of the incident positively traveling wave as

$$\Gamma_L = \frac{V_-(t + l/c)}{V_+(t - l/c)} = \frac{R_L - Z_0}{R_L + Z_0} \quad (8)$$

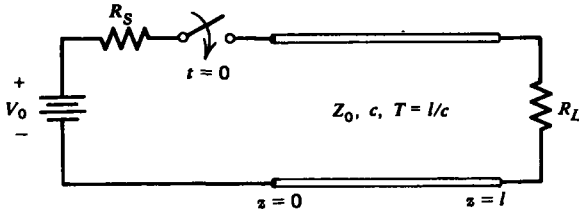
where  $\Gamma_L$  is known as the reflection coefficient that is of the same form as the reflection coefficient  $R$  in Section 7-6-1 for normally incident uniform plane waves on a dielectric.

The reflection coefficient gives us the relative amplitude of the returning  $V_-$  wave compared to the incident  $V_+$  wave. There are several important limits of (8):

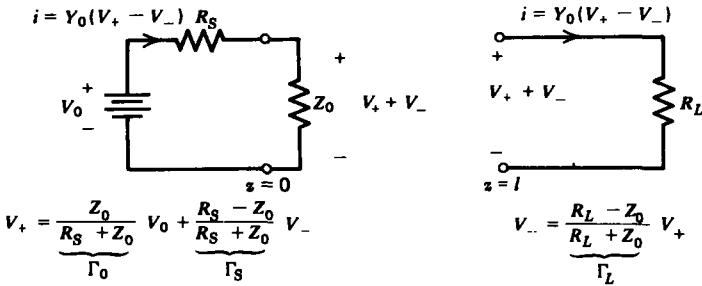
- (i) If  $R_L = Z_0$ , the reflection coefficient is zero ( $\Gamma_L = 0$ ) so that there is no reflected wave and the line is said to be matched.
- (ii) If the line is short circuited ( $R_L = 0$ ), then  $\Gamma_L = -1$ . The reflected wave is equal in amplitude but opposite in sign to the incident wave. In general, if  $R_L < Z_0$ , the reflected voltage wave has its polarity reversed.
- (iii) If the line is open circuited ( $R_L = \infty$ ), then  $\Gamma_L = +1$ . The reflected wave is identical to the incident wave. In general, if  $R_L > Z_0$ , the reflected voltage wave is of the same polarity as the incident wave.

#### (b) Step Voltage

A dc battery of voltage  $V_0$  with series resistance  $R$ , is switched onto the transmission line at  $t=0$ , as shown in Figure 8-8a. At  $z=0$ , the source has no knowledge of the



(a)



(b)

Figure 8-8 (a) A dc voltage  $V_0$  is switched onto a resistively loaded transmission line through a source resistance  $R_s$ . (b) The equivalent circuits at  $z = 0$  and  $z = l$  allow us to calculate the reflected voltage wave amplitudes in terms of the incident waves.

line's length or load termination, so as for an infinitely long line the transmission line looks like a resistor of value  $Z_0$  to the source. There is no  $V_-$  wave initially. The  $V_+$  wave is determined by the voltage divider ratio of the series source resistance and transmission line characteristic impedance as given by (6).

This  $V_+$  wave travels down the line at speed  $c$  where it is reflected at  $z = l$  for  $t > T$ , where  $T = l/c$  is the transit time for a wave propagating between the two ends. The new  $V_-$  wave generated is related to the incident  $V_+$  wave by the reflection coefficient  $\Gamma_L$ . As the  $V_+$  wave continues to propagate in the positive  $z$  direction, the  $V_-$  wave propagates back towards the source. The total voltage at any point on the line is equal to the sum of  $V_+$  and  $V_-$  while the current is proportional to their difference.

When the  $V_-$  wave reaches the end of the transmission line at  $z = 0$  at time  $2T$ , in general a new  $V_+$  wave is generated, which can be found by solving the equivalent circuit shown in Figure 8-8b:

$$v(0, t) + i(0, t)R_s = V_0 \Rightarrow V_+(0, t) + V_-(0, t) + Y_0R_s[V_+(0, t) - V_-(0, t)] = V_0 \quad (9)$$

to yield

$$V_+(0, t) = \Gamma_s V_-(0, t) + \frac{Z_0 V_0}{Z_0 + R_s}, \quad \Gamma_s = \frac{R_s - Z_0}{R_s + Z_0} \quad (10)$$

where  $\Gamma_s$  is just the reflection coefficient at the source end. This new  $V_+$  wave propagates towards the load again generating a new  $V_-$  wave as the reflections continue.

If the source resistance is matched to the line,  $R_s = Z_0$  so that  $\Gamma_s = 0$ , then  $V_+$  is constant for all time and the steady state is reached for  $t > 2T$ . If the load was matched, the steady state is reached for  $t > T$  no matter the value of  $R_s$ . There are no further reflections from the end of a matched line. In Figure 8-9 we plot representative voltage and current spatial distributions for various times assuming the source is matched to the line for the load being matched, open, or short circuited.

(i) Matched Line

When  $R_L = Z_0$  the load reflection coefficient is zero so that  $V_+ = V_0/2$  for all time. The wavefront propagates down the line with the voltage and current being identical in shape. The system is in the dc steady state for  $t \geq T$ .

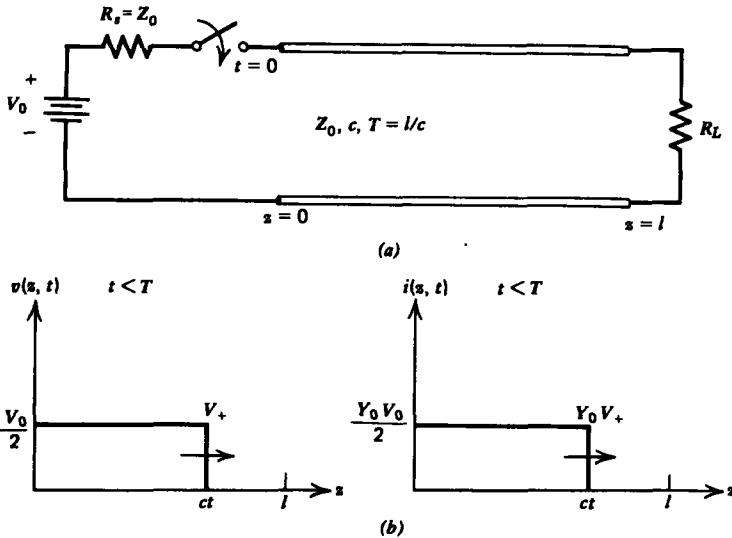


Figure 8-9 (a) A dc voltage is switched onto a transmission line with load resistance  $R_L$  through a source resistance  $R_s$  matched to the line. (b) Regardless of the load resistance, half the source voltage propagates down the line towards the load. If the load is also matched to the line ( $R_L = Z_0$ ), there are no reflections and the steady state of  $v(z, t \geq T) = V_0/2$ ,  $i(z, t \geq T) = Y_0 V_0/2$  is reached for  $t \geq T$ . (c) If the line is short circuited ( $R_L = 0$ ), then  $\Gamma_L = -1$  so that the  $V_+$  and  $V_-$  waves cancel for the voltage but add for the current wherever they overlap in space. Since the source end is matched, no further reflections arise at  $z = 0$  so that the steady state is reached for  $t \geq 2T$ . (d) If the line is open circuited ( $R_L = \infty$ ) so that  $\Gamma_L = +1$ , the  $V_+$  and  $V_-$  waves add for the voltage but cancel for the current.

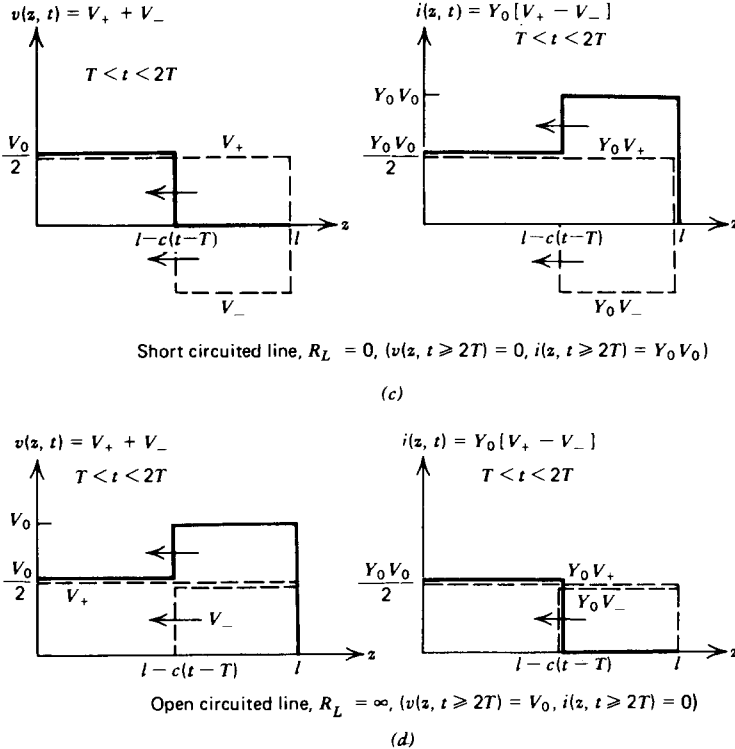


Figure 8-9

**(ii) Open Circuited Line**

When  $R_L = \infty$  the reflection coefficient is unity so that  $V_+ = V_-$ . When the incident and reflected waves overlap in space the voltages add to a staircase pulse shape while the current is zero. For  $t \geq 2T$ , the voltage is  $V_0$  everywhere on the line while the current is zero.

**(iii) Short Circuited Line**

When  $R_L = 0$  the load reflection coefficient is  $-1$  so that  $V_+ = -V_-$ . When the incident and reflected waves overlap in space, the total voltage is zero while the current is now a staircase pulse shape. For  $t \geq 2T$  the voltage is zero everywhere on the line while the current is  $V_0/Z_0$ .

**8-2-3 Approach to the dc Steady State**

If the load end is matched, the steady state is reached after one transit time  $T = l/c$  for the wave to propagate from the source to the load. If the source end is matched, after one

round trip  $2T = 2l/c$  no further reflections occur. If neither end is matched, reflections continue on forever. However, for nonzero and noninfinite source and load resistances, the reflection coefficient is always less than unity in magnitude so that each successive reflection is reduced in amplitude. After a few round-trips, the changes in  $V_+$  and  $V_-$  become smaller and eventually negligible. If the source resistance is zero and the load resistance is either zero or infinite, the transient pulses continue to propagate back and forth forever in the lossless line, as the magnitude of the reflection coefficients are unity.

Consider again the dc voltage source in Figure 8-8a switched through a source resistance  $R_s$  at  $t=0$  onto a transmission line loaded at its  $z=l$  end with a load resistor  $R_L$ . We showed in (10) that the  $V_+$  wave generated at the  $z=0$  end is related to the source and an incoming  $V_-$  wave as

$$V_+ = \Gamma_0 V_0 + \Gamma_s V_-, \quad \Gamma_0 = \frac{Z_0}{R_s + Z_0}, \quad \Gamma_s = \frac{R_s - Z_0}{R_s + Z_0} \quad (11)$$

Similarly, at  $z=l$ , an incident  $V_+$  wave is converted into a  $V_-$  wave through the load reflection coefficient:

$$V_- = \Gamma_L V_+, \quad \Gamma_L = \frac{R_L - Z_0}{R_L + Z_0} \quad (12)$$

We can now tabulate the voltage at  $z=l$  using the following reasoning:

- (i) For the time interval  $t < T$  the voltage at  $z=l$  is zero as no wave has yet reached the end.
- (ii) At  $z=0$  for  $0 \leq t \leq 2T$ ,  $V_- = 0$  resulting in a  $V_+$  wave emanating from  $z=0$  with amplitude  $V_+ = \Gamma_0 V_0$ .
- (iii) When this  $V_+$  wave reaches  $z=l$ , a  $V_-$  wave is generated with amplitude  $V_- = \Gamma_L V_+$ . The incident  $V_+$  wave at  $z=l$  remains unchanged until another interval of  $2T$ , whereupon the just generated  $V_-$  wave after being reflected from  $z=0$  as a new  $V_+$  wave given by (11) again returns to  $z=l$ .
- (iv) Thus, the voltage at  $z=l$  only changes at times  $(2n-1)T$ ,  $n=1, 2, \dots$ , while the voltage at  $z=0$  changes at times  $2(n-1)T$ . The resulting voltage waveforms at the ends are stairstep patterns with steps at these times.

The  $n$ th traveling  $V_+$  wave is then related to the source and the  $(n-1)$ th  $V_-$  wave at  $z=0$  as

$$V_{+n} = \Gamma_0 V_0 + \Gamma_s V_{-(n-1)} \quad (13)$$

while the  $(n - 1)$ th  $V_-$  wave is related to the incident  $(n - 1)$ th  $V_+$  wave at  $z = l$  as

$$V_{-(n-1)} = \Gamma_L V_{+(n-1)} \tag{14}$$

Using (14) in (13) yields a single linear constant coefficient difference equation in  $V_{+n}$ :

$$V_{+n} - \Gamma_s \Gamma_L V_{+(n-1)} = \Gamma_0 V_0 \tag{15}$$

For a particular solution we see that  $V_{+n}$  being a constant satisfies (15):

$$V_{+n} = C \Rightarrow C(1 - \Gamma_s \Gamma_L) = \Gamma_0 V_0 \Rightarrow C = \frac{\Gamma_0}{1 - \Gamma_s \Gamma_L} V_0 \tag{16}$$

To this solution we can add any homogeneous solution assuming the right-hand side of (15) is zero:

$$V_{+n} - \Gamma_s \Gamma_L V_{+(n-1)} = 0 \tag{17}$$

We try a solution of the form

$$V_{+n} = A \lambda^n \tag{18}$$

which when substituted into (17) requires

$$A \lambda^{n-1} (\lambda - \Gamma_s \Gamma_L) = 0 \Rightarrow \lambda = \Gamma_s \Gamma_L \tag{19}$$

The total solution is then a sum of the particular and homogeneous solutions:

$$V_{+n} = \frac{\Gamma_0}{1 - \Gamma_s \Gamma_L} V_0 + A (\Gamma_s \Gamma_L)^n \tag{20}$$

The constant  $A$  is found by realizing that the first transient wave is

$$\dot{V}_{+1} = \Gamma_0 V_0 = \frac{\Gamma_0}{1 - \Gamma_s \Gamma_L} V_0 + A (\Gamma_s \Gamma_L) \tag{21}$$

which requires  $A$  to be

$$A = -\frac{\Gamma_0 V_0}{1 - \Gamma_s \Gamma_L} \tag{22}$$

so that (20) becomes

$$V_{+n} = \frac{\Gamma_0 V_0}{1 - \Gamma_s \Gamma_L} [1 - (\Gamma_s \Gamma_L)^n] \tag{23}$$

Raising the index of (14) by one then gives the  $n$ th  $V_-$  wave as

$$V_{-n} = \Gamma_L V_{+n} \tag{24}$$

so that the total voltage at  $z = l$  after  $n$  reflections at times  $(2n - 1)T$ ,  $n = 1, 2, \dots$ , is

$$V_n = V_{+n} + V_{-n} = \frac{V_0 \Gamma_0 (1 + \Gamma_L)}{1 - \Gamma_s \Gamma_L} [1 - (\Gamma_s \Gamma_L)^n] \quad (25)$$

or in terms of the source and load resistances

$$V_n = \frac{R_L}{R_L + R_s} V_0 [1 - (\Gamma_s \Gamma_L)^n] \quad (26)$$

The steady-state results as  $n \rightarrow \infty$ . If either  $R_s$  or  $R_L$  are nonzero or noninfinite, the product of  $\Gamma_s \Gamma_L$  must be less than unity. Under these conditions

$$\lim_{\substack{n \rightarrow \infty \\ (|\Gamma_s \Gamma_L| < 1)}} (\Gamma_s \Gamma_L)^n = 0 \quad (27)$$

so that in the steady state

$$\lim_{n \rightarrow \infty} V_n = \frac{R_L}{R_s + R_L} V_0 \quad (28)$$

which is just the voltage divider ratio as if the transmission line was just a pair of zero-resistance connecting wires. Note also that if either end is matched so that either  $\Gamma_s$  or  $\Gamma_L$  is zero, the voltage at the load end is immediately in the steady state after the time  $T$ .

In Figure 8-10 the load is plotted versus time with  $R_s = 0$  and  $R_L = 3Z_0$  so that  $\Gamma_s \Gamma_L = -\frac{1}{2}$  and with  $R_L = \frac{1}{3}Z_0$  so that

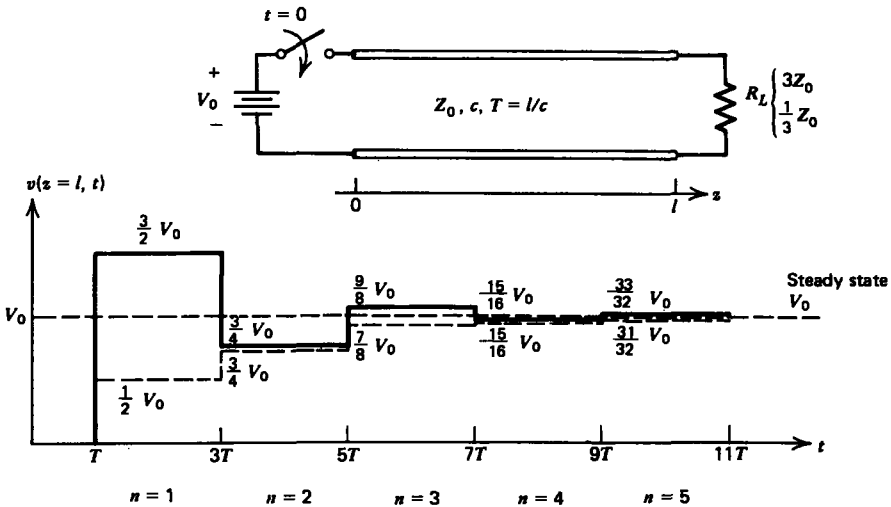


Figure 8-10 The load voltage as a function of time when  $R_s = 0$  and  $R_L = 3Z_0$  so that  $\Gamma_s \Gamma_L = -\frac{1}{2}$  (solid) and with  $R_L = \frac{1}{3}Z_0$  so that  $\Gamma_s \Gamma_L = \frac{1}{2}$  (dashed). The dc steady state is the same as if the transmission line were considered a pair of perfectly conducting wires in a circuit.

$\Gamma_s \Gamma_L = +\frac{1}{2}$ . Then (26) becomes

$$V_n = \begin{cases} V_0 [1 - (-\frac{1}{2})^n], & R_L = 3Z_0 \\ V_0 [1 - (\frac{1}{2})^n], & R_L = \frac{1}{3}Z_0 \end{cases} \quad (29)$$

The step changes in load voltage oscillate about the steady-state value  $V_\infty = V_0$ . The steps rapidly become smaller having less than one-percent variation for  $n > 7$ .

If the source resistance is zero and the load resistance is either zero or infinite (short or open circuits), a lossless transmission line never reaches a dc steady state as the limit of (27) does not hold with  $\Gamma_s \Gamma_L = \pm 1$ . Continuous reflections with no decrease in amplitude results in pulse waveforms for all time. However, in a real transmission line, small losses in the conductors and dielectric allow a steady state to be eventually reached.

Consider the case when  $R_s = 0$  and  $R_L = \infty$  so that  $\Gamma_s \Gamma_L = -1$ . Then from (26) we have

$$V_n = \begin{cases} 0, & n \text{ even} \\ 2V_0, & n \text{ odd} \end{cases} \quad (30)$$

which is sketched in Figure 8-11a.

For any source and load resistances the current through the load resistor at  $z = l$  is

$$\begin{aligned} I_n &= \frac{V_n}{R_L} = \frac{V_0 \Gamma_0 (1 + \Gamma_L)}{R_L (1 - \Gamma_s \Gamma_L)} [1 - (\Gamma_s \Gamma_L)^n] \\ &= \frac{2V_0 \Gamma_0}{R_L + Z_0} \frac{[1 - (\Gamma_s \Gamma_L)^n]}{(1 - \Gamma_s \Gamma_L)} \end{aligned} \quad (31)$$

If both  $R_s$  and  $R_L$  are zero so that  $\Gamma_s \Gamma_L = 1$ , the short circuit current in (31) is in the indeterminate form  $0/0$ , which can be evaluated using l'Hôpital's rule:

$$\begin{aligned} \lim_{\Gamma_s \Gamma_L \rightarrow 1} I_n &= \frac{2V_0 \Gamma_0}{R_L + Z_0} \frac{[-n(\Gamma_s \Gamma_L)^{n-1}]}{(-1)} \\ &= \frac{2V_0 n}{Z_0} \end{aligned} \quad (32)$$

As shown by the solid line in Figure 8-11b, the current continually increases in a stepwise fashion. As  $n$  increases to infinity, the current also becomes infinite, which is expected for a battery connected across a short circuit.

## 8-2-4 Inductors and Capacitors as Quasi-static Approximations to Transmission Lines

If the transmission line was one meter long with a free space dielectric medium, the round trip transit time  $2T = 2l/c$

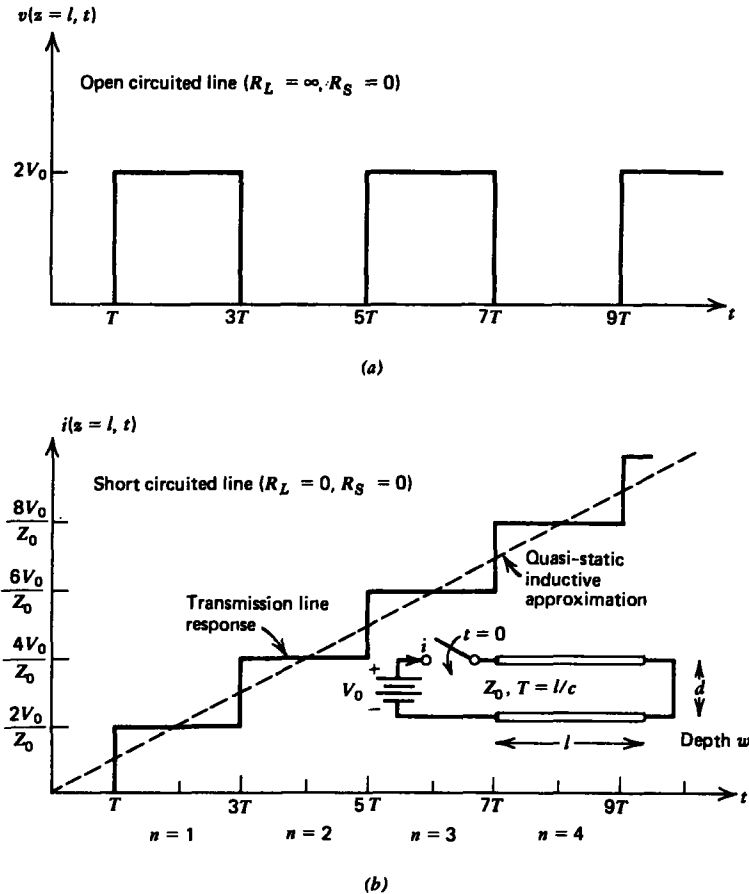


Figure 8-11 The (a) open circuit voltage and (b) short circuit current at the  $z = l$  end of the transmission line for  $R_L = 0$ . No dc steady state is reached because the system is lossless. If the short circuited transmission line is modeled as an inductor in the quasi-static limit, a step voltage input results in a linearly increasing current (shown dashed). The exact transmission line response is the solid staircase waveform.

is approximately 6 nsec. For many circuit applications this time is so fast that it may be considered instantaneous. In this limit the quasi-static circuit element approximation is valid.

For example, consider again the short circuited transmission line ( $R_L = 0$ ) of length  $l$  with zero source resistance. In the magnetic quasi-static limit we would call the structure an inductor with inductance  $Ll$  (remember,  $L$  is the inductance per unit length) so that the terminal voltage and current are related as

$$v = (Ll) \frac{di}{dt} \tag{33}$$

If a constant voltage  $V_0$  is applied at  $t=0$ , the current is obtained by integration of (33) as

$$i = \frac{V_0}{Ll} t \quad (34)$$

where we use the initial condition of zero current at  $t=0$ . The linear time dependence of the current, plotted as the dashed line in Figure 8-11*b*, approximates the rising staircase waveform obtained from the exact transmission line analysis of (32).

Similarly, if the transmission line were open circuited with  $R_L = \infty$ , it would be a capacitor of value  $Cl$  in the electric quasi-static limit so that the voltage on the line charges up through the source resistance  $R_s$  with time constant  $\tau = R_s Cl$  as

$$v(t) = V_0(1 - e^{-t/\tau}) \quad (35)$$

The exact transmission line voltage at the  $z=l$  end is given by (26) with  $R_L = \infty$  so that  $\Gamma_L = 1$ :

$$V_n = V_0(1 - \Gamma_s^n) \quad (36)$$

where the source reflection coefficient can be written as

$$\begin{aligned} \Gamma_s &= \frac{R_s - Z_0}{R_s + Z_0} \\ &= \frac{R_s - \sqrt{L/C}}{R_s + \sqrt{L/C}} \end{aligned} \quad (37)$$

If we multiply the numerator and denominator of (37) through by  $Cl$ , we have

$$\begin{aligned} \Gamma_s &= \frac{R_s Cl - l\sqrt{LC}}{R_s Cl + l\sqrt{LC}} \\ &= \frac{\tau - T}{\tau + T} = \frac{1 - T/\tau}{1 + T/\tau} \end{aligned} \quad (38)$$

where

$$T = l\sqrt{LC} = \ell c \quad (39)$$

For the quasi-static limit to be valid, the wave transit time  $T$  must be much faster than any other time scale of interest so that  $T/\tau \ll 1$ . In Figure 8-12 we plot (35) and (36) for two values of  $T/\tau$  and see that the quasi-static and transmission line results approach each other as  $T/\tau$  becomes small.

When the roundtrip wave transit time is so small compared to the time scale of interest so as to appear to be instantaneous, the circuit treatment is an excellent approximation.

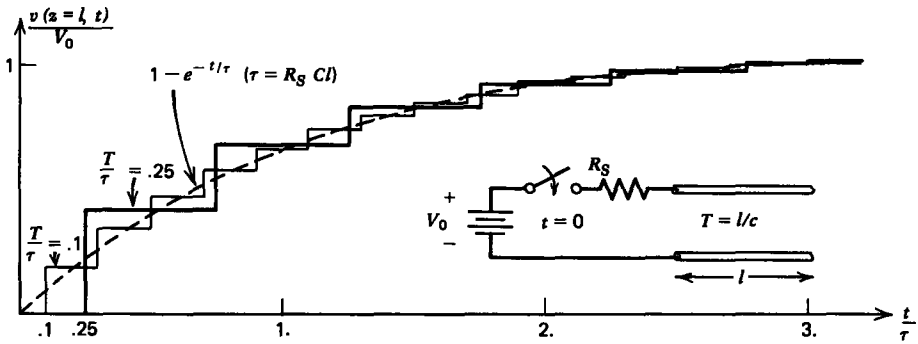


Figure 8-12 The open circuit voltage at  $z=l$  for a step voltage applied at  $t=0$  through a source resistance  $R_s$  for various values of  $T/\tau$ , which is the ratio of propagation time  $T=l/c$  to quasi-static charging time  $\tau=R_s C l$ . The dashed curve shows the exponential rise obtained by a circuit analysis assuming the open circuited transmission line is a capacitor.

If this propagation time is significant, then the transmission line equations must be used.

8-2-5 Reflections from Arbitrary Terminations

For resistive terminations we have been able to relate reflected wave amplitudes in terms of an incident wave amplitude through the use of a reflection coefficient because the voltage and current in the resistor are algebraically related. For an arbitrary termination, which may include any component such as capacitors, inductors, diodes, transistors, or even another transmission line with perhaps a different characteristic impedance, it is necessary to solve a circuit problem at the end of the line. For the arbitrary element with voltage  $V_L$  and current  $I_L$  at  $z=l$ , shown in Figure 8-13a, the voltage and current at the end of line are related as

$$v(z=l, t) = V_L(t) = V_+(t-l/c) + V_-(t+l/c) \tag{40}$$

$$i(z=l, t) = I_L(t) = Y_0[V_+(t-l/c) - V_-(t+l/c)] \tag{41}$$

We assume that we know the incident  $V_+$  wave and wish to find the reflected  $V_-$  wave. We then eliminate the unknown  $V_-$  in (40) and (41) to obtain

$$2V_+(t-l/c) = V_L(t) + I_L(t)Z_0 \tag{42}$$

which suggests the equivalent circuit in Figure 8-13b.

For a particular lumped termination we solve the equivalent circuit for  $V_L(t)$  or  $I_L(t)$ . Since  $V_+(t-l/c)$  is already known as it is incident upon the termination, once  $V_L(t)$  or

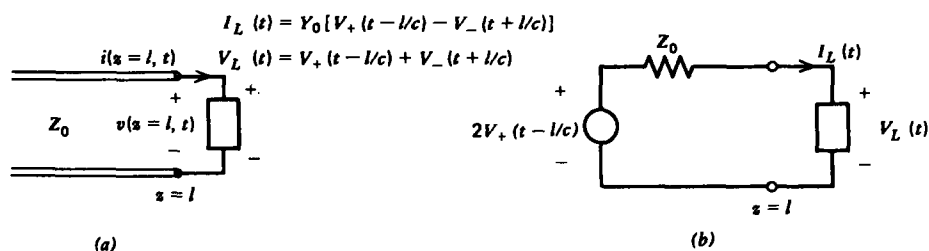


Figure 8-13 A transmission line with an (a) arbitrary load at the  $z=l$  end can be analyzed from the equivalent circuit in (b). Since  $V_+$  is known, calculation of the load current or voltage yields the reflected wave  $V_-$ .

$I_L(t)$  is calculated from the equivalent circuit,  $V_-(t+l/c)$  can be calculated as  $V_- = V_L - V_+$ .

For instance, consider the lossless transmission lines of length  $l$  shown in Figure 8-14a terminated at the end with either a lumped capacitor  $C_L$  or an inductor  $L_L$ . A step voltage at  $t=0$  is applied at  $z=0$  through a source resistor matched to the line.

The source at  $z=0$  is unaware of the termination at  $z=l$  until a time  $2T$ . Until this time it launches a  $V_+$  wave of amplitude  $V_0/2$ . At  $z=l$ , the equivalent circuit for the capacitive termination is shown in Figure 8-14b. Whereas resistive terminations just altered wave amplitudes upon reflection, inductive and capacitive terminations introduce differential equations.

From (42), the voltage across the capacitor  $v_c$  obeys the differential equation

$$Z_0 C_L \frac{dv_c}{dt} + v_c = 2V_+ = V_0, \quad t > T \quad (43)$$

with solution

$$v_c(t) = V_0 [1 - e^{-(t-T)/Z_0 C_L}], \quad t > T \quad (44)$$

Note that the voltage waveform plotted in Figure 8-14b begins at time  $T=l/c$ .

Thus, the returning  $V_-$  wave is given as

$$V_- = v_c - V_+ = V_0/2 + V_0 e^{-(t-T)/Z_0 C_L} \quad (45)$$

This reflected wave travels back to  $z=0$ , where no further reflections occur since the source end is matched. The current at  $z=l$  is then

$$i_c = C_L \frac{dv_c}{dt} = \frac{V_0}{Z_0} e^{-(t-T)/Z_0 C_L}, \quad t > T \quad (46)$$

and is also plotted in Figure 8-14b.

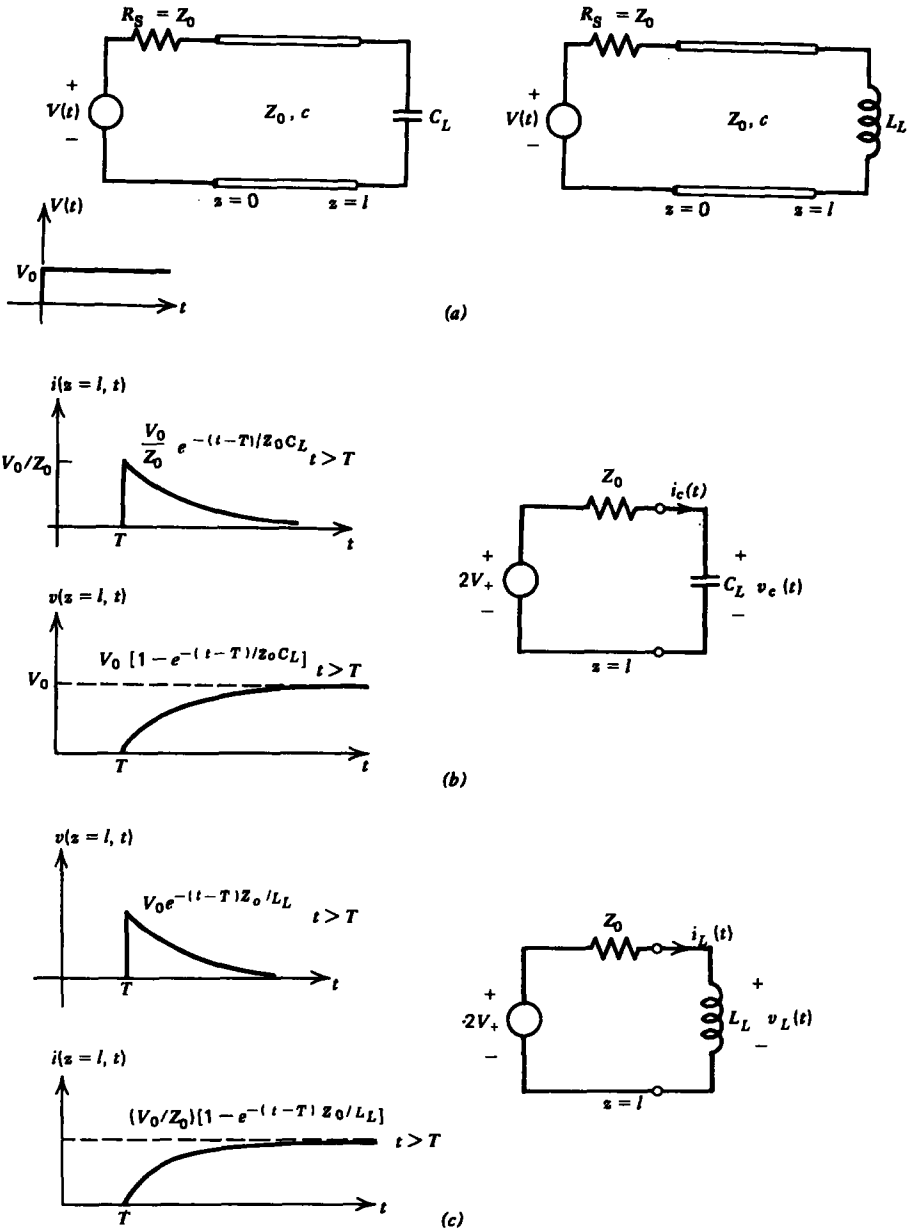


Figure 8-14 (a) A step voltage is applied to transmission lines loaded at  $z = l$  with a capacitor  $C_L$  or inductor  $L_L$ . The load voltage and current are calculated from the (b) resistive-capacitive or (c) resistive-inductive equivalent circuits at  $z = l$  to yield exponential waveforms with respective time constants  $\tau = Z_0 C_L$  and  $\tau = L_L / Z_0$  as the solutions approach the dc steady state. The waveforms begin after the initial  $V_+$  wave arrives at  $z = l$  after a time  $T = l/c$ . There are no further reflections as the source end is matched.

If the end at  $z = 0$  were not matched, a new  $V_+$  would be generated. When it reached  $z = l$ , we would again solve the  $RC$  circuit with the capacitor now initially charged. The reflections would continue, eventually becoming negligible if  $R_1$  is nonzero.

Similarly, the governing differential equation for the inductive load obtained from the equivalent circuit in Figure 8-14c is

$$L_L \frac{di_L}{dt} + i_L Z_0 = 2V_+ = V_0, \quad t > T \quad (47)$$

with solution

$$i_L = \frac{V_0}{Z_0} (1 - e^{-(t-T)Z_0/L_L}), \quad t > T \quad (48)$$

The voltage across the inductor is

$$v_L = L_L \frac{di_L}{dt} = V_0 e^{-(t-T)Z_0/L_L}, \quad t > T \quad (49)$$

Again since the end at  $z = 0$  is matched, the returning  $V_-$  wave from  $z = l$  is not reflected at  $z = 0$ . Thus the total voltage and current for all time at  $z = l$  is given by (48) and (49) and is sketched in Figure 8-14c.

### 8-3 SINUSOIDAL TIME VARIATIONS

#### 8-3-1 Solutions to the Transmission Line Equations

Often transmission lines are excited by sinusoidally varying sources so that the line voltage and current also vary sinusoidally with time:

$$\begin{aligned} v(z, t) &= \text{Re} [\hat{v}(z) e^{j\omega t}] \\ i(z, t) &= \text{Re} [\hat{i}(z) e^{j\omega t}] \end{aligned} \quad (1)$$

Then as we found for TEM waves in Section 7-4, the voltage and current are found from the wave equation solutions of Section 8-1-5 as linear combinations of exponential functions with arguments  $t - z/c$  and  $t + z/c$ :

$$\begin{aligned} v(z, t) &= \text{Re} [\hat{V}_+ e^{j\omega(t-z/c)} + \hat{V}_- e^{j\omega(t+z/c)}] \\ i(z, t) &= Y_0 \text{Re} [\hat{V}_+ e^{j\omega(t-z/c)} - \hat{V}_- e^{j\omega(t+z/c)}] \end{aligned} \quad (2)$$

Now the phasor amplitudes  $\hat{V}_+$  and  $\hat{V}_-$  are complex numbers and do not depend on  $z$  or  $t$ .

By factoring out the sinusoidal time dependence in (2), the spatial dependences of the voltage and current are

$$\begin{aligned}\hat{v}(z) &= \hat{V}_+ e^{-jkz} + \hat{V}_- e^{+jkz} \\ \hat{i}(z) &= Y_0(\hat{V}_+ e^{-jkz} - \hat{V}_- e^{+jkz})\end{aligned}\quad (3)$$

where the wavenumber is again defined as

$$k = \omega/c \quad (4)$$

### 8-3-2 Lossless Terminations

#### (a) Short Circuited Line

The transmission line shown in Figure 8-15a is excited by a sinusoidal voltage source at  $z = -l$  imposing the boundary condition

$$\begin{aligned}v(z = -l, t) &= V_0 \cos \omega t \\ &= \text{Re}(V_0 e^{j\omega t}) \Rightarrow \hat{v}(z = -l) = V_0 = \hat{V}_+ e^{jkl} + \hat{V}_- e^{-jkl}\end{aligned}\quad (5)$$

Note that to use (3) we must write all sinusoids in complex notation. Then since all time variations are of the form  $e^{j\omega t}$ , we may suppress writing it each time and work only with the spatial variations of (3).

Because the transmission line is short circuited, we have the additional boundary condition

$$v(z = 0, t) = 0 \Rightarrow \hat{v}(z = 0) = 0 = \hat{V}_+ + \hat{V}_- \quad (6)$$

which when simultaneously solved with (5) yields

$$\hat{V}_+ = -\hat{V}_- = \frac{V_0}{2j \sin kl} \quad (7)$$

The spatial dependences of the voltage and current are then

$$\begin{aligned}\hat{v}(z) &= \frac{V_0(e^{-jkz} - e^{jkz})}{2j \sin kl} = -\frac{V_0 \sin kz}{\sin kl} \\ \hat{i}(z) &= \frac{V_0 Y_0(e^{-jkz} + e^{jkz})}{2j \sin kl} = -j \frac{V_0 Y_0 \cos kz}{\sin kl}\end{aligned}\quad (8)$$

The instantaneous voltage and current as functions of space and time are then

$$\begin{aligned}v(z, t) &= \text{Re}[\hat{v}(z) e^{j\omega t}] = -V_0 \frac{\sin kz}{\sin kl} \cos \omega t \\ i(z, t) &= \text{Re}[\hat{i}(z) e^{j\omega t}] = \frac{V_0 Y_0 \cos kz \sin \omega t}{\sin kl}\end{aligned}\quad (9)$$

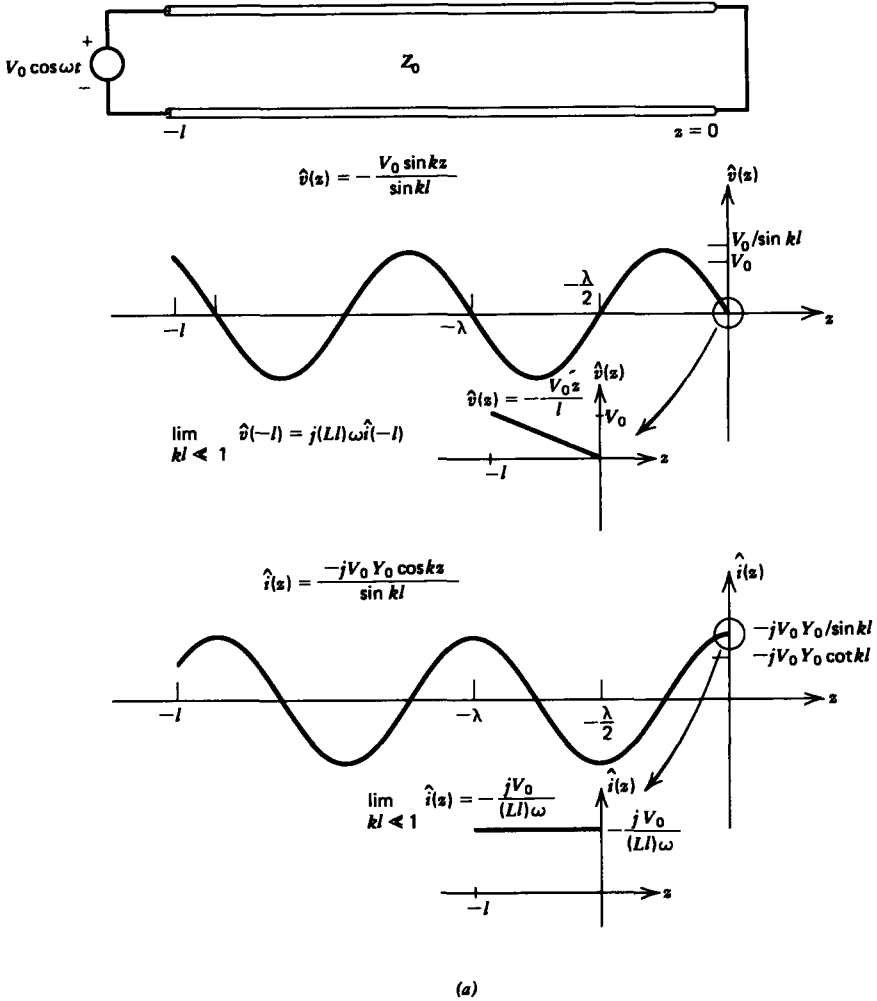


Figure 8-15 The voltage and current distributions on a (a) short circuited and (b) open circuited transmission line excited by sinusoidal voltage sources at  $z = -l$ . If the lines are much shorter than a wavelength, they act like reactive circuit elements. (c) As the frequency is raised, the impedance reflected back as a function of  $z$  can look capacitive or inductive making the transition through open or short circuits.

The spatial distributions of voltage and current as a function of  $z$  at a specific instant of time are plotted in Figure 8-15a and are seen to be  $90^\circ$  out of phase with one another in space with their distributions periodic with wavelength  $\lambda$  given by

$$\lambda = \frac{2\pi}{k} = \frac{2\pi c}{\omega} \tag{10}$$

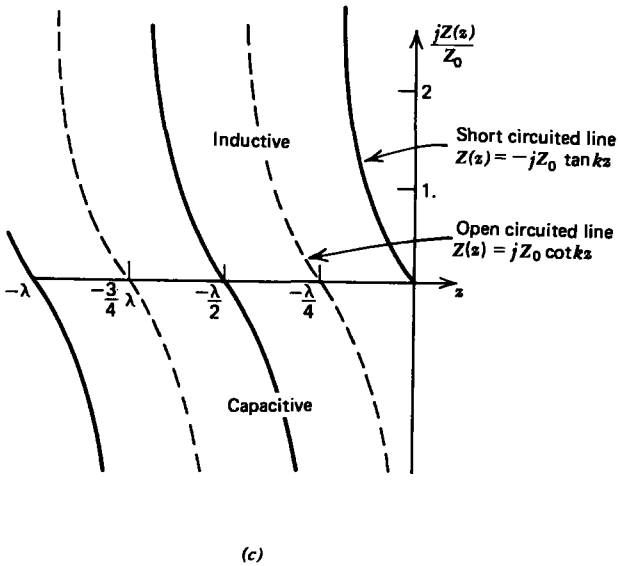
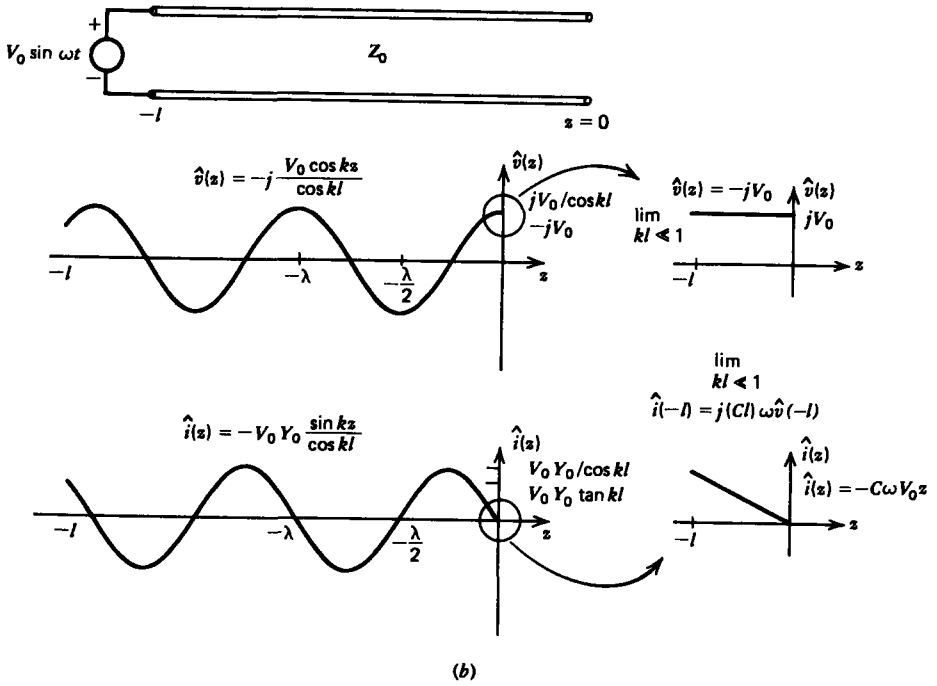


Figure 8-15

The complex impedance at any position  $z$  is defined as

$$Z(z) = \frac{\hat{v}(z)}{\hat{i}(z)} \quad (11)$$

which for this special case of a short circuited line is found from (8) as

$$Z(z) = -jZ_0 \tan kz \quad (12)$$

In particular, at  $z = -l$ , the transmission line appears to the generator as an impedance of value

$$Z(z = -l) = jZ_0 \tan kl \quad (13)$$

From the solid lines in Figure 8-15c we see that there are various regimes of interest:

- (i) When the line is an integer multiple of a half wavelength long so that  $kl = n\pi$ ,  $n = 1, 2, 3, \dots$ , the impedance at  $z = -l$  is zero and the transmission line looks like a short circuit.
- (ii) When the line is an odd integer multiple of a quarter wavelength long so that  $kl = (2n-1)\pi/2$ ,  $n = 1, 2, \dots$ , the impedance at  $z = -l$  is infinite and the transmission line looks like an open circuit.
- (iii) Between the short and open circuit limits  $(n-1)\pi < kl < (2n-1)\pi/2$ ,  $n = 1, 2, 3, \dots$ ,  $Z(z = -l)$  has a positive reactance and hence looks like an inductor.
- (iv) Between the open and short circuit limits  $(n-\frac{1}{2})\pi < kl < n\pi$ ,  $n = 1, 2, \dots$ ,  $Z(z = -l)$  has a negative reactance and so looks like a capacitor.

Thus, the short circuited transmission line takes on all reactive values, both positive (inductive) and negative (capacitive), including open and short circuits as a function of  $kl$ . Thus, if either the length of the line  $l$  or the frequency is changed, the impedance of the transmission line is changed.

Examining (8) we also notice that if  $\sin kl = 0$ , ( $kl = n\pi$ ,  $n = 1, 2, \dots$ ), the voltage and current become infinite (in practice the voltage and current become large limited only by losses). Under these conditions, the system is said to be resonant with the resonant frequencies given by

$$\omega_n = n\pi c/l, \quad n = 1, 2, 3, \dots \quad (14)$$

Any voltage source applied at these frequencies will result in very large voltages and currents on the line.

### (b) Open Circuited Line

If the short circuit is replaced by an open circuit, as in Figure 8-15b, and for variety we change the source at  $z = -l$  to

$V_0 \sin \omega t$  the boundary conditions are

$$\begin{aligned} i(z=0, t) &= 0 \\ v(z=-l, t) &= V_0 \sin \omega t = \operatorname{Re}(-jV_0 e^{j\omega t}) \end{aligned} \quad (15)$$

Using (3) the complex amplitudes obey the relations

$$\begin{aligned} \hat{i}(z=0) &= 0 = Y_0(\hat{V}_+ - \hat{V}_-) \\ \hat{v}(z=-l) &= -jV_0 = \hat{V}_+ e^{jkl} + \hat{V}_- e^{-jkl} \end{aligned} \quad (16)$$

which has solutions

$$\hat{V}_+ = \hat{V}_- = \frac{-jV_0}{2 \cos kl} \quad (17)$$

The spatial dependences of the voltage and current are then

$$\begin{aligned} \hat{v}(z) &= \frac{-jV_0}{2 \cos kl} (e^{-jkl} + e^{jkl}) = \frac{-jV_0}{\cos kl} \cos kz \\ \hat{i}(z) &= \frac{-jV_0 Y_0}{2 \cos kl} (e^{-jkl} - e^{jkl}) = -\frac{V_0 Y_0}{\cos kl} \sin kz \end{aligned} \quad (18)$$

with instantaneous solutions as a function of space and time:

$$\begin{aligned} v(z, t) &= \operatorname{Re}[\hat{v}(z) e^{j\omega t}] = \frac{V_0 \cos kz}{\cos kl} \sin \omega t \\ i(z, t) &= \operatorname{Re}[\hat{i}(z) e^{j\omega t}] = -\frac{V_0 Y_0}{\cos kl} \sin kz \cos \omega t \end{aligned} \quad (19)$$

The impedance at  $z = -l$  is

$$Z(z=-l) = \frac{\hat{v}(-l)}{\hat{i}(-l)} = -jZ_0 \cot kl \quad (20)$$

Again the impedance is purely reactive, as shown by the dashed lines in Figure 8-15c, alternating signs every quarter wavelength so that the open circuit load looks to the voltage source as an inductor, capacitor, short or open circuit depending on the frequency and length of the line.

Resonance will occur if

$$\cos kl = 0 \quad (21)$$

or

$$kl = (2n-1)\pi/2, \quad n = 1, 2, 3, \dots \quad (22)$$

so that the resonant frequencies are

$$\omega_n = \frac{(2n-1)\pi c}{2l} \quad (23)$$

### 8-3-3 Reactive Circuit Elements as Approximations to Short Transmission Lines

Let us re-examine the results obtained for short and open circuited lines in the limit when  $l$  is much shorter than the wavelength  $\lambda$  so that in this long wavelength limit the spatial trigonometric functions can be approximated as

$$\lim_{kl \ll 1} \begin{cases} \sin kz \approx kz \\ \cos kz \approx 1 \end{cases} \quad (24)$$

Using these approximations, the voltage, current, and impedance for the short circuited line excited by a voltage source  $V_0 \cos \omega t$  can be obtained from (9) and (13) as

$$\lim_{kl \ll 1} \begin{cases} v(z, t) = -\frac{V_0 z}{l} \cos \omega t, & v(-l, t) = V_0 \cos \omega t \\ i(z, t) = \frac{V_0 Y_0}{kl} \sin \omega t, & i(-l, t) = \frac{V_0 \sin \omega t}{(Ll)\omega} \\ Z(-l) = jZ_0 kl = j\frac{\omega Z_0 l}{c} = j\omega(Ll) \end{cases} \quad (25)$$

We see that the short circuited transmission line acts as an inductor of value  $(Ll)$  (remember that  $L$  is the inductance per unit length), where we used the relations

$$Z_0 = \frac{1}{Y_0} = \sqrt{\frac{L}{C}}, \quad c = \frac{1}{\sqrt{LC}} \quad (26)$$

Note that at  $z = -l$ ,

$$v(-l, t) = (Ll) \frac{di(-l, t)}{dt} \quad (27)$$

Similarly for the open circuited line we obtain:

$$\lim_{kl \ll 1} \begin{cases} v(z, t) = V_0 \sin \omega t \\ i(z, t) = -V_0 Y_0 kz \cos \omega t, & i(-l, t) = (Cl)\omega V_0 \cos \omega t \\ Z(-l) = \frac{-jZ_0}{kl} = \frac{-j}{(Cl)\omega} \end{cases} \quad (28)$$

For the open circuited transmission line, the terminal voltage and current are simply related as for a capacitor,

$$i(-l, t) = (Cl) \frac{dv(-l, t)}{dt} \quad (29)$$

with capacitance given by  $(Cl)$ .

In general, if the frequency of excitation is low enough so that the length of a transmission line is much shorter than the

wavelength, the circuit approximations of inductance and capacitance are appropriate. However, it must be remembered that if the frequencies of interest are so high that the length of a circuit element is comparable to the wavelength, it no longer acts like that element. In fact, as found in Section 8-3-2, a capacitor can even look like an inductor, a short circuit, or an open circuit at high enough frequency while vice versa an inductor can also look capacitive, a short or an open circuit.

In general, if the termination is neither a short nor an open circuit, the voltage and current distribution becomes more involved to calculate and is the subject of Section 8-4.

### 8-3-4 Effects of Line Losses

#### (a) Distributed Circuit Approach

If the dielectric and transmission line walls have Ohmic losses, the voltage and current waves decay as they propagate. Because the governing equations of Section 8-1-3 are linear with constant coefficients, in the sinusoidal steady state we assume solutions of the form

$$\begin{aligned} v(z, t) &= \text{Re} (\hat{V} e^{j(\omega t - kz)}) \\ i(z, t) &= \text{Re} (\hat{I} e^{j(\omega t - kz)}) \end{aligned} \quad (30)$$

where now  $\omega$  and  $k$  are not simply related as the nondispersive relation in (4). Rather we substitute (30) into Eq. (28) in Section 8-1-3:

$$\begin{aligned} \frac{\partial i}{\partial z} &= -C \frac{\partial v}{\partial t} - Gv \Rightarrow -jk\hat{I} = -(Cj\omega + G)\hat{V} \\ \frac{\partial v}{\partial z} &= -L \frac{\partial i}{\partial t} - iR \Rightarrow -jk\hat{V} = -(Lj\omega + R)\hat{I} \end{aligned} \quad (31)$$

which requires that

$$\frac{\hat{V}}{\hat{I}} = \frac{jk}{(Cj\omega + G)} = \frac{Lj\omega + R}{jk} \quad (32)$$

We solve (32) self-consistently for  $k$  as

$$k^2 = -(Lj\omega + R)(Cj\omega + G) = LC\omega^2 - j\omega(RC + LG) - RG \quad (33)$$

The wavenumber is thus complex so that we find the real and imaginary parts from (33) as

$$\begin{aligned} k^2 = k_r + jk_i \Rightarrow k_r^2 - k_i^2 &= LC\omega^2 - RG \\ 2k_r k_i &= -\omega(RC + LG) \end{aligned} \quad (34)$$

In the low loss limit where  $\omega RC \ll 1$  and  $\omega LG \ll 1$ , the spatial decay of  $k_i$  is small compared to the propagation wavenumber  $k_r$ . In this limit we have the following approximate solution:

$$\lim_{\substack{\omega RC \ll 1 \\ \omega LG \ll 1}} \begin{cases} k_r \approx \pm \omega \sqrt{LC} = \pm \omega/c \\ k_i = -\frac{\omega(RC + LG)}{2k_r} \approx \mp \frac{1}{2} \left[ R\sqrt{\frac{C}{L}} + G\sqrt{\frac{L}{C}} \right] \\ \qquad \qquad \qquad \approx \mp \frac{1}{2} (RY_0 + GZ_0) \end{cases} \quad (35)$$

We use the upper sign for waves propagating in the  $+z$  direction and the lower sign for waves traveling in the  $-z$  direction.

### (b) Distortionless lines

Using the value of  $k$  of (33),

$$k = \pm [-(Lj\omega + R)(Cj\omega + G)]^{1/2} \quad (36)$$

in (32) gives us the frequency dependent wave impedance for waves traveling in the  $\pm z$  direction as

$$\frac{\hat{V}}{\hat{I}} = \pm \left( \frac{Lj\omega + R}{Cj\omega + G} \right)^{1/2} = \pm \sqrt{\frac{L}{C} \left( \frac{j\omega + R/L}{j\omega + G/C} \right)^{1/2}} \quad (37)$$

If the line parameters are adjusted so that

$$\frac{R}{L} = \frac{G}{C} \quad (38)$$

the impedance in (37) becomes frequency independent and equal to the lossless line impedance. Under the conditions of (38) the complex wavenumber reduces to

$$k_r = \pm \omega \sqrt{LC}, \quad k_i = \mp \sqrt{RG} \quad (39)$$

Although the waves are attenuated, all frequencies propagate at the same phase and group velocities as for a lossless line

$$\begin{aligned} v_p &= \frac{\omega}{k_r} = \pm \frac{1}{\sqrt{LC}} \\ v_g &= \frac{d\omega}{dk_r} = \pm \frac{1}{\sqrt{LC}} \end{aligned} \quad (40)$$

Since all the Fourier components of a pulse excitation will travel at the same speed, the shape of the pulse remains unchanged as it propagates down the line. Such lines are called distortionless.

**(c) Fields Approach**

If  $R = 0$ , we can directly find the TEM wave solutions using the same solutions found for plane waves in Section 7-4-3. There we found that a dielectric with permittivity  $\epsilon$  and small Ohmic conductivity  $\sigma$  has a complex wavenumber:

$$\lim_{\sigma/\omega\epsilon \ll 1} k \approx \pm \left( \frac{\omega}{c} - \frac{j\sigma\eta}{2} \right) \quad (41)$$

Equating (41) to (35) with  $R = 0$  requires that  $GZ_0 = \sigma\eta$ .

The tangential component of  $\mathbf{H}$  at the perfectly conducting transmission line walls is discontinuous by a surface current. However, if the wall has a large but noninfinite Ohmic conductivity  $\sigma_w$ , the fields penetrate in with a characteristic distance equal to the skin depth  $\delta = \sqrt{2/\omega\mu\sigma_w}$ . The resulting  $z$ -directed current gives rise to a  $z$ -directed electric field so that the waves are no longer purely TEM.

Because we assume this loss to be small, we can use an approximate perturbation method to find the spatial decay rate of the fields. We assume that the fields between parallel plane electrodes are essentially the same as when the system is lossless except now being exponentially attenuated as  $e^{-\alpha z}$ , where  $\alpha = -k_i$ :

$$\begin{aligned} E_x(z, t) &= \text{Re} \left[ \hat{E} e^{j(\omega t - k_r z)} e^{-\alpha z} \right] \\ H_y(z, t) &= \text{Re} \left[ \frac{\hat{E}}{\eta} e^{j(\omega t - k_r z)} e^{-\alpha z} \right], \quad k_r = \frac{\omega}{c} \end{aligned} \quad (42)$$

From the real part of the complex Poynting's theorem derived in Section 7-2-4, we relate the divergence of the time-average electromagnetic power density to the time-average dissipated power:

$$\nabla \cdot \langle \mathbf{S} \rangle = -\langle P_d \rangle \quad (43)$$

Using the divergence theorem we integrate (43) over a volume of thickness  $\Delta z$  that encompasses the entire width and thickness of the line, as shown in Figure 8-16:

$$\begin{aligned} \int_V \nabla \cdot \langle \mathbf{S} \rangle dV &= \oint_S \langle \mathbf{S} \rangle \cdot d\mathbf{S} \\ &= \int_{z+\Delta z} \langle S_z(z+\Delta z) \rangle dS \\ &\quad - \int_z \langle S_z(z) \rangle dS = - \int_V \langle P_d \rangle dV \end{aligned} \quad (44)$$

The power  $\langle P_d \rangle$  is dissipated in the dielectric and in the walls. Defining the total electromagnetic power as

$$\langle P(z) \rangle = \int \langle S_z(z) \rangle dS \quad (45)$$

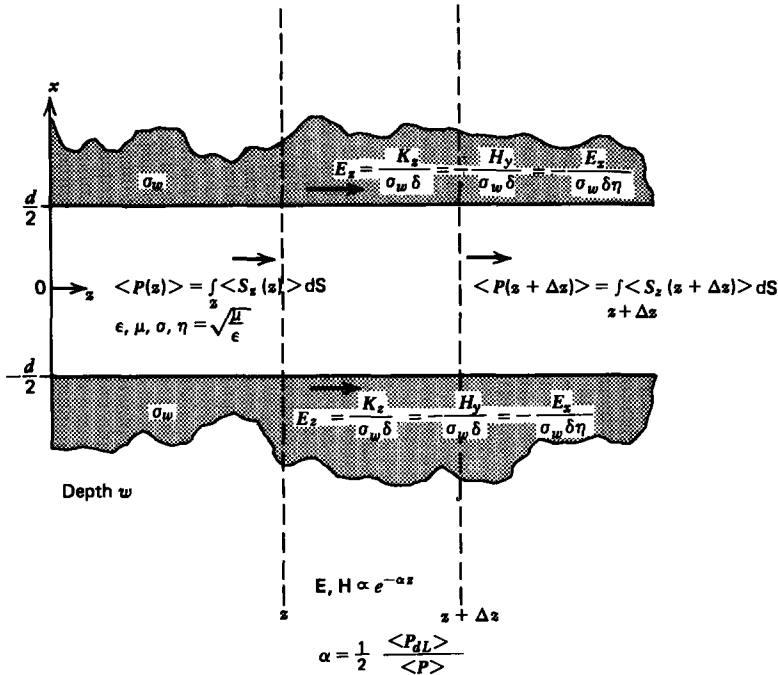


Figure 8-16 A transmission line with lossy walls and dielectric results in waves that decay as they propagate. The spatial decay rate  $\alpha$  of the fields is approximately proportional to the ratio of time average dissipated power per unit length  $\langle P_{dL} \rangle$  to the total time average electromagnetic power flow  $\langle P \rangle$  down the line.

(44) can be rewritten as

$$\langle P(z + \Delta z) \rangle - \langle P(z) \rangle = - \int \langle P_d \rangle dx dy dz \quad (46)$$

Dividing through by  $dz = \Delta z$ , we have in the infinitesimal limit

$$\lim_{\Delta z \rightarrow 0} \frac{\langle P(z + \Delta z) \rangle - \langle P(z) \rangle}{\Delta z} = \frac{d\langle P \rangle}{dz} = - \int_S \langle P_d \rangle dx dy = - \langle P_{dL} \rangle \quad (47)$$

where  $\langle P_{dL} \rangle$  is the power dissipated per unit length. Since the fields vary as  $e^{-\alpha z}$ , the power flow that is proportional to the square of the fields must vary as  $e^{-2\alpha z}$  so that

$$\frac{d\langle P \rangle}{dz} = -2\alpha \langle P \rangle = - \langle P_{dL} \rangle \quad (48)$$

which when solved for the spatial decay rate is proportional to the ratio of dissipated power per unit length to the total

electromagnetic power flowing down the transmission line:

$$\alpha = \frac{1}{2} \frac{\langle P_{dL} \rangle}{\langle P \rangle} \quad (49)$$

For our lossy transmission line, the power is dissipated both in the walls and in the dielectric. Fortunately, it is not necessary to solve the complicated field problem within the walls because we already approximately know the magnetic field at the walls from (42). Since the wall current is effectively confined to the skin depth  $\delta$ , the cross-sectional area through which the current flows is essentially  $w\delta$  so that we can define the surface conductivity as  $\sigma_w\delta$ , where the electric field at the wall is related to the lossless surface current as

$$\mathbf{K}_w = \sigma_w \delta \mathbf{E}_w \quad (50)$$

The surface current in the wall is approximately found from the magnetic field in (42) as

$$K_z = -H_y = -E_x / \eta \quad (51)$$

The time-average power dissipated in the wall is then

$$\langle P_{dL} \rangle_{\text{wall}} = \frac{w}{2} \text{Re} (\mathbf{E}_w \cdot \mathbf{K}_w^*) = \frac{1}{2} \frac{|\mathbf{K}_w|^2 w}{\sigma_w \delta} = \frac{1}{2} \frac{|\hat{E}|^2 w}{\sigma_w \delta \eta^2} \quad (52)$$

The total time-average dissipated power in the walls and dielectric per unit length for a transmission line system of depth  $w$  and plate spacing  $d$  is then

$$\begin{aligned} \langle P_{dL} \rangle &= 2 \langle P_{dL} \rangle_{\text{wall}} + \frac{1}{2} \sigma |\hat{E}|^2 w d \\ &= \frac{1}{2} |\hat{E}|^2 w \left( \frac{2}{\eta^2 \sigma_w \delta} + \sigma d \right) \end{aligned} \quad (53)$$

where we multiply (52) by two because of the losses in both electrodes. The time-average electromagnetic power is

$$\langle P \rangle = \frac{1}{2} \frac{|\hat{E}|^2}{\eta} w d \quad (54)$$

so that the spatial decay rate is found from (49) as

$$\alpha = -k_i = \frac{1}{2} \left( \frac{2}{\eta^2 \sigma_w \delta} + \sigma d \right) \frac{\eta}{d} = \frac{1}{2} \left( \sigma \eta + \frac{2}{\eta \sigma_w \delta d} \right) \quad (55)$$

Comparing (55) to (35) we see that

$$\begin{aligned} GZ_0 &= \sigma \eta, & RY_0 &= \frac{2}{\eta \sigma_w \delta d} \\ \Rightarrow Z_0 &= \frac{1}{Y_0} = \frac{d}{w} \eta, & G &= \frac{\sigma w}{d}, & R &= \frac{2}{\sigma_w w \delta} \end{aligned} \quad (56)$$

## 8-4 ARBITRARY IMPEDANCE TERMINATIONS

### 8-4-1 The Generalized Reflection Coefficient

A lossless transmission line excited at  $z = -l$  with a sinusoidal voltage source is now terminated at its other end at  $z = 0$  with an arbitrary impedance  $Z_L$ , which in general can be a complex number. Defining the load voltage and current at  $z = 0$  as

$$\begin{aligned} v(z = 0, t) &= v_L(t) = \text{Re}(V_L e^{j\omega t}) \\ i(z = 0, t) &= i_L(t) = \text{Re}(I_L e^{j\omega t}), \quad I_L = V_L/Z_L \end{aligned} \quad (1)$$

where  $V_L$  and  $I_L$  are complex amplitudes, the boundary conditions at  $z = 0$  are

$$V_+ + V_- = V_L \quad (2)$$

$$Y_0(V_+ - V_-) = I_L = V_L/Z_L$$

We define the reflection coefficient as the ratio

$$\Gamma_L = V_-/V_+ \quad (3)$$

and solve as

$$\Gamma_L = \frac{Z_L - Z_0}{Z_L + Z_0} \quad (4)$$

Here in the sinusoidal steady state with reactive loads,  $\Gamma_L$  can be a complex number as  $Z_L$  may be complex. For transient pulse waveforms,  $\Gamma_L$  was only defined for resistive loads. For capacitive and inductive terminations, the reflections were given by solutions to differential equations in time. Now that we are only considering sinusoidal time variations so that time derivatives are replaced by  $j\omega$ , we can generalize  $\Gamma_L$  for the sinusoidal steady state.

It is convenient to further define the generalized reflection coefficient as

$$\Gamma(z) = \frac{V_- e^{jkz}}{V_+ e^{-jkz}} = \frac{V_-}{V_+} e^{2jkz} = \Gamma_L e^{2jkz} \quad (5)$$

where  $\Gamma_L$  is just  $\Gamma(z = 0)$ . Then the voltage and current on the line can be expressed as

$$\begin{aligned} \hat{v}(z) &= V_+ e^{-jkz} [1 + \Gamma(z)] \\ \hat{i}(z) &= Y_0 V_+ e^{-jkz} [1 - \Gamma(z)] \end{aligned} \quad (6)$$

The advantage to this notation is that now the impedance along the line can be expressed as

$$Z_n(z) = \frac{Z(z)}{Z_0} = \frac{\hat{v}(z)}{\hat{i}(z)Z_0} = \frac{1 + \Gamma(z)}{1 - \Gamma(z)} \quad (7)$$

where  $Z_n$  is defined as the normalized impedance. We can now solve (7) for  $\Gamma(z)$  as

$$\Gamma(z) = \frac{Z_n(z) - 1}{Z_n(z) + 1} \quad (8)$$

Note the following properties of  $Z_n(z)$  and  $\Gamma(z)$  for passive loads:

- (i)  $Z_n(z)$  is generally complex. For passive loads its real part is allowed over the range from zero to infinity while its imaginary part can extend from negative to positive infinity.
- (ii) The magnitude of  $\Gamma(z)$ ,  $|\Gamma_L|$  must be less than or equal to 1 for passive loads.
- (iii) From (5), if  $z$  is increased or decreased by a half wavelength,  $\Gamma(z)$  and hence  $Z_n(z)$  remain unchanged. Thus, if the impedance is known at any position, the impedance of all-points integer multiples of a half wavelength away have the same impedance.
- (iv) From (5), if  $z$  is increased or decreased by a quarter wavelength,  $\Gamma(z)$  changes sign, while from (7)  $Z_n(z)$  goes to its reciprocal  $\Rightarrow 1/Z_n(z) = Y_n(z)$ .
- (v) If the line is matched,  $Z_L = Z_0$ , then  $\Gamma_L = 0$  and  $Z_n(z) = 1$ . The impedance is the same everywhere along the line.

### 8-4-2 Simple Examples

#### (a) Load Impedance Reflected Back to the Source

Properties (iii)–(v) allow simple computations for transmission line systems that have lengths which are integer multiples of quarter or half wavelengths. Often it is desired to maximize the power delivered to a load at the end of a transmission line by adding a lumped admittance  $Y$  across the line. For the system shown in Figure 8-17a, the impedance of the load is reflected back to the generator and then added in parallel to the lumped reactive admittance  $Y$ . The normalized load impedance of  $(R_L + jX_L)/Z_0$  inverts when reflected back to the source by a quarter wavelength to  $Z_0/(R_L + jX_L)$ . Since this is the normalized impedance the actual impedance is found by multiplying by  $Z_0$  to yield  $Z(z = -\lambda/4) = Z_0^2/(R_L + jX_L)$ . The admittance of this reflected load then adds in parallel to  $Y$  to yield a total admittance of  $Y + (R_L + jX_L)/Z_0^2$ . If  $Y$  is pure imaginary and of opposite sign to the reflected load susceptance with value  $-jX_L/Z_0^2$ , maximum power is delivered to the line if the source resistance  $R_S$  also equals the resulting line input impedance,  $R_S = Z_0^2/R_L$ . Since  $Y$  is purely

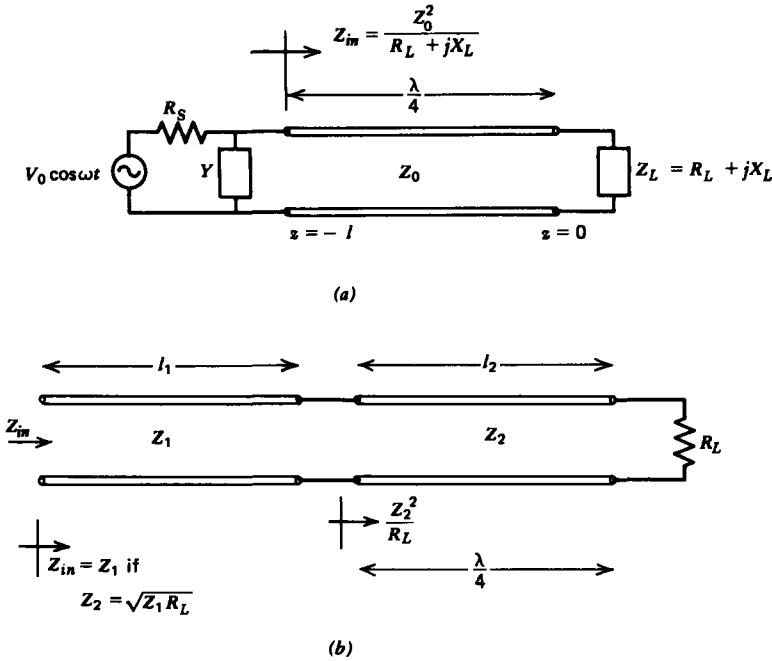


Figure 8-17 The normalized impedance reflected back through a quarter-wave-long line inverts. (a) The time-average power delivered to a complex load can be maximized if  $Y$  is adjusted to just cancel the reactive admittance of the load reflected back to the source with  $R_s$  equaling the resulting input resistance. (b) If the length  $l_2$  of the second transmission line shown is a quarter wave long or an odd integer multiple of  $\lambda/4$  and its characteristic impedance is equal to the geometric average of  $Z_1$  and  $R_L$ , the input impedance  $Z_{in}$  is matched to  $Z_1$ .

reactive and the transmission line is lossless, half the time-average power delivered by the source is dissipated in the load:

$$\langle P \rangle = \frac{1}{8} \frac{V_0^2}{R_S} = \frac{1}{8} \frac{R_L V_0^2}{Z_0^2} \tag{9}$$

Such a reactive element  $Y$  is usually made from a variable length short circuited transmission line called a stub. As shown in Section 8-3-2a, a short circuited lossless line always has a pure reactive impedance.

To verify that the power in (9) is actually dissipated in the load, we write the spatial distribution of voltage and current along the line as

$$\begin{aligned} \hat{v}(z) &= V_+ e^{-jkz} (1 + \Gamma_L e^{2jkz}) \\ \hat{i}(z) &= Y_0 V_+ e^{-jkz} (1 - \Gamma_L e^{2jkz}) \end{aligned} \tag{10}$$

where the reflection coefficient for this load is given by (4) as

$$\Gamma_L = \frac{R_L + jX_L - Z_0}{R_L + jX_L + Z_0} \quad (11)$$

At  $z = -l = -\lambda/4$  we have the boundary condition

$$\begin{aligned} \hat{v}(z = -l) &= V_0/2 = V_+ e^{jkl}(1 + \Gamma_L e^{-2jkl}) \\ &= jV_+(1 - \Gamma_L) \end{aligned} \quad (12)$$

which allows us to solve for  $V_+$  as

$$V_+ = \frac{-jV_0}{2(1 - \Gamma_L)} = \frac{-jV_0}{4Z_0}(R_L + jX_L + Z_0) \quad (13)$$

The time-average power dissipated in the load is then

$$\begin{aligned} \langle P_L \rangle &= \frac{1}{2} \operatorname{Re} [\hat{v}(z = 0)\hat{i}^*(z = 0)] \\ &= \frac{1}{2} |\hat{i}(z = 0)|^2 R_L \\ &= \frac{1}{2} |V_+|^2 |1 - \Gamma_L|^2 Y_0^2 R_L \\ &= \frac{1}{8} V_0^2 Y_0^2 R_L \end{aligned} \quad (14)$$

which agrees with (9).

### (b) Quarter Wavelength Matching

It is desired to match the load resistor  $R_L$  to the transmission line with characteristic impedance  $Z_1$  for any value of its length  $l_1$ . As shown in Figure 8-17b, we connect the load to  $Z_1$  via another transmission line with characteristic impedance  $Z_2$ . We wish to find the values of  $Z_2$  and  $l_2$  necessary to match  $R_L$  to  $Z_1$ .

This problem is analogous to the dielectric coating problem of Example 7-1, where it was found that reflections could be eliminated if the coating thickness between two different dielectric media was an odd integer multiple of a quarter wavelength and whose wave impedance was equal to the geometric average of the impedance in each adjacent region. The normalized load on  $Z_2$  is then  $Z_{n2} = R_L/Z_2$ . If  $l_2$  is an odd integer multiple of a quarter wavelength long, the normalized impedance  $Z_{n2}$  reflected back to the first line inverts to  $Z_2/R_L$ . The actual impedance is obtained by multiplying this normalized impedance by  $Z_2$  to give  $Z_2^2/R_L$ . For  $Z_{in}$  to be matched to  $Z_1$  for any value of  $l_1$ , this impedance must be matched to  $Z_1$ :

$$Z_1 = Z_2^2/R_L \Rightarrow Z_2 = \sqrt{Z_1 R_L} \quad (15)$$

### 8-4-3 The Smith Chart

Because the range of allowed values of  $\Gamma_L$  must be contained within a unit circle in the complex plane, all values of  $Z_n(z)$  can be mapped by a transformation within this unit circle using (8). This transformation is what makes the substitutions of (3)–(8) so valuable. A graphical aid of this mathematical transformation was developed by P. H. Smith in 1939 and is known as the Smith chart. Using the Smith chart avoids the tedium in problem solving with complex numbers.

Let us define the real and imaginary parts of the normalized impedance at some value of  $z$  as

$$Z_n(z) = r + jx \quad (16)$$

The reflection coefficient similarly has real and imaginary parts given as

$$\Gamma(z) = \Gamma_r + j\Gamma_i \quad (17)$$

Using (7) we have

$$r + jx = \frac{1 + \Gamma_r + j\Gamma_i}{1 - \Gamma_r - j\Gamma_i} \quad (18)$$

Multiplying numerator and denominator by the complex conjugate of the denominator  $(1 - \Gamma_r + j\Gamma_i)$  and separating real and imaginary parts yields

$$\begin{aligned} r &= \frac{1 - \Gamma_r^2 - \Gamma_i^2}{(1 - \Gamma_r)^2 + \Gamma_i^2} \\ x &= \frac{2\Gamma_i}{(1 - \Gamma_r)^2 + \Gamma_i^2} \end{aligned} \quad (19)$$

Since we wish to plot (19) in the  $\Gamma_r - \Gamma_i$  plane we rewrite these equations as

$$\begin{aligned} \left(\Gamma_r - \frac{r}{1+r}\right)^2 + \Gamma_i^2 &= \frac{1}{(1+r)^2} \\ (\Gamma_r - 1)^2 + \left(\Gamma_i - \frac{1}{x}\right)^2 &= \frac{1}{x^2} \end{aligned} \quad (20)$$

Both equations in (20) describe a family of orthogonal circles. The upper equation is that of a circle of radius  $1/(1+r)$  whose center is at the position  $\Gamma_i = 0$ ,  $\Gamma_r = r/(1+r)$ . The lower equation is a circle of radius  $|1/x|$  centered at the position  $\Gamma_r = 1$ ,  $\Gamma_i = 1/x$ . Figure 8-18a illustrates these circles for a particular value of  $r$  and  $x$ , while Figure 8-18b shows a few representative values of  $r$  and  $x$ . In Figure 8-19, we have a complete Smith chart. Only those parts of the circles that lie within the unit circle in the  $\Gamma$  plane are considered for passive

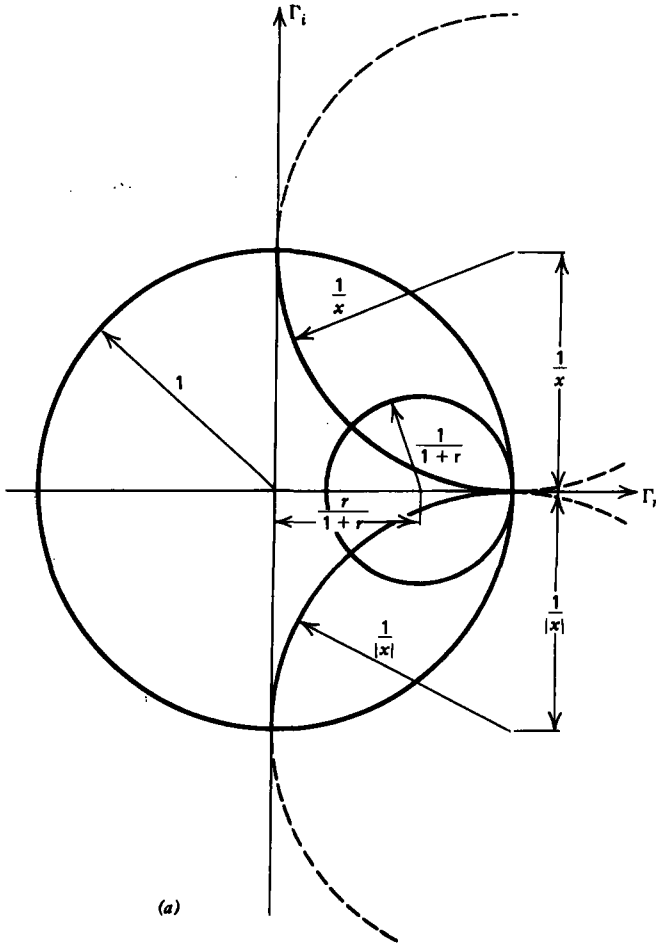


Figure 8-18 For passive loads the Smith chart is constructed within the unit circle in the complex  $\Gamma$  plane. (a) Circles of constant normalized resistance  $r$  and reactance  $x$  are constructed with the centers and radii shown. (b) Smith chart construction for various values of  $r$  and  $x$ .

resistive-reactive loads. The values of  $\Gamma(z)$  themselves are usually not important and so are not listed, though they can be easily found from (8). Note that all circles pass through the point  $\Gamma_r = 1, \Gamma_i = 0$ .

The outside of the circle is calibrated in wavelengths toward the generator, so if the impedance is known at any point on the transmission line (usually at the load end), the impedance at any other point on the line can be found using just a compass and a ruler. From the definition of  $\Gamma(z)$  in (5) with  $z$  negative, we move clockwise around the Smith chart when heading towards the source and counterclockwise when moving towards the load.

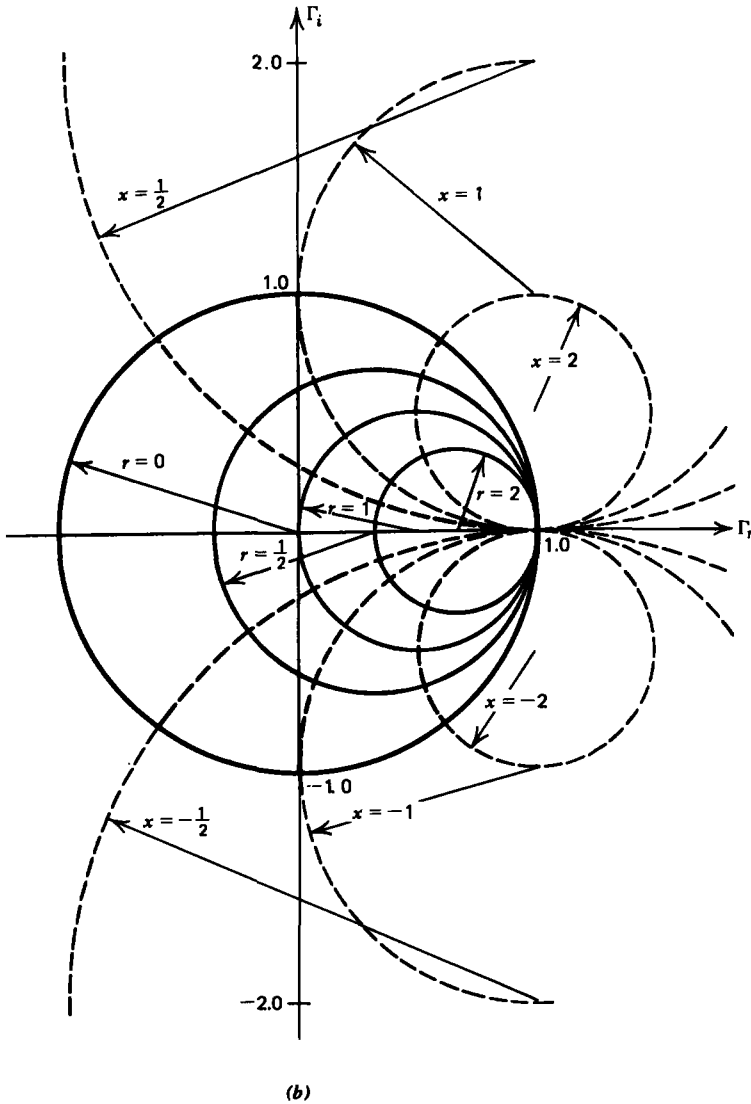


Figure 8-18

In particular, consider the transmission line system in Figure 8-20a. The normalized load impedance is  $Z_n = 1 + j$ . Using the Smith chart in Figure 8-20b, we find the load impedance at position A. The effective impedance reflected back to  $z = -l$  must lie on the circle of constant radius returning to A whenever  $l$  is an integer multiple of a half wavelength. The table in Figure 8-20 lists the impedance at  $z = -l$  for various line lengths. Note that at point C, where  $l = \lambda/4$ , that the normalized impedance is the reciprocal of

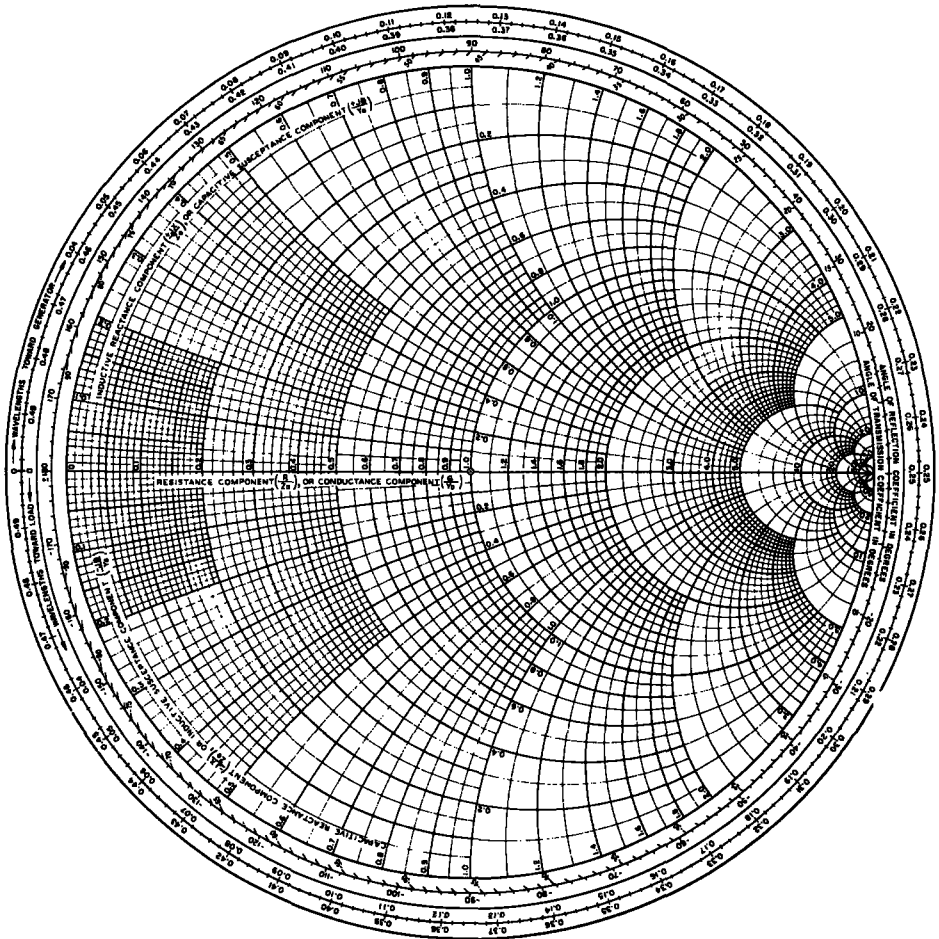


Figure 8-19 A complete Smith chart.

that at  $A$ . Similarly the normalized impedance at  $B$  is the reciprocal of that at  $D$ .

The current from the voltage source is found using the equivalent circuit shown in Figure 8-20c as

$$i = |\hat{I}| \sin(\omega t - \phi) \quad (21)$$

where the current magnitude and phase angle are

$$|\hat{I}| = \frac{V_0}{|50 + Z(z = -l)|}, \quad \phi = \tan^{-1} \frac{\text{Im}[Z(z = -l)]}{50 + \text{Re}[Z(z = -l)]} \quad (22)$$

Representative numerical values are listed in Figure 8-20.

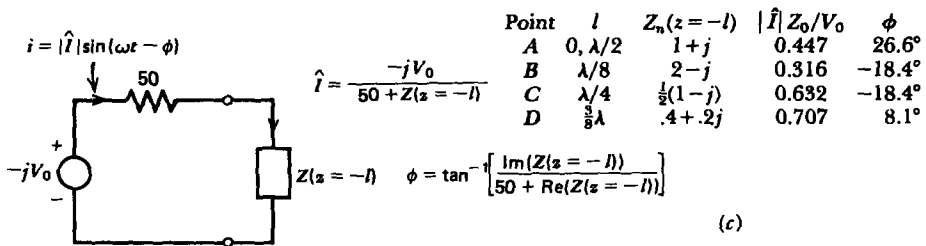
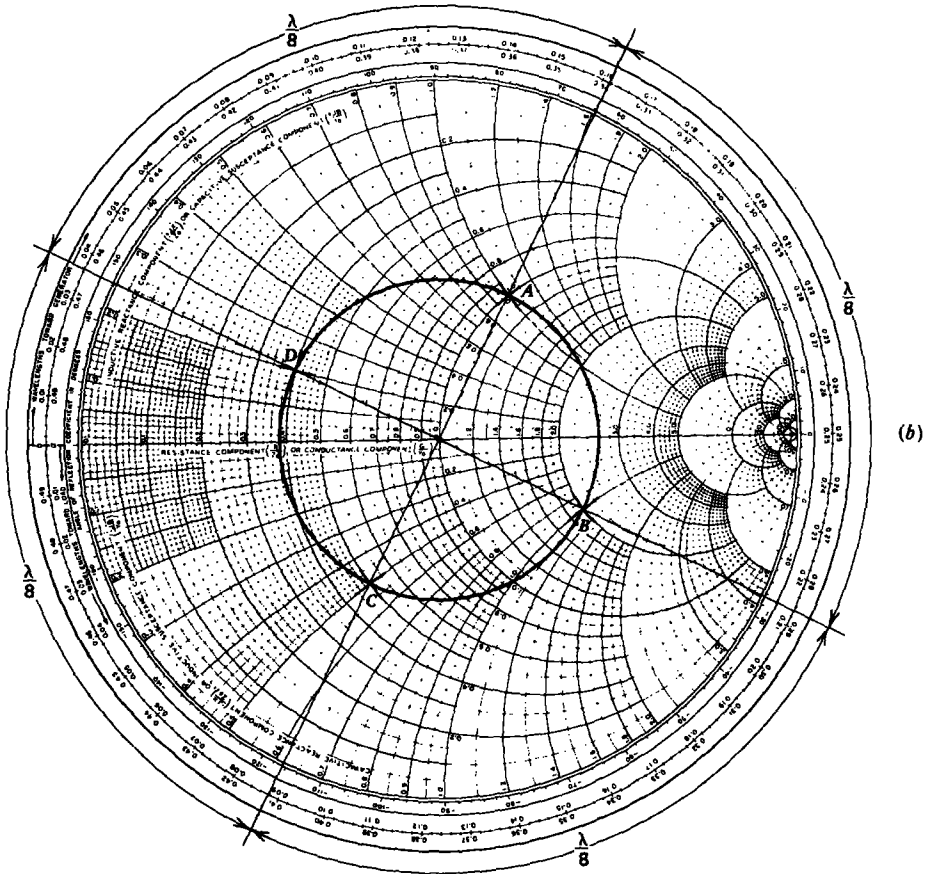
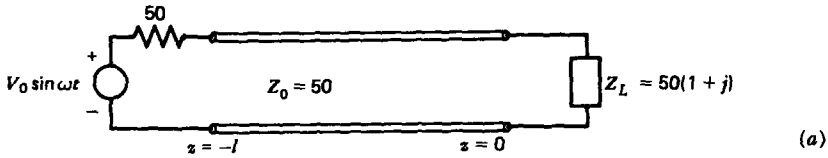


Figure 8-20 (a) The load impedance at  $z = 0$  reflected back to the source is found using the (b) Smith chart for various line lengths. Once this impedance is known the source current is found by solving the simple series circuit in (c).

8-4-4 Standing Wave Parameters

The impedance and reflection coefficient are not easily directly measured at microwave frequencies. In practice, one slides an ac voltmeter across a slotted transmission line and measures the magnitude of the peak or rms voltage and not its phase angle.

From (6) the magnitude of the voltage and current at any position  $z$  is

$$\begin{aligned} |\hat{v}(z)| &= |V_+| |1 + \Gamma(z)| \\ |\hat{i}(z)| &= Y_0 |V_+| |1 - \Gamma(z)| \end{aligned} \tag{23}$$

From (23), the variations of the voltage and current magnitudes can be drawn by a simple construction in the  $\Gamma$  plane, as shown in Figure 8-21. Note again that  $|V_+|$  is just a real number independent of  $z$  and that  $|\Gamma(z)| \leq 1$  for a passive termination. We plot  $|1 + \Gamma(z)|$  and  $|1 - \Gamma(z)|$  since these terms are proportional to the voltage and current magnitudes, respectively. The following properties from this con-

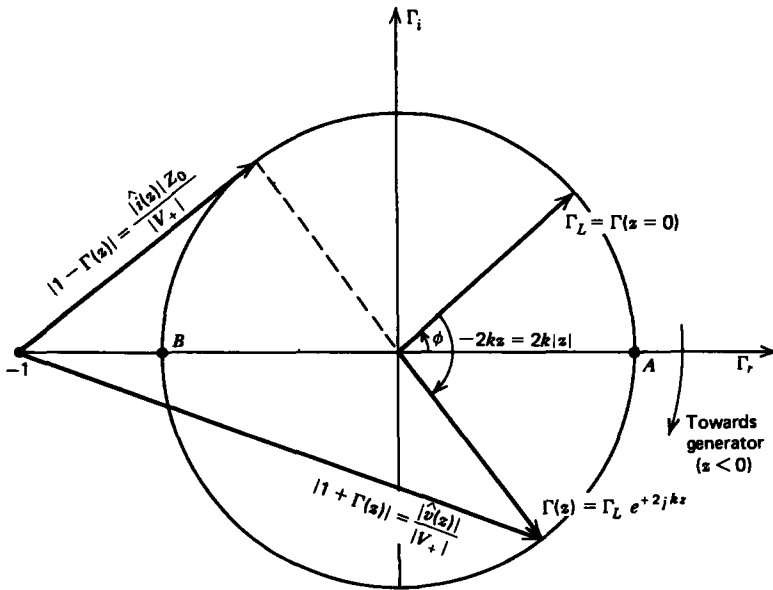


Figure 8-21 The voltage and current magnitudes along a transmission line are respectively proportional to the lengths of the vectors  $|1 + \Gamma(z)|$  and  $|1 - \Gamma(z)|$  in the complex  $\Gamma$  plane.

struction are apparent:

- (i) The magnitude of the current is smallest and the voltage magnitude largest when  $\Gamma(z) = 1$  at point *A* and vice versa when  $\Gamma(z) = -1$  at point *B*.
- (ii) The voltage and current are in phase at the points of maximum or minimum magnitude of either at points *A* or *B*.
- (iii) A rotation of  $\Gamma(z)$  by an angle  $\pi$  corresponds to a change of  $\lambda/4$  in  $z$ , thus any voltage (or current) maximum is separated by  $\lambda/4$  from its nearest minima on either side.

By plotting the lengths of the phasors  $|1 \pm \Gamma(z)|$ , as in Figure 8-22, we obtain a plot of what is called the standing wave pattern on the line. Observe that the curves are not sinusoidal. The minima are sharper than the maxima so the minima are usually located in position more precisely by measurement than the maxima.

From Figures 8-21 and 8-22, the ratio of the maximum voltage magnitude to the minimum voltage magnitude is defined as the voltage standing wave ratio, or VSWR for short:

$$\frac{|\hat{v}(z)|_{\max}}{|\hat{v}(z)|_{\min}} = \frac{1 + |\Gamma_L|}{1 - |\Gamma_L|} = \text{VSWR} \quad (24)$$

The VSWR is measured by simply recording the largest and smallest readings of a sliding voltmeter. Once the VSWR is measured, the reflection coefficient magnitude can be calculated from (24) as

$$|\Gamma_L| = \frac{\text{VSWR} - 1}{\text{VSWR} + 1} \quad (25)$$

The angle  $\phi$  of the reflection coefficient

$$\Gamma_L = |\Gamma_L| e^{j\phi} \quad (26)$$

can also be determined from these standing wave measurements. According to Figure 8-21,  $\Gamma(z)$  must swing clockwise through an angle  $\phi + \pi$  as we move from the load at  $z = 0$  toward the generator to the first voltage minimum at *B*. The shortest distance  $d_{\min}$  that we must move to reach the first voltage minimum is given by

$$2kd_{\min} = \phi + \pi \quad (27)$$

or

$$\frac{\phi}{\pi} = 4 \frac{d_{\min}}{\lambda} - 1 \quad (28)$$

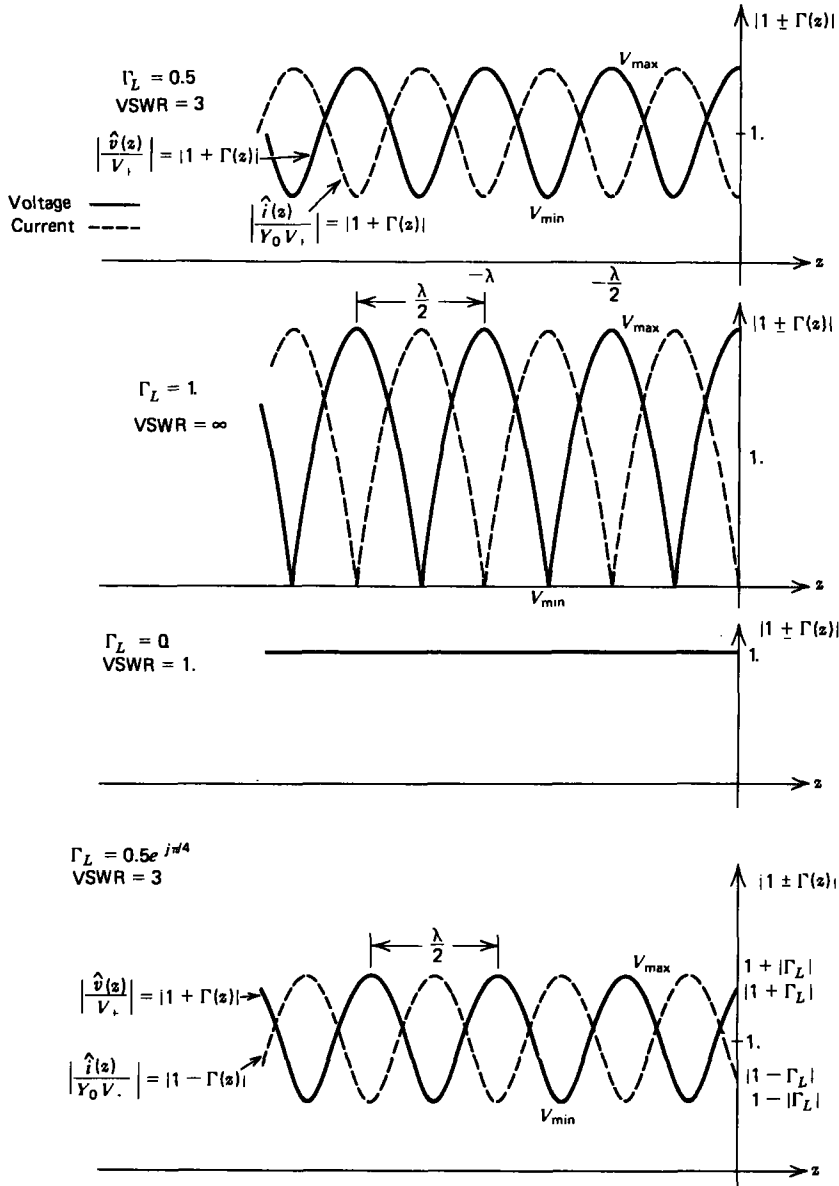


Figure 8-22 Voltage and current standing wave patterns plotted for various values of the VSWR.

A measurement of  $d_{min}$ , as well as a determination of the wavelength (the distance between successive minima or maxima is  $\lambda/2$ ) yields the complex reflection coefficient of the load using (25) and (28). Once we know the complex reflection coefficient we can calculate the load impedance

from (7). These standing wave measurements are sufficient to determine the terminating load impedance  $Z_L$ . These measurement properties of the load reflection coefficient and its relation to the load impedance are of great importance at high frequencies where the absolute measurement of voltage or current may be difficult. Some special cases of interest are:

- (i) Matched line—If  $\Gamma_L = 0$ , then  $VSWR = 1$ . The voltage magnitude is constant everywhere on the line.
- (ii) Short or open circuited line—If  $|\Gamma_L| = 1$ , then  $VSWR = \infty$ . The minimum voltage on the line is zero.
- (iii) The peak normalized voltage  $|\hat{v}(z)/V_+|$  is  $1 + |\Gamma_L|$  while the minimum normalized voltage is  $1 - |\Gamma_L|$ .
- (iv) The normalized voltage at  $z = 0$  is  $|1 + \Gamma_L|$  while the normalized current  $|\hat{i}(z)/Y_0 V_+|$  at  $z = 0$  is  $|1 - \Gamma_L|$ .
- (v) If the load impedance is real ( $Z_L = R_L$ ), then (4) shows us that  $\Gamma_L$  is real. Then evaluating (7) at  $z = 0$ , where  $\Gamma(z = 0) = \Gamma_L$ , we see that when  $Z_L > Z_0$  that  $VSWR = Z_L/Z_0$  while if  $Z_L < Z_0$ ,  $VSWR = Z_0/Z_L$ .

For a general termination, if we know the VSWR and  $d_{\min}$ , we can calculate the load impedance from (7) as

$$\begin{aligned} Z_L &= Z_0 \frac{1 + |\Gamma_L| e^{j\phi}}{1 - |\Gamma_L| e^{j\phi}} \\ &= Z_0 \frac{[VSWR + 1 + (VSWR - 1) e^{j\phi}]}{[VSWR + 1 - (VSWR - 1) e^{j\phi}]} \end{aligned} \quad (29)$$

Multiplying through by  $e^{-j\phi/2}$  and then simplifying yields

$$\begin{aligned} Z_L &= \frac{Z_0 [VSWR - j \tan(\phi/2)]}{[1 - j VSWR \tan(\phi/2)]} \\ &= \frac{Z_0 [1 - j VSWR \tan kd_{\min}]}{[VSWR - j \tan kd_{\min}]} \end{aligned} \quad (30)$$

### EXAMPLE 8-2 VOLTAGE STANDING WAVE RATIO

The VSWR on a 50-Ohm (characteristic impedance) transmission line is 2. The distance between successive voltage minima is 40 cm while the distance from the load to the first minima is 10 cm. What is the reflection coefficient and load impedance?

**SOLUTION**

We are given

$$\text{VSWR} = 2$$

$$kd_{\min} = \frac{2\pi(10)}{2(40)} = \frac{\pi}{4}$$

The reflection coefficient is given from (25)–(28) as

$$\Gamma_L = \frac{1}{3} e^{-j\pi/2} = \frac{-j}{3}$$

while the load impedance is found from (30) as

$$\begin{aligned} Z_L &= \frac{50(1-2j)}{2-j} \\ &= 40 - 30j \text{ ohm} \end{aligned}$$

**8-5 STUB TUNING**

In practice, most sources are connected to a transmission line through a series resistance matched to the line. This eliminates transient reflections when the excitation is turned on or off. To maximize the power flow to a load, it is also necessary for the load impedance reflected back to the source to be equal to the source impedance and thus equal to the characteristic impedance of the line,  $Z_0$ . This matching of the load to the line for an arbitrary termination can only be performed by adding additional elements along the line.

Usually these elements are short circuited transmission lines, called stubs, whose lengths can be varied. The reactance of the stub can be changed over the range from  $-j\infty$  to  $j\infty$  simply by varying its length, as found in Section 8-3-2, for the short circuited line. Because stubs are usually connected in parallel to a transmission line, it is more convenient to work with admittances rather than impedances as admittances in parallel simply add.

**8-5-1 Use of the Smith Chart for Admittance Calculations**

Fortunately the Smith chart can also be directly used for admittance calculations where the normalized admittance is defined as

$$Y_n(z) = \frac{Y(z)}{Y_0} = \frac{1}{Z_n(z)} \quad (1)$$

If the normalized load admittance  $Y_{nL}$  is known, straightforward impedance calculations first require the computation

$$Z_{nL} = 1/Y_{nL} \quad (2)$$

so that we could enter the Smith chart at  $Z_{nL}$ . Then we rotate by the required angle corresponding to  $2kz$  and read the new  $Z_n(z)$ . Then we again compute its reciprocal to find

$$Y_n(z) = 1/Z_n(z) \quad (3)$$

The two operations of taking the reciprocal are tedious. We can use the Smith chart itself to invert the impedance by using the fact that the normalized impedance is inverted by a  $\lambda/4$  section of line, so that a rotation of  $\Gamma(z)$  by  $180^\circ$  changes a normalized impedance into its reciprocal. Hence, if the admittance is given, we enter the Smith chart with a given value of normalized admittance  $Y_n$  and rotate by  $180^\circ$  to find  $Z_n$ . We then rotate by the appropriate number of wavelengths to find  $Z_n(z)$ . Finally, we again rotate by  $180^\circ$  to find  $Y_n(z) = 1/Z_n(z)$ . We have actually rotated the reflection coefficient by an angle of  $2\pi + 2kz$ . Rotation by  $2\pi$  on the Smith chart, however, brings us back to wherever we started, so that only the  $2kz$  rotation is significant. As long as we do an even number of  $\pi$  rotations by entering the Smith chart with an admittance and leaving again with an admittance, we can use the Smith chart with normalized admittances exactly as if they were normalized impedances.

### EXAMPLE 8-3 USE OF THE SMITH CHART FOR ADMITTANCE CALCULATIONS

The load impedance on a 50-Ohm line is

$$Z_L = 50(1 + j)$$

What is the admittance of the load?

#### SOLUTION

---

By direct computation we have

$$Y_L = \frac{1}{Z_L} = \frac{1}{50(1 + j)} = \frac{(1 - j)}{100}$$

To use the Smith chart we find the normalized impedance at A in Figure 8-23:

$$Z_{nL} = 1 + j$$

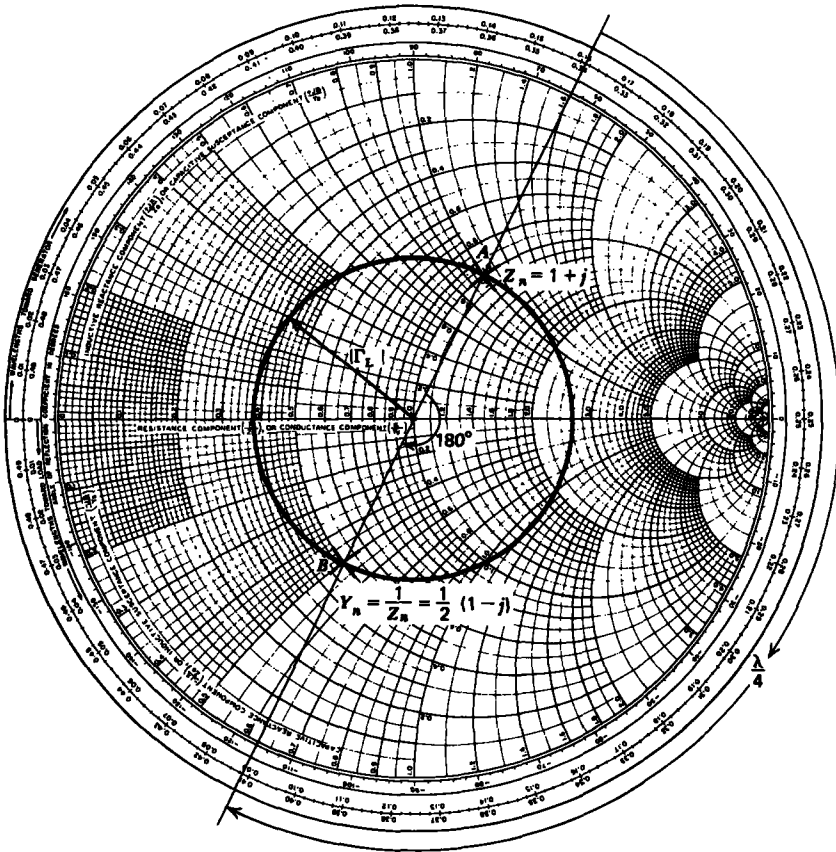


Figure 8-23 The Smith chart offers a convenient way to find the reciprocal of a complex number using the property that the normalized impedance reflected back by a quarter wavelength inverts. Thus, the normalized admittance is found by locating the normalized impedance and rotating this point by  $180^\circ$  about the constant  $|\Gamma_L|$  circle.

The normalized admittance that is the reciprocal of the normalized impedance is found by locating the impedance a distance  $\lambda/4$  away from the load end at B:

$$Y_{nL} = 0.5(1 - j) \Rightarrow Y_L = Y_n Y_0 = (1 - j)/100$$

Note that the point B is just  $180^\circ$  away from A on the constant  $|\Gamma_L|$  circle. For more complicated loads the Smith chart is a convenient way to find the reciprocal of a complex number.

### 8-5-2 Single-Stub Matching

A termination of value  $Z_L = 50(1+j)$  on a 50-Ohm transmission line is to be matched by means of a short circuited stub at a distance  $l_1$  from the load, as shown in Figure 8-24a. We need to find the line length  $l_1$  and the length of the stub  $l_2$  such that the impedance at the junction is matched to the line ( $Z_{in} = 50 \text{ Ohm}$ ). Then we know that all further points to the left of the junction have the same impedance of 50 Ohms.

Because of the parallel connection, it is simpler to use the Smith chart as an admittance transformation. The normalized load admittance can be computed using the Smith chart by rotating by  $180^\circ$  from the normalized load impedance at  $A$ , as was shown in Figure 8-23 and Example 8-3,

$$Z_{nL} = 1 + j \quad (4)$$

to yield

$$Y_{nL} = 0.5(1 - j) \quad (5)$$

at the point  $B$ .

Now we know from Section 8-3-2 that the short circuited stub can only add an imaginary component to the admittance. Since we want the total normalized admittance to be unity to the left of the stub in Figure 8-24

$$Y_{in} = Y_1 + Y_2 = 1 \quad (6)$$

when  $Y_{nL}$  is reflected back to be  $Y_1$  it must wind up on the circle whose real part is 1 (as  $Y_2$  can only be imaginary), which occurs either at  $C$  or back at  $A$  allowing  $l_1$  to be either  $0.25\lambda$  at  $A$  or  $(0.25 + 0.177)\lambda = 0.427\lambda$  at  $C$  (or these values plus any integer multiple of  $\lambda/2$ ). Then  $Y_1$  is either of the following two conjugate values:

$$Y_1 = \begin{cases} 1 + j, & l_1 = 0.25\lambda \text{ (A)} \\ 1 - j, & l_1 = 0.427\lambda \text{ (C)} \end{cases} \quad (7)$$

For  $Y_{in}$  to be unity we must pick  $Y_2$  to have an imaginary part to just cancel the imaginary part of  $Y_1$ :

$$Y_2 = \begin{cases} -j, & l_1 = 0.25\lambda \\ +j, & l_1 = 0.427\lambda \end{cases} \quad (8)$$

which means, since the shorted end has an infinite admittance at  $D$  that the stub must be of length such as to rotate the admittance to the points  $E$  or  $F$  requiring a stub length  $l_2$  of  $(\lambda/8)(E)$  or  $(3\lambda/8)(F)$  (or these values plus any integer multiple



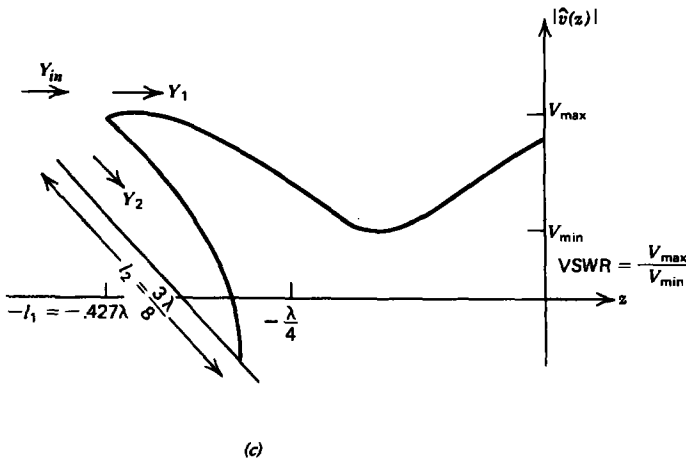


Figure 8-24

of  $\lambda/2$ ). Thus, the solutions can be summarized as

$$\begin{aligned} l_1 &= 0.25\lambda + n\lambda/2, & l_2 &= \lambda/8 + m\lambda/2 \\ \text{or} & & & \\ l_1 &= 0.427\lambda + n\lambda/2, & l_2 &= 3\lambda/8 + m\lambda/2 \end{aligned} \quad (9)$$

where  $n$  and  $m$  are any nonnegative integers (including zero).

When the load is matched by the stub to the line, the VSWR to the left of the stub is unity, while to the right of the stub over the length  $l_1$  the reflection coefficient is

$$\Gamma_L = \frac{Z_{nL} - 1}{Z_{nL} + 1} = \frac{j}{2 + j} \quad (10)$$

which has magnitude

$$|\Gamma_L| = 1/\sqrt{5} \approx 0.447 \quad (11)$$

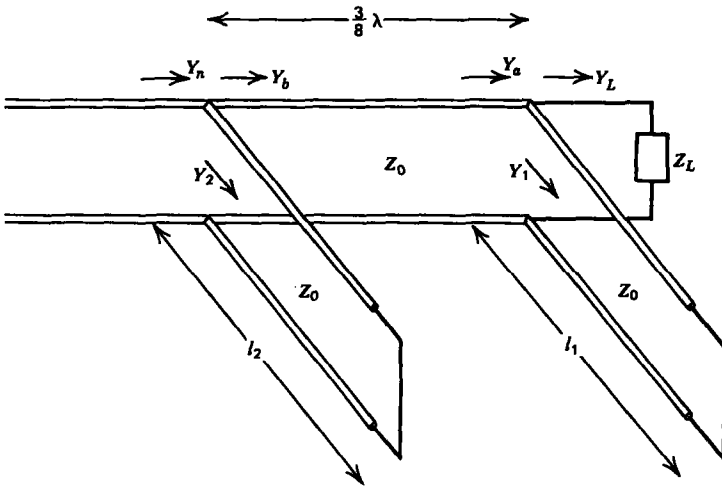
so that the voltage standing wave ratio is

$$\text{VSWR} = \frac{1 + |\Gamma_L|}{1 - |\Gamma_L|} \approx 2.62 \quad (12)$$

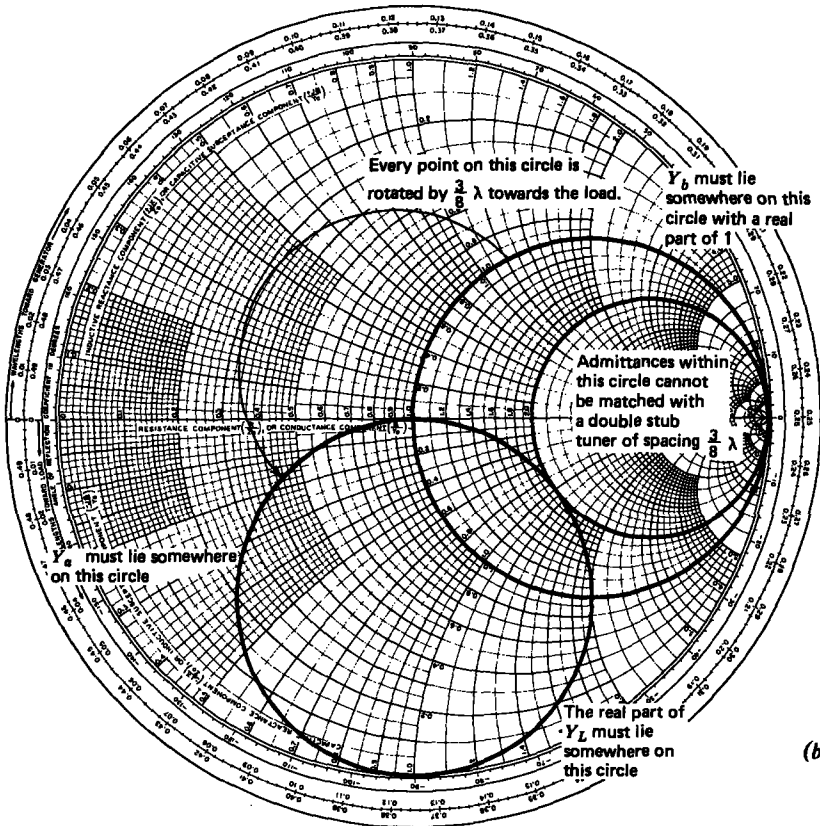
The disadvantage to single-stub tuning is that it is not easy to vary the length  $l_1$ . Generally new elements can only be connected at the ends of the line and not inbetween.

### 8-5-3 Double-Stub Matching

This difficulty of not having a variable length line can be overcome by using two short circuited stubs a fixed length apart, as shown in Figure 8-25a. This fixed length is usually  $\frac{3}{8}\lambda$ . A match is made by adjusting the length of the stubs  $l_1$  and



(a)



(b)

Figure 8-25 (a) A double stub tuner of fixed spacing cannot match all loads but is useful because additional elements can only be placed at transmission line terminations and not at any general position along a line as required for a single-stub tuner. (b) Smith chart construction. If the stubs are  $\frac{3}{8}\lambda$  apart, normalized load admittances whose real part exceeds 2 cannot be matched.

$l_2$ . One problem with the double-stub tuner is that not all loads can be matched for a given stub spacing.

The normalized admittances at each junction are related as

$$\begin{aligned} Y_a &= Y_1 + Y_L \\ Y_n &= Y_2 + Y_b \end{aligned} \quad (13)$$

where  $Y_1$  and  $Y_2$  are the purely reactive admittances of the stubs reflected back to the junctions while  $Y_b$  is the admittance of  $Y_a$  reflected back towards the load by  $\frac{3}{8}\lambda$ . For a match we require that  $Y_n$  be unity. Since  $Y_2$  is purely imaginary, the real part of  $Y_b$  must lie on the circle with a real part of unity. Then  $Y_a$  must lie somewhere on this circle when each point on the circle is reflected back by  $\frac{3}{8}\lambda$ . This generates another circle that is  $\frac{3}{2}\pi$  back in the counterclockwise direction as we are moving toward the load, as illustrated in Figure 8-25*b*. To find the conditions for a match, we work from left to right towards the load using the following reasoning:

- (i) Since  $Y_2$  is purely imaginary, the real part of  $Y_b$  must lie on the circle with a real part of unity, as in Figure 8-25*b*.
- (ii) Every possible point on  $Y_b$  must be reflected towards the load by  $\frac{3}{8}\lambda$  to find the locus of possible match for  $Y_a$ . This generates another circle that is  $\frac{3}{2}\pi$  back in the counterclockwise direction as we move towards the load, as in Figure 8-25*b*.

Again since  $Y_1$  is purely imaginary, the real part of  $Y_a$  must also equal the real part of the load admittance. This yields two possible solutions if the load admittance is outside the forbidden circle enclosing all load admittances with a real part greater than 2. Only loads with normalized admittances whose real part is less than 2 can be matched by the double-stub tuner of  $\frac{3}{8}\lambda$  spacing. Of course, if a load is within the forbidden circle, it can be matched by a double-stub tuner if the stub spacing is different than  $\frac{3}{8}\lambda$ .

#### EXAMPLE 8-4 DOUBLE-STUB MATCHING

The load impedance  $Z_L = 50(1 + j)$  on a 50-Ohm line is to be matched by a double-stub tuner of  $\frac{3}{8}\lambda$  spacing. What stub lengths  $l_1$  and  $l_2$  are necessary?

#### SOLUTION

The normalized load impedance  $Z_{nL} = 1 + j$  corresponds to a normalized load admittance:

$$Y_{nL} = 0.5(1 - j)$$



Then the two solutions for  $Y_a$  lie on the intersection of the circle shown in Figure 8-26a with the  $r = 0.5$  circle:

$$Y_{a1} = 0.5 - 0.14j$$

$$Y_{a2} = 0.5 - 1.85j$$

We then find  $Y_1$  by solving for the imaginary part of the upper equation in (13):

$$Y_1 = j \operatorname{Im}(Y_a - Y_L) = \begin{cases} 0.36j \Rightarrow l_1 = 0.305\lambda & (F) \\ -1.35j \Rightarrow l_1 = 0.1\lambda & (E) \end{cases}$$

By rotating the  $Y_a$  solutions by  $\frac{3}{8}\lambda$  back to the generator ( $270^\circ$  clockwise, which is equivalent to  $90^\circ$  counterclockwise), their intersection with the  $r = 1$  circle gives the solutions for  $Y_b$  as

$$Y_{b1} = 1.0 - 0.72j$$

$$Y_{b2} = 1.0 + 2.7j$$

This requires  $Y_2$  to be

$$Y_2 = -j \operatorname{Im}(Y_b) = \begin{cases} 0.72j \Rightarrow l_2 = 0.349\lambda & (G) \\ -2.7j \Rightarrow l_2 = 0.056\lambda & (H) \end{cases}$$

The voltage standing wave pattern along the line and stubs is shown in Figure 8.26b. Note the continuity of voltage at the junctions. The actual stub lengths can be those listed plus any integer multiple of  $\lambda/2$ .

## 8-6 THE RECTANGULAR WAVEGUIDE

We showed in Section 8-1-2 that the electric and magnetic fields for TEM waves have the same form of solutions in the plane transverse to the transmission line axis as for statics. The inner conductor within a closed transmission line structure such as a coaxial cable is necessary for TEM waves since it carries a surface current and a surface charge distribution, which are the source for the magnetic and electric fields. A hollow conducting structure, called a waveguide, cannot propagate TEM waves since the static fields inside a conducting structure enclosing no current or charge is zero.

However, new solutions with electric or magnetic fields along the waveguide axis as well as in the transverse plane are allowed. Such solutions can also propagate along transmission lines. Here the axial displacement current can act as a source

of the transverse magnetic field giving rise to transverse magnetic (TM) modes as the magnetic field lies entirely within the transverse plane. Similarly, an axial time varying magnetic field generates transverse electric (TE) modes. The most general allowed solutions on a transmission line are TEM, TM, and TE modes. Removing the inner conductor on a closed transmission line leaves a waveguide that can only propagate TM and TE modes.

### 8-6-1 Governing Equations

To develop these general solutions we return to Maxwell's equations in a linear source-free material:

$$\begin{aligned}\nabla \times \mathbf{E} &= -\mu \frac{\partial \mathbf{H}}{\partial t} \\ \nabla \times \mathbf{H} &= \epsilon \frac{\partial \mathbf{E}}{\partial t} \\ \epsilon \nabla \cdot \mathbf{E} &= 0 \\ \mu \nabla \cdot \mathbf{H} &= 0\end{aligned}\tag{1}$$

Taking the curl of Faraday's law, we expand the double cross product and then substitute Ampere's law to obtain a simple vector equation in  $\mathbf{E}$  alone:

$$\begin{aligned}\nabla \times (\nabla \times \mathbf{E}) &= \nabla(\nabla \cdot \mathbf{E}) - \nabla^2 \mathbf{E} \\ &= -\mu \frac{\partial}{\partial t} (\nabla \times \mathbf{H}) \\ &= -\epsilon \mu \frac{\partial^2 \mathbf{E}}{\partial t^2}\end{aligned}\tag{2}$$

Since  $\nabla \cdot \mathbf{E} = 0$  from Gauss's law when the charge density is zero, (2) reduces to the vector wave equation in  $\mathbf{E}$ :

$$\nabla^2 \mathbf{E} = \frac{1}{c^2} \frac{\partial^2 \mathbf{E}}{\partial t^2}, \quad c^2 = \frac{1}{\epsilon \mu}\tag{3}$$

If we take the curl of Ampere's law and perform similar operations, we also obtain the vector wave equation in  $\mathbf{H}$ :

$$\nabla^2 \mathbf{H} = \frac{1}{c^2} \frac{\partial^2 \mathbf{H}}{\partial t^2}\tag{4}$$

The solutions for  $\mathbf{E}$  and  $\mathbf{H}$  in (3) and (4) are not independent. If we solve for either  $\mathbf{E}$  or  $\mathbf{H}$ , the other field is obtained from (1). The vector wave equations in (3) and (4) are valid for any shaped waveguide. In particular, we limit ourselves in this text to waveguides whose cross-sectional shape is rectangular, as shown in Figure 8-27.

### 8-6-2 Transverse Magnetic (TM) Modes

We first consider TM modes where the magnetic field has  $x$  and  $y$  components but no  $z$  component. It is simplest to solve (3) for the  $z$  component of electric field and then obtain the other electric and magnetic field components in terms of  $E_z$  directly from Maxwell's equations in (1).

We thus assume solutions of the form

$$E_z = \text{Re} [\hat{E}_z(x, y) e^{j(\omega t - k_z z)}] \quad (5)$$

where an exponential  $z$  dependence is assumed because the cross-sectional area of the waveguide is assumed to be uniform in  $z$  so that none of the coefficients in (1) depends on  $z$ . Then substituting into (3) yields the Helmholtz equation:

$$\frac{\partial^2 E_z}{\partial x^2} + \frac{\partial^2 E_z}{\partial y^2} - \left( k_z^2 - \frac{\omega^2}{c^2} \right) \hat{E}_z = 0 \quad (6)$$

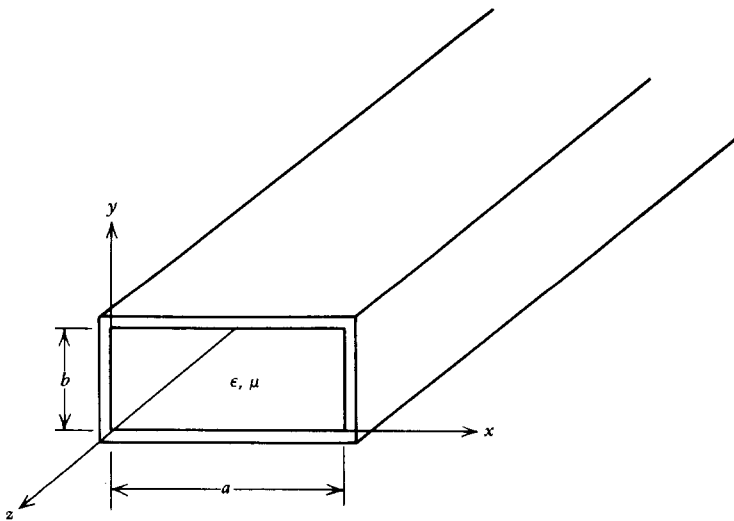


Figure 8-27 A lossless waveguide with rectangular cross section.

This equation can be solved by assuming the same product solution as used for solving Laplace's equation in Section 4-2-1, of the form

$$\hat{E}_z(x, y) = X(x)Y(y) \quad (7)$$

where  $X(x)$  is only a function of the  $x$  coordinate and  $Y(y)$  is only a function of  $y$ . Substituting this assumed form of solution into (6) and dividing through by  $X(x)Y(y)$  yields

$$\frac{1}{X} \frac{d^2 X}{dx^2} + \frac{1}{Y} \frac{d^2 Y}{dy^2} = k_z^2 - \frac{\omega^2}{c^2} \quad (8)$$

When solving Laplace's equation in Section 4-2-1 the right-hand side was zero. Here the reasoning is the same. The first term on the left-hand side in (8) is only a function of  $x$  while the second term is only a function of  $y$ . The only way a function of  $x$  and a function of  $y$  can add up to a constant for all  $x$  and  $y$  is if each function alone is a constant,

$$\begin{aligned} \frac{1}{X} \frac{d^2 X}{dx^2} &= -k_x^2 \\ \frac{1}{Y} \frac{d^2 Y}{dy^2} &= -k_y^2 \end{aligned} \quad (9)$$

where the separation constants must obey the relation

$$k_x^2 + k_y^2 + k_z^2 = k^2 = \omega^2/c^2 \quad (10)$$

When we solved Laplace's equation in Section 4-2-6, there was no time dependence so that  $\omega = 0$ . Then we found that at least one of the wavenumbers was imaginary, yielding decaying solutions. For finite frequencies it is possible for all three wavenumbers to be real for pure propagation. The values of these wavenumbers will be determined by the dimensions of the waveguide through the boundary conditions.

The solutions to (9) are sinusoids so that the transverse dependence of the axial electric field  $\hat{E}_z(x, y)$  is

$$\hat{E}_z(x, y) = (A_1 \sin k_x x + A_2 \cos k_x x)(B_1 \sin k_y y + B_2 \cos k_y y) \quad (11)$$

Because the rectangular waveguide in Figure 8-27 is composed of perfectly conducting walls, the tangential component of electric field at the walls is zero:

$$\begin{aligned} \hat{E}_z(x, y=0) &= 0, & \hat{E}_z(x=0, y) &= 0 \\ \hat{E}_z(x, y=b) &= 0, & \hat{E}_z(x=a, y) &= 0 \end{aligned} \quad (12)$$

These boundary conditions then require that  $A_2$  and  $B_2$  are zero so that (11) simplifies to

$$\hat{E}_z(x, y) = E_0 \sin k_x x \sin k_y y \quad (13)$$

where  $E_0$  is a field amplitude related to a source strength and the transverse wavenumbers must obey the equalities

$$\begin{aligned} k_x &= m\pi/a, & m &= 1, 2, 3, \dots \\ k_y &= n\pi/b, & n &= 1, 2, 3, \dots \end{aligned} \quad (14)$$

Note that if either  $m$  or  $n$  is zero in (13), the axial electric field is zero. The waveguide solutions are thus described as  $\text{TM}_{mn}$  modes where both  $m$  and  $n$  are integers greater than zero.

The other electric field components are found from the  $z$  component of Faraday's law, where  $\mathbf{H}_z = 0$  and the charge-free Gauss's law in (1):

$$\begin{aligned} \frac{\partial E_y}{\partial x} &= \frac{\partial E_x}{\partial y} \\ \frac{\partial E_x}{\partial x} + \frac{\partial E_y}{\partial y} + \frac{\partial E_z}{\partial z} &= 0 \end{aligned} \quad (15)$$

By taking  $\partial/\partial x$  of the top equation and  $\partial/\partial y$  of the lower equation, we eliminate  $E_x$  to obtain

$$\frac{\partial^2 E_y}{\partial x^2} + \frac{\partial^2 E_y}{\partial y^2} = -\frac{\partial^2 E_z}{\partial y \partial z} \quad (16)$$

where the right-hand side is known from (13). The general solution for  $E_y$  must be of the same form as (11), again requiring the tangential component of electric field to be zero at the waveguide walls,

$$\hat{E}_y(x=0, y) = 0, \quad \hat{E}_y(x=a, y) = 0 \quad (17)$$

so that the solution to (16) is

$$\hat{E}_y = -\frac{jk_y k_z E_0}{k_x^2 + k_y^2} \sin k_x x \cos k_y y \quad (18)$$

We then solve for  $E_x$  using the upper equation in (15):

$$\hat{E}_x = -\frac{jk_x k_z E_0}{k_x^2 + k_y^2} \cos k_x x \sin k_y y \quad (19)$$

where we see that the boundary conditions

$$\hat{E}_x(x, y=0) = 0, \quad \hat{E}_x(x, y=b) = 0 \quad (20)$$

are satisfied.

The magnetic field is most easily found from Faraday's law

$$\hat{\mathbf{H}}(\mathbf{x}, y) = -\frac{1}{j\omega\mu} \nabla \times \hat{\mathbf{E}}(\mathbf{x}, y) \quad (21)$$

to yield

$$\begin{aligned} \hat{H}_x &= -\frac{1}{j\omega\mu} \left( \frac{\partial \hat{E}_z}{\partial y} - \frac{\partial \hat{E}_y}{\partial z} \right) \\ &= -\frac{k_y k^2}{j\omega\mu (k_x^2 + k_y^2)} E_0 \sin k_x x \cos k_y y \\ &= \frac{j\omega\epsilon k_y}{k_x^2 + k_y^2} E_0 \sin k_x x \cos k_y y \\ \hat{H}_y &= -\frac{1}{j\omega\mu} \left( \frac{\partial \hat{E}_z}{\partial x} - \frac{\partial \hat{E}_x}{\partial z} \right) \\ &= \frac{k_x k^2 E_0}{j\omega\mu (k_x^2 + k_y^2)} \cos k_x x \sin k_y y \\ &= -\frac{j\omega\epsilon k_x}{k_x^2 + k_y^2} E_0 \cos k_x x \sin k_y y \\ \hat{H}_z &= 0 \end{aligned} \quad (22)$$

Note the boundary conditions of the normal component of  $\mathbf{H}$  being zero at the waveguide walls are automatically satisfied:

$$\begin{aligned} \hat{H}_y(x, y=0) &= 0, & \hat{H}_y(x, y=b) &= 0 \\ \hat{H}_x(x=0, y) &= 0, & \hat{H}_x(x=a, y) &= 0 \end{aligned} \quad (23)$$

The surface charge distribution on the waveguide walls is found from the discontinuity of normal  $\mathbf{D}$  fields:

$$\begin{aligned} \hat{\sigma}_f(x=0, y) &= \epsilon \hat{E}_x(x=0, y) = -\frac{jk_x k_x \epsilon}{k_x^2 + k_y^2} E_0 \sin k_y y \\ \hat{\sigma}_f(x=a, y) &= -\epsilon \hat{E}_x(x=a, y) = \frac{jk_x k_x \epsilon}{k_x^2 + k_y^2} E_0 \cos m\pi \sin k_y y \\ \hat{\sigma}_f(x, y=0) &= \epsilon \hat{E}_y(x, y=0) = -\frac{jk_x k_y \epsilon}{k_x^2 + k_y^2} E_0 \sin k_x x \\ \hat{\sigma}_f(x, y=b) &= -\epsilon \hat{E}_y(x, y=b) = \frac{jk_x k_y \epsilon}{k_x^2 + k_y^2} E_0 \cos n\pi \sin k_x x \end{aligned} \quad (24)$$

Similarly, the surface currents are found by the discontinuity in the tangential components of  $\mathbf{H}$  to be purely  $z$  directed:

$$\begin{aligned}\hat{K}_z(x, y = 0) &= -\hat{H}_x(x, y = 0) = \frac{k_y k^2 E_0 \sin k_x x}{j\omega\mu(k_x^2 + k_y^2)} \\ \hat{K}_z(x, y = b) &= \hat{H}_x(x, y = b) = -\frac{k_y k^2 E_0}{j\omega\mu(k_x^2 + k_y^2)} \sin k_x x \cos n\pi \\ \hat{K}_z(x = 0, y) &= \hat{H}_y(x = 0, y) = \frac{k_x k^2 E_0}{j\omega\mu(k_x^2 + k_y^2)} \sin k_y y \\ \hat{K}_z(x = a, y) &= -\hat{H}_y(x = a, y) = -\frac{k_x k^2 E_0 \cos m\pi \sin k_y y}{j\omega\mu(k_x^2 + k_y^2)}\end{aligned}\quad (25)$$

We see that if  $m$  or  $n$  are even, the surface charges and surface currents on opposite walls are of opposite sign, while if  $m$  or  $n$  are odd, they are of the same sign. This helps us in plotting the field lines for the various  $\text{TM}_{mn}$  modes shown in Figure 8-28. The electric field is always normal and the magnetic field tangential to the waveguide walls. Where the surface charge is positive, the electric field points out of the wall, while it points in where the surface charge is negative. For higher order modes the field patterns shown in Figure 8-28 repeat within the waveguide.

Slots are often cut in waveguide walls to allow the insertion of a small sliding probe that measures the electric field. These slots must be placed at positions of zero surface current so that the field distributions of a particular mode are only negligibly disturbed. If a slot is cut along the  $z$  direction on the  $y = b$  surface at  $x = a/2$ , the surface current given in (25) is zero for  $\text{TM}$  modes if  $\sin(k_x a/2) = 0$ , which is true for the  $m = \text{even}$  modes.

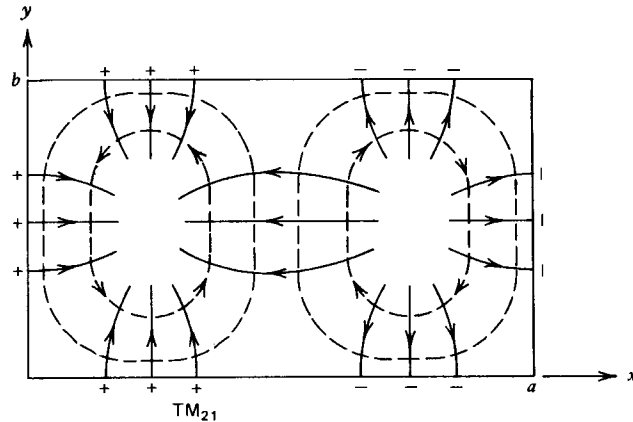
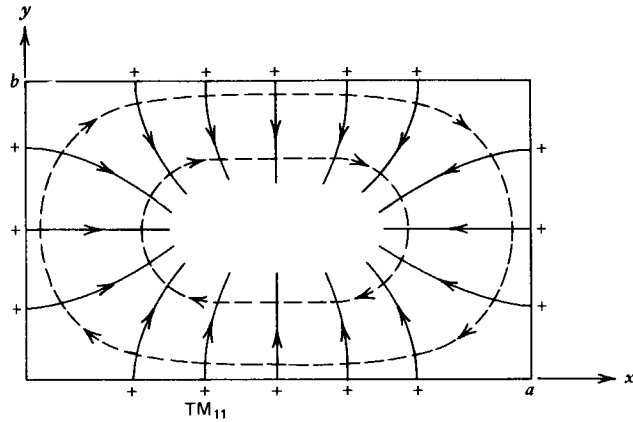
### 8-6-3 Transverse Electric (TE) Modes

When the electric field lies entirely in the  $xy$  plane, it is most convenient to first solve (4) for  $H_z$ . Then as for  $\text{TM}$  modes we assume a solution of the form

$$H_z = \text{Re} [\hat{H}_z(x, y) e^{j(\omega t - k_z z)}] \quad (26)$$

which when substituted into (4) yields

$$\frac{\partial^2 \hat{H}_z}{\partial x^2} + \frac{\partial^2 \hat{H}_z}{\partial y^2} - \left(k_z^2 - \frac{\omega^2}{c^2}\right) \hat{H}_z = 0 \quad (27)$$



Electric field (—)

$$\hat{E}_x = \frac{-jk_x k_y E_0}{k_x^2 + k_y^2} \cos k_x x \sin k_y y$$

$$\hat{E}_y = \frac{-jk_y k_x E_0}{k_x^2 + k_y^2} \sin k_x x \cos k_y y$$

$$\hat{E}_z = E_0 \sin k_x x \sin k_y y$$

$$\frac{dy}{dx} = \frac{E_y}{E_x} = \frac{k_y \tan k_x x}{k_x \tan k_y y}$$

$$\Rightarrow \frac{[\cos k_x x]^{(k_y/k_x)^2}}{\cos k_y y} = \text{const}$$

Magnetic field (----)

$$\hat{H}_x = \frac{j\omega\epsilon k_y}{k_x^2 + k_y^2} E_0 \sin k_x x \cos k_y y$$

$$\hat{H}_y = \frac{-j\omega\epsilon k_x}{k_x^2 + k_y^2} E_0 \cos k_x x \sin k_y y$$

$$\frac{dy}{dx} = \frac{H_y}{H_x} = \frac{-k_x \cot k_x x}{k_y \cot k_y y}$$

$$\Rightarrow \sin k_x x \sin k_y y = \text{const}$$

$$k_x = \frac{m\pi}{a}, \quad k_y = \frac{n\pi}{b}, \quad k_z = \left[ \frac{\omega^2}{c^2} - k_x^2 - k_y^2 \right]^{1/2}$$

Figure 8-28 The transverse electric and magnetic field lines for the  $TM_{11}$  and  $TM_{21}$  modes. The electric field is purely  $z$  directed where the field lines converge.

Again this equation is solved by assuming a product solution and separating to yield a solution of the same form as (11):

$$\hat{H}_z(x, y) = (A_1 \sin k_x x + A_2 \cos k_x x)(B_1 \sin k_y y + B_2 \cos k_y y) \quad (28)$$

The boundary conditions of zero normal components of  $\mathbf{H}$  at the waveguide walls require that

$$\begin{aligned} \hat{H}_x(x=0, y) = 0, \quad \hat{H}_x(x=a, y) = 0 \\ \hat{H}_y(x, y=0) = 0, \quad \hat{H}_y(x, y=b) = 0 \end{aligned} \quad (29)$$

Using identical operations as in (15)–(20) for the TM modes the magnetic field solutions are

$$\begin{aligned} \hat{H}_x &= \frac{jk_x k_y H_0}{k_x^2 + k_y^2} \sin k_x x \cos k_y y, \quad k_x = \frac{m\pi}{a}, \quad k_y = \frac{n\pi}{b} \\ \hat{H}_y &= \frac{jk_x k_y H_0}{k_x^2 + k_y^2} \cos k_x x \sin k_y y \\ \hat{H}_z &= H_0 \cos k_x x \cos k_y y \end{aligned} \quad (30)$$

The electric field is then most easily obtained from Ampere's law in (1),

$$\hat{\mathbf{E}} = \frac{1}{j\omega\epsilon} \nabla \times \hat{\mathbf{H}} \quad (31)$$

to yield

$$\begin{aligned} \hat{E}_x &= \frac{1}{j\omega\epsilon} \left( \frac{\partial}{\partial y} \hat{H}_z - \frac{\partial}{\partial z} \hat{H}_y \right) \\ &= -\frac{k_y k^2 H_0}{j\omega\epsilon (k_x^2 + k_y^2)} \cos k_x x \sin k_y y \\ &= \frac{j\omega\mu k_y}{k_x^2 + k_y^2} H_0 \cos k_x x \sin k_y y \\ \hat{E}_y &= \frac{1}{j\omega\epsilon} \left( \frac{\partial \hat{H}_x}{\partial z} - \frac{\partial \hat{H}_z}{\partial x} \right) \\ &= \frac{k_x k^2 H_0}{j\omega\epsilon (k_x^2 + k_y^2)} \sin k_x x \cos k_y y \\ &= -\frac{j\omega\mu k_x}{k_x^2 + k_y^2} H_0 \sin k_x x \cos k_y y \\ \hat{E}_z &= 0 \end{aligned} \quad (32)$$

We see in (32) that as required the tangential components of the electric field at the waveguide walls are zero. The

surface charge densities on each of the walls are:

$$\begin{aligned}
 \hat{\sigma}_f(x=0, y) &= \varepsilon \hat{E}_x(x=0, y) = \frac{-k_y k^2 H_0}{j\omega(k_x^2 + k_y^2)} \sin k_y y \\
 \hat{\sigma}_f(x=a, y) &= -\varepsilon \hat{E}_x(x=a, y) = \frac{k_y k^2 H_0}{j\omega(k_x^2 + k_y^2)} \cos m\pi \sin k_y y \\
 \hat{\sigma}_f(x, y=0) &= \varepsilon \hat{E}_y(x, y=0) = \frac{k_x k^2 H_0}{j\omega(k_x^2 + k_y^2)} \sin k_x x \\
 \hat{\sigma}_f(x, y=b) &= -\varepsilon \hat{E}_y(x, y=b) = -\frac{k_x k^2 H_0}{j\omega(k_x^2 + k_y^2)} \cos n\pi \sin k_x x
 \end{aligned} \tag{33}$$

For TE modes, the surface currents determined from the discontinuity of tangential  $\mathbf{H}$  now flow in closed paths on the waveguide walls:

$$\begin{aligned}
 \hat{\mathbf{K}}(x=0, y) &= \mathbf{i}_x \times \hat{\mathbf{H}}(x=0, y) \\
 &= \mathbf{i}_z \hat{H}_y(x=0, y) - \mathbf{i}_y \hat{H}_z(x=0, y) \\
 \hat{\mathbf{K}}(x=a, y) &= -\mathbf{i}_x \times \hat{\mathbf{H}}(x=a, y) \\
 &= -\mathbf{i}_z \hat{H}_y(x=a, y) + \mathbf{i}_y \hat{H}_z(x=a, y) \\
 \hat{\mathbf{K}}(x, y=0) &= \mathbf{i}_y \times \hat{\mathbf{H}}(x, y=0) \\
 &= -\mathbf{i}_z \hat{H}_x(x, y=0) + \mathbf{i}_x \hat{H}_z(x, y=0) \\
 \hat{\mathbf{K}}(x, y=b) &= -\mathbf{i}_y \times \hat{\mathbf{H}}(x, y=b) \\
 &= \mathbf{i}_z \hat{H}_x(x, y=b) - \mathbf{i}_x \hat{H}_z(x, y=b)
 \end{aligned} \tag{34}$$

Note that for TE modes either  $n$  or  $m$  (but not both) can be zero and still yield a nontrivial set of solutions. As shown in Figure 8-29, when  $n$  is zero there is no variation in the fields in the  $y$  direction and the electric field is purely  $y$  directed while the magnetic field has no  $y$  component. The  $\text{TE}_{11}$  and  $\text{TE}_{21}$  field patterns are representative of the higher order modes.

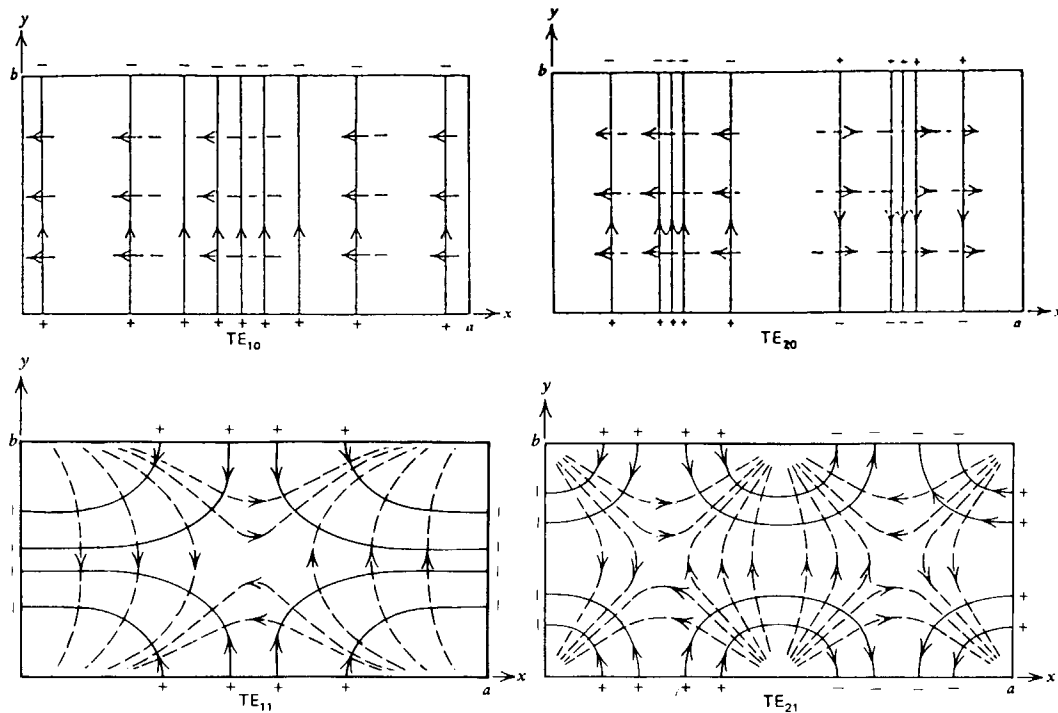
#### 8-6-4 Cut-Off

The transverse wavenumbers are

$$k_x = \frac{m\pi}{a}, \quad k_y = \frac{n\pi}{b} \tag{35}$$

so that the axial variation of the fields is obtained from (10) as

$$k_z = \left[ \frac{\omega^2}{c^2} - k_x^2 - k_y^2 \right]^{1/2} = \left[ \frac{\omega^2}{c^2} - \left( \frac{m\pi}{a} \right)^2 - \left( \frac{n\pi}{b} \right)^2 \right]^{1/2} \tag{36}$$



Electric field (—)

$$\hat{E}_x = \frac{j\omega\mu k_y}{k_x^2 + k_y^2} H_0 \cos k_x x \sin k_y y$$

$$\hat{E}_y = \frac{-j\omega\mu k_x}{k_x^2 + k_y^2} H_0 \sin k_x x \cos k_y y$$

$$k_x = \frac{m\pi}{a}, \quad k_y = \frac{n\pi}{b}, \quad k_z = \left[ \frac{\omega^2}{c^2} - k_x^2 - k_y^2 \right]^{1/2}$$

$$\frac{dy}{dx} = \frac{E_y}{E_x} = \frac{-k_x \tan k_x x}{k_y \tan k_y y}$$

$$\Rightarrow \cos k_x x \cos k_y y = \text{const}$$

Magnetic field (---)

$$\hat{H}_x = \frac{jk_z k_x H_0}{k_x^2 + k_y^2} \sin k_x x \cos k_y y$$

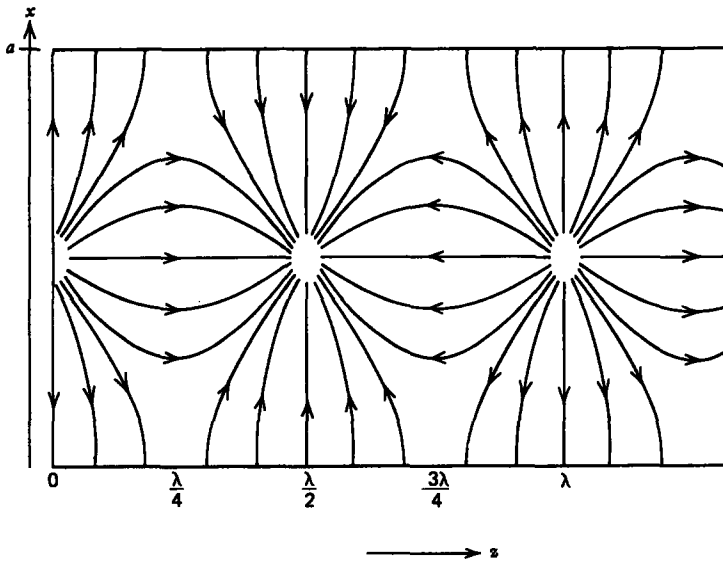
$$\hat{H}_y = \frac{jk_z k_y H_0}{k_x^2 + k_y^2} \cos k_x x \sin k_y y$$

$$\hat{H}_z = H_0 \cos k_x x \cos k_y y$$

$$\frac{dy}{dx} = \frac{H_y}{H_x} = \frac{k_y \cot k_x x}{k_x \cot k_y y}$$

$$\Rightarrow \frac{[\sin k_x x]^{(k_y/k_x)^2}}{\sin k_y y} = \text{const}$$

Figure 8-29 (a) The transverse electric and magnetic field lines for various TE modes. The magnetic field is purely z directed where the field lines converge. The  $TE_{10}$  mode is called the dominant mode since it has the lowest cut-off frequency. (b) Surface current lines for the  $TE_{10}$  mode.



(b)

Figure 8-29

Thus, although  $k_x$  and  $k_y$  are real,  $k_z$  can be either pure real or pure imaginary. A real value of  $k_z$  represents power flow down the waveguide in the  $z$  direction. An imaginary value of  $k_z$  means exponential decay with no time-average power flow. The transition from propagating waves ( $k_z$  real) to evanescence ( $k_z$  imaginary) occurs for  $k_z = 0$ . The frequency when  $k_z$  is zero is called the cut-off frequency  $\omega_c$ :

$$\omega_c = c \left[ \left( \frac{m\pi}{a} \right)^2 + \left( \frac{n\pi}{b} \right)^2 \right]^{1/2} \quad (37)$$

This frequency varies for each mode with the mode parameters  $m$  and  $n$ . If we assume that  $a$  is greater than  $b$ , the lowest cut-off frequency occurs for the  $\text{TE}_{10}$  mode, which is called the dominant or fundamental mode. No modes can propagate below this lowest critical frequency  $\omega_{c0}$ :

$$\omega_{c0} = \frac{\pi c}{a} \Rightarrow f_{c0} = \frac{\omega_{c0}}{2\pi} = \frac{c}{2a} \text{ Hz} \quad (38)$$

If an air-filled waveguide has  $a = 1 \text{ cm}$ , then  $f_{c0} = 1.5 \times 10^{10} \text{ Hz}$ , while if  $a = 10 \text{ m}$ , then  $f_{c0} = 15 \text{ MHz}$ . This explains why we usually cannot hear the radio when driving through a tunnel. As the frequency is raised above  $\omega_{c0}$ , further modes can propagate.

The phase and group velocity of the waves are

$$v_p = \frac{\omega}{k_z} = \frac{\omega}{\left[ \frac{\omega^2}{c^2} - \left( \frac{m\pi}{a} \right)^2 - \left( \frac{n\pi}{b} \right)^2 \right]^{1/2}} \tag{39}$$

$$v_g = \frac{d\omega}{dk_z} = \frac{k_z c^2}{\omega} = \frac{c^2}{v_p} \Rightarrow v_g v_p = c^2$$

At cut-off,  $v_g = 0$  and  $v_p = \infty$  with their product always a constant.

### 8-6-5 Waveguide Power Flow

The time-averaged power flow per unit area through the waveguide is found from the Poynting vector:

$$\langle \mathbf{S} \rangle = \frac{1}{2} \text{Re} (\hat{\mathbf{E}} \times \hat{\mathbf{H}}^*) \tag{40}$$

#### (a) Power Flow for the TM Modes

Substituting the field solutions found in Section 8-6-2 into (40) yields

$$\begin{aligned} \langle \mathbf{S} \rangle &= \frac{1}{2} \text{Re} [(\hat{E}_x \mathbf{i}_x + \hat{E}_y \mathbf{i}_y + \hat{E}_z \mathbf{i}_z) e^{-jk_z z} \times (\hat{H}_x^* \mathbf{i}_x + \hat{H}_y^* \mathbf{i}_y) e^{+jk_z^* z}] \\ &= \frac{1}{2} \text{Re} [(\hat{E}_x \hat{H}_y^* - \hat{E}_y \hat{H}_x^*) \mathbf{i}_z + \hat{E}_z (\hat{H}_x^* \mathbf{i}_y - \hat{H}_y^* \mathbf{i}_x)] e^{-j(k_z - k_z^*)z} \end{aligned} \tag{41}$$

where we remember that  $k_z$  may be imaginary for a particular mode if the frequency is below cut-off. For propagating modes where  $k_z$  is real so that  $k_z = k_z^*$ , there is no  $z$  dependence in (41). For evanescent modes where  $k_z$  is pure imaginary, the  $z$  dependence of the Poynting vector is a real decaying exponential of the form  $e^{-2|k_z|z}$ . For either case we see from (13) and (22) that the product of  $\hat{E}_z$  with  $\hat{H}_x$  and  $\hat{H}_y$  is pure imaginary so that the real parts of the  $x$ - and  $y$ -directed time average power flow are zero in (41). Only the  $z$ -directed power flow can have a time average:

$$\begin{aligned} \langle \mathbf{S} \rangle &= \frac{\omega \epsilon |E_0|^2}{2(k_x^2 + k_y^2)} \text{Re} [k_z e^{-j(k_z - k_z^*)z} (k_x^2 \cos^2 k_x x \sin^2 k_y y \\ &\quad + k_y^2 \sin^2 k_x x \cos^2 k_y y)] \mathbf{i}_z \end{aligned} \tag{42}$$

If  $k_z$  is imaginary, we have that  $\langle \mathbf{S} \rangle = 0$  while a real  $k_z$  results in a nonzero time-average power flow. The total  $z$ -directed

power flow is found by integrating (42) over the cross-sectional area of the waveguide:

$$\begin{aligned} \langle P \rangle &= \int_{x=0}^a \int_{y=0}^b \langle S_z \rangle dx dy \\ &= \frac{\omega \epsilon k_z ab E_0^2}{8(k_x^2 + k_y^2)} \end{aligned} \quad (43)$$

where it is assumed that  $k_z$  is real, and we used the following identities:

$$\begin{aligned} \int_0^a \sin^2 \frac{m\pi x}{a} dx &= \frac{a}{m\pi} \left( \frac{1}{2} \frac{m\pi x}{a} - \frac{1}{4} \sin \frac{2m\pi x}{a} \right) \Big|_0^a \\ &= \begin{cases} a/2, & m \neq 0 \\ 0, & m = 0 \end{cases} \\ \int_0^a \cos^2 \frac{m\pi x}{a} dx &= \frac{a}{m\pi} \left( \frac{1}{2} \frac{m\pi x}{a} + \frac{1}{4} \sin \frac{2m\pi x}{a} \right) \Big|_0^a \\ &= \begin{cases} a/2, & m \neq 0 \\ a, & m = 0 \end{cases} \end{aligned} \quad (44)$$

For the TM modes, both  $m$  and  $n$  must be nonzero.

#### (b) Power Flow for the TE Modes

The same reasoning is used for the electromagnetic fields found in Section 8-6-3 substituted into (40):

$$\begin{aligned} \langle S \rangle &= \frac{1}{2} \text{Re} [(\hat{E}_x \mathbf{i}_x + \hat{E}_y \mathbf{i}_y) e^{-jk_z z} \times (\hat{H}_x^* \mathbf{i}_x + \hat{H}_y^* \mathbf{i}_y + \hat{H}_z^* \mathbf{i}_z) e^{+jk_z^* z}] \\ &= \frac{1}{2} \text{Re} [(\hat{E}_x \hat{H}_y^* - \hat{E}_y \hat{H}_x^*) \mathbf{i}_z - \hat{H}_z^* (\hat{E}_x \mathbf{i}_y - \hat{E}_y \mathbf{i}_x)] e^{-j(k_z - k_z^*)z} \end{aligned} \quad (45)$$

Similarly, again we have that the product of  $H_z^*$  with  $\hat{E}_x$  and  $\hat{E}_y$  is pure imaginary so that there are no x- and y-directed time average power flows. The z-directed power flow reduces to

$$\begin{aligned} \langle S_z \rangle &= \frac{1}{2} \frac{\omega \mu H_0^2}{(k_x^2 + k_y^2)} (k_y^2 \cos^2 k_x x \sin^2 k_y y \\ &\quad + k_x^2 \sin^2 k_x x \cos^2 k_y y) \text{Re} (k_z e^{-j(k_z - k_z^*)z}) \end{aligned} \quad (46)$$

Again we have nonzero z-directed time average power flow only if  $k_z$  is real. Then the total z-directed power is

$$\langle P \rangle = \int_{x=0}^a \int_{y=0}^b \langle S_z \rangle dx dy = \begin{cases} \frac{\omega \mu k_z ab H_0^2}{8(k_x^2 + k_y^2)}, & m, n \neq 0 \\ \frac{\omega \mu k_z ab H_0^2}{4(k_x^2 + k_y^2)}, & m \text{ or } n = 0 \end{cases} \quad (47)$$

where we again used the identities of (44). Note the factor of 2 differences in (47) for either the  $TE_{10}$  or  $TE_{01}$  modes. Both  $m$  and  $n$  cannot be zero as the  $TE_{00}$  mode reduces to the trivial spatially constant uncoupled  $z$ -directed magnetic field.

### 8-6-6 Wall Losses

If the waveguide walls have a high but noninfinite Ohmic conductivity  $\sigma_w$ , we can calculate the spatial attenuation rate using the approximate perturbation approach described in Section 8-3-4b. The fields decay as  $e^{-\alpha z}$ , where

$$\alpha = \frac{1}{2} \frac{\langle P_{dL} \rangle}{\langle P \rangle} \quad (48)$$

where  $\langle P_{dL} \rangle$  is the time-average dissipated power per unit length and  $\langle P \rangle$  is the electromagnetic power flow in the lossless waveguide derived in Section 8-6-5 for each of the modes.

In particular, we calculate  $\alpha$  for the  $TE_{10}$  mode ( $k_x = \pi/a$ ,  $k_y = 0$ ). The waveguide fields are then

$$\begin{aligned} \hat{\mathbf{H}} &= H_0 \left( \mathbf{i}_x \frac{jk_z a}{\pi} \sin \frac{\pi x}{a} + \cos \frac{\pi x}{a} \mathbf{i}_z \right) \\ \hat{\mathbf{E}} &= -\frac{j\omega\mu a}{\pi} H_0 \sin \frac{\pi x}{a} \mathbf{i}_y \end{aligned} \quad (49)$$

The surface current on each wall is found from (34) as

$$\begin{aligned} \hat{\mathbf{K}}(x=0, y) &= \hat{\mathbf{K}}(x=a, y) = -H_0 \mathbf{i}_y \\ \hat{\mathbf{K}}(x, y=0) &= -\hat{\mathbf{K}}(x, y=b) = H_0 \left( -\mathbf{i}_z \frac{jk_z a}{\pi} \sin \frac{\pi x}{a} + \mathbf{i}_x \cos \frac{\pi x}{a} \right) \end{aligned} \quad (50)$$

With lossy walls the electric field component  $\mathbf{E}_w$  within the walls is in the same direction as the surface current proportional by a surface conductivity  $\sigma_w \delta$ , where  $\delta$  is the skin depth as found in Section 8-3-4b. The time-average dissipated power density per unit area in the walls is then:

$$\begin{aligned} \langle P_d(x=0, y) \rangle &= \langle P_d(x=a, y) \rangle \\ &= \frac{1}{2} \text{Re} (\hat{\mathbf{E}}_w \cdot \hat{\mathbf{K}}^*) = \frac{1}{2} \frac{H_0^2}{\sigma_w \delta} \\ \langle P_d(x, y=0) \rangle &= \langle P_d(x, y=b) \rangle \\ &= \frac{1}{2} \frac{H_0^2}{\sigma_w \delta} \left[ \left( \frac{k_z a}{\pi} \right)^2 \sin^2 \frac{\pi x}{a} + \cos^2 \frac{\pi x}{a} \right] \end{aligned} \quad (51)$$

The total time average dissipated power per unit length  $\langle P_{dL} \rangle$  required in (48) is obtained by integrating each of the

terms in (51) along the waveguide walls:

$$\begin{aligned}
 \langle P_{dL} \rangle &= \int_0^b [\langle P_d(x=0, y) \rangle + \langle P_d(x=a, y) \rangle] dy \\
 &\quad + \int_0^a [\langle P_d(x, y=0) \rangle + \langle P_d(x, y=b) \rangle] dx \\
 &= \frac{H_0^2 b}{\sigma_w \delta} + \frac{H_0^2}{\sigma_w \delta} \int_0^a \left[ \left( \frac{k_z a}{\pi} \right)^2 \sin^2 \frac{\pi x}{a} + \cos^2 \frac{\pi x}{a} \right] dx \\
 &= \frac{H_0^2}{\sigma_w \delta} \left\{ b + \frac{a}{2} \left[ \left( \frac{k_z a}{\pi} \right)^2 + 1 \right] \right\} = \frac{H_0^2}{\sigma_w \delta} \left[ b + \frac{a}{2} \left( \frac{\omega^2 a^2}{\pi^2 c^2} \right) \right] \quad (52)
 \end{aligned}$$

while the electromagnetic power above cut-off for the TE<sub>10</sub> mode is given by (47),

$$\langle P \rangle = \frac{\omega \mu k_z a b H_0^2}{4(\pi/a)^2} \quad (53)$$

so that

$$\alpha = \frac{1}{2} \frac{\langle P_{dL} \rangle}{\langle P \rangle} = \frac{2 \left( \frac{\pi}{a} \right)^2 \left[ b + \frac{a}{2} \left( \frac{\omega^2 a^2}{\pi^2 c^2} \right) \right]}{\omega \mu a b k_z \sigma_w \delta} \quad (54)$$

where

$$k_z = \left[ \frac{\omega^2}{c^2} - \left( \frac{\pi}{a} \right)^2 \right]^{1/2}; \quad \frac{\omega}{c} > \frac{\pi}{a} \quad (55)$$

## 8-7 DIELECTRIC WAVEGUIDE

We found in Section 7-10-6 for fiber optics that electromagnetic waves can also be guided by dielectric structures if the wave travels from the dielectric to free space at an angle of incidence greater than the critical angle. Waves propagating along the dielectric of thickness  $2d$  in Figure 8-30 are still described by the vector wave equations derived in Section 8-6-1.

### 8-7-1 TM Solutions

We wish to find solutions where the fields are essentially confined within the dielectric. We neglect variations with  $y$  so that for TM waves propagating in the  $z$  direction the  $z$  component of electric field is given in Section 8-6-2 as

$$E_z(x, t) = \begin{cases} \operatorname{Re} [A_2 e^{-\alpha(x-d)} e^{j(\omega t - k_z z)}], & x \geq d \\ \operatorname{Re} [(A_1 \sin k_x x + B_1 \cos k_x x) e^{j(\omega t - k_z z)}], & |x| \leq d \\ \operatorname{Re} [A_3 e^{\alpha(x+d)} e^{j(\omega t - k_z z)}], & x \leq -d \end{cases} \quad (1)$$

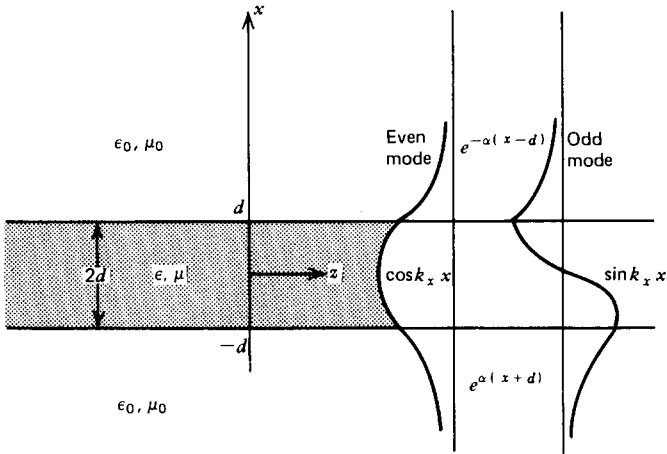


Figure 8-30 TE and TM modes can also propagate along dielectric structures. The fields can be essentially confined to the dielectric over a frequency range if the speed of the wave in the dielectric is less than that outside. It is convenient to separate the solutions into even and odd modes.

where we choose to write the solution outside the dielectric in the decaying wave form so that the fields are predominantly localized around the dielectric.

The wavenumbers and decay rate obey the relations

$$\begin{aligned} k_x^2 + k_z^2 &= \omega^2 \epsilon \mu \\ -\alpha^2 + k_z^2 &= \omega^2 \epsilon_0 \mu_0 \end{aligned} \quad (2)$$

The  $z$  component of the wavenumber must be the same in all regions so that the boundary conditions can be met at each interface. For propagation in the dielectric and evanescence in free space, we must have that

$$\omega^2 \epsilon_0 \mu_0 < k_z^2 < \omega^2 \epsilon \mu \quad (3)$$

All the other electric and magnetic field components can be found from (1) in the same fashion as for metal waveguides in Section 8-6-2. However, it is convenient to separately consider each of the solutions for  $E_z$  within the dielectric.

### (a) Odd Solutions

If  $E_z$  in each half-plane above and below the centerline are oppositely directed, the field within the dielectric must vary solely as  $\sin k_x x$ :

$$\hat{E}_z = \begin{cases} A_2 e^{-\alpha(x-d)}, & x \geq d \\ A_1 \sin k_x x, & |x| \leq d \\ A_3 e^{\alpha(x+d)}, & x \leq -d \end{cases} \quad (4)$$

Then because in the absence of volume charge the electric field has no divergence,

$$\frac{\partial \hat{E}_x}{\partial x} - jk_z \hat{E}_z \Rightarrow \hat{E}_x = \begin{cases} -\frac{jk_z}{\alpha} A_2 e^{-\alpha(x-d)}, & x \geq d \\ -\frac{jk_z}{k_x} A_1 \cos k_x x, & |x| \leq d \\ \frac{jk_z}{\alpha} A_3 e^{\alpha(x+d)}, & x \leq -d \end{cases} \quad (5)$$

while from Faraday's law the magnetic field is

$$\hat{H}_y = -\frac{1}{j\omega\mu} \left( -jk_z \hat{E}_x - \frac{\partial \hat{E}_z}{\partial x} \right)$$

$$\Rightarrow \hat{H}_y = \begin{cases} -\frac{j\omega\epsilon_0 A_2}{\alpha} e^{-\alpha(x-d)}, & x \geq d \\ -\frac{j\omega\epsilon A_1}{k_x} \cos k_x x, & |x| \leq d \\ \frac{j\omega\epsilon_0 A_3}{\alpha} e^{\alpha(x+d)}, & x \leq -d \end{cases} \quad (6)$$

At the boundaries where  $x = \pm d$  the tangential electric and magnetic fields are continuous:

$$E_z(x = \pm d_-) = E_z(x = \pm d_+) \Rightarrow A_1 \sin k_x d = A_2$$

$$-A_1 \sin k_x d = A_3$$

$$H_y(x = \pm d_-) = H_y(x = \pm d_+) \Rightarrow \frac{-j\omega\epsilon A_1}{k_x} \cos k_x d = \frac{-j\omega\epsilon_0 A_2}{\alpha} \quad (7)$$

$$\frac{-j\omega\epsilon A_1}{k_x} \cos k_x d = \frac{j\omega\epsilon_0 A_3}{\alpha}$$

which when simultaneously solved yields

$$\left. \begin{aligned} \frac{A_2}{A_1} = \sin k_x d &= \frac{\epsilon\alpha}{\epsilon_0 k_x} \cos k_x d \\ \frac{A_3}{A_1} = -\sin k_x d &= -\frac{\epsilon\alpha}{\epsilon_0 k_x} \cos k_x d \end{aligned} \right\} \Rightarrow \alpha = \frac{\epsilon_0}{\epsilon} k_x \tan k_x d \quad (8)$$

The allowed values of  $\alpha$  and  $k_x$  are obtained by self-consistently solving (8) and (2), which in general requires a numerical method. The critical condition for a guided wave occurs when  $\alpha = 0$ , which requires that  $k_x d = n\pi$  and  $k_z^2 = \omega^2 \epsilon_0 \mu_0$ . The critical frequency is then obtained from (2) as

$$\omega^2 = \frac{k_x^2}{\epsilon\mu - \epsilon_0\mu_0} = \frac{(n\pi/d)^2}{\epsilon\mu - \epsilon_0\mu_0} \quad (9)$$

Note that this occurs for real frequencies only if  $\epsilon\mu > \epsilon_0\mu_0$ .

**(b) Even Solutions**

If  $E_z$  is in the same direction above and below the dielectric, solutions are similarly

$$\hat{E}_z = \begin{cases} B_2 e^{-\alpha(x-d)}, & x \geq d \\ B_1 \cos k_x x, & |x| \leq d \\ B_3 e^{\alpha(x+d)}, & x \leq -d \end{cases} \quad (10)$$

$$\hat{E}_x = \begin{cases} -\frac{jk_x}{\alpha} B_2 e^{-\alpha(x-d)}, & x \geq d \\ \frac{jk_x}{k_x} B_1 \sin k_x x, & |x| \leq d \\ \frac{jk_x}{\alpha} B_3 e^{\alpha(x+d)}, & x \leq -d \end{cases} \quad (11)$$

$$\hat{H}_y = \begin{cases} -\frac{j\omega\epsilon_0}{\alpha} B_2 e^{-\alpha(x-d)}, & x \geq d \\ \frac{j\omega\epsilon}{k_x} B_1 \sin k_x x, & |x| \leq d \\ \frac{j\omega\epsilon_0}{\alpha} B_3 e^{\alpha(x+d)}, & x \leq -d \end{cases} \quad (12)$$

Continuity of tangential electric and magnetic fields at  $x = \pm d$  requires

$$\begin{aligned} B_1 \cos k_x d &= B_2, & B_1 \cos k_x d &= B_3 \\ \frac{j\omega\epsilon}{k_x} B_1 \sin k_x d &= -\frac{j\omega\epsilon_0}{\alpha} B_2, & -\frac{j\omega\epsilon B_1}{k_x} \sin k_x d &= \frac{j\omega\epsilon_0 B_3}{\alpha} \end{aligned} \quad (13)$$

or

$$\left. \begin{aligned} \frac{B_2}{B_1} = \cos k_x d &= -\frac{\epsilon\alpha}{\epsilon_0 k_x} \sin k_x d \\ \frac{B_3}{B_1} = \cos k_x d &= -\frac{\epsilon\alpha}{\epsilon_0 k_x} \sin k_x d \end{aligned} \right\} \Rightarrow \alpha = -\frac{\epsilon_0 k_x}{\epsilon} \cot k_x d \quad (14)$$

**8-7-2 TE Solutions**

The same procedure is performed for the TE solutions by first solving for  $H_z$ .

**(a) Odd Solutions**

$$\hat{H}_z = \begin{cases} A_2 e^{-\alpha(x-d)}, & x \geq d \\ A_1 \sin k_x x, & |x| \leq d \\ A_3 e^{\alpha(x+d)}, & x \leq -d \end{cases} \quad (15)$$

$$\hat{H}_x = \begin{cases} -\frac{jk_z}{\alpha} A_2 e^{-\alpha(x-d)}, & x \geq d \\ -\frac{jk_z}{k_x} A_1 \cos k_x x, & |x| \leq d \\ \frac{jk_z}{\alpha} A_3 e^{\alpha(x+d)}, & x \leq -d \end{cases} \quad (16)$$

$$\hat{E}_y = \begin{cases} \frac{j\omega\mu_0}{\alpha} A_2 e^{-\alpha(x-d)}, & x \geq d \\ \frac{j\omega\mu}{k_x} A_1 \cos k_x x, & |x| \leq d \\ -\frac{j\omega\mu_0}{\alpha} A_3 e^{\alpha(x+d)}, & x \leq -d \end{cases} \quad (17)$$

where continuity of tangential  $\mathbf{E}$  and  $\mathbf{H}$  across the boundaries requires

$$\alpha = \frac{\mu_0}{\mu} k_x \tan k_x d \quad (18)$$

**(b) Even Solutions**

$$\hat{H}_z = \begin{cases} B_2 e^{-\alpha(x-d)}, & x \geq d \\ B_1 \cos k_x x, & |x| \leq d \\ B_3 e^{\alpha(x+d)}, & x \leq -d \end{cases} \quad (19)$$

$$\hat{H}_x = \begin{cases} -\frac{jk_z}{\alpha} B_2 e^{-\alpha(x-d)}, & x \geq d \\ \frac{jk_z}{k_x} B_1 \sin k_x x, & |x| \leq d \\ \frac{jk_z}{\alpha} B_3 e^{\alpha(x+d)}, & x \leq -d \end{cases} \quad (20)$$

$$\hat{E}_y = \begin{cases} \frac{j\omega\mu_0}{\alpha} B_2 e^{-\alpha(x-d)}, & x \geq d \\ -\frac{j\omega\mu}{k_x} B_1 \sin k_x x, & |x| \leq d \\ -\frac{j\omega\mu_0}{\alpha} B_3 e^{\alpha(x+d)}, & x \leq -d \end{cases} \quad (21)$$

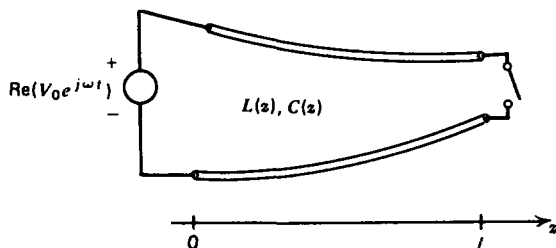
where  $\alpha$  and  $k_x$  are related as

$$\alpha = -\frac{\mu_0}{\mu} k_x \cot k_x d \quad (22)$$

**PROBLEMS**

Section 8-1

1. Find the inductance and capacitance per unit length and the characteristic impedance for the wire above plane and two wire line shown in Figure 8-3. (Hint: See Section 2-6-4c.)
2. The inductance and capacitance per unit length on a lossless transmission line is a weak function of  $z$  as the distance between electrodes changes slowly with  $z$ .



- (a) For this case write the transmission line equations as single equations in voltage and current.
- (b) Consider an exponential line, where

$$L(z) = L_0 e^{\alpha z}, \quad C(z) = C_0 e^{-\alpha z}$$

If the voltage and current vary sinusoidally with time as

$$v(z, t) = \text{Re} [\hat{v}(z) e^{j\omega t}], \quad i(z, t) = \text{Re} [\hat{i}(z) e^{j\omega t}]$$

find the general form of solution for the spatial distributions of  $\hat{v}(z)$  and  $\hat{i}(z)$ .

(c) The transmission line is excited by a voltage source  $V_0 \cos \omega t$  at  $z = 0$ . What are the voltage and current distributions if the line is short or open circuited at  $z = l$ ?

(d) For what range of frequency do the waves strictly decay with distance? What is the cut-off frequency for wave propagation?

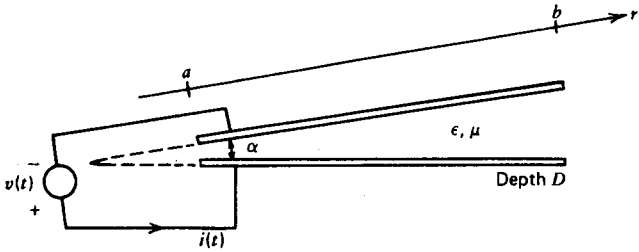
(e) What are the resonant frequencies of the short circuited line?

(f) What condition determines the resonant frequencies of the open circuited line.

3. Two conductors of length  $l$  extending over the radial distance  $a \leq r \leq b$  are at a constant angle  $\alpha$  apart.

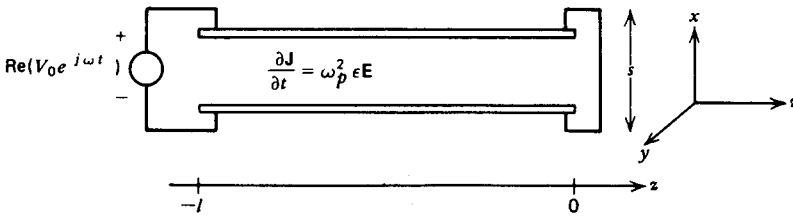
(a) What are the electric and magnetic fields in terms of the voltage and current?

(b) Find the inductance and capacitance per unit length. What is the characteristic impedance?



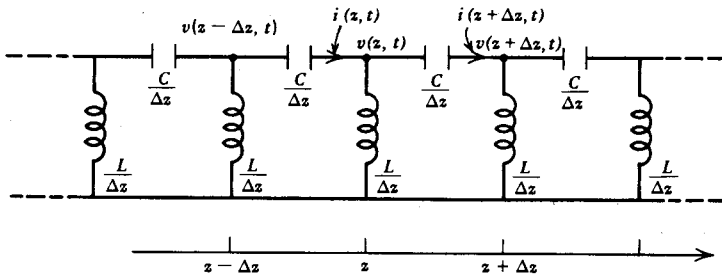
4. A parallel plate transmission line is filled with a conducting plasma with constitutive law

$$\frac{\partial \mathbf{J}}{\partial t} = \omega_p^2 \epsilon \mathbf{E}$$



- (a) How are the electric and magnetic fields related?
- (b) What are the transmission line equations for the voltage and current?
- (c) For sinusoidal signals of the form  $e^{j(\omega t - kz)}$ , how are  $\omega$  and  $k$  related? Over what frequency range do we have propagation or decay?
- (d) The transmission line is short circuited at  $z = 0$  and excited by a voltage source  $V_0 \cos \omega t$  at  $z = -l$ . What are the voltage and current distributions?
- (e) What are the resonant frequencies of the system?

5. An unusual type of distributed system is formed by series capacitors and shunt inductors.

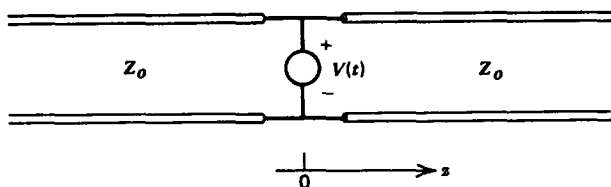


- (a) What are the governing partial differential equations relating the voltage and current?

- (b) What is the dispersion relation between  $\omega$  and  $k$  for signals of the form  $e^{j(\omega t - kz)}$ ?
- (c) What are the group and phase velocities of the waves? Why are such systems called "backward wave"?
- (d) A voltage  $V_0 \cos \omega t$  is applied at  $z = -l$  with the  $z = 0$  end short circuited. What are the voltage and current distributions along the line?
- (e) What are the resonant frequencies of the system?

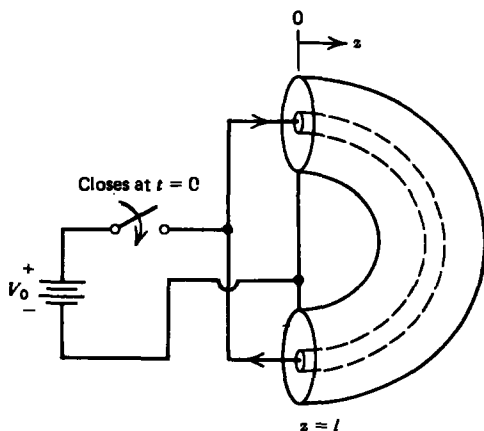
Section 8-2

6. An infinitely long transmission line is excited at its center by a step voltage  $V_0$  turned on at  $t = 0$ . The line is initially at rest.



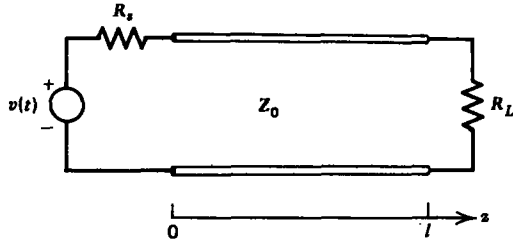
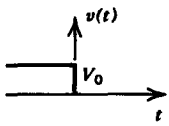
- (a) Plot the voltage and current distributions at time  $T$ .
- (b) At this time  $T$  the voltage is set to zero. Plot the voltage and current everywhere at time  $2T$ .

7. A transmission line of length  $l$  excited by a step voltage source has its ends connected together. Plot the voltage and current at  $z = l/4, l/2,$  and  $3l/4$  as a function of time.



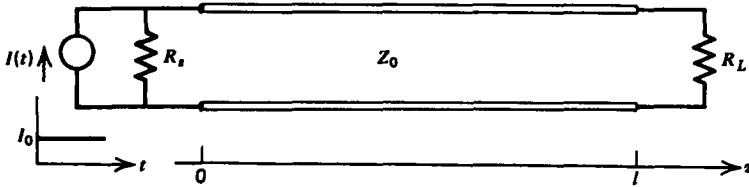
8. The dc steady state is reached for a transmission line loaded at  $z = l$  with a resistor  $R_L$  and excited at  $z = 0$  by a dc voltage  $V_0$  applied through a source resistor  $R_s$ . The voltage source is suddenly set to zero at  $t = 0$ .

- (a) What is the initial voltage and current along the line?



(b) Find the voltage at the  $z = l$  end as a function of time. (Hint: Use difference equations.)

9. A step current source turned on at  $t = 0$  is connected to the  $z = 0$  end of a transmission line in parallel with a source resistance  $R_s$ . A load resistor  $R_L$  is connected at  $z = l$ .



(a) What is the load voltage and current as a function of time? (Hint: Use a Thevenin equivalent network at  $z = 0$  with the results of Section 8-2-3.)

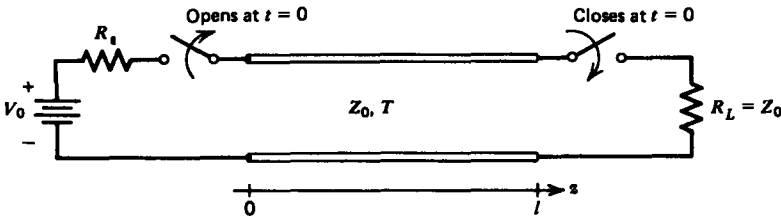
(b) With  $R_s = \infty$  plot versus time the load voltage when  $R_L = \infty$  and the load current when  $R_L = 0$ .

(c) If  $R_s = \infty$  and  $R_L = \infty$ , solve for the load voltage in the quasi-static limit assuming the transmission line is a capacitor. Compare with (b).

(d) If  $R_s$  is finite but  $R_L = 0$ , what is the time dependence of the load current?

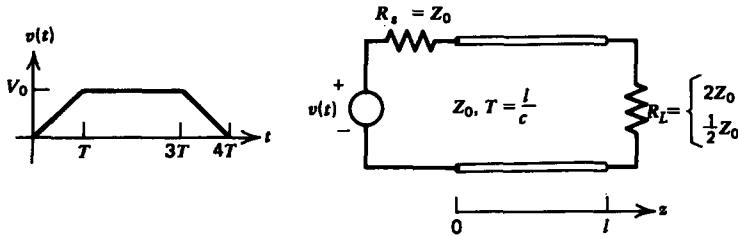
(e) Repeat (d) in the quasi-static limit where the transmission line behaves as an inductor. When are the results of (d) and (e) approximately equal?

10. Switched transmission line systems with an initial dc voltage can be used to generate high voltage pulses of short time duration. The line shown is charged up to a dc voltage  $V_0$  when at  $t = 0$  the load switch is closed and the source switch is opened.

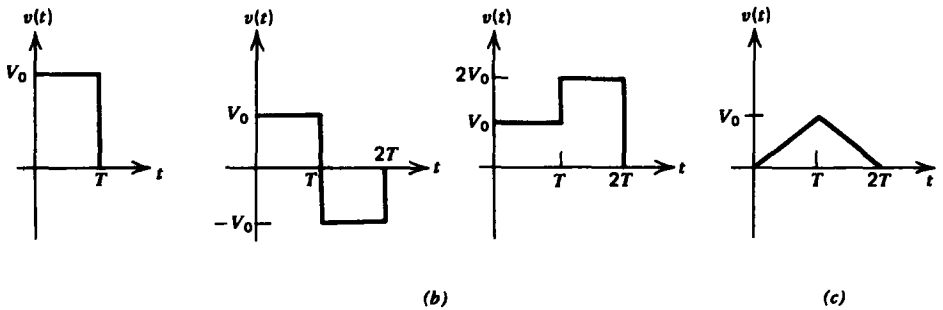
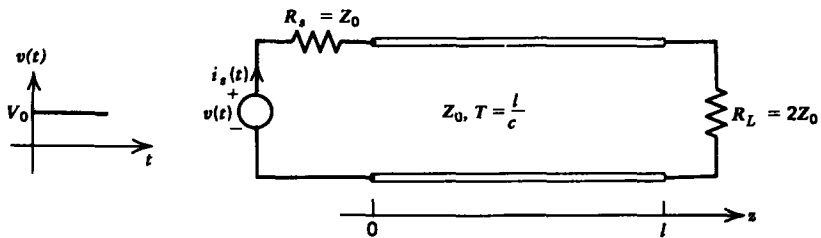


- (a) What are the initial line voltage and current? What are  $V_+$  and  $V_-$ ?  
 (b) Sketch the time dependence of the load voltage.

11. For the trapezoidal voltage excitation shown, plot versus time the current waveforms at  $z = 0$  and  $z = l$  for  $R_L = 2Z_0$  and  $R_L = \frac{1}{2}Z_0$ .



12. A step voltage is applied to a loaded transmission line with  $R_L = 2Z_0$  through a matching source resistor.

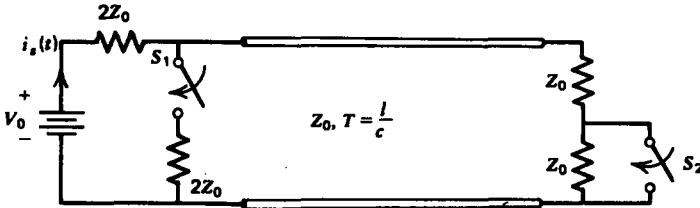


- (a) Sketch the source current  $i_s(t)$ .  
 (b) Using superposition of delayed step voltages find the time dependence of  $i_s(t)$  for the various pulse voltages shown.  
 (c) By integrating the appropriate solution of (b), find  $i_s(t)$  if the applied voltage is the triangle wave shown.

13. A dc voltage has been applied for a long time to the transmission line circuit shown with switches  $S_1$  and  $S_2$  open

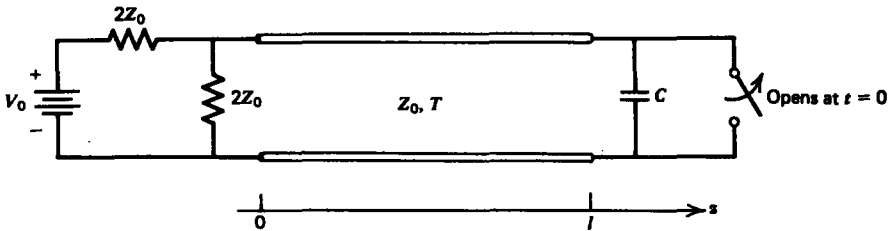
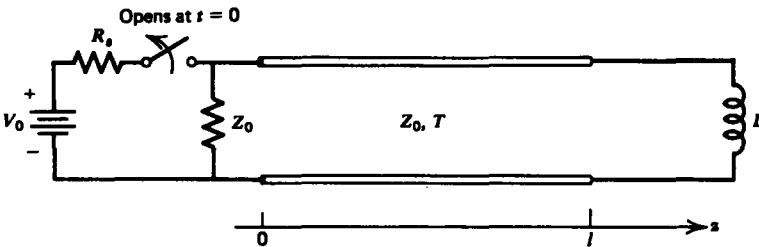
when at  $t = 0$ :

- (a)  $S_2$  is suddenly closed with  $S_1$  kept open;
- (b)  $S_1$  is suddenly closed with  $S_2$  kept open;
- (c) Both  $S_1$  and  $S_2$  are closed.



For each of these cases plot the source current  $i_s(t)$  versus time.

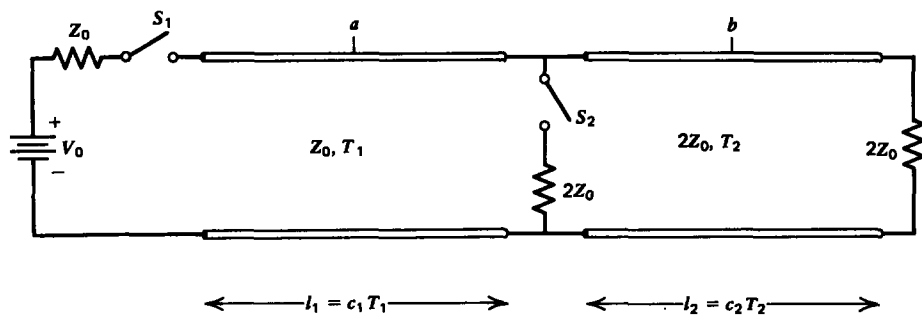
14. For each of the transmission line circuits shown, the switch opens at  $t = 0$  after the dc voltage has been applied for a long time.



- (a) What are the transmission line voltages and currents right before the switches open? What are  $V_+$  and  $V_-$  at  $t = 0$ ?
- (b) Plot the voltage and current as a function of time at  $z = l/2$ .

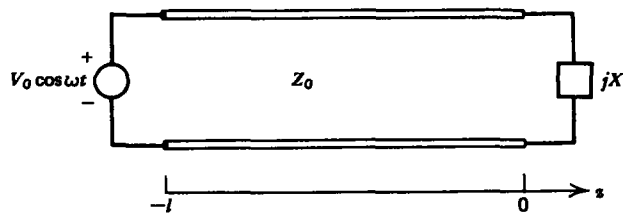
15. A transmission line is connected to another transmission line with double the characteristic impedance.

- (a) With switch  $S_2$  open, switch  $S_1$  is suddenly closed at  $t = 0$ . Plot the voltage and current as a function of time half-way down each line at points  $a$  and  $b$ .
- (b) Repeat (a) if  $S_2$  is closed.



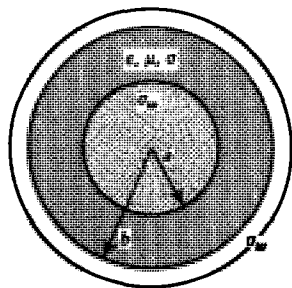
Section 8-3

16. A transmission line is excited by a voltage source  $V_0 \cos \omega t$  at  $z = -l$ . The transmission line is loaded with a purely reactive load with impedance  $jX$  at  $z = 0$ .



- (a) Find the voltage and current distribution along the line.
- (b) Find an expression for the resonant frequencies of the system if the load is capacitive or inductive. What is the solution if  $|X| = Z_0$ ?
- (c) Repeat (a) and (b) if the transmission line is excited by a current source  $I_0 \cos \omega t$  at  $z = -l$ .

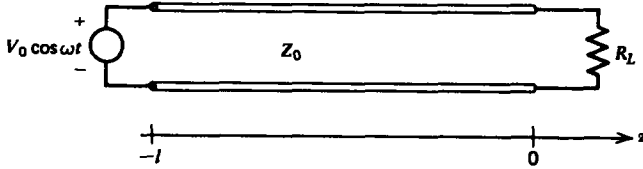
17. (a) Find the resistance and conductance per unit lengths for a coaxial cable whose dielectric has a small Ohmic conductivity  $\sigma$  and walls have a large conductivity  $\sigma_w$ . (Hint: The skin depth  $\delta$  is much smaller than the radii or thickness of either conductor.)



- (b) What is the decay rate of the fields due to the losses?
- (c) If the dielectric is lossless ( $\sigma = 0$ ) with a fixed value of

outer radius  $b$ , what value of inner radius  $a$  will minimize the decay rate? (Hint:  $1 + 1/3.6 \approx \ln 3.6$ .)

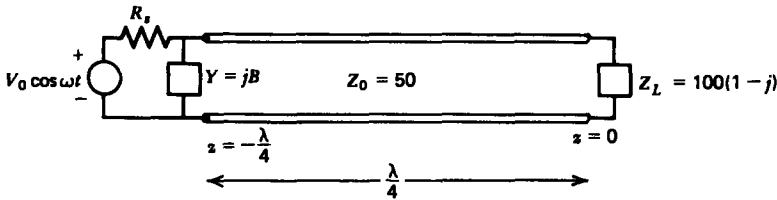
18. A transmission line of length  $l$  is loaded by a resistor  $R_L$ .



- (a) Find the voltage and current distributions along the line.
- (b) Reduce the solutions of (a) when the line is much shorter than a wavelength.
- (c) Find the approximate equivalent circuits in the long wavelength limit ( $kl \ll 1$ ) when  $R_L$  is very small ( $R_L \ll Z_0$ ) and when it is very large ( $R_L \gg Z_0$ ).

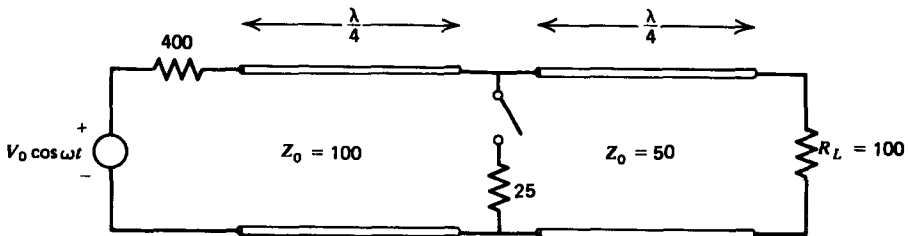
Section 8-4

19. For the transmission line shown:



- (a) Find the values of lumped reactive admittance  $Y = jB$  and non-zero source resistance  $R_s$  that maximizes the power delivered by the source. (Hint: Do not use the Smith chart.)
- (b) What is the time-average power dissipated in the load?

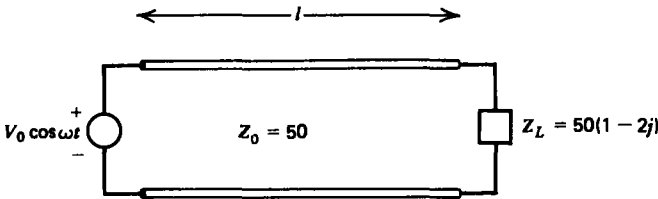
20. (a) Find the time-average power delivered by the source for the transmission line system shown when the switch is open or closed. (Hint: Do not use the Smith chart.)



- (b) For each switch position, what is the time average power dissipated in the load resistor  $R_L$ ?

(c) For each switch position what is the VSWR on each line?

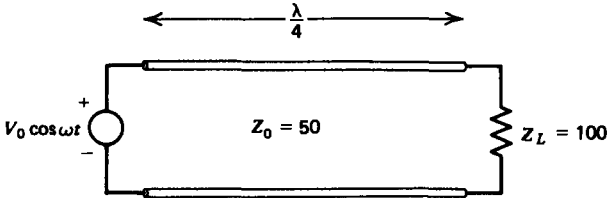
21. (a) Using the Smith chart find the source current delivered (magnitude and phase) for the transmission line system shown, for  $l = \lambda/8, \lambda/4, 3\lambda/8,$  and  $\lambda/2$ .



(b) For each value of  $l$ , what are the time-average powers delivered by the source and dissipated in the load impedance  $Z_L$ ?

(c) What is the VSWR?

22. (a) Without using the Smith chart find the voltage and current distributions for the transmission line system shown.



(b) What is the VSWR?

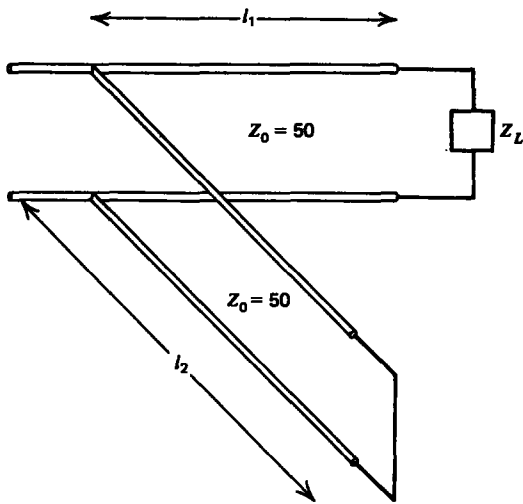
(c) At what positions are the voltages a maximum or a minimum? What is the voltage magnitude at these positions?

23. The VSWR on a 100-Ohm transmission line is 3. The distance between successive voltage minima is 50 cm while the distance from the load to the first minima is 20 cm. What are the reflection coefficient and load impedance?

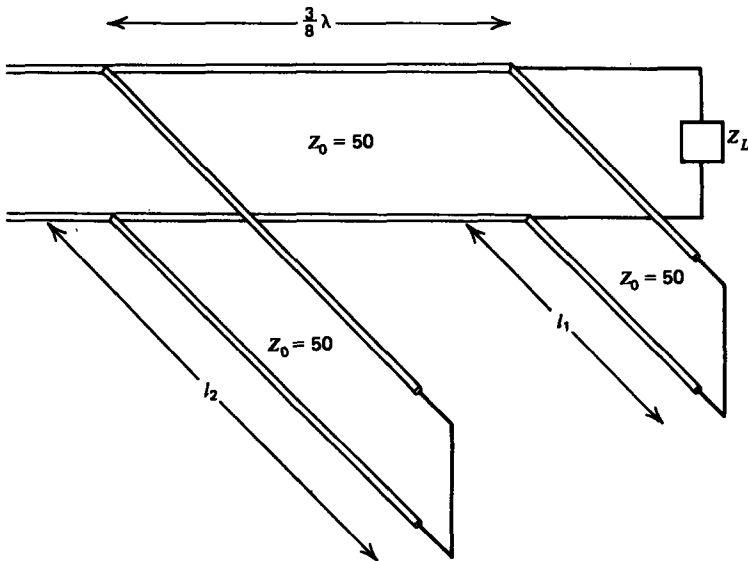
Section 8-5

24. For each of the following load impedances in the single-stub tuning transmission line system shown, find all values of the length of the line  $l_1$  and stub length  $l_2$  necessary to match the load to the line.

- (a)  $Z_L = 100(1 - j)$
- (b)  $Z_L = 50(1 + 2j)$
- (c)  $Z_L = 25(2 - j)$
- (d)  $Z_L = 25(1 + 2j)$

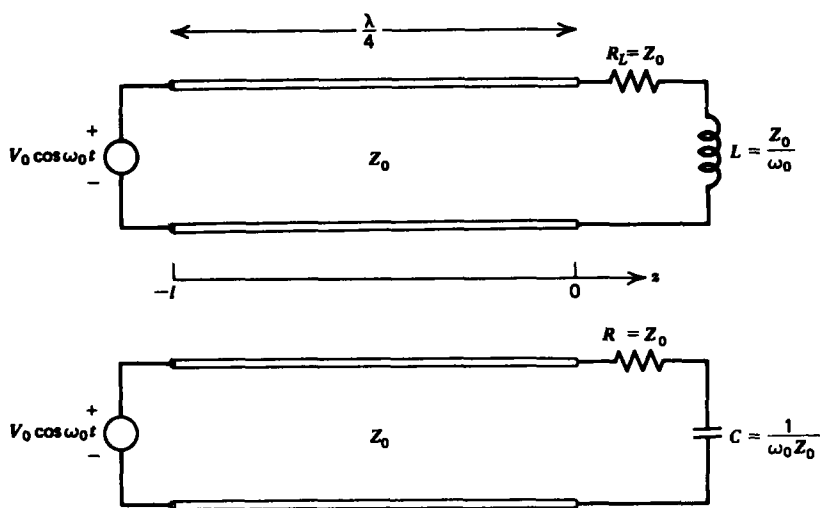


25. For each of the following load impedances in the double-stub tuning transmission line system shown, find stub lengths  $l_1$  and  $l_2$  to match the load to the line.



- (a)  $Z_L = 100(1-j)$       (c)  $Z_L = 25(2-j)$   
 (b)  $Z_L = 50(1+2j)$       (d)  $Z_L = 25(1+2j)$

26. (a) Without using the Smith chart, find the input impedance  $Z_{in}$  at  $z = -l = -\lambda/4$  for each of the loads shown.  
 (b) What is the input current  $i(z = -l, t)$  for each of the loads?



(c) The frequency of the source is doubled to  $2\omega_0$ . The line length  $l$  and loads  $L$  and  $C$  remain unchanged. Repeat (a) and (b).

(d) The frequency of the source is halved to  $\frac{1}{2}\omega_0$ . Repeat (a) and (b).

Section 8-6

27. A rectangular metal waveguide is filled with a plasma with constitutive law

$$\frac{\partial \mathbf{J}_f}{\partial t} = \omega_p^2 \epsilon \mathbf{E}$$

(a) Find the TE and TM solutions that satisfy the boundary conditions.

(b) What is the wavenumber  $k_z$  along the axis? What is the cut-off frequency?

(c) What are the phase and group velocities of the waves?

(d) What is the total electromagnetic power flowing down the waveguide for each of the modes?

(e) If the walls have a large but finite conductivity, what is the spatial decay rate for TE<sub>10</sub> propagating waves?

28. (a) Find the power dissipated in the walls of a waveguide with large but finite conductivity  $\sigma_w$  for the TM<sub>*m*n</sub> modes (Hint: Use Equation (25).)

(b) What is the spatial decay rate for propagating waves?

29. (a) Find the equations of the electric and magnetic field lines in the  $xy$  plane for the TE and TM modes.

(b) Find the surface current field lines on each of the

waveguide surfaces for the  $TE_{mn}$  modes. **Hint:**

$$\int \tan x dx = -\ln \cos x$$

$$\int \cot x dx = \ln \sin x$$

(c) For all modes verify the conservation of charge relation on the  $x = 0$  surface:

$$\nabla_{\Sigma} \cdot \mathbf{K} + \frac{\partial \sigma_f}{\partial t} = 0$$

30. (a) Find the first ten lowest cut-off frequencies if  $a = b = 1$  cm in a free space waveguide.

(b) What are the necessary dimensions for a square free space waveguide to have a lowest cut-off frequency of  $10^{10}$ ,  $10^8$ ,  $10^6$ ,  $10^4$ , or  $10^2$  Hz?

31. A rectangular waveguide of height  $b$  and width  $a$  is short circuited by perfectly conducting planes at  $z = 0$  and  $z = l$ .

(a) Find the general form of the TE and TM electric and magnetic fields. (**Hint:** Remember to consider waves traveling in the  $\pm z$  directions.)

(b) What are the natural frequencies of this resonator?

(c) If the walls have a large conductivity  $\sigma_w$  find the total time-average power  $\langle P_d \rangle$  dissipated in the  $TE_{101}$  mode.

(d) What is the total time-average electromagnetic energy  $\langle W \rangle$  stored in the resonator?

(e) Find the  $Q$  of the resonator, defined as

$$Q = \frac{\omega_0 \langle W \rangle}{\langle P_d \rangle}$$

where  $\omega_0$  is the resonant frequency.

### Section 8.7

32. (a) Find the critical frequency where the spatial decay rate  $\alpha$  is zero for all the dielectric modes considered.

(b) Find approximate values of  $\alpha$ ,  $k_x$ , and  $k_z$  for a very thin dielectric, where  $k_x d \ll 1$ .

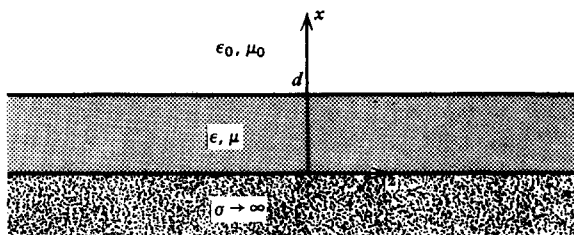
(c) For each of the solutions find the time-average power per unit length in each region.

(d) If the dielectric has a small Ohmic conductivity  $\sigma$ , what is the approximate attenuation rate of the fields.

33. A dielectric waveguide of thickness  $d$  is placed upon a perfect conductor.

(a) Which modes can propagate along the dielectric?

(b) For each of these modes, what are the surface current and charges on the conductor?



(c) Verify the conservation of charge relation:

$$\nabla_{\Sigma} \cdot \mathbf{K} + \frac{\partial \sigma_f}{\partial t} = 0$$

(d) If the conductor has a large but noninfinite Ohmic conductivity  $\sigma_w$ , what is the approximate power per unit area dissipated?

(e) What is the approximate attenuation rate of the fields?

.



# chapter 9

*radiation*

In low-frequency electric circuits and along transmission lines, power is guided from a source to a load along highly conducting wires with the fields predominantly confined to the region around the wires. At very high frequencies these wires become antennas as this power can radiate away into space without the need of any guiding structure.

## 9-1 THE RETARDED POTENTIALS

### 9-1-1 Nonhomogeneous Wave Equations

Maxwell's equations in complete generality are

$$\nabla \times \mathbf{E} = -\frac{\partial \mathbf{B}}{\partial t} \quad (1)$$

$$\nabla \times \mathbf{H} = \mathbf{J}_f + \frac{\partial \mathbf{D}}{\partial t} \quad (2)$$

$$\nabla \cdot \mathbf{B} = 0 \quad (3)$$

$$\nabla \cdot \mathbf{D} = \rho_f \quad (4)$$

In our development we will use the following vector identities

$$\nabla \times (\nabla V) = 0 \quad (5)$$

$$\nabla \cdot (\nabla \times \mathbf{A}) = 0 \quad (6)$$

$$\nabla \times (\nabla \times \mathbf{A}) = \nabla(\nabla \cdot \mathbf{A}) - \nabla^2 \mathbf{A} \quad (7)$$

where  $\mathbf{A}$  and  $V$  can be any functions but in particular will be the magnetic vector potential and electric scalar potential, respectively.

Because in (3) the magnetic field has no divergence, the identity in (6) allows us to again define the vector potential  $\mathbf{A}$  as we had for quasi-statics in Section 5-4:

$$\mathbf{B} = \nabla \times \mathbf{A} \quad (8)$$

so that Faraday's law in (1) can be rewritten as

$$\nabla \times \left( \mathbf{E} + \frac{\partial \mathbf{A}}{\partial t} \right) = 0 \quad (9)$$

Then (5) tells us that any curl-free vector can be written as the gradient of a scalar so that (9) becomes

$$\mathbf{E} + \frac{\partial \mathbf{A}}{\partial t} = -\nabla V \quad (10)$$

where we introduce the negative sign on the right-hand side so that  $V$  becomes the electric potential in a static situation when  $\mathbf{A}$  is independent of time. We solve (10) for the electric field and with (8) rewrite (2) for linear dielectric media ( $\mathbf{D} = \epsilon \mathbf{E}$ ,  $\mathbf{B} = \mu \mathbf{H}$ ):

$$\nabla \times (\nabla \times \mathbf{A}) = \mu \mathbf{J}_f + \frac{1}{c^2} \left[ -\nabla \left( \frac{\partial V}{\partial t} \right) - \frac{\partial^2 \mathbf{A}}{\partial t^2} \right], \quad c^2 = \frac{1}{\epsilon \mu} \quad (11)$$

The vector identity of (7) allows us to reduce (11) to

$$\nabla^2 \mathbf{A} - \nabla \left[ \nabla \cdot \mathbf{A} + \frac{1}{c^2} \frac{\partial V}{\partial t} \right] - \frac{1}{c^2} \frac{\partial^2 \mathbf{A}}{\partial t^2} = -\mu \mathbf{J}_f \quad (12)$$

Thus far, we have only specified the curl of  $\mathbf{A}$  in (8). The Helmholtz theorem discussed in Section 5-4-1 told us that to uniquely specify the vector potential we must also specify the divergence of  $\mathbf{A}$ . This is called setting the gauge. Examining (12) we see that if we set

$$\nabla \cdot \mathbf{A} = -\frac{1}{c^2} \frac{\partial V}{\partial t} \quad (13)$$

the middle term on the left-hand side of (12) becomes zero so that the resulting relation between  $\mathbf{A}$  and  $\mathbf{J}_f$  is the non-homogeneous vector wave equation:

$$\nabla^2 \mathbf{A} - \frac{1}{c^2} \frac{\partial^2 \mathbf{A}}{\partial t^2} = -\mu \mathbf{J}_f \quad (14)$$

The condition of (13) is called the Lorentz gauge. Note that for static conditions,  $\nabla \cdot \mathbf{A} = 0$ , which is the value also picked in Section 5-4-2 for the magneto-quasi-static field. With (14) we can solve for  $\mathbf{A}$  when the current distribution  $\mathbf{J}_f$  is given and then use (13) to solve for  $V$ . The scalar potential can also be found directly by using (10) in Gauss's law of (4) as

$$\nabla^2 V + \frac{\partial}{\partial t} (\nabla \cdot \mathbf{A}) = \frac{-\rho_f}{\epsilon} \quad (15)$$

The second term can be put in terms of  $V$  by using the Lorentz gauge condition of (13) to yield the scalar wave equation:

$$\nabla^2 V - \frac{1}{c^2} \frac{\partial^2 V}{\partial t^2} = \frac{-\rho_f}{\epsilon} \quad (16)$$

Note again that for static situations this relation reduces to Poisson's equation, the governing equation for the quasi-static electric potential.

### 9-1-2 Solutions to the Wave Equation

We see that the three scalar equations of (14) (one equation for each vector component) and that of (16) are in the same form. If we can thus find the general solution to any one of these equations, we know the general solution to all of them.

As we had earlier proceeded for quasi-static fields, we will find the solution to (16) for a point charge source. Then the solution for any charge distribution is obtained using superposition by integrating the solution for a point charge over all incremental charge elements.

In particular, consider a stationary point charge at  $r=0$  that is an arbitrary function of time  $Q(t)$ . By symmetry, the resulting potential can only be a function of  $r$  so that (16) becomes

$$\frac{1}{r^2} \frac{\partial}{\partial r} \left( r^2 \frac{\partial V}{\partial r} \right) - \frac{1}{c^2} \frac{\partial^2 V}{\partial t^2} = 0, \quad r > 0 \quad (17)$$

where the right-hand side is zero because the charge density is zero everywhere except at  $r=0$ . By multiplying (17) through by  $r$  and realizing that

$$\frac{1}{r} \frac{\partial}{\partial r} \left( r^2 \frac{\partial V}{\partial r} \right) = \frac{\partial^2}{\partial r^2} (rV) \quad (18)$$

we rewrite (17) as a homogeneous wave equation in the variable  $(rV)$ :

$$\frac{\partial^2}{\partial r^2} (rV) - \frac{1}{c^2} \frac{\partial^2}{\partial t^2} (rV) = 0 \quad (19)$$

which we know from Section 7-3-2 has solutions

$$rV = f_+ \left( t - \frac{r}{c} \right) + f_- \left( t + \frac{r}{c} \right) \quad (20)$$

We throw out the negatively traveling wave solution as there are no sources for  $r > 0$  so that all waves emanate radially outward from the point charge at  $r=0$ . The arbitrary function  $f_+$  is evaluated by realizing that as  $r \rightarrow 0$  there can be no propagation delay effects so that the potential should approach the quasi-static Coulomb potential of a point charge:

$$\lim_{r \rightarrow 0} V = \frac{Q(t)}{4\pi\epsilon r} \Rightarrow f_+(t) = \frac{Q(t)}{4\pi\epsilon} \quad (21)$$

The potential due to a point charge is then obtained from (20) and (21) replacing time  $t$  with the retarded time  $t - r/c$ :

$$V(r, t) = \frac{Q(t - r/c)}{4\pi\epsilon r} \quad (22)$$

The potential at time  $t$  depends not on the present value of charge but on the charge value a propagation time  $r/c$  earlier when the wave now received was launched.

The potential due to an arbitrary volume distribution of charge  $\rho_f(t)$  is obtained by replacing  $Q(t)$  with the differential charge element  $\rho_f(t) dV$  and integrating over the volume of charge:

$$V(r, t) = \int_{\text{all charge}} \frac{\rho_f(t - r_{QP}/c)}{4\pi\epsilon r_{QP}} dV \quad (23)$$

where  $r_{QP}$  is the distance between the charge as a source at point  $Q$  and the field point at  $P$ .

The vector potential in (14) is in the same direction as the current density  $\mathbf{J}_f$ . The solution for  $\mathbf{A}$  can be directly obtained from (23) realizing that each component of  $\mathbf{A}$  obeys the same equation as (16) if we replace  $\rho_f/\epsilon$  by  $\mu\mathbf{J}_f$ :

$$\mathbf{A}(r, t) = \int_{\text{all current}} \frac{\mu\mathbf{J}_f(t - r_{QP}/c)}{4\pi r_{QP}} dV \quad (24)$$

## 9-2 RADIATION FROM POINT DIPOLES

### 9-2-1 The Electric Dipole

The simplest building block for a transmitting antenna is that of a uniform current flowing along a conductor of incremental length  $dl$  as shown in Figure 9-1. We assume that this current varies sinusoidally with time as

$$i(t) = \text{Re}(\hat{I} e^{j\omega t}) \quad (1)$$

Because the current is discontinuous at the ends, charge must be deposited there being of opposite sign at each end [ $q(t) = \text{Re}(\hat{Q} e^{j\omega t})$ ]:

$$i(t) = \pm \frac{dq}{dt} \Rightarrow \hat{I} = \pm j\omega \hat{Q}, \quad z = \pm \frac{dl}{2} \quad (2)$$

This forms an electric dipole with moment

$$\mathbf{p} = q dl \mathbf{i}_z \quad (3)$$

If we can find the potentials and fields from this simple element, the solution for any current distribution is easily found by superposition.

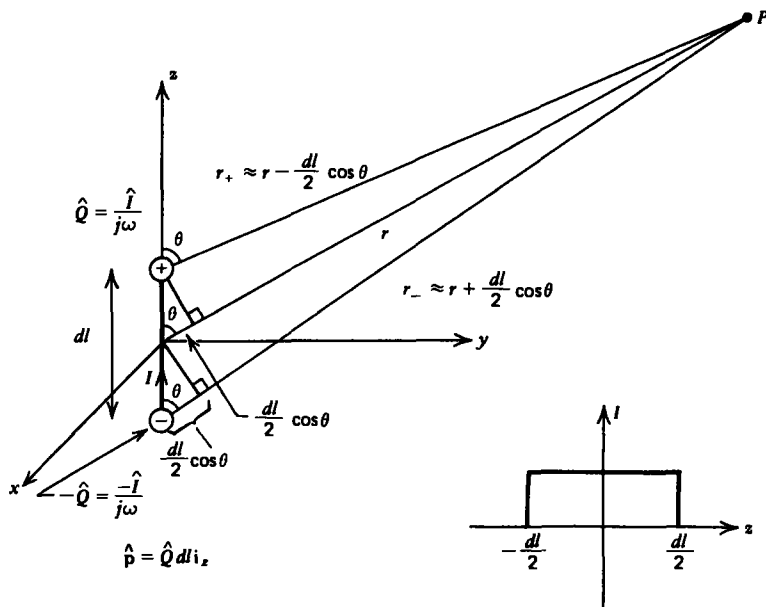


Figure 9-1 A point dipole antenna is composed of a very short uniformly distributed current-carrying wire. Because the current is discontinuous at the ends, equal magnitude but opposite polarity charges accumulate there forming an electric dipole.

By symmetry, the vector potential cannot depend on the angle  $\phi$ ,

$$A_z = \text{Re} [\hat{A}_z(r, \theta) e^{j\omega t}] \quad (4)$$

and must be in the same direction as the current:

$$A_z(r, t) = \text{Re} \left[ \int_{-dl/2}^{+dl/2} \frac{\mu \hat{I} e^{j[\omega(t-r_{QP}/c)]}}{4\pi r_{QP}} dz \right] \quad (5)$$

Because the dipole is of infinitesimal length, the distance from the dipole to any field point is just the spherical radial distance  $r$  and is constant for all points on the short wire. Then the integral in (5) reduces to a pure multiplication to yield

$$\hat{A}_z = \frac{\mu \hat{I} dl}{4\pi r} e^{-jkr}, \quad A_z(r, t) = \text{Re} [\hat{A}_z(r) e^{j\omega t}] \quad (6)$$

where we again introduce the wavenumber  $k = \omega/c$  and neglect writing the sinusoidal time dependence present in all field and source quantities. The spherical components of  $\hat{A}_z$

are ( $\hat{\mathbf{i}}_z = \hat{\mathbf{i}}_r \cos \theta - \hat{\mathbf{i}}_\theta \sin \theta$ ):

$$\hat{A}_r = \hat{A}_z \cos \theta, \quad \hat{A}_\theta = -\hat{A}_z \sin \theta, \quad \hat{A}_\phi = 0 \quad (7)$$

Once the vector potential is known, the electric and magnetic fields are most easily found from

$$\begin{aligned} \hat{\mathbf{H}} &= \frac{1}{\mu} \nabla \times \hat{\mathbf{A}}, & \mathbf{H}(r, t) &= \text{Re} [\hat{\mathbf{H}}(r, \theta) e^{j\omega t}] \\ \hat{\mathbf{E}} &= \frac{1}{j\omega\epsilon} \nabla \times \hat{\mathbf{H}}, & \mathbf{E}(r, t) &= \text{Re} [\hat{\mathbf{E}}(r, \theta) e^{j\omega t}] \end{aligned} \quad (8)$$

Before we find these fields, let's examine an alternate approach.

### 9-2-2 Alternate Derivation Using the Scalar Potential

It was easiest to find the vector potential for the point electric dipole because the integration in (5) reduced to a simple multiplication. The scalar potential is due solely to the opposite point charges at each end of the dipole,

$$\hat{V} = \frac{\hat{Q}}{4\pi\epsilon} \left( \frac{e^{-jk r_+}}{r_+} - \frac{e^{-jk r_-}}{r_-} \right) \quad (9)$$

where  $r_+$  and  $r_-$  are the distances from the respective dipole charges to any field point, as shown in Figure 9-1. Just as we found for the quasi-static electric dipole in Section 3-1-1, we cannot let  $r_+$  and  $r_-$  equal  $r$  as a zero potential would result. As we showed in Section 3-1-1, a first-order correction must be made, where

$$\begin{aligned} r_+ &\approx r - \frac{dl}{2} \cos \theta \\ r_- &\approx r + \frac{dl}{2} \cos \theta \end{aligned} \quad (10)$$

so that (9) becomes

$$\hat{V} \approx \frac{\hat{Q}}{4\pi\epsilon r} e^{-jkr} \left( \frac{e^{jk(dl/2)\cos\theta}}{\left(1 - \frac{dl}{2r}\cos\theta\right)} - \frac{e^{-jk(dl/2)\cos\theta}}{\left(1 + \frac{dl}{2r}\cos\theta\right)} \right) \quad (11)$$

Because the dipole length  $dl$  is assumed much smaller than the field distance  $r$  and the wavelength, the phase factors in the exponentials are small so they and the  $1/r$  dependence in the denominators can be expanded in a first-order Taylor

series to result in:

$$\begin{aligned} \lim_{\substack{k dl \ll 1 \\ dl/r \ll 1}} \hat{V} &\approx \frac{\hat{Q}}{4\pi\epsilon r} e^{-jkr} \left[ \left(1 + j\frac{k dl}{2} \cos \theta\right) \left(1 + \frac{dl}{2r} \cos \theta\right) \right. \\ &\quad \left. - \left(1 - jk\frac{dl}{2} \cos \theta\right) \left(1 - \frac{dl}{2r} \cos \theta\right) \right] \\ &= \frac{\hat{Q} dl}{4\pi\epsilon r^2} e^{-jkr} \cos \theta (1 + jkr) \end{aligned} \quad (12)$$

When the frequency becomes very low so that the wavenumber also becomes small, (12) reduces to the quasi-static electric dipole potential found in Section 3-1-1 with dipole moment  $\hat{p} = \hat{Q} dl$ . However, we see that the radiation correction terms in (12) dominate at higher frequencies (large  $k$ ) far from the dipole ( $kr \gg 1$ ) so that the potential only dies off as  $1/r$  rather than the quasi-static  $1/r^2$ . Using the relationships  $\hat{Q} = \hat{I}/j\omega$  and  $c = 1/\sqrt{\epsilon\mu}$ , (12) could have been obtained immediately from (6) and (7) with the Lorentz gauge condition of Eq. (13) in Section 9-1-1:

$$\begin{aligned} \hat{V} = \frac{-c^2}{j\omega} \nabla \cdot \hat{A} &= \frac{-c^2}{j\omega} \left( \frac{1}{r^2} \frac{\partial}{\partial r} (r^2 \hat{A}_r) + \frac{1}{r \sin \theta} \frac{\partial}{\partial \theta} (\hat{A}_\theta \sin \theta) \right) \\ &= \frac{\mu \hat{I} dl c^2}{4\pi j\omega} \frac{(1 + jkr)}{r^2} e^{-jkr} \cos \theta \\ &= \frac{\hat{Q} dl}{4\pi\epsilon r^2} (1 + jkr) e^{-jkr} \cos \theta \end{aligned} \quad (13)$$

### 9-2-3 The Electric and Magnetic Fields

Using (6), the fields are directly found from (8) as

$$\begin{aligned} \hat{H} &= \frac{1}{\mu} \nabla \times \hat{A} \\ &= \hat{i}_\phi \frac{1}{\mu r} \left( \frac{\partial}{\partial r} (r \hat{A}_\theta) - \frac{\partial \hat{A}_r}{\partial \theta} \right) \\ &= -\hat{i}_\phi \frac{\hat{I} dl}{4\pi} k^2 \sin \theta \left( \frac{1}{jkr} + \frac{1}{(jkr)^2} \right) e^{-jkr} \end{aligned} \quad (14)$$

$$\begin{aligned}
 \hat{\mathbf{E}} &= \frac{1}{j\omega\epsilon} \nabla \times \hat{\mathbf{H}} \\
 &= \frac{1}{j\omega\epsilon} \left( \frac{1}{r \sin \theta} \frac{\partial}{\partial \theta} (\hat{H}_\phi \sin \theta) \mathbf{i}_r - \frac{1}{r} \frac{\partial}{\partial r} (r \hat{H}_\phi) \mathbf{i}_\theta \right) \\
 &= -\frac{\hat{I} dl k^2}{4\pi} \sqrt{\frac{\mu}{\epsilon}} \left\{ \mathbf{i}_r \left[ 2 \cos \theta \left( \frac{1}{(jkr)^2} + \frac{1}{(jkr)^3} \right) \right] \right. \\
 &\quad \left. + \mathbf{i}_\theta \left[ \sin \theta \left( \frac{1}{jkr} + \frac{1}{(jkr)^2} + \frac{1}{(jkr)^3} \right) \right] \right\} e^{-jkr} \quad (15)
 \end{aligned}$$

Note that even this simple source generates a fairly complicated electromagnetic field. The magnetic field in (14) points purely in the  $\phi$  direction as expected by the right-hand rule for a  $z$ -directed current. The term that varies as  $1/r^2$  is called the induction field or near field for it predominates at distances close to the dipole and exists even at zero frequency. The new term, which varies as  $1/r$ , is called the radiation field since it dominates at distances far from the dipole and will be shown to be responsible for time-average power flow away from the source. The near field term does not contribute to power flow but is due to the stored energy in the magnetic field and thus results in reactive power.

The  $1/r^3$  terms in (15) are just the electric dipole field terms present even at zero frequency and so are often called the electrostatic solution. They predominate at distances close to the dipole and thus are the near fields. The electric field also has an intermediate field that varies as  $1/r^2$ , but more important is the radiation field term in the  $\mathbf{i}_\theta$  component, which varies as  $1/r$ . At large distances ( $kr \gg 1$ ) this term dominates.

In the far field limit ( $kr \gg 1$ ), the electric and magnetic fields are related to each other in the same way as for plane waves:

$$\lim_{kr \gg 1} \hat{E}_\theta = \sqrt{\frac{\mu}{\epsilon}} \hat{H}_\phi = \frac{\hat{E}_0}{jkr} \sin \theta e^{-jkr}, \quad \hat{E}_0 = -\frac{\hat{I} dl k^2}{4\pi} \sqrt{\frac{\mu}{\epsilon}} \quad (16)$$

The electric and magnetic fields are perpendicular and their ratio is equal to the wave impedance  $\eta = \sqrt{\mu/\epsilon}$ . This is because in the far field limit the spherical wavefronts approximate a plane.

### 9-2-4 Electric Field Lines

Outside the dipole the volume charge density is zero, which allows us to define an electric vector potential  $\mathbf{C}$ :

$$\nabla \cdot \mathbf{E} = 0 \Rightarrow \mathbf{E} = \nabla \times \mathbf{C} \quad (17)$$

Because the electric field in (15) only has  $r$  and  $\theta$  components,  $\mathbf{C}$  must only have a  $\phi$  component,  $C_\phi(r, \theta)$ :

$$\mathbf{E} = \nabla \times \mathbf{C} = \frac{1}{r \sin \theta} \frac{\partial}{\partial \theta} (\sin \theta C_\phi) \mathbf{i}_r - \frac{1}{r} \frac{\partial}{\partial r} (r C_\phi) \mathbf{i}_\theta \quad (18)$$

We follow the same procedure developed in Section 4-4-3*b*, where the electric field lines are given by

$$\frac{dr}{r d\theta} = \frac{E_r}{E_\theta} = - \frac{\frac{\partial}{\partial \theta} (\sin \theta C_\phi)}{\sin \theta \frac{\partial}{\partial r} (r C_\phi)} \quad (19)$$

which can be rewritten as an exact differential,

$$\frac{\partial}{\partial r} (r \sin \theta C_\phi) dr + \frac{\partial}{\partial \theta} (r \sin \theta C_\phi) d\theta = 0 \Rightarrow d(r \sin \theta C_\phi) = 0 \quad (20)$$

so that the field lines are just lines of constant stream-function  $r \sin \theta C_\phi$ .  $C_\phi$  is found by equating each vector component in (18) to the solution in (15):

$$\begin{aligned} & \frac{1}{r \sin \theta} \frac{\partial}{\partial \theta} (\sin \theta \hat{C}_\phi) \\ &= \hat{E}_r = - \frac{\hat{I} dl k^2}{4\pi} \sqrt{\frac{\mu}{\epsilon}} \left[ 2 \cos \theta \left( \frac{1}{(jkr)^2} + \frac{1}{(jkr)^3} \right) \right] e^{-jkr} \\ & - \frac{1}{r} \frac{\partial}{\partial r} (r \hat{C}_\phi) \\ &= \hat{E}_\theta = - \frac{\hat{I} dl k^2}{4\pi} \sqrt{\frac{\mu}{\epsilon}} \left[ \sin \theta \left( \frac{1}{(jkr)} + \frac{1}{(jkr)^2} + \frac{1}{(jkr)^3} \right) \right] e^{-jkr} \end{aligned} \quad (21)$$

which integrates to

$$\hat{C}_\phi = \frac{\hat{I} dl}{4\pi} \sqrt{\frac{\mu}{\epsilon}} \frac{\sin \theta}{r} \left( 1 - \frac{j}{kr} \right) e^{-jkr} \quad (22)$$

Then assuming  $\hat{I}$  is real, the instantaneous value of  $C_\phi$  is

$$\begin{aligned} C_\phi &= \text{Re} (\hat{C}_\phi e^{j\omega t}) \\ &= \frac{\hat{I} dl}{4\pi} \sqrt{\frac{\mu}{\epsilon}} \frac{\sin \theta}{r} \left( \cos(\omega t - kr) + \frac{\sin(\omega t - kr)}{kr} \right) \end{aligned} \quad (23)$$

so that, omitting the constant amplitude factor in (23), the field lines are

$$r C_\phi \sin \theta = \text{const} \Rightarrow \sin^2 \theta \left( \cos(\omega t - kr) + \frac{\sin(\omega t - kr)}{kr} \right) = \text{const} \quad (24)$$

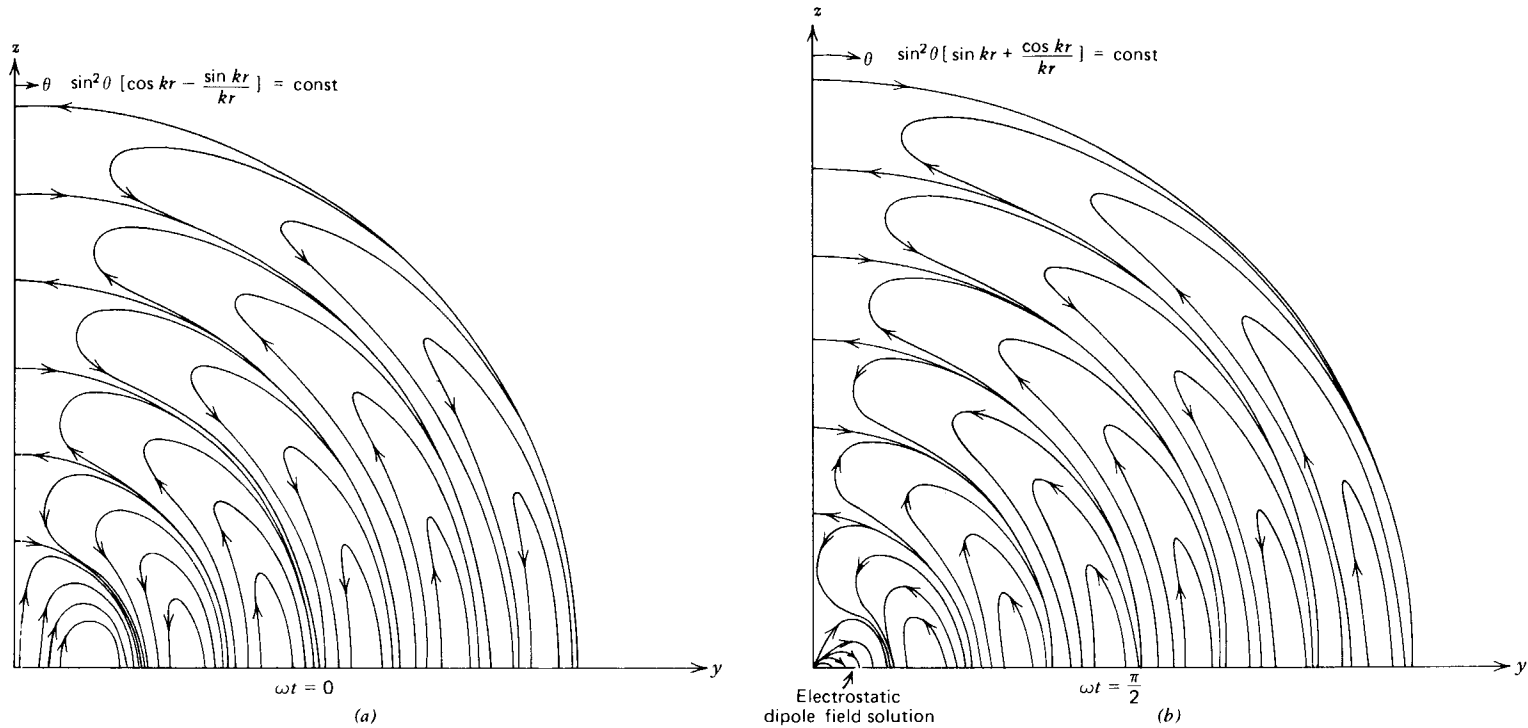


Figure 9-2 The electric field lines for a point electric dipole at  $\omega t = 0$  and  $\omega t = \pi/2$ .

These field lines are plotted in Figure 9-2 at two values of time. We can check our result with the static field lines for a dipole given in Section 3-1-1. Remembering that  $k = \omega/c$ , at low frequencies,

$$\lim_{\omega \rightarrow 0} \begin{cases} \cos(\omega t - kr) \approx 1 \\ \frac{\sin(\omega t - kr)}{kr} \approx \frac{(t - r/c)}{r/c} \approx \frac{t}{r/c} - 1 \end{cases} \quad (25)$$

so that, in the low-frequency limit at a fixed time, (24) approaches the result of Eq. (6) of Section 3-1-1:

$$\lim_{\omega \rightarrow 0} \sin^2 \theta \left( \frac{ct}{r} \right) = \text{const} \quad (26)$$

Note that the field lines near the dipole are those of a static dipole field, as drawn in Figure 3-2. In the far field limit

$$\lim_{kr \gg 1} \sin^2 \theta \cos(\omega t - kr) = \text{const} \quad (27)$$

the field lines repeat with period  $\lambda = 2\pi/k$ .

### 9-2-5 Radiation Resistance

Using the electric and magnetic fields of Section 9-2-3, the time-average power density is

$$\begin{aligned} \langle \mathbf{S} \rangle &= \frac{1}{2} \text{Re} (\hat{\mathbf{E}} \times \hat{\mathbf{H}}^*) \\ &= \text{Re} \left\{ \frac{|\hat{I} dl|^2 \eta k^4}{2(4\pi)^2} \left[ -\mathbf{i}_\theta \sin 2\theta \left( -\frac{1}{(jkr)^3} + \frac{1}{(jkr)^5} \right) \right] \right. \\ &\quad \left. + \mathbf{i}_r \sin^2 \theta \left( -\frac{1}{(jkr)^2} + \frac{1}{(jkr)^5} \right) \right\} \\ &= \frac{1}{2} |\hat{I} dl|^2 \left( \frac{k}{4\pi} \right)^2 \frac{\eta}{r^2} \sin^2 \theta \mathbf{i}_r \\ &= \frac{1}{2} \frac{|\hat{\mathbf{E}}_0|^2}{\eta} \frac{\sin^2 \theta}{(kr)^2} \mathbf{i}_r \end{aligned} \quad (28)$$

where  $\hat{\mathbf{E}}_0$  is defined in (16).

Only the far fields contributed to the time-average power flow. The near and intermediate fields contributed only imaginary terms in (28) representing reactive power.

The power density varies with the angle  $\theta$ , being zero along the electric dipole's axis ( $\theta = 0, \pi$ ) and maximum at right angles to it ( $\theta = \pi/2$ ), illustrated by the radiation power pattern in Fig. 9-3. The strength of the power density is proportional to the length of the vector from the origin to the

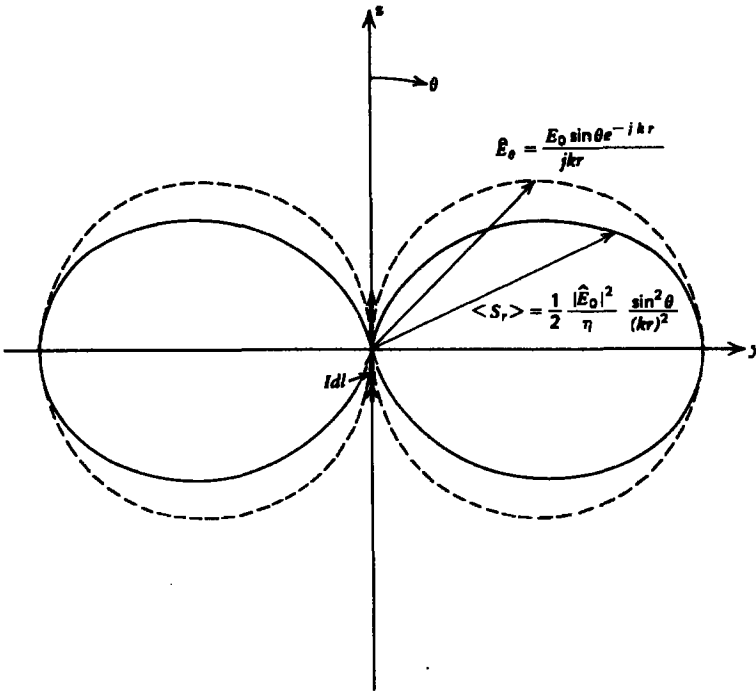


Figure 9-3 The strength of the electric field and power density due to a  $z$ -directed point dipole as a function of angle  $\theta$  is proportional to the length of the vector from the origin to the radiation pattern.

radiation pattern. These directional properties are useful in beam steering, where the directions of power flow can be controlled.

The total time-average power radiated by the electric dipole is found by integrating the Poynting vector over a spherical surface at any radius  $r$ :

$$\begin{aligned}
 \langle P \rangle &= \int_{\theta=0}^{\pi} \int_{\phi=0}^{2\pi} \langle S_r \rangle r^2 \sin \theta \, d\theta \, d\phi \\
 &= \frac{1}{2} |\hat{I} dl|^2 \left( \frac{k}{4\pi} \right)^2 \eta 2\pi \int_{\theta=0}^{\pi} \sin^3 \theta \, d\theta \\
 &= \frac{|\hat{I} dl|^2}{16\pi} \eta k^2 \left[ -\frac{1}{3} \cos \theta (\sin^2 \theta + 2) \right]_0^{\pi} \\
 &= \frac{|\hat{I} dl|^2}{12\pi} \eta k^2
 \end{aligned} \tag{29}$$

As far as the dipole is concerned, this radiated power is lost in the same way as if it were dissipated in a resistance  $R$ ,

$$\langle P \rangle = \frac{1}{2} |\hat{I}|^2 R \quad (30)$$

where this equivalent resistance is called the radiation resistance:

$$R = \frac{\eta}{6\pi} (k dl)^2 = \frac{2\pi\eta}{3} \left(\frac{dl}{\lambda}\right)^2, \quad k = \frac{2\pi}{\lambda} \quad (31)$$

In free space  $\eta_0 = \sqrt{\mu_0/\epsilon_0} \approx 120\pi$ , the radiation resistance is

$$R_0 = 80\pi^2 \left(\frac{dl}{\lambda}\right)^2 \quad (\text{free space}) \quad (32)$$

These results are only true for point dipoles, where  $dl$  is much less than a wavelength ( $dl/\lambda \ll 1$ ). This verifies the validity of the quasi-static approximation for geometries much smaller than a radiated wavelength, as the radiated power is then negligible.

If the current on a dipole is not constant but rather varies with  $z$  over the length, the only term that varies with  $z$  for the vector potential in (5) is  $\hat{I}(z)$ :

$$\hat{A}_z(r) = \text{Re} \left[ \int_{-dl/2}^{+dl/2} \frac{\mu \hat{I}(z) e^{-jk r_{QP}}}{4\pi r_{QP}} dz \right] \approx \text{Re} \left[ \frac{\mu e^{-jk r_{QP}}}{4\pi r_{QP}} \int_{-dl/2}^{+dl/2} \hat{I}(z) dz \right] \quad (33)$$

where, because the dipole is of infinitesimal length, the distance  $r_{QP}$  from any point on the dipole to any field point far from the dipole is essentially  $r$ , independent of  $z$ . Then, all further results for the electric and magnetic fields are the same as in Section 9-2-3 if we replace the actual dipole length  $dl$  by its effective length,

$$dl_{\text{eff}} = \frac{1}{\hat{I}_0} \int_{-dl/2}^{+dl/2} \hat{I}(z) dz \quad (34)$$

where  $\hat{I}_0$  is the terminal current feeding the center of the dipole.

Generally the current is zero at the open circuited ends, as for the linear distribution shown in Figure 9-4,

$$\hat{I}(z) = \begin{cases} I_0(1 - 2z/dl), & 0 \leq z \leq dl/2 \\ I_0(1 + 2z/dl), & -dl/2 \leq z \leq 0 \end{cases} \quad (35)$$

so that the effective length is half the actual length:

$$dl_{\text{eff}} = \frac{1}{I_0} \int_{-dl/2}^{+dl/2} \hat{I}(z) dz = \frac{dl}{2} \quad (36)$$

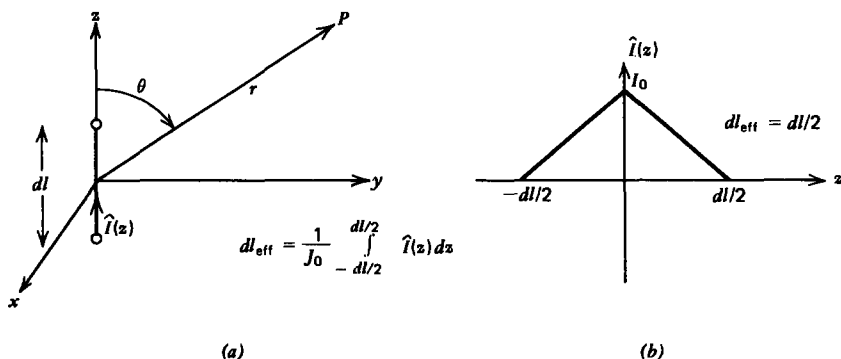


Figure 9-4 (a) If a point electric dipole has a nonuniform current distribution, the solutions are of the same form if we replace the actual dipole length  $dl$  by an effective length  $dl_{\text{eff}}$ . (b) For a triangular current distribution the effective length is half the true length.

Because the fields are reduced by half, the radiation resistance is then reduced by  $\frac{1}{4}$ :

$$R = \frac{2\pi\eta}{3} \left( \frac{dl_{\text{eff}}}{\lambda} \right)^2 = 20\pi^2 \sqrt{\frac{\mu_r}{\epsilon_r}} \left( \frac{dl}{\lambda} \right)^2 \quad (37)$$

In free space the relative permeability  $\mu_r$  and relative permittivity  $\epsilon_r$  are unity.

Note also that with a spatially dependent current distribution, a line charge distribution is found over the whole length of the dipole and not just on the ends:

$$\hat{\lambda} = -\frac{1}{j\omega} \frac{d\hat{I}}{dz} \quad (38)$$

For the linear current distribution described by (35), we see that:

$$\hat{\lambda} = \pm \frac{2I_0}{j\omega dl} \begin{cases} 0 \leq z \leq dl/2 \\ -dl/2 \leq z \leq 0 \end{cases} \quad (39)$$

### 9-2-6 Rayleigh Scattering (or why is the sky blue?)

If a plane wave electric field  $\text{Re} [E_0 e^{j\omega t} \mathbf{i}_x]$  is incident upon an atom that is much smaller than the wavelength, the induced dipole moment also contributes to the resultant field, as illustrated in Figure 9-5. The scattered power is perpendicular to the induced dipole moment. Using the dipole model developed in Section 3-1-4, where a negative spherical electron cloud of radius  $R_0$  with total charge  $-Q$  surrounds a fixed

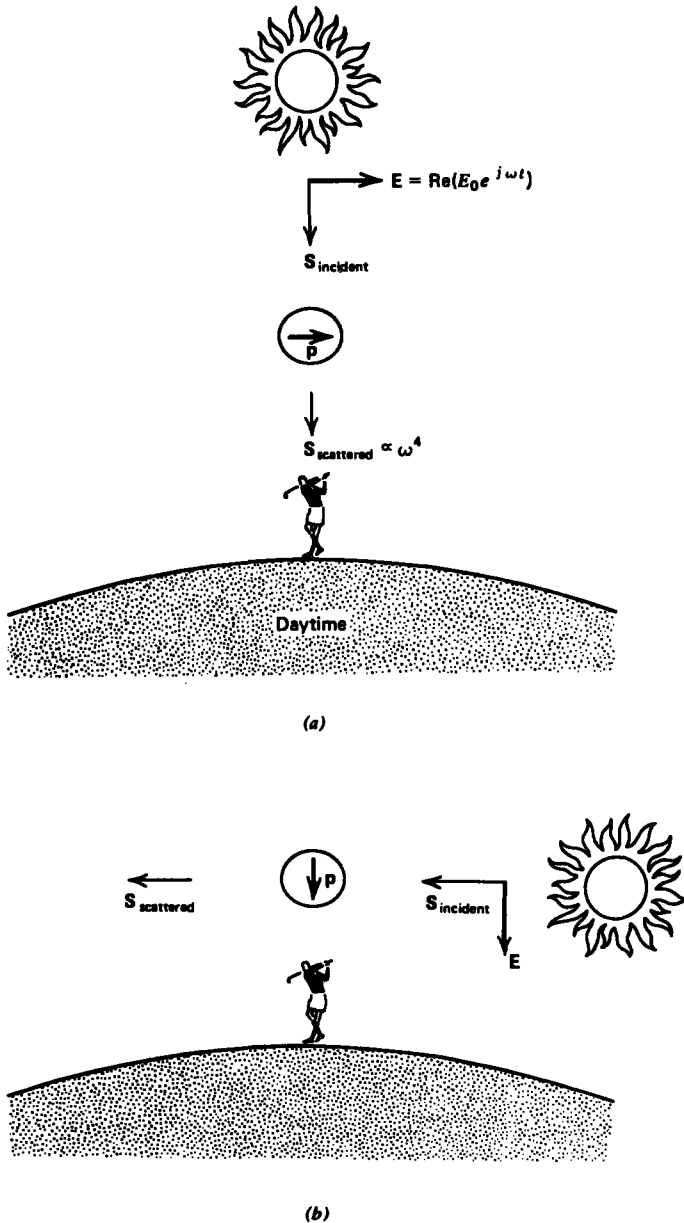


Figure 9-5 An incident electric field polarizes dipoles that then re-radiate their energy primarily perpendicular to the polarizing electric field. The time-average scattered power increases with the fourth power of frequency so shorter wavelengths of light are scattered more than longer wavelengths. (a) During the daytime an earth observer sees more of the blue scattered light so the sky looks blue (short wavelengths). (b) Near sunset the light reaching the observer lacks blue so the sky appears reddish (long wavelength).

positive point nucleus, Newton's law for the charged cloud with mass  $m$  is:

$$\frac{d^2x}{dt^2} + \omega_0^2 x = \text{Re} \left( \frac{QE_0}{m} e^{j\omega t} \right), \quad \omega_0^2 = \frac{Q^2}{4\pi\epsilon m R_0^3} \quad (40)$$

The resulting dipole moment is then

$$\hat{p} = Q\hat{x} = \frac{Q^2 E_0/m}{\omega_0^2 - \omega^2} \quad (41)$$

where we neglect damping effects. This dipole then re-radiates with solutions given in Sections 9-2-1-9-2-5 using the dipole moment of (41) ( $\hat{I} dl \rightarrow j\omega\hat{p}$ ). The total time-average power radiated is then found from (29) as

$$\langle P \rangle = \frac{\omega^4 |\hat{p}|^2 \eta}{12\pi c^2} = \frac{\omega^4 \eta (Q^2 E_0/m)^2}{12\pi c^2 (\omega_0^2 - \omega^2)^2} \quad (42)$$

To approximately compute  $\omega_0$ , we use the approximate radius of the electron found in Section 3-8-2 by equating the energy stored in Einstein's relativistic formula relating mass to energy:

$$mc^2 = \frac{3Q^2}{20\pi\epsilon R_0} \Rightarrow R_0 = \frac{3Q^2}{20\pi\epsilon mc^2} \approx 1.69 \times 10^{-15} \text{ m} \quad (43)$$

Then from (40)

$$\omega_0 = \frac{\sqrt{5/3} 20\pi\epsilon mc^3}{3Q^2} \approx 2.3 \times 10^{23} \text{ radian/sec} \quad (44)$$

is much greater than light frequencies ( $\omega \approx 10^{15}$ ) so that (42) becomes approximately

$$\lim_{\omega_0 \gg \omega} \langle P \rangle \approx \frac{\eta}{12\pi} \left( \frac{Q^2 E_0 \omega^2}{m c \omega_0^2} \right)^2 \quad (45)$$

This result was originally derived by Rayleigh to explain the blueness of the sky. Since the scattered power is proportional to  $\omega^4$ , shorter wavelength light dominates. However, near sunset the light is scattered parallel to the earth rather than towards it. The blue light received by an observer at the earth is diminished so that the longer wavelengths dominate and the sky appears reddish.

### 9-2-7 Radiation from a Point Magnetic Dipole

A closed sinusoidally varying current loop of very small size flowing in the  $z = 0$  plane also generates radiating waves. Because the loop is closed, the current has no divergence so

that there is no charge and the scalar potential is zero. The vector potential phasor amplitude is then

$$\hat{\mathbf{A}}(\mathbf{r}) = \int \frac{\mu \hat{\mathbf{I}} e^{-jk r_{QP}}}{4\pi r_{QP}} dl \quad (46)$$

We assume the dipole to be much smaller than a wavelength,  $k(r_{QP} - r) \ll 1$ , so that the exponential factor in (46) can be linearized to

$$\lim_{k(r_{QP}-r) \ll 1} e^{-jk r_{QP}} = e^{-jk r} e^{-jk(r_{QP}-r)} \approx e^{-jk r} [1 - jk(r_{QP} - r)] \quad (47)$$

Then (46) reduces to

$$\begin{aligned} \hat{\mathbf{A}}(\mathbf{r}) &= \int \frac{\mu \hat{\mathbf{I}}}{4\pi} e^{-jk r} \left( \frac{1 + jkr}{r_{QP}} - jk \right) dl \\ &= e^{-jk r} \int \frac{\mu \hat{\mathbf{I}}}{4\pi} \left( \frac{1 + jkr}{r_{QP}} - jk \right) dl \\ &= \frac{\mu}{4\pi} e^{-jk r} \left( (1 + jkr) \int \frac{\hat{\mathbf{I}} dl}{r_{QP}} - jk \int \hat{\mathbf{I}} dl \right) \end{aligned} \quad (48)$$

where all terms that depend on  $r$  can be taken outside the integrals because  $r$  is independent of  $dl$ . The second integral is zero because the vector current has constant magnitude and flows in a closed loop so that its average direction integrated over the loop is zero. This is most easily seen with a rectangular loop where opposite sides of the loop contribute equal magnitude but opposite signs to the integral, which thus sums to zero. If the loop is circular with radius  $a$ ,

$$\hat{\mathbf{I}} dl = \hat{\mathbf{I}}_{\phi} a d\phi \Rightarrow \int_0^{2\pi} \mathbf{i}_{\phi} d\phi = \int_0^{2\pi} (-\sin \phi \mathbf{i}_x + \cos \phi \mathbf{i}_y) d\phi = 0 \quad (49)$$

the integral is again zero as the average value of the unit vector  $\mathbf{i}_{\phi}$  around the loop is zero.

The remaining integral is the same as for quasi-statics except that it is multiplied by the factor  $(1 + jkr) e^{-jk r}$ . Using the results of Section 5-5-1, the quasi-static vector potential is also multiplied by this quantity:

$$\hat{\mathbf{A}} = \frac{\mu \hat{m}}{4\pi r^2} \sin \theta (1 + jkr) e^{-jk r} \mathbf{i}_{\phi}, \quad \hat{m} = \hat{\mathbf{I}} dS \quad (50)$$

The electric and magnetic fields are then

$$\begin{aligned}\hat{\mathbf{H}} &= \frac{1}{\mu} \nabla \times \hat{\mathbf{A}} = -\frac{\hat{m}}{4\pi} jk^3 e^{-jkr} \left\{ \mathbf{i}_r \left[ 2 \cos \theta \left( \frac{1}{(jkr)^2} + \frac{1}{(jkr)^3} \right) \right] \right. \\ &\quad \left. + \mathbf{i}_\theta \left[ \sin \theta \left( \frac{1}{jkr} + \frac{1}{(jkr)^2} + \frac{1}{(jkr)^3} \right) \right] \right\} \quad (51) \\ \hat{\mathbf{E}} &= \frac{1}{j\omega\epsilon} \nabla \times \hat{\mathbf{H}} = \frac{\hat{m}jk^3}{4\pi} \eta e^{-jkr} \sin \theta \left( \frac{1}{(jkr)} + \frac{1}{(jkr)^2} \right) \mathbf{i}_\phi\end{aligned}$$

The magnetic dipole field solutions are the dual to those of the electric dipole where the electric and magnetic fields reverse roles if we replace the electric dipole moment with the magnetic dipole moment:

$$\frac{\mathbf{p}}{\epsilon} = \frac{q \, d\mathbf{l}}{\epsilon} = \frac{\mathbf{I} \, dl}{j\omega\epsilon} \rightarrow \mathbf{m} \quad (52)$$

### 9-3 POINT DIPOLE ARRAYS

The power density for a point electric dipole varies with the broad angular distribution  $\sin^2 \theta$ . Often it is desired that the power pattern be highly directive with certain angles carrying most of the power with negligible power density at other angles. It is also necessary that the directions for maximum power flow be controllable with no mechanical motion of the antenna. These requirements can be met by using more dipoles in a periodic array.

#### 9-3-1 A Simple Two Element Array

To illustrate the basic principles of antenna arrays we consider the two element electric dipole array shown in Figure 9-6. We assume each element carries uniform currents  $\hat{I}_1$  and  $\hat{I}_2$  and has lengths  $dl_1$  and  $dl_2$ , respectively. The elements are a distance  $2a$  apart. The fields at any point  $P$  are given by the superposition of fields due to each dipole alone. Since we are only interested in the far field radiation pattern where  $\theta_1 \approx \theta_2 \approx \theta$ , we use the solutions of Eq. (16) in Section 9-2-3 to write:

$$\hat{E}_\theta = \eta \hat{H}_\phi = \frac{\hat{E}_1 \sin \theta e^{-jkr_1}}{jkr_1} + \frac{\hat{E}_2 \sin \theta e^{-jkr_2}}{jkr_2} \quad (1)$$

where

$$\hat{E}_1 = -\frac{\hat{I}_1 dl_1 k^2}{4\pi} \eta, \quad \hat{E}_2 = -\frac{\hat{I}_2 dl_2 k^2}{4\pi} \eta$$

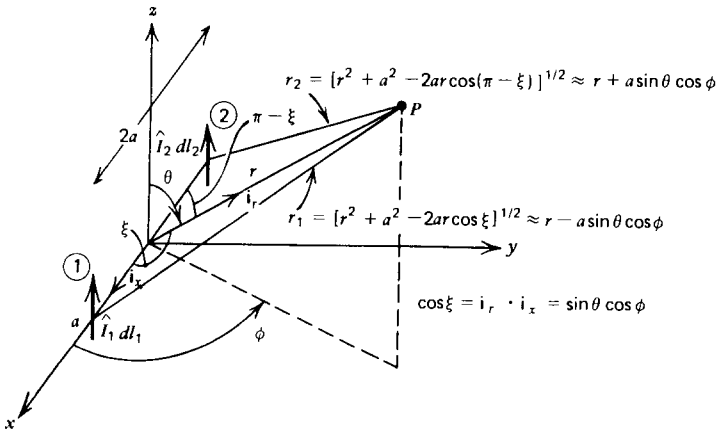


Figure 9-6 The field at any point *P* due to two-point dipoles is just the sum of the fields due to each dipole alone taking into account the difference in distances to each dipole.

Remember, we can superpose the fields but we cannot superpose the power flows.

From the law of cosines the distances  $r_1$  and  $r_2$  are related as

$$\begin{aligned} r_2 &= [r^2 + a^2 - 2ar \cos(\pi - \xi)]^{1/2} = [r^2 + a^2 + 2ar \cos \xi]^{1/2} \\ r_1 &= [r^2 + a^2 - 2ar \cos \xi]^{1/2} \end{aligned} \tag{2}$$

where  $\xi$  is the angle between the unit radial vector  $\mathbf{i}_r$  and the *x* axis:

$$\cos \xi = \mathbf{i}_r \cdot \mathbf{i}_x = \sin \theta \cos \phi$$

Since we are interested in the far field pattern, we linearize (2) to

$$\lim_{r \gg a} \begin{cases} r_2 \approx r \left[ 1 + \frac{1}{2} \left( \frac{a^2}{r^2} + \frac{2a}{r} \sin \theta \cos \phi \right) \right] \approx r + a \sin \theta \cos \phi \\ r_1 \approx r \left[ 1 + \frac{1}{2} \left( \frac{a^2}{r^2} - \frac{2a}{r} \sin \theta \cos \phi \right) \right] \approx r - a \sin \theta \cos \phi \end{cases} \tag{3}$$

In this far field limit, the correction terms have little effect in the denominators of (1) but can have significant effect in the exponential phase factors if *a* is comparable to a wavelength so that *ka* is near or greater than unity. In this spirit we include the first-order correction terms of (3) in the phase

factors of (1), but not anywhere else, so that (1) is rewritten as

$$\hat{E}_\theta = \eta \hat{H}_\phi$$

$$= \underbrace{\frac{jk\eta}{4\pi r} \sin \theta e^{-jkr}}_{\text{element factor}} \underbrace{(\hat{I}_1 dl_1 e^{jka \sin \theta \cos \phi} + \hat{I}_2 dl_2 e^{-jka \sin \theta \cos \phi})}_{\text{array factor}} \quad (4)$$

The first factor is called the element factor because it is the radiation field per unit current element ( $\hat{I} dl$ ) due to a single dipole at the origin. The second factor is called the array factor because it only depends on the geometry and excitations (magnitude and phase) of each dipole element in the array.

To examine (4) in greater detail, we assume the two dipoles are identical in length and that the currents have the same magnitude but can differ in phase  $\chi$ :

$$dl_1 = dl_2 \equiv dl$$

$$\hat{I}_1 = \hat{I}, \quad \hat{I}_2 = \hat{I} e^{j\chi} \Rightarrow \hat{E}_1 = \hat{E}_0, \quad \hat{E}_2 = \hat{E}_0 e^{j\chi} \quad (5)$$

so that (4) can be written as

$$\hat{E}_\theta = \eta \hat{H}_\phi = \frac{2\hat{E}_0^*}{jkr} e^{-jkr} \sin \theta e^{j\chi/2} \cos \left( ka \sin \theta \cos \phi - \frac{\chi}{2} \right) \quad (6)$$

Now the far fields also depend on  $\phi$ . In particular, we focus attention on the  $\theta = \pi/2$  plane. Then the power flow,

$$\lim_{\theta=\pi/2} \langle S_r \rangle = \frac{1}{2\eta} |\hat{E}_\theta|^2 = \frac{2|\hat{E}_0|^2}{\eta(kr)^2} \cos^2 \left( ka \cos \phi - \frac{\chi}{2} \right) \quad (7)$$

depends strongly on the dipole spacing  $2a$  and current phase difference  $\chi$ .

**(a) Broadside Array**

Consider the case where the currents are in phase ( $\chi = 0$ ) but the dipole spacing is a half wavelength ( $2a = \lambda/2$ ). Then, as illustrated by the radiation pattern in Figure 9-7a, the field strengths cancel along the  $x$  axis while they add along the  $y$  axis. This is because along the  $y$  axis  $r_1 = r_2$ , so the fields due to each dipole add, while along the  $x$  axis the distances differ by a half wavelength so that the dipole fields cancel. Wherever the array factor phase ( $ka \cos \phi - \chi/2$ ) is an integer multiple of  $\pi$ , the power density is maximum, while wherever it is an odd integer multiple of  $\pi/2$ , the power density is zero. Because this radiation pattern is maximum in the direction perpendicular to the array, it is called a broadside pattern.

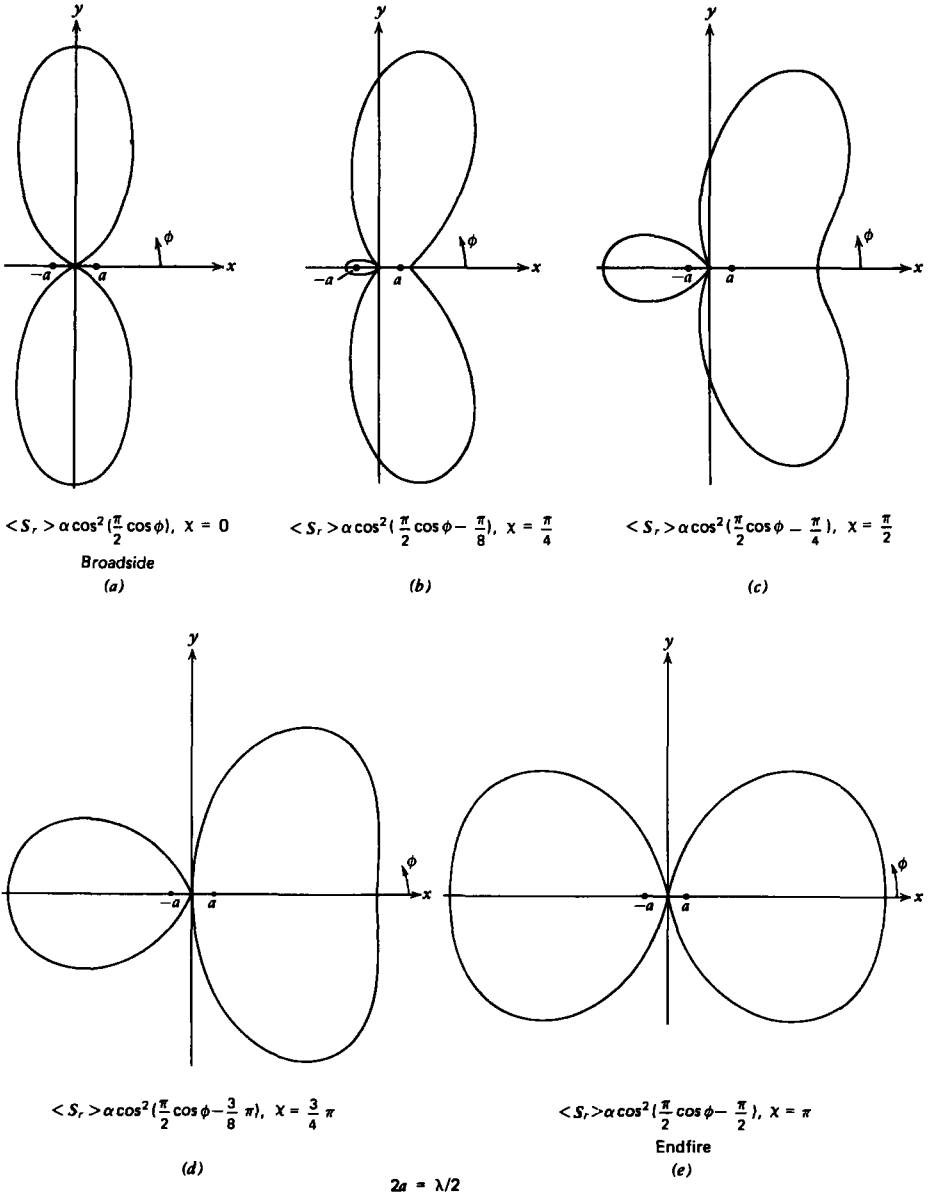


Figure 9-7 The power radiation pattern due to two-point dipoles depends strongly on the dipole spacing and current phases. With a half wavelength dipole spacing ( $2a = \lambda/2$ ), the radiation pattern is drawn for various values of current phase difference in the  $\theta = \pi/2$  plane. The broadside array in (a) with the currents in phase ( $\chi = 0$ ) has the power lobe in the direction perpendicular to the array while the end-fire array in (e) has out-of-phase currents ( $\chi = \pi$ ) with the power lobe in the direction along the array.

**(b) End-fire Array**

If, however, for the same half wavelength spacing the currents are out of phase ( $\chi = \pi$ ), the fields add along the  $x$  axis but cancel along the  $y$  axis. Here, even though the path lengths along the  $y$  axis are the same for each dipole, because the currents are out of phase the fields cancel. Along the  $x$  axis the extra  $\pi$  phase because of the half wavelength path difference is just canceled by the current phase difference of  $\pi$  so that the fields due to each dipole add. The radiation pattern is called end-fire because the power is maximum in the direction along the array, as shown in Figure 9-7e.

**(c) Arbitrary Current Phase**

For arbitrary current phase angles and dipole spacings, a great variety of radiation patterns can be obtained, as illustrated by the sequences in Figures 9-7 and 9-8. More power lobes appear as the dipole spacing is increased.

**9-3-2 An  $N$  Dipole Array**

If we have  $(2N + 1)$  equally spaced dipoles, as shown in Figure 9-9, the  $n$ th dipole's distance to the far field point is approximately,

$$\lim_{r \gg |na|} r_n \approx r - na \sin \theta \cos \phi \quad (8)$$

so that the array factor of (4) generalizes to

$$AF = \sum_{-N}^{+N} \hat{I}_n dl_n e^{jkn a \sin \theta \cos \phi} \quad (9)$$

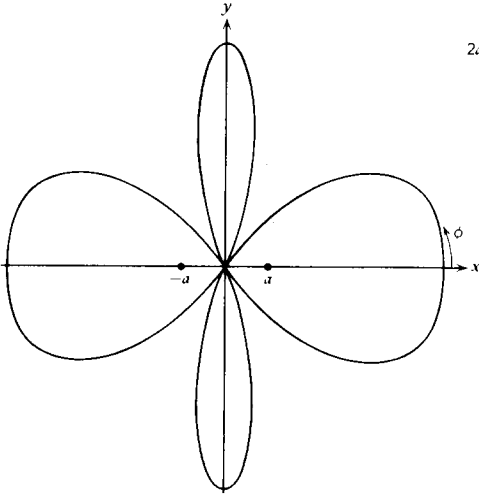
where for symmetry we assume that there are as many dipoles to the left (negative  $n$ ) as to the right (positive  $n$ ) of the  $z$  axis, including one at the origin ( $n = 0$ ). In the event that a dipole is not present at a given location, we simply let its current be zero. The array factor can be varied by changing the current magnitude or phase in the dipoles. For simplicity here, we assume that all dipoles have the same length  $dl$ , the same current magnitude  $I_0$ , and differ in phase from its neighbors by a constant angle  $\chi_0$  so that

$$\hat{I}_n = I_0 e^{-jn\chi_0}, \quad -N \leq n \leq N \quad (10)$$

and (9) becomes

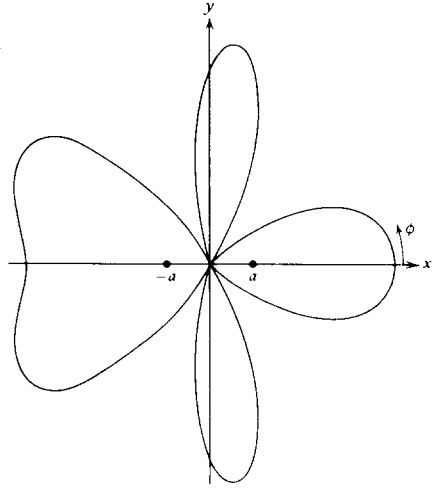
$$AF = I_0 dl \sum_{-N}^{+N} e^{jn(ha \sin \theta \cos \phi - \chi_0)} \quad (11)$$

$2a = \lambda$



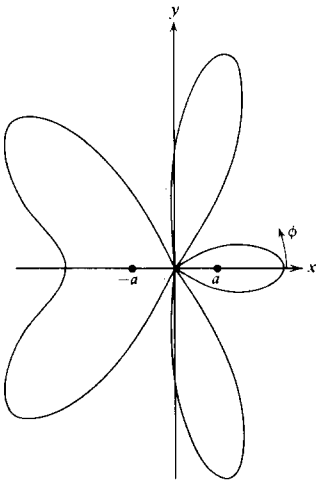
$\langle S_r \rangle \propto \alpha \cos^2(\pi \cos \phi), \chi = 0$

(a)



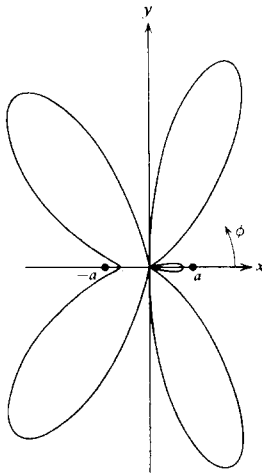
$\langle S_r \rangle \propto \alpha \cos^2(\pi \cos \phi - \frac{\pi}{8}), \chi = \pi/4$

(b)



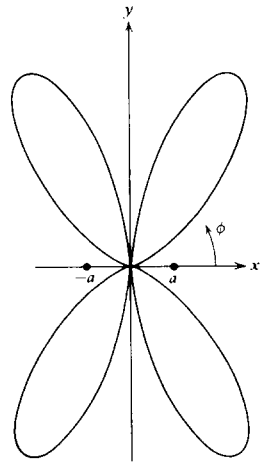
$\langle S_r \rangle \propto \alpha \cos^2(\pi \cos \phi - \frac{\pi}{4}), \chi = \frac{\pi}{2}$

(c)



$\langle S_r \rangle \propto \alpha \cos^2(\pi \cos \phi - \frac{3\pi}{8}), \chi = \frac{3}{4} \pi$

(d)



$\langle S_r \rangle \propto \alpha \cos^2(\pi \cos \phi - \frac{\pi}{2}), \chi = \pi$

(e)

Figure 9-8 With a full wavelength dipole spacing ( $2a = \lambda$ ) there are four main power lobes.

Defining the parameter

$$\beta = e^{j(ka \sin \theta \cos \phi - \chi_0)} \quad (12)$$

the geometric series in (11) can be written as

$$S = \sum_{-N}^{+N} \beta^n = \beta^{-N} + \beta^{-N+1} + \dots + \beta^{-2} + \beta^{-1} + 1 + \beta + \beta^2 + \dots + \beta^{N-1} + \beta^N \quad (13)$$

If we multiply this series by  $\beta$  and subtract from (13), we have

$$S(1 - \beta) = \beta^{-N} - \beta^{N+1} \quad (14)$$

which allows us to write the series sum in closed form as

$$S = \frac{\beta^{-N} - \beta^{N+1}}{1 - \beta} = \frac{\beta^{-(N+1/2)} - \beta^{(N+1/2)}}{\beta^{-1/2} - \beta^{1/2}} = \frac{\sin [(N + \frac{1}{2})(ka \sin \theta \cos \phi - \chi_0)]}{\sin [\frac{1}{2}(ka \sin \theta \cos \phi - \chi_0)]} \quad (15)$$

In particular, we again focus on the solution in the  $\theta = \pi/2$  plane so that the array factor is

$$AF = I_0 dl \frac{\sin [(N + \frac{1}{2})(ka \cos \phi - \chi_0)]}{\sin [\frac{1}{2}(ka \cos \phi - \chi_0)]} \quad (16)$$

The radiation pattern is proportional to the square of the array factor. Maxima occur where

$$ka \cos \phi - \chi_0 = 2n\pi \quad n = 0, 1, 2, \dots \quad (17)$$

The principal maximum is for  $n = 0$  as illustrated in Figure 9-10 for various values of  $ka$  and  $\chi_0$ . The larger the number of dipoles  $N$ , the narrower the principal maximum with smaller amplitude side lobes. This allows for a highly directive beam at angle  $\phi$  controlled by the incremental current phase angle  $\chi_0$ , so that  $\cos \phi = \chi_0/ka$ , which allows for electronic beam steering by simply changing  $\chi_0$ .

#### 9-4 LONG DIPOLE ANTENNAS

The radiated power, proportional to  $(dl/\lambda)^2$ , is small for point dipole antennas where the dipole's length  $dl$  is much less than the wavelength  $\lambda$ . More power can be radiated if the length of the antenna is increased. Then however, the fields due to each section of the antenna may not add constructively.

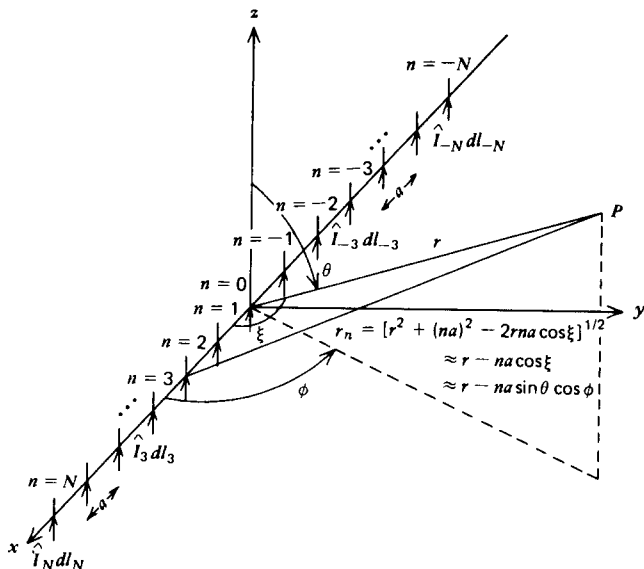


Figure 9-9 A linear point dipole array with  $2N+1$  equally spaced dipoles.

#### 9-4-1 Far Field Solution

Consider the long dipole antenna in Figure 9-11 carrying a current  $\hat{I}(z)$ . For simplicity we restrict ourselves to the far field pattern where  $r \gg L$ . Then, as we found for dipole arrays, the differences in radial distance for each incremental current element of length  $dz$  are only important in the exponential phase factors and not in the  $1/r$  dependences.

From Section 9-2-3, the incremental current element at position  $z$  generates a far electric field:

$$d\hat{E}_\theta = \eta d\hat{H}_\phi = \frac{jk\eta}{4\pi} \frac{\hat{I}(z) dz}{r} \sin \theta e^{-jk(r-z \cos \theta)} \quad (1)$$

where we again assume that in the far field the angle  $\theta$  is the same for all incremental current elements.

The total far electric field due to the entire current distribution is obtained by integration over all current elements:

$$\hat{E}_\theta = \eta \hat{H}_\phi = \frac{jk\eta}{4\pi r} \sin \theta e^{-jkr} \int_{-L/2}^{+L/2} \hat{I}(z) e^{jkz \cos \theta} dz \quad (2)$$

If the current distribution is known, the integral in (2) can be directly evaluated. The practical problem is difficult because the current distribution along the antenna is determined by the near fields through the boundary conditions.

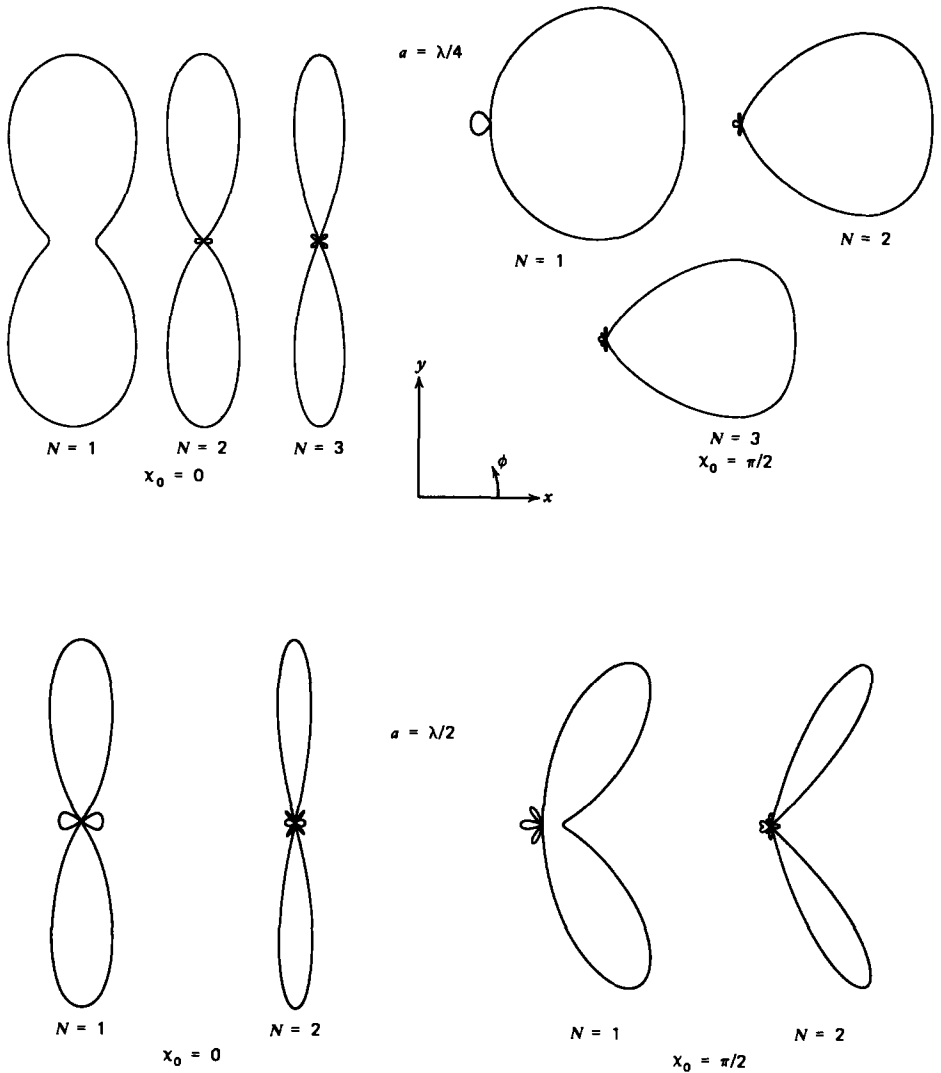


Figure 9-10 The radiation pattern for an  $N$  dipole linear array for various values of  $N$ , dipole spacing  $2a$ , and relative current phase  $\chi_0$  in the  $\theta = \pi/2$  plane.

Since the fields and currents are coupled, an exact solution is impossible no matter how simple the antenna geometry. In practice, one guesses a current distribution and calculates the resultant (near and far) fields. If all boundary conditions along the antenna are satisfied, then the solution has been found. Unfortunately, this never happens with the first guess. Thus based on the field solution obtained from the originally guessed current, a corrected current distribution is used and

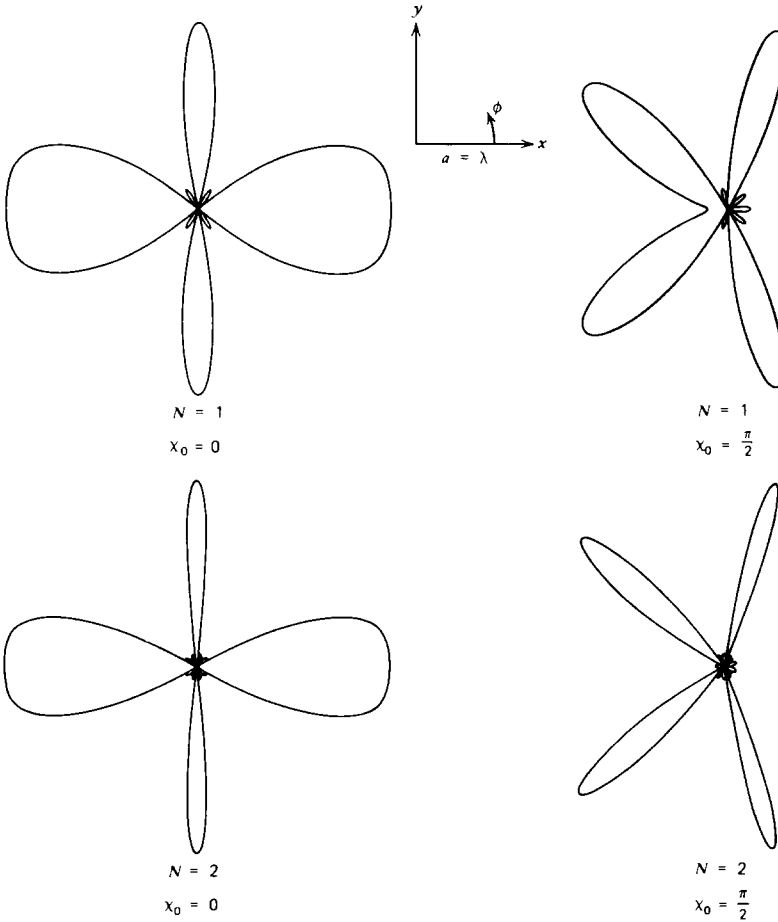


Figure 9-10

the resulting fields are again calculated. This procedure is numerically iterated until convergence is obtained with self-consistent fields and currents.

### 9-4-2 Uniform Current

A particularly simple case is when  $\hat{I}(z) = \hat{I}_0$  is a constant. Then (2) becomes:

$$\begin{aligned}
 \hat{E}_\theta &= \eta \hat{H}_\phi = \frac{jk\eta}{4\pi r} \sin \theta e^{-jkr} \hat{I}_0 \int_{-L/2}^{+L/2} e^{jkz \cos \theta} dz \\
 &= \frac{jk\eta}{4\pi r} \sin \theta e^{-jkr} \hat{I}_0 \left. \frac{e^{jkz \cos \theta}}{jk \cos \theta} \right|_{-L/2}^{+L/2} \\
 &= \frac{\hat{I}_0 \eta}{4\pi r} \tan \theta e^{-jkr} \left[ 2j \sin \left( \frac{kL}{2} \cos \theta \right) \right] \quad (3)
 \end{aligned}$$

The time-average power density is then

$$\langle S_r \rangle = \frac{1}{2\eta} |\hat{E}_\theta|^2 = \frac{|\hat{E}_0|^2 \tan^2 \theta \sin^2 [(kL/2) \cos \theta]}{2\eta(kr)^2(kL/2)^2} \quad (4)$$

where

$$\hat{E}_0 = \frac{\hat{I}_0 L \eta k^2}{4\pi} \quad (5)$$

This power density is plotted versus angle  $\theta$  in Figure 9-12 for various lengths  $L$ . The principal maximum always appears at  $\theta = \pi/2$ , becoming sharper as  $L$  increases. For  $L > \lambda$ , zero power density occurs at angles

$$\cos \theta = \frac{2n\pi}{kL} = \frac{n\lambda}{L}, \quad n = 1, 2, \dots \quad (6)$$

Secondary maxima then occur at nearby angles but at much smaller amplitudes compared to the main lobe at  $\theta = \pi/2$ .

### 9-4-3 Radiation Resistance

The total time-average radiated power is obtained by integrating (4) over all angles:

$$\begin{aligned} \langle P \rangle &= \int_{\phi=0}^{2\pi} \int_{\theta=0}^{\pi} \langle S_r \rangle r^2 \sin \theta \, d\theta \, d\phi \\ &= \frac{|\hat{E}_0|^2 \pi}{k^2 \eta (kL/2)^2} \int_{\theta=0}^{\pi} \frac{\sin^3 \theta}{\cos^2 \theta} \sin^2 \left( \frac{kL}{2} \cos \theta \right) d\theta \end{aligned} \quad (7)$$

If we introduce the change of variable,

$$v = \frac{kL}{2} \cos \theta, \quad dv = -\frac{kL}{2} \sin \theta \, d\theta \quad (8)$$

the integral of (7) becomes

$$\langle P \rangle = \frac{|\hat{E}_0|^2 \pi}{k^2 \eta (kL/2)^2} \int_{+kL/2}^{-kL/2} \left( \frac{2}{kL} \sin^2 v \, dv - \frac{kL}{2} \frac{\sin^2 v}{v^2} \right) dv \quad (9)$$

The first term is easily integrable as

$$\int \sin^2 v \, dv = \frac{1}{2}v - \frac{1}{4} \sin 2v \quad (10)$$

The second integral results in a new tabulated function  $Si(x)$  called the sine integral, defined as:

$$Si(x) = \int_0^x \frac{\sin t}{t} dt \quad (11)$$

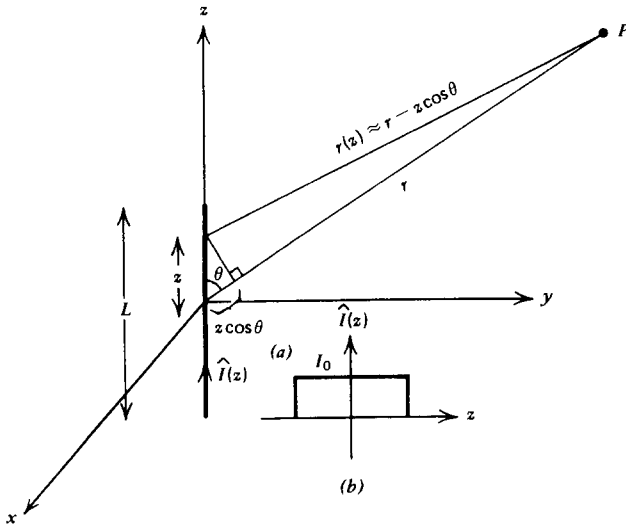


Figure 9-11 (a) For a long dipole antenna, each incremental current element at coordinate  $z$  is at a slightly different distance to any field point  $P$ . (b) The simplest case study has the current uniformly distributed over the length of the dipole.

which is plotted in Figure 9-13. Then the second integral in (9) can be expanded and integrated by parts:

$$\begin{aligned}
 \int \frac{\sin^2 v}{v^2} dv &= \int \frac{(1 - \cos 2v)}{2v^2} dv \\
 &= -\frac{1}{2v} - \int \cos 2v \frac{dv}{2v^2} \\
 &= -\frac{1}{2v} + \frac{\cos 2v}{2v} + \int \frac{\sin 2v d(2v)}{2v} \\
 &= -\frac{1}{2v} + \frac{\cos 2v}{2v} + \text{Si}(2v) \quad (12)
 \end{aligned}$$

Then evaluating the integrals of (10) and (12) in (9) at the upper and lower limits yields the time-average power as:

$$\langle P \rangle = \frac{|\hat{E}_0|^2 \pi}{k^2 \eta (kL/2)^2} \left( \frac{\sin kL}{kL} + \cos kL - 2 + kL \text{Si}(kL) \right) \quad (13)$$

where we used the fact that the sine integral is an odd function  $\text{Si}(x) = -\text{Si}(-x)$ .

Using (5), the radiation resistance is then

$$R = \frac{2\langle P \rangle}{|\hat{I}_0|^2} = \frac{\eta}{2\pi} \left( \frac{\sin kL}{kL} + \cos kL - 2 + kL \text{Si}(kL) \right) \quad (14)$$

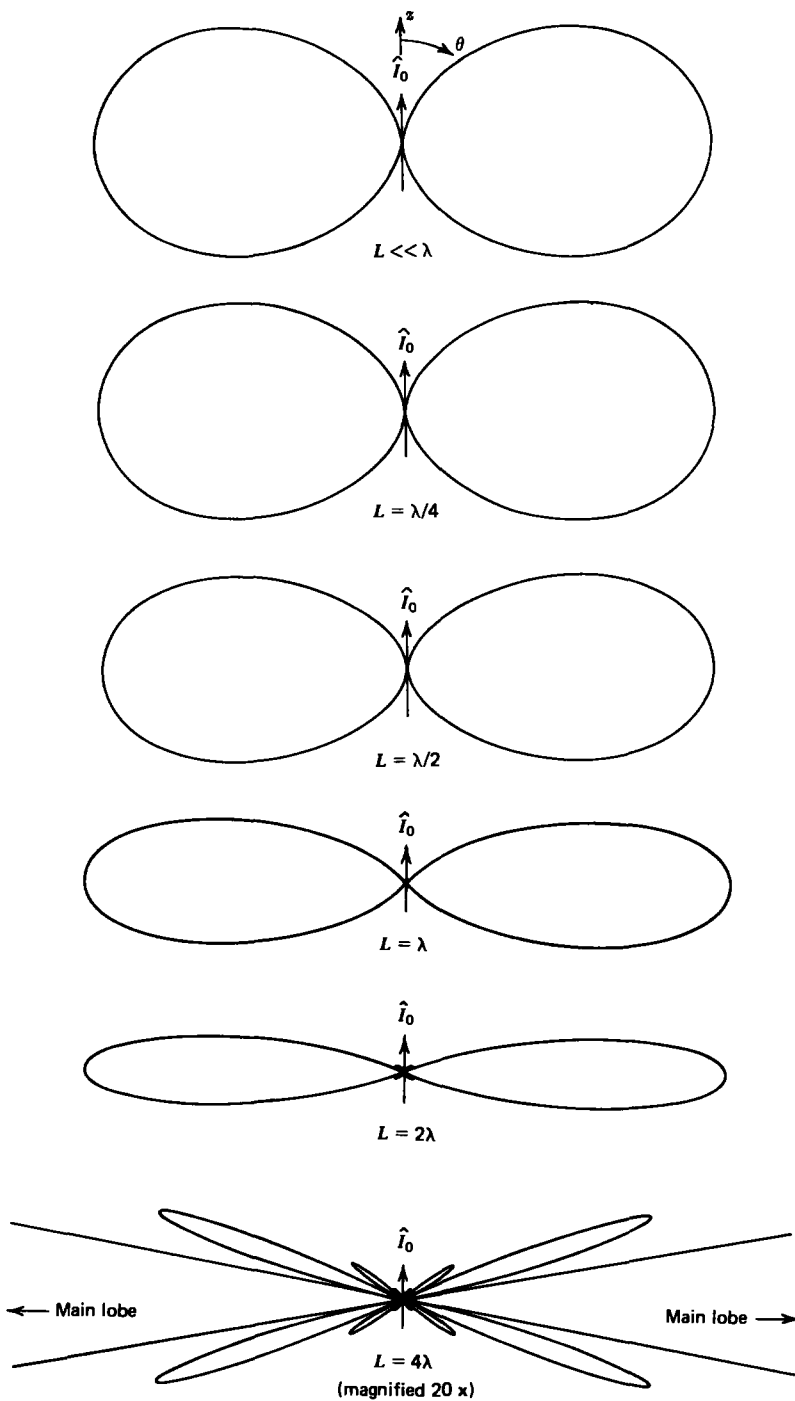


Figure 9-12 The radiation pattern for a long dipole for various values of its length.

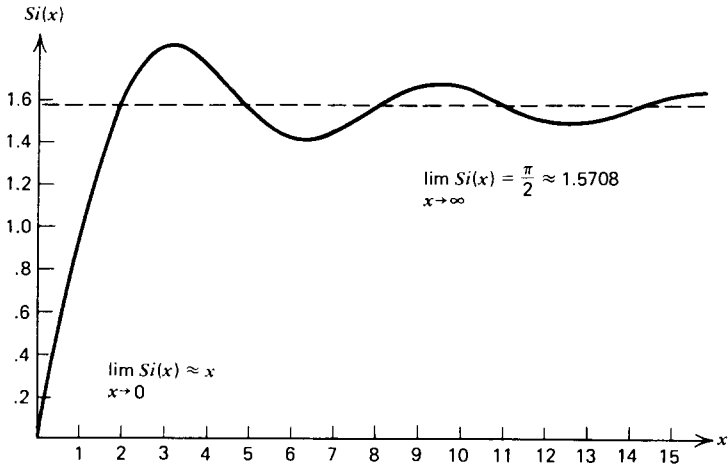


Figure 9-13 The sine integral  $Si(x)$  increases linearly for small arguments and approaches  $\pi/2$  for large arguments oscillating about this value for intermediate arguments.

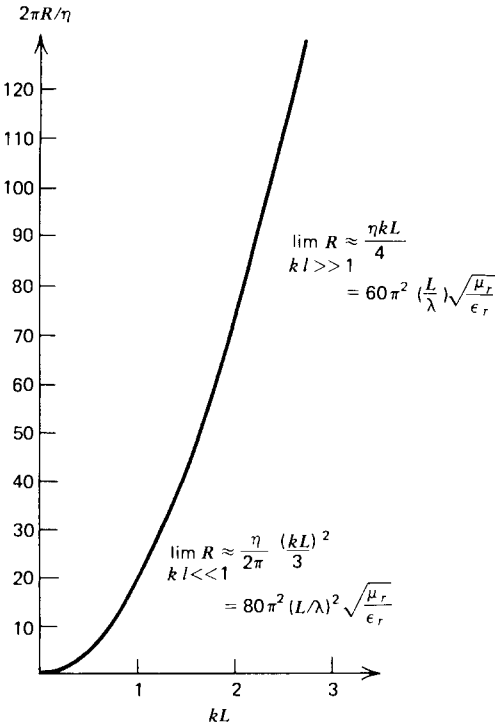


Figure 9-14 The radiation resistance for a dipole antenna carrying a uniformly distributed current increases with the square of its length when it is short ( $L/\lambda \ll 1$ ) and only linearly with its length when it is long ( $L/\lambda \gg 1$ ). For short lengths, the radiation resistance approximates that of a point dipole.

which is plotted versus  $kL$  in Fig. 9-14. This result can be checked in the limit as  $L$  becomes very small ( $kL \ll 1$ ) since the radiation resistance should approach that of a point dipole given in Section 9-2-5. In this short dipole limit the bracketed terms in (14) are

$$\lim_{kL \ll 1} \left\{ \begin{array}{l} \frac{\sin kL}{kL} \approx 1 - \frac{(kL)^2}{6} \\ \cos kL \approx 1 - \frac{(kL)^2}{2} \\ kL \text{Si}(kL) \approx (kL)^2 \end{array} \right. \quad (15)$$

so that (14) reduces to

$$\lim_{kL \ll 1} R \approx \frac{\eta}{2\pi} \frac{(kL)^2}{3} = \frac{2\pi\eta}{3} \left(\frac{L}{\lambda}\right)^2 = 80\pi^2 \left(\frac{L}{\lambda}\right)^2 \sqrt{\frac{\mu_r}{\epsilon_r}} \quad (16)$$

which agrees with the results in Section 9-2-5. Note that for large dipoles ( $kL \gg 1$ ), the sine integral term dominates with  $\text{Si}(kL)$  approaching a constant value of  $\pi/2$  so that

$$\lim_{kL \gg 1} R \approx \frac{\eta kL}{4} = 60 \sqrt{\frac{\mu_r}{\epsilon_r}} \pi^2 \frac{L}{\lambda} \quad (17)$$

## PROBLEMS

---

### Section 9-1

1. We wish to find the properties of waves propagating within a linear dielectric medium that also has an Ohmic conductivity  $\sigma$ .

- (a) What are Maxwell's equations in this medium?
- (b) Defining vector and scalar potentials, what gauge condition decouples these potentials?
- (c) A point charge at  $r = 0$  varies sinusoidally with time as  $Q(t) = \text{Re}(\hat{Q} e^{j\omega t})$ . What is the scalar potential?
- (d) Repeat (a)–(c) for waves in a plasma medium with constitutive law

$$\frac{\partial \mathbf{J}_f}{\partial t} = \omega_p^2 \epsilon \mathbf{E}$$

2. An infinite current sheet at  $z = 0$  varies as  $\text{Re}[K_0 e^{j(\omega t - k_x x)} \mathbf{i}_x]$ .

- (a) Find the vector and scalar potentials.
- (b) What are the electric and magnetic fields?

(c) Repeat (a) and (b) if the current is uniformly distributed over a planar slab of thickness  $2a$ :

$$\mathbf{J}_f = \begin{cases} J_0 e^{j(\omega t - k_x x)} \mathbf{i}_x, & -a < z < a \\ 0, & |z| > a \end{cases}$$

3. A sphere of radius  $R$  has a uniform surface charge distribution  $\sigma_f = \text{Re}(\hat{\sigma}_0 e^{j\omega t})$  where the time varying surface charge is due to a purely radial conduction current.

(a) Find the scalar and vector potentials, inside and outside the sphere. (**Hint:**  $r_{QP}^2 = r^2 + R^2 - 2rR \cos \theta$ ;  $r_{QP} dr_{QP} = rR \sin \theta d\theta$ .)

(b) What are the electric and magnetic fields everywhere?

### Section 9.2

4. Find the effective lengths, radiation resistances and line charge distributions for each of the following current distributions valid for  $|z| < dl/2$  on a point electric dipole with short length  $dl$ :

(a)  $\hat{I}(z) = I_0 \cos \alpha z$

(b)  $\hat{I}(z) = I_0 e^{-\alpha|z|}$

(c)  $\hat{I}(z) = I_0 \cosh \alpha z$

5. What is the time-average power density, total time-average power, and radiation resistance of a point magnetic dipole?

6. A plane wave electric field  $\text{Re}(\mathbf{E}_0 e^{j\omega t})$  is incident upon a perfectly conducting spherical particle of radius  $R$  that is much smaller than the wavelength.

(a) What is the induced dipole moment? (**Hint:** See Section 4-4-3.)

(b) If the small particle is, instead, a pure lossless dielectric with permittivity  $\epsilon$ , what is the induced dipole moment?

(c) For both of these cases, what is the time-average scattered power?

7. A plane wave magnetic field  $\text{Re}(\mathbf{H}_0 e^{j\omega t})$  is incident upon a perfectly conducting particle that is much smaller than the wavelength.

(a) What is the induced magnetic dipole moment? (**Hint:** See Section 5-7-2ii and 5-5-1.)

(b) What are the re-radiated electric and magnetic fields?

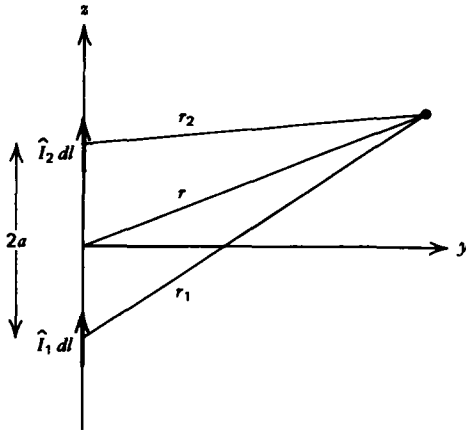
(c) What is the time-average scattered power? How does it vary with frequency?

8. (a) For the magnetic dipole, how are the magnetic field lines related to the vector potential  $\mathbf{A}$ ?

(b) What is the equation of these field lines?

### Section 9.3

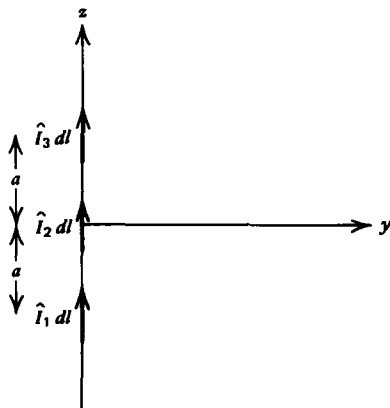
9. Two aligned dipoles  $\hat{I}_1 dl$  and  $\hat{I}_2 dl$  are placed along the  $z$  axis a distance  $2a$  apart. The dipoles have the same length



while the currents have equal magnitudes but phase difference  $\chi$ .

- (a) What are the far electric and magnetic fields?
- (b) What is the time-average power density?
- (c) At what angles is the power density zero or maximum?
- (d) For  $2a = \lambda/2$ , what values of  $\chi$  give a broadside or end-fire array?
- (e) Repeat (a)–(c) for  $2N + 1$  equally spaced aligned dipoles along the  $z$  axis with incremental phase difference  $\chi_0$ .

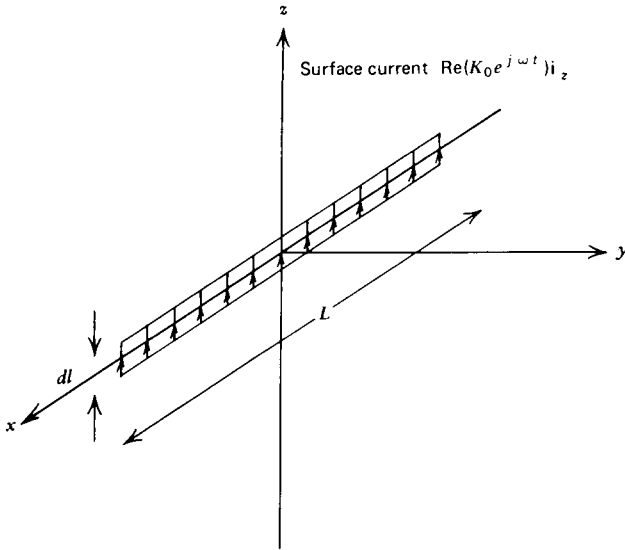
10. Three dipoles of equal length  $dl$  are placed along the  $z$  axis.



- (a) Find the far electric and magnetic fields.
- (b) What is the time average power density?
- (c) For each of the following cases find the angles where the power density is zero or maximum.

- (i)  $\hat{I}_1 = \hat{I}_3 = I_0, \hat{I}_2 = 2I_0$
- (ii)  $\hat{I}_1 = \hat{I}_3 = I_0, \hat{I}_2 = -2I_0$
- (iii)  $\hat{I}_1 = -\hat{I}_3 = I_0, \hat{I}_2 = 2jI_0$

11. Many closely spaced point dipoles of length  $dl$  placed along the  $x$  axis driven in phase approximate a  $z$ -directed current sheet  $\text{Re}(K_0 e^{j\omega t} \mathbf{i}_z)$  of length  $L$ .



- (a) Find the far fields from this current sheet.
- (b) At what angles is the power density minimum or maximum?

Section 9.4

12. Find the far fields and time-average power density for each of the following current distributions on a long dipole:

$$(a) \hat{I}(z) = \begin{cases} I_0(1 - 2z/L), & 0 < z < L/2 \\ I_0(1 + 2z/L), & -L/2 < z < 0 \end{cases}$$

**Hint:**

$$\int z e^{az} dz = \frac{e^{az}}{a^2}(az - 1)$$

$$(b) \hat{I}(z) = I_0 \cos \pi z/L, \quad -L/2 < z < L/2$$

**Hint:**

$$\int e^{az} \cos pz dz = e^{az} \frac{(a \cos pz + p \sin pz)}{(a^2 + p^2)}$$

- (c) For these cases find the radiation resistance when  $kL \ll 1$ .

## SOLUTIONS TO SELECTED PROBLEMS

## Chapter 1

1. Area =  $\pi a^2$
3. (a)  $\mathbf{A} + \mathbf{B} = 6\mathbf{i}_x - 2\mathbf{i}_y - 6\mathbf{i}_z$   
 (b)  $\mathbf{A} \cdot \mathbf{B} = 6$   
 (c)  $\mathbf{A} \times \mathbf{B} = -14\mathbf{i}_x + 12\mathbf{i}_y - 18\mathbf{i}_z$
5. (b)  $\mathbf{B}_{\parallel} = 2(-\mathbf{i}_x + 2\mathbf{i}_y - \mathbf{i}_z)$ ,  $\mathbf{B}_{\perp} = 5\mathbf{i}_x + \mathbf{i}_y - 3\mathbf{i}_z$
7. (a)  $\mathbf{A} \cdot \mathbf{B} = -75$   
 (b)  $\mathbf{A} \times \mathbf{B} = -100\mathbf{i}_z$   
 (c)  $\theta = 126.87^\circ$
12. (a)  $\nabla f = (az + 3bx^2y)\mathbf{i}_x + bx^3\mathbf{i}_y + ax\mathbf{i}_z$
14. (a)  $\nabla \cdot \mathbf{A} = 3$
17. (b)  $\Phi = \frac{1}{2}abc$
18. (a)  $\nabla \times \mathbf{A} = (x - y^2)\mathbf{i}_x - y\mathbf{i}_y - x^2\mathbf{i}_z$
23. (b)  $\nabla f = \frac{1}{h_u} \frac{\partial f}{\partial u} \mathbf{i}_u + \frac{1}{h_v} \frac{\partial f}{\partial v} \mathbf{i}_v + \frac{1}{h_w} \frac{\partial f}{\partial w} \mathbf{i}_w$   
 (c)  $dV = h_u h_v h_w du dv dw$   
 (d)  $\nabla \cdot \mathbf{A} = \frac{1}{h_u h_v h_w} \left[ \frac{\partial}{\partial u} (h_v h_w A_u) + \frac{\partial}{\partial v} (h_u h_w A_v) + \frac{\partial}{\partial w} (h_u h_v A_w) \right]$   
 $(\nabla \times \mathbf{A})_u = \frac{1}{h_v h_w} \left[ \frac{\partial (h_w A_w)}{\partial v} - \frac{\partial (h_v A_v)}{\partial w} \right]$
25. (a)  $r_{QP} = \sqrt{30}$ , (b)  $\mathbf{i}_{QP} = \frac{\mathbf{r}_{QP}}{r_{QP}} = \frac{\mathbf{i}_x - 5\mathbf{i}_y + 2\mathbf{i}_z}{\sqrt{30}}$ ,  
 (c)  $\mathbf{n} = \frac{5\mathbf{i}_x + \mathbf{i}_y}{\sqrt{26}}$

## Chapter 2

3.  $E_0 = \frac{4}{3} \frac{\pi R^3 \rho_m g}{q}$
4.  $Q_2 = \frac{2\pi\epsilon_0 d^3 Mg}{Q_1 \sqrt{l^2 - \left(\frac{d}{2}\right)^2}}$
5. (a)  $\omega = \left[ \frac{Q_1 Q_2}{4\pi\epsilon_0 R^3 m} \right]^{1/2}$

$$7. (a) m = \frac{m_1 m_2}{m_1 + m_2},$$

$$(b) v = \pm \sqrt{\frac{-q_1 q_2}{2\pi\epsilon_0 m} \left( \frac{1}{r} - \frac{1}{r_0} \right)},$$

$$(d) t = \frac{\pi}{2} r_0^{3/2} \left[ \frac{2\pi m \epsilon_0}{-q_1 q_2} \right]^{1/2}$$

$$8. h = \frac{qE_0 L^2}{2mv_0^2}$$

$$10. (b) q = \frac{6\sqrt{3}}{7^{3/2}} Q$$

$$12. (a) q = 2\lambda_0 a, \quad (b) q = \frac{4}{3}\pi\rho_0 a^3, \quad (c) q = 2\sigma_0 ab\pi$$

$$15. \theta = \tan^{-1} \left[ \frac{Q\sigma_0}{2\epsilon_0 Mg} \right]$$

$$16. (a) E_r = \frac{\lambda L}{2\pi\epsilon_0 r \sqrt{L^2 + r^2}},$$

$$(b) E_x = \frac{\sigma_0}{2\pi\epsilon_0} \left[ \sin^{-1} \left( \frac{L^2 - x^2}{L^2 + x^2} \right) + \frac{\pi}{2} \right]; \quad x > 0$$

$$18. (a) E_y = \frac{-\lambda_0 a^2}{\pi \epsilon_0 [z^2 + a^2]^{3/2}}$$

$$(b) E_y = \frac{-\sigma_0}{\pi\epsilon_0} \left\{ \frac{-a}{\sqrt{z^2 + a^2}} + \ln \left[ \frac{a + \sqrt{z^2 + a^2}}{|z|} \right] \right\}$$

$$20. (a) E_y = -\frac{\lambda_0 a^2}{\pi\epsilon_0 (a^2 + z^2)^{3/2}}$$

$$21. E_y = \frac{\lambda_0 z^2}{2\pi\epsilon_0 (a^2 + z^2)^{3/2}}$$

$$22. (a) Q_T = 4\pi\epsilon_0 AR^4$$

$$23. (c) E_x = \begin{cases} \frac{\rho_0}{2\epsilon_0 d} (x^2 - d^2) & |x| < d \\ 0 & |x| > d \end{cases}$$

$$25. (c) E_r = \begin{cases} \frac{\rho_0 r^2}{3\epsilon_0 a} & r < a \\ \frac{\rho_0 a^2}{3\epsilon_0 r} & r > a \end{cases}$$

$$26. \mathbf{E} = \frac{\rho_0 d}{2\epsilon_0} \mathbf{i}_x$$

$$27. W = -\frac{\lambda\sigma_0 l^2}{4\epsilon_0}$$

$$28. (a) v_0 \geq \sqrt{\frac{qQ}{2\pi\epsilon_0 Rm}}, \quad (b) r = 4R$$

$$29. (a) \mathbf{E} = -2Ax\mathbf{i}_x, \rho_f = -2A\epsilon_0$$

$$31. (a) \Delta v = \frac{\sigma_0 a}{\epsilon_0}$$

$$32. (a) dq = -\frac{Q}{R} dz'$$

$$33. (c) V \approx \frac{q_0 a}{4\pi\epsilon_0 r^2} \cos \theta, \quad (d) r = r_0 \sin^2 \theta$$

$$34. (d) q_c = -\frac{qV_p}{V_c}$$

$$36. (a) E_y = -\frac{\sigma_0}{2\pi\epsilon_0} \ln\left(1 - \frac{d}{y}\right)$$

$$38. (a) x_0 = \sqrt{\frac{q}{16\pi\epsilon_0 E_0}}, \quad (b) v_0 > \frac{1}{2} \sqrt{\frac{q}{m} \left[\frac{qE_0}{\pi\epsilon_0}\right]^{1/4}},$$

$$(c) W = \frac{q^2}{16\pi\epsilon_0 d}$$

$$43. (e) \lambda = \pm \sqrt{\frac{R_1}{R_2}}, \alpha = \pm \frac{R_1}{R_2}$$

$$44. (g) q_T = -4\pi\epsilon_0 R^2 \frac{\pi^2}{6}$$

### Chapter 3

$$2. (a) p_z = \lambda_0 L^2, \quad (e) p_z = QR$$

$$4. (a) \rho_0 = \frac{3Q}{\pi R_0^3}$$

$$7. (a) \mathbf{d} = \frac{4\pi\epsilon_0 R_0^3 \mathbf{E}_0}{Q}$$

$$8. (b) \frac{Q}{L^2} = 2\pi\epsilon_0 E_0$$

$$10. (a) \mathbf{p}_{\text{ind}} = \mathbf{p} \frac{R^3}{D^3}$$

$$12. (a) V(x) = \frac{V_0}{2} \frac{\sinh x/l_d}{\sinh l/l_d}$$

$$15. (b) Q = \frac{m\omega R A \sigma}{q}$$

$$17. (a) D_r = \frac{\lambda}{2\pi r}$$

$$19. (a) \lambda' = -\lambda'' = \frac{\lambda(\epsilon_2 - \epsilon_1)}{\epsilon_1 + \epsilon_2}, \lambda''' = \frac{2\epsilon_2\lambda}{\epsilon_1 + \epsilon_2}$$

$$23. (a) E_r = \begin{cases} -\frac{P_0 r}{\epsilon_0 R} & r < R \\ 0 & r > R \end{cases}$$

$$26. (a) R = \frac{s \ln \frac{\sigma_2}{\sigma_1}}{lD(\sigma_2 - \sigma_1)}$$

$$31. C = \frac{2\pi l(\epsilon_2 a - \epsilon_1 b)}{(b-a) \ln \frac{\epsilon_2 a}{\epsilon_1 b}}$$

$$33. \sigma_f(r=a_1) = \frac{\rho_0 a_0^2}{3a_1} (1 - e^{-4\tau}); \tau = \epsilon/\sigma$$

$$35. \rho_f = \rho_0 e^{-\sigma r^3/(3\epsilon A)}$$

$$38. (a) v(z) = -\frac{V_0 \sinh \sqrt{2RG}(z-l)}{\sinh \sqrt{2RG}l}$$

$$41. (b) \frac{\epsilon\mu}{2}[E^2(l) - E^2(0)] + \epsilon \frac{dv}{dt} = J(t)l$$

$$(c) E(l) = \frac{V_0/l}{1 - \frac{\mu t V_0}{2l^2}}, \quad (f) \tau = \frac{2l^2}{\mu V_0} (1 - e^{-1/2})$$

$$42. (c) E_i^2 = \left( \frac{V_0}{R_0 - R_i} \right)^2 = \frac{I}{2\pi\epsilon\mu l}$$

$$43. (a) W = -\frac{1}{2}\mathbf{p} \cdot \mathbf{E}$$

$$44. W = \frac{p^2}{12\pi\epsilon_0 R^3}$$

$$47. (a) W = \frac{-Q^2}{8\pi\epsilon_0 R}$$

$$48. (a) W_{\text{init}} = \frac{1}{2}CV_0^2, \quad (b) W_{\text{final}} = \frac{1}{4}CV_0^2$$

$$49. (b) W = -pE(\cos \theta - 1)$$

$$50. h = \frac{1}{2}(\epsilon - \epsilon_0) \frac{V_0^2}{\rho_m g s^2}$$

$$52. (b) f_y = \frac{1}{2} \frac{\epsilon_0 A}{(s+d)^2} \left[ V_0 + \frac{P_0 d}{\epsilon_0} \right]^2$$

$$54. (b) f_z = \frac{\pi V_0^2}{\ln \frac{b}{a}} (\epsilon - \epsilon_0)$$

$$55. f_x = -\frac{1}{2} \frac{\epsilon_0 d}{s} V_0^2$$

$$56. (c) T = \frac{1}{2} v^2 \frac{dC}{d\theta} = \frac{-NV_0^2 R^2 \epsilon_0}{s}$$

$$57. (a) v(t) = \frac{\sigma_f U \omega t}{4\pi \epsilon_0 R}$$

$$58. (a) \rho_f = \rho_0 e^{-\sigma_f / \epsilon U}$$

$$59. (a) nC_i > \frac{1}{R} + \frac{2}{R_L}, \quad (c) \frac{nC_i}{2} > \frac{1}{R}, \quad \omega_0 = \frac{\sqrt{3}}{2} \frac{nC_i}{C}$$

#### Chapter 4

$$2. (a) V = \begin{cases} \frac{\sigma_0}{2\epsilon a} \cos ay e^{-ax} & x > 0 \\ \frac{\sigma_0}{2\epsilon a} \cos ay e^{ax} & x < 0 \end{cases}$$

$$4. (a) V = \frac{4V_1}{\pi} \sum_{\substack{n=1 \\ \text{odd}}}^{\infty} \frac{\sin \frac{n\pi y}{d} \sinh \frac{n\pi(l-x)}{d}}{n \sinh \frac{n\pi l}{d}}$$

$$7. (a) V_p = \frac{\rho_0}{\epsilon_0 a^2} \sin ax$$

$$12. V(r, \phi) = \begin{cases} \left[ \frac{P_2 - P_1}{2\epsilon_0} - E_0 \right] r \cos \phi & 0 \leq r \leq a \\ \left[ -E_0 r + \frac{(P_2 - P_1)a^2}{2\epsilon_0 r} \right] \cos \phi & r > a \end{cases}$$

$$13. (a) \mathbf{E} = \left[ E_0 \left( 1 + \frac{a^2}{r^2} \right) \cos \phi + \frac{\lambda(t)}{2\pi \epsilon r} \right] \mathbf{i}_r - E_0 \left( 1 - \frac{a^2}{r^2} \right) \sin \phi \mathbf{i}_\phi$$

$$(b) \cos \phi < -\frac{\lambda(t)}{4\pi \epsilon a E_0}, \quad (c) \lambda_{\max} = 4\pi \epsilon a E_0$$

$$15. (a) V(r, z) = \begin{cases} \frac{V_0 z}{l} \ln \frac{r}{a} & a \leq r \leq b \\ \frac{V_0 z}{l} & b \leq r \leq c \end{cases}$$

$$17. (b) E_0 \geq \sqrt{\frac{8\rho_m g R}{27\epsilon}}$$

$$22. V(2, 2) = V(3, 2) = V(2, 3) = V(3, 3) = -4.$$

$$23. (a) V(2, 2) = -1.0000, V(3, 2) = -.5000, V(2, 3) = -.5000, V(3, 3) = .0000$$

$$(b) V(2, 2) = 1.2500, V(3, 2) = -.2500, V(2, 3) = .2500, V(3, 3) = -1.2500$$

### Chapter 5

$$2. (b) B_0^2 > \frac{2mV_0}{es^2}, \quad (e) B_0^2 > \frac{8b^2 m V_0}{e(b^2 - a^2)^2}$$

$$3. B_0 = \frac{-mg}{qv_0}$$

$$4. (d) \frac{e}{m} = \frac{E_y}{RB_0^2}$$

$$8. (c) \mathbf{J} = \sigma(\mathbf{E} + \mathbf{v} \times \mathbf{B})$$

$$10. (a) B_z = \frac{2\mu_0 I (a^2 + b^2)^{1/2}}{\pi ab}, \quad (c) B_z = \frac{n\mu_0 I}{2\pi a} \tan \frac{\pi}{n}$$

$$12. (a) B_z = \frac{\mu_0 K_0 \pi}{4}$$

$$13. (a) B_\phi = \frac{\mu_0 I L}{2\pi r \sqrt{L^2 + r^2}}$$

$$15. (b) B_y = \frac{\mu_0 J_0 d}{2}$$

$$17. (b) B_x = \begin{cases} -\frac{\mu_0 J_0}{2a} (y^2 - a^2) & |y| < a \\ 0 & |y| > a \end{cases}$$

$$18. (d) y = \frac{y_0}{2} \text{ at } x = -\infty$$

$$21. (a) m_z = \frac{1}{2} q \omega a^2$$

$$23. \omega_0 = \sqrt{\gamma B_0}$$

$$27. (a) I' = \frac{(\mu_2 - \mu_1)}{(\mu_1 + \mu_2)} I, I'' = \frac{2\mu_1 I}{\mu_1 + \mu_2}$$

$$34. (a) \mathbf{H} = \begin{cases} \frac{-M_0 i_x}{2} \\ \frac{M_0 a^2}{2r^2} [\cos \phi i_r + \sin \phi i_\phi] \end{cases}$$

$$35. (a) H_z(x) = -\frac{I}{Dd}(x-d), \quad (b) f_x = \frac{1}{2} \mu_0 \frac{I^2 s}{D}$$

$$36. (a) f_x = \frac{1}{2}(\mu - \mu_0) H_0^2 D s, \quad (b) f_x = \mu_0 M_0 D s [H_0 + M_0]$$

### Chapter 6

$$1. (a) M = \mu_0 [D - \sqrt{D^2 - a^2}], \quad (e) f_r = \mu_0 I i \left[ \frac{D}{\sqrt{D^2 - a^2}} - 1 \right]$$

$$3. (d) v(t) = v_0 \left[ \frac{\alpha}{2\beta} \sin \beta t + \cos \beta t \right] e^{-\alpha t/2}; \quad \beta = \sqrt{\omega_0^2 - \left(\frac{\alpha}{2}\right)^2}$$

$$i(t) = \frac{m v_0 \omega_0^2}{B_0 b \beta} \sin \beta t e^{-\alpha t/2}$$

$$(e) v_0 > \frac{B_0 b s}{\sqrt{mL}}$$

$$4. (a) M = \frac{\mu_0 N s}{2\pi} \ln \frac{a}{b}, \quad M = \mu_0 N [R - \sqrt{R^2 - a^2}]$$

$$7. (c) f_z = \frac{3\mu_0 (I d s)^2}{32\pi d^4}$$

$$8. (a) H_z = K(t), \quad (b) K(t) = K_0 \left( \frac{x_0}{x_0 - Vt} \right)^{(1-1/R_m)}$$

$$9. (a) i = \frac{r \sigma d}{2} \frac{dB}{dt} dr, \quad (c) P = \frac{\pi \sigma d a^4}{8} \left( \frac{dB}{dt} \right)^2$$

$$10. L = \mu_0 N^2 [b - \sqrt{b^2 - a^2}]$$

$$14. (a) \frac{v_2}{v_1} = \frac{N_2}{2N_1}, \quad \frac{i_2}{i_1} = \frac{2N_1}{N_2}$$

$$16. (a) V_{oc} = J_x B_z d \frac{(\mu_+^2 n_+ - \mu_-^2 n_-)}{q(\mu_+ n_+ + \mu_- n_-)^2}$$

$$17. (b), (c) \text{ EMF} = -\frac{\mu_0 V_0 I}{2\pi} \ln \frac{R_2}{R_1},$$

$$(d) \text{ EMF} = -\frac{(\mu - \mu_0) I V_0}{2\pi} \ln \frac{R_2}{R_1}$$

$$18. (a) \mathbf{H} = 0, \mathbf{B} = \mu_0 M_0 \mathbf{i}_z, \quad (b) v_{oc} = \frac{\omega B_z}{2} (b^2 - a^2)$$

$$20. (b) V > \frac{1}{\mu_0 \sigma N D}$$

$$21. (a) \omega > \frac{(R_r + R_f) G}{C}$$

$$(b) C_{\text{crit}} = \frac{4L_f}{[R_r + R_f - G\omega]^2}; \quad C > C_{\text{crit}}(dc), \quad C < C_{\text{crit}}(ac)$$

$$(c) \omega_0 \left[ \frac{1}{L_f C} - \left[ \frac{R_r + R_f - G\omega}{2L_f} \right]^2 \right]^{1/2}$$

$$22. (b) H_z(x, t) = \sum_{\substack{n=1 \\ n \text{ odd}}}^{\infty} \frac{2I_0}{n\pi D} \sin \frac{n\pi x}{d} e^{-\alpha_n t}$$

$$23. (c) H_y(x, t) = H_0 - \sum_{\substack{n=1 \\ n \text{ odd}}}^{\infty} \frac{4H_0}{n\pi} \sin \frac{n\pi x}{d} e^{-\alpha_n t}$$

$$25. (b) H_z(y, t) = -K_0 + \sum_{n=0}^{\infty} \frac{(-1)^n 4K_0}{\pi(2n+1)} \cos \left[ \frac{(2n+1)\pi y}{2D} \right] e^{-\alpha_n t}$$

$$(d) \hat{H}_z(y) = K_0 \left[ \frac{e^{(1+j)y/\delta} + e^{-(1+j)y/\delta}}{e^{(1+j)D/\delta} + e^{-(1+j)D/\delta}} \right]$$

$$26. (a) H_z(x) = \frac{K_0}{1 - e^{-R_m}} [2e^{R_m x/l} - (1 + e^{R_m})]$$

$$27. (a) \hat{H}_z(x) = K_0 e^{-\beta x} e^{R_m x/2l}; \quad \beta = \frac{R_m}{2l} \sqrt{1 + \frac{2j l^2}{R_m^2 \delta^2}}$$

$$28. (a)$$

$$\hat{\mathbf{H}}(\mathbf{x}) = \begin{cases} \frac{K_0 \left\{ \left( 1 - \frac{\mu}{\mu_0} \frac{k}{\gamma} \right) e^{k(x-s)} (\mathbf{i}_z + j\mathbf{i}_x) + \left( 1 + \frac{\mu}{\mu_0} \frac{k}{\gamma} \right) e^{-k(x-s)} (\mathbf{i}_z - j\mathbf{i}_x) \right\}}{\left[ 1 - \frac{\mu}{\mu_0} \frac{k}{\gamma} \right] e^{-ks} + \left[ 1 + \frac{\mu}{\mu_0} \frac{k}{\gamma} \right] e^{ks}} & 0 < x < s \\ \frac{2K_0 e^{-\gamma(x-s)} \left[ \mathbf{i}_z - \frac{j k}{\gamma} \mathbf{i}_x \right]}{\left[ 1 - \frac{\mu}{\mu_0} \frac{k}{\gamma} \right] e^{-ks} + \left[ 1 + \frac{\mu}{\mu_0} \frac{k}{\gamma} \right] e^{ks}} & x > s \end{cases}$$

29. (a)  $H_y = H_0 \frac{\cosh k(x-d/2)}{\cosh kd/2}$
32. (b)  $\hat{H}_\phi(r) = \frac{I_0}{2\pi a} \frac{J_1[(r/\delta)(1-j)]}{J_1[(a/\delta)(1-j)]}$
33. (a)  $T = -L_1 I_0^2 \cos^2 \omega_0 t \sin 2\theta$
34. (c)  $T = M_0 I_1 I_2 \cos \theta$ ,
- (f)  $\theta(t) = \theta_0 \left[ \cos \beta t + \frac{\alpha}{2\beta} \sin \beta t \right] e^{-\alpha t/2}$
35. (a)  $L(x) = \frac{\mu_0 x}{2\pi} \ln \frac{b}{a}$ , (b)  $f_x = \frac{\mu_0 i^2}{4\pi} \ln \frac{b}{a}$
37.  $h = \frac{I^2(\mu - \mu_0) \ln \frac{b}{a}}{4\pi^2 \rho_m g (b^2 - a^2)}$

## Chapter 7

4. (b)  $W = 4[P_s E_c + \mu_0 M_s H_c]$
9. (b)  $\hat{E}_x(z) = \begin{cases} \frac{j\eta_0 J_0 \sin kd e^{-j\eta_0(z+d)}}{\omega\epsilon[\eta_0 \sin kd - j\eta \cos kd]} & z > d \\ -\frac{J_0 \eta \cos kz}{\omega\epsilon[\eta_0 \sin kd - j\eta \cos kd]} & z < -d \\ \frac{J_0 \eta \cos kz}{\omega\epsilon[\eta_0 \sin kd - j\eta \cos kd]} & |z| < d \end{cases}$
10. (b)  $E_x = E_0 e^{j(\omega t \mp \beta z)} e^{\mp(\alpha z/2)}$   $\begin{matrix} z > 0 \\ z < 0 \end{matrix}$ ;  $\beta = \sqrt{\omega^2 \epsilon \mu - \frac{\alpha^2}{4}}$
11. (a)  $t'_1 - t'_2 = \frac{\gamma v}{c_0^2} (z_2 - z_1)$ ,
- (b)  $t'_1 - t'_2 = \gamma(t_1 - t_2)$ , (c)  $z'_2 - z'_1 = \gamma L$
12. (a)  $u'_z = \frac{\dot{u}_z - v}{1 - v u_z/c_0^2}$ ,  $u'_{x,y} = \frac{u_{x,y} \sqrt{1 - (v/c_0)^2}}{1 - v u_z/c_0^2}$
15. (b)  $\epsilon(\omega) = \epsilon_0 \left[ 1 + \frac{\omega_p^2}{\omega_0^2 - \omega^2} \right]$
16. (c)  $k^2 = \frac{\omega^2}{c^2} \left[ 1 - \frac{\omega_p^2}{\omega(\omega \mp \omega_0)} \right]$
20. (a)  $\mathbf{E} = E_0 \left[ \cos \omega \left( t - \frac{z}{c} \right) - \cos \omega \left[ \left( 1 - \frac{2v}{c} \right) \left( t - \frac{z}{c} \right) \right] \right] \mathbf{i}_y$
22.  $\alpha^2 - k^2 = -\omega^2 \epsilon \mu$ ,  $\boldsymbol{\alpha} \cdot \mathbf{k} = \frac{1}{\delta^2}$

$$26. (a) L_1 + L_2 = s_i \sin \theta_i + s_r \sin \theta_r = h_1 \tan \theta_i + h_2 \tan \theta_r$$

$$31. \theta_i \approx 41.7^\circ$$

$$33. (a) \left(\frac{x}{R}\right)^2 > 1 - \frac{(n^2 - 2)^2}{4}; \sqrt{2} \leq n \leq 2$$

$$(b) R' = \frac{\alpha R}{[\sqrt{n^2(1 - \alpha^2)}\sqrt{n^2 - \alpha^2} + \alpha^2]}$$

### Chapter 8

$$2. (c) \hat{v}(z) = -\frac{V_0 \sin \beta(z-l) e^{\alpha z/2}}{\sin \beta l} \quad (\text{Short circuited end})$$

$$4. (c) \omega^2 = \omega_p^2 + k^2 c^2, \quad (d) v(z, t) = -\frac{V_0 \sin kz \cos \omega t}{\sin kl}$$

$$5. (b) k = \frac{1}{\omega \sqrt{LC}}$$

$$14. (a) V_+ = -V_- = \frac{V_0 Z_0}{2R_s}$$

$$16. (b) \tan kl = -XY_0$$

$$21. (c) VSWR = \frac{1 + \sqrt{2}}{\sqrt{2} - 1} \approx 5.83$$

$$22. (b) VSWR = 2$$

$$23. Z_L = 170.08 - 133.29j$$

$$24. (a) l_1 = .137\lambda + \frac{n\lambda}{2}, l_2 = .089\lambda + \frac{m\lambda}{2}$$

$$l_1 = .279\lambda + \frac{n\lambda}{2}, l_2 = .411\lambda + \frac{m\lambda}{2}$$

$$25. (a) l_1 = .166\lambda + \frac{n\lambda}{2}, l_2 = .411\lambda + \frac{m\lambda}{2}$$

$$l_1 = .077\lambda + \frac{n\lambda}{2}, l_2 = .043\lambda + \frac{m\lambda}{2}$$

$$27. (e) \alpha = \frac{2(\pi/a)^2 [b + (a/2)(\omega^2 a^2 / \pi^2 c^2)]}{\omega \mu a b k_x \sigma_w \delta}$$

$$28. (b) = \frac{2\omega \epsilon (b k_x^2 + a k_y^2)}{\sigma_w \delta k_x a b (k_x^2 + k_y^2)}$$

29. (a) TE mode:

electric field:  $\cos k_x x \cos k_y y = \text{const}$

magnetic field:  $\frac{\sin (k_x x)^{(k_y/k_x)^2}}{\sin k_y y} = \text{const}$

$$31. (b) \frac{\omega^2}{c^2} = \left(\frac{m\pi}{a}\right)^2 + \left(\frac{n\pi}{b}\right)^2 + \left(\frac{p\pi}{l}\right)^2,$$

$$32. (a) \omega^2 = \frac{k_x^2}{\epsilon\mu - \epsilon_0\mu_0}$$

### Chapter 9

$$1. (c) \hat{V} = \frac{\hat{Q}}{4\pi\epsilon r} e^{-jr\sqrt{\omega^2/c^2 - j\omega\mu\sigma}}$$

$$4. (a) dl_{\text{eff}} = \frac{2 \sin(\alpha dl/2)}{\alpha}, \quad \hat{\lambda}(z) = \frac{I_0 \alpha}{j\omega} \sin \alpha z$$

$$6. (a) \hat{p}_z = 4\pi\epsilon_0 R^3 \hat{E}_0$$

$$(c) \langle P \rangle = \frac{\omega^4 |\hat{p}_z|^2 \eta}{12\pi c^2}$$

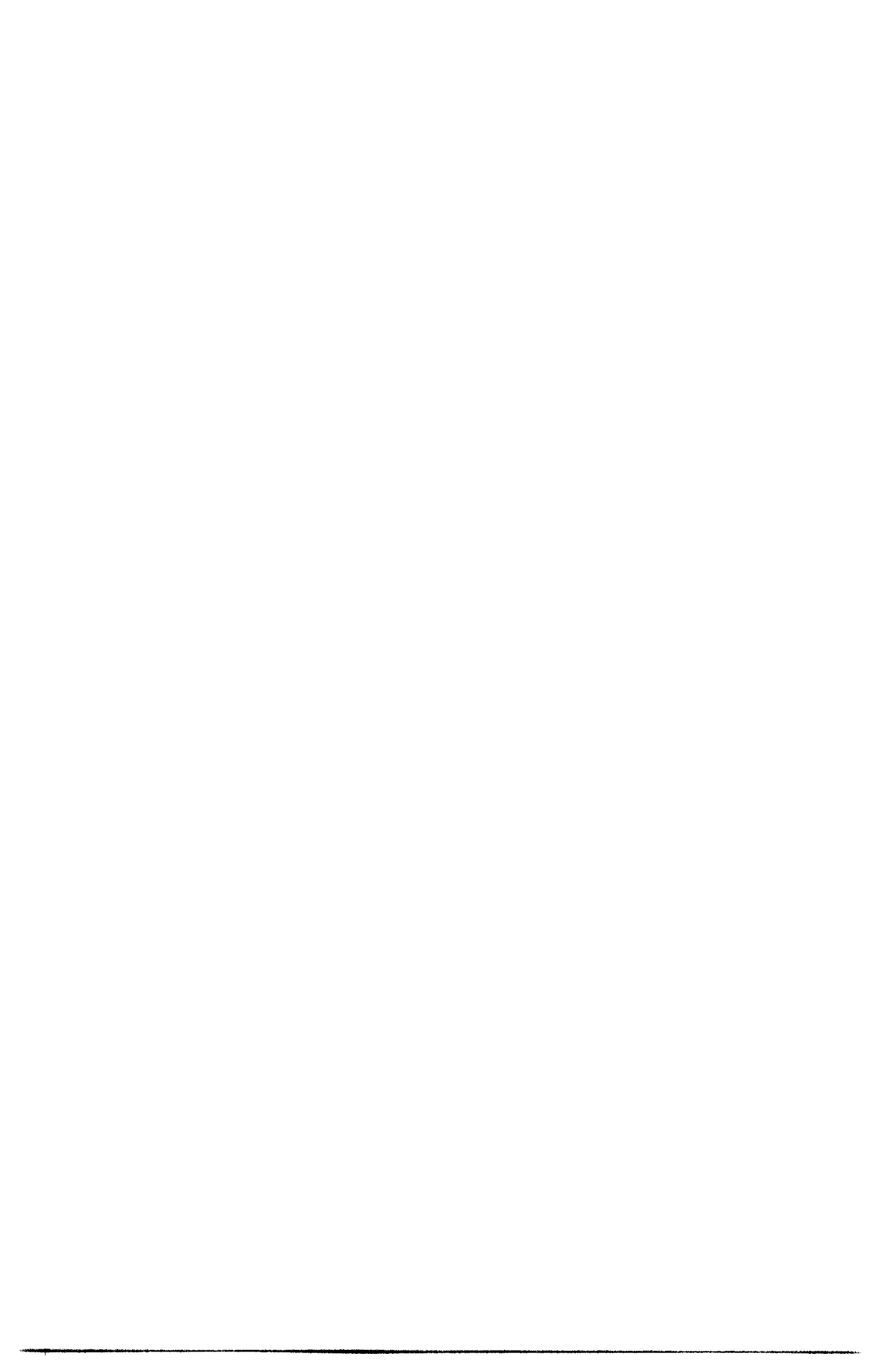
$$7. (a) m_{\text{ind}} = 2\pi H_0 R^3$$

$$8. (b) \sin^2 \theta \left[ \frac{\cos(\omega t - kr)}{kr} - \sin(\omega t - kr) \right] = \text{const}$$

$$9. (a) \hat{E}_\theta \approx \frac{2\hat{E}_0}{jkr} \sin \theta e^{-j(kr - \chi/2)} \left[ \cos \left( ka \cos \theta - \frac{\chi}{2} \right) \right]$$

$$11. \hat{E}_\theta = \frac{2jK_0 dl \eta e^{-jkr}}{4\pi r \cos \phi} \sin \left( \frac{kL}{2} \sin \theta \cos \phi \right)$$

$$12. (a) \hat{E}_\theta = \frac{\eta I_0 \sin \theta e^{-jkr}}{j\pi k r L \cos^2 \theta} \cos \left[ \left( \frac{kL}{2} \cos \theta \right) - 1 \right]$$



## INDEX

- Addition, vector, 9-10  
Admittance, characteristic, 579  
A field, 336. *See also* Vector potential  
Amber, 50  
Ampere, unit, 55  
Ampere's circuital law, 334  
  displacement current correction to, 488  
Ampere's experiments, 322  
Amperian currents, 348  
Analyzer, 518  
Angular momentum, 350  
Anisotropic media, 516-520  
Antennas:  
  long dipole, 687-695  
  N element array, 685-687  
  point electric dipole, 667-677  
  point magnetic dipole, 679-681  
  two element array, 681-685  
Array:  
  broadside, 683  
  endfire, 685  
  factor, 683, 685, 687  
  N element, 685-687  
  two element, 681-685  
Atmosphere, as leaky spherical capacitor,  
  195-197  
Atom, binding energy of, 211-212  
Attenuation constant:  
  dielectric waveguide, 646-648  
  lossy transmission line, 602-606  
  lossy rectangular waveguide, 644  
  non-uniform plane waves, 531-532  
Autotransformer, 474  
Avogadro's number, 136  
Axisymmetric solutions to Laplace's  
  equation, 286-288  
  
Backward wave distributed system, 651  
Barium titanate, 150  
Base units, 55  
Batteries due to lightning, 197  
Bessel's equation, 280, 482  
  functions, 281  
Betatron, 402-404  
  oscillations, 404  
Bewley, L. V., 433, 475  
B field, *see* Magnetic field  
Binding energy, of atom, 211-212  
  of crystal, 205-206  
Biot-Savart law, 322-323  
Birefringence, 518-520  
Bohr atomic model, 111-112  
  
Bohr magneton, 350  
Bohr radius, 63  
Boltzmann constant, 155  
Boltzmann distribution, 156  
Boundary conditions:  
  normal component of:  
    current density  $J$ , 168-169  
    displacement field  $D$ , 163-164  
    magnetic field  $B$ , 366  
    polarization  $P$ , 165-166  
     $\epsilon_0 E$ , 165-166  
  tangential component of:  
    electric field  $E$ , 162-163  
    magnetic field  $H$ , 359-360  
    magnetization  $M$ , 360  
Breakdown, electric strength, 93, 223  
  electromechanical, 252  
Brewster's angle, 540-543  
  and polarization by reflection, 547  
Broadside array, 683  
  
Capacitance:  
  as approximation to short transmission  
    line, 589-592, 601  
  coaxial cylindrical electrodes, 176-177  
  concentric spherical electrodes, 176-  
    177  
  energy stored in, 212-213  
  force on, 219-223  
  any geometry, 172  
  isolated sphere, 178, 213  
  parallel plate electrodes, 173-177  
  per unit length on transmission line,  
    570, 572  
  power flow in, 491-493  
  reflections from at end of transmission  
    line, 593-594  
  and resistance, 177  
  in series or parallel, 242-243  
  slanted conducting planes, 273  
  two contacting spheres, 178-181  
  two wire line, 101-103  
Cartesian coordinates, 29-30  
Cauchy's equation, 563  
Cauchy-Riemann equations, 305  
Chalmers, J. A., 293  
Characteristic admittance, 579  
Characteristic impedance, 579  
Charge:  
  by contact, 50  
  differential elements, 60  
  distributions, 59-63

- and electric field, 56-57
- force between two electrons, 56
- forces on, 51-52
- and Gauss's law, 74-76
- polarization, 140-142, 149
- Charge relaxation, series lossy capacitor, 184-189
  - time, 182-184
  - transient, 182
  - uniformly charged sphere, 183-184
- Child-Langmuir law, 200
- Circuit theory as quasi-static approximation, 490
- Circular polarization, 515-516
- Circulation, 29
  - differential sized contour, 30
  - and Stokes' theorem, 35
- Coaxial cable, capacitance, 176-177
  - inductance, 456-458
  - resistance, 172
- Coefficient of coupling, 415
- Coercive electric field, 151
- Coercive magnetic field, 356-357
- Cole-Cole plot, 234
- Collision frequency, 154
- Commutator, 429
- Complex permittivity, 509, 524
- Complex Poynting's theorem, 494-496
- Complex propagation constant, 530-532
- Conductance per unit length, 190
- Conduction, 51
  - drift-diffusion, 156-159
  - Ohmic, 159-160
  - superconductors, 160-161
- Conductivity, 159-160
  - of earth's atmosphere, 195
  - and resistance, 170
- Conjugate functions, 305
- Conservation of charge, 152-154
  - boundary condition, 168-169
  - inconsistency with Ampere's law, 488-489
  - on perfect conductor with time varying surface charge, 537
- Conservation of energy, 199
- Constitutive laws:
  - linear dielectrics, 143-146
  - linear magnetic materials, 352, 356
  - Ohm's law, 159-160
  - superconductors, 160-161
- Convection currents, 182, 194-195
- Coordinate systems, 2-7
  - Cartesian (rectangular), 2-4
  - circular cylindrical, 4-7
  - inertial, 417
  - spherical, 4-7
- Coulomb's force law, 54-55
- Critical angle, 541-544
- Cross (Vector) product, 13-16
  - and curl operation, 30
- Crystal binding energy, 205-206
- Curl:
  - Cartesian (rectangular) coordinates, 29-30
  - circulation, 29-31
  - curvilinear coordinates, 31
  - cylindrical coordinates, 31-33
  - of electric field, 86
  - of gradient, 38-39
  - of magnetic field, 333
  - spherical coordinates, 33-35
  - and Stokes' theorem, 35-38
- Current, 152-154
  - boundary condition, 168-169
  - density, 153-154
  - over earth, 196
  - between electrodes, 169-170
  - through lossless capacitor, 178
  - through series lossy capacitor, 187-189
  - sheet, as source of non-uniform plane waves, 532-534
  - as source of uniform plane waves, 500-503
- Curvilinear coordinates, general, 46
- Cut-off in rectangular waveguides, 638-641
- Cyclotron, 319-321
  - frequency, 316
- Cylinder:
  - magnetically permeable, 357-359
  - and method of images, 97-103
  - permanently polarized, 166-168
  - surface charged, 80-82
  - with surface current, 335-336
  - in uniform electric field, 273-277
    - perfectly conducting, 278
    - perfectly insulating, 279
  - volume charged, 72, 82
  - with volume current, 336
- Cylindrical coordinates, curl, 31
  - divergence, 24-26
  - gradient, 17
- Debye length, 157-159
- Debye unit, 139
- Dees, 319
- Del operator, 16
  - and complex propagation vector, 531
  - and curl, 30
  - and divergence, 24

- and gradient, 16
- Delta function, 187
- Diamagnetism, 349-352
- Dichroism, 517
- Dielectric, 143
  - coating, 525-528
  - constant, 146-147
  - linear, 146-147
  - modeled as dilute suspension of conducting spheres, 293
  - and point charge, 164-165
  - waveguide, 644-648
- Difference equations:
  - capacitance of two contacting spheres, 179-181
  - distributed circuits, 47-48
  - self-excited electrostatic induction machines, 227-230
  - transient transmission line waves, 586-587
- Differential:
  - charge elements, 60
  - current elements, 323
  - cylindrical charge element, 81-82
  - lengths and del operator, 16-17
  - line, surface, and volume elements, 4
  - planar charge element, 68
  - spherical charge element, 79-80
- Diffusion, coefficient, 156
  - equation, 191
- Diode, vacuum tube, 198-201
- Dipole electric field:
  - far from permanently polarized cylinder, 168
  - far from two oppositely charged electrodes, 169, 172
  - along symmetry axis, 58-59
  - two dimensional, 231, 274
- Dipole moment, electric, 137
  - magnetic, 345
- Directional cosines, 41
- Dispersion, complex waves, 531
  - light, 563
- Displacement current, 154, 178
  - as correction to Ampere's law, 488-489
- Displacement field, 143
  - boundary condition, 163-164
  - parallel plate capacitor, 175
  - permanently polarized cylinder, 166-168
  - in series capacitor, 185
- Distortionless transmission line, 603
- Distributed circuits:
  - backward wave, 650
  - inductive-capacitive, 47-48
  - resistive-capacitive, 189-194
  - transmission line model, 575-576
- Divergence:
  - Cartesian (rectangular) coordinates, 23-24
  - of curl, 39
  - curvilinear coordinates, 24
  - cylindrical coordinates, 24-26
  - of electric field, 83
  - of magnetic field, 333
  - spherical coordinates, 26
  - theorem, 26-28
    - and Gauss's law, 82-83
    - relating curl over volume to surface integral, 44
    - relating gradient over volume to surface integral, 43
- Domains, ferroelectric, 50
  - ferromagnetic, 356-357
- Dominant waveguide mode, 640
- Doppler frequency shifts, 507-508
- Dot (scalar) product, 11-13
  - and divergence operation, 24
  - and gradient operation, 16
- Double refraction, 518-520
- Double stub matching, 625-629
- Drift-diffusion conduction, 156-159
- Earth, fair weather electric field, 195
  - magnetic field, 424-425
- Eddy currents, 401
- Effective length of radiating electric dipole, 676-677
- Einstein's relation, 156
- Einstein's theory of relativity, 207
- Electrets, 151
  - force on, 218
  - measurement of polarization, 239-240
- Electric breakdown, 93, 223-224
  - mechanical, 252
- Electric dipole, 136
  - electric field, 139
  - moment, 137-140, 231
  - potential, 136-137
  - radiating, 667-671
  - units, 139
- Electric field, 56-57
  - boundary conditions, normal component, 83, 165-166
  - tangential component, 162-163
  - of charge distribution, 63-64
  - of charged particle precipitation onto sphere, 293
  - of cylinder with, surface charge, 71, 80-82

- volume charge, 72, 82
  - in conducting box, 269
  - discontinuity across surface charge, 83
  - of disk with surface charge, 69-71
  - due to lossy charged sphere, 183
  - due to spatially periodic potential sheet, 266
  - due to superposition of point charges, 57-58
  - energy density, 208-209
  - and Faraday's law, 395
  - of finite length line charge, 89
  - and gradient of potential, 86
  - around high voltage insulator bushing, 284
  - of hoop with line charge, 69
  - between hyperbolic electrodes, 262
  - of infinitely long line charge, 64-65
  - of infinite sheets of surface charge, 65-69
  - line integral, 85-86
  - local field around electric dipole, 145-146
  - around lossy cylinder, 276
  - around lossy sphere, 289
  - numerical method, 298
  - around permanently polarized cylinder, 166-168
  - of permanently polarized cylinder, 166-168
  - of point charge above dielectric boundary, 165
  - of point charge near grounded plane, 107
  - of point charge near grounded sphere, 106
  - of radiating electric dipole, 671
  - in resistive box, 263
  - in resistor, coaxial cylinder, 172
    - concentric sphere, 173
    - parallel plate, 171
  - of sphere with, surface charge, 76-79
    - volume charge, 79-80
    - transformation, 417
  - between two cones, 286
  - of two infinitely long opposite polarity line charges, 94
  - of two point charges, 58-59
  - of uniformly charged volume, 68-69
- Electric field lines:
  - around charged sphere in uniform field, 297
  - around cylinder in uniform field, 276-277
  - due to spatially periodic potential sheet, 267
  - of electric dipole, 139
  - around high voltage insulator bushing, 284
  - between hyperbolic electrodes, 262
  - of radiating electric dipole, 671-673
  - within rectangular waveguide, 636, 639
  - around two infinitely long opposite polarity line charges, 95-96
  - around uncharged sphere in uniform field, 290-291
- Electric potential, 86-87
  - of charge distribution, 87
  - within closed conducting box, 268, 300
  - due to spatially periodic potential sheet, 266
  - and electric field, 86-87
  - of finite length line charge, 88-89
  - around high voltage insulator bushing, 282-284
  - between hyperbolic electrodes, 262
  - of infinitely long line charge, 94
  - inside square conducting box, 299-301
  - of isolated sphere with charge, 109
  - around lossy cylinder in uniform electric field, 274
  - around lossy sphere in uniform electric field, 288
  - within open resistive box, 263
  - of point charge, 87
  - of point charge above dielectric boundary, 165
  - of point charge and grounded plane, 107
  - of point charge and grounded sphere, 103
  - of sphere with, surface charge, 90-91
    - volume charge, 90-91
  - between two cones, 286
  - of two infinitely long line charges, 94
  - between upper atmosphere and earth's surface, 196-197
  - and zero potential reference, ground, 87
- Electric susceptibility, 146
- Electromechanical breakdown, 252
- Electromotive force (EMF), 395
  - due to switching, 433
  - due to time varying number of coil turns, 433-435
  - in magnetic circuits, 406
- Electron, beam injection into dielectrics, 201
  - charge and mass of, 56
  - radius of, 207

- Electronic polarization, 136  
 Electron volts, 206  
 Electroscope, 53-54  
 Electrostatic generators, and Faraday's  
   ice pail experiment, 53-54  
   induction machines, 224-230  
   Van de Graaff, 223-224  
 Electrostatic induction, 51-53  
   Faraday's ice pail experiment, 53-54  
   machines, 224-230  
 Electrostatic precipitation, 293, 307  
 Electrostatic radiating field, 671  
 Electrostriction, 151  
 Elliptical polarization, 515  
 Element factor, 683  
 Endfire array, 685  
 Energy:  
   binding, of atom, 211-212  
   of crystal, 205-206  
   and capacitance, 212-213, 220  
   and charge distributions, 204-208  
   conservation theorem, 199  
   and current distributions, 454  
   density, electric field, 208-209  
   magnetic field, 441-455  
   and inductance, 454  
   stored in charged spheres, 210  
 Equipotential, 84-85  
 Euerle, W. C., 227  
 Exponential transmission line, 649  
 External inductance, 456-457  
  
 Fair weather electric field, 195  
 Farad, 175  
 Faraday, M., 394  
   cage, 78  
   disk, 420-422  
   ice pail experiment, 53-54  
 Faraday's law of induction, 394-397,  
   489  
   and betatron, 403  
   for moving media, 417  
   and paradoxes, 430-435  
   and resistive loop, 412  
   and Stokes' theorem, 404  
 Far field radiation, 671  
 Fermat's principle, 562  
 Ferroelectrics, 149-151  
 Ferromagnetism, 357  
 Fiber optics, 550-552  
 Field emission, 109  
 Field lines, *see* Electric field lines;  
   Magnetic field lines  
 Flux, 22  
   and divergence, 21-26  
   and divergence theorem, 26-28  
   and Gauss's law, 74-75  
   and magnetic field, 338  
   magnetic through square loop, 342-343  
   and sources, 21-22  
   and vector potential, 338  
 Force:  
   on capacitor, 219-223  
   Coulomb's law, 54-56  
   on current carrying slab, 441, 444  
   between current sheets, 329  
   due to pressure gradient, 155  
   on electric dipole, 216  
   gravitational, 56  
   on inductor, 461  
   interfacial, 264  
   on linear induction machine, 449-450  
   between line charge and cylinder, 99  
   between line charge and plane, 97  
   between line current and perfect con-  
   ductor or infinitely permeable  
   medium, 363  
   between line currents, 314-315  
   on magnetically permeable medium,  
   363  
   on magnetic block, 465  
   on magnetic dipole, 352, 368-370  
   on magnetizable current loop, 370-375  
   on MHD machine, 430  
   on moving charge, 314-315  
   on one turn loop, 464  
   between point charge and dielectric  
   boundary, 165  
   between point charge and grounded  
   plane, 108  
   between point charge and grounded  
   sphere, 105  
   between point charges, 51-56  
   between point charge and sphere of  
   constant charge, 109  
   between point charge and sphere of  
   constant potential, 110  
   on polarizable medium, 215-219  
   on relay, 463  
   on surface charge, 213-215  
   between two contacting spheres, 181  
   between two cylinders, 100  
 Fourier series, 267  
 Frequency, 505-506  
 Fringing fields, 173-175  
 Fundamental waveguide mode, 640  
  
 Galilean coordinate transformation, 505  
 Galilean electric field transformation, 417  
 Garton, C. G., 252

- Gas conduction model, 154-155  
 Gauge, setting, 665  
 Gauss's law, 75, 489  
   and boundary conditions:  
     normal component of current density, 168  
     normal component of displacement field, 163-164  
     normal component of polarization, 165-166  
     normal component of  $\epsilon_0 E$ , 83, 165-166  
   and charge distributions, 75  
   and charge injection into dielectrics, 201-202  
   and conservation of charge, 154  
   and cylinders of charge, 80-82  
   and displacement field, 143  
   and divergence theorem, 82-83  
   and lossy charged spheres, 183-184  
   for magnetic field, 333  
   and point charge inside or outside volume, 74-75  
   and polarization field, 142  
   and resistors, coaxial cylinder, 172  
     parallel plate, 171  
     spherical, 173  
   and spheres of charge, 76-80  
 Generalized reflection coefficient, 607-608  
 Generators, 427-429  
 Geometric relations between coordinate systems, 7  
 Gibbs phenomenon, 269  
 Gradient:  
   in Cartesian (rectangular) coordinates, 16-17  
   in cylindrical coordinates, 17  
   and del operator, 16  
   and electric potential, 86  
   and line integral, 18-21  
   of reciprocal distance, 73  
   in spherical coordinates, 17-18  
   theorem, 43-44, 334, 370  
 Gravitational force, 56  
 Green's reciprocity theorem, 124  
 Green's theorem, 44  
 Ground, 87  
 Group velocity, 513  
   on distortionless transmission line, 603  
   in waveguide, 641  
 Guard ring, 173-174  
 Gyromagnetic ratio, 385  
 Half wave plate, 519  
 Hall effect, 321-322  
 Hall voltage, 322  
 Harmonics, 267-269  
 Helix, 317  
 Helmholtz coil, 331  
 Helmholtz equation, 631  
 Helmholtz theorem, 337-338, 665  
 H field, *see* Magnetic field  
 High voltage bushing, 282-284  
 Holes, 154, 321  
 Homopolar generator, 420-422  
   periodic speed reversals, 426-427  
   self-excited, 422-424  
   self-excited ac operation, 424-425  
 Horenstein, M. N., 282  
 Hyperbolic electrodes, 261-262  
 Hyperbolic functions, 264-265  
 Hysteresis, ferroelectric, 150-151  
   magnetic, 356-357  
   and Poynting's theorem, 553  
 Identities, vector, 38-39, 46-47  
 Images, *see* Method of Images  
 Impedance, characteristic, 579  
   of free space, 498  
   wave, 498  
 Impulse current, 187  
 Index of refraction, 540  
 Inductance:  
   of coaxial cable, 456-458, 575  
   external, 456-457  
   and ideal transformer, 414-415  
   internal, 457-458  
   and magnetic circuits, 407-411  
   mutual, 398  
   as quasi-static approximations to transmission lines, 589-592, 601  
   reflections from at end of transmission line, 594-595  
   and resistance and capacitance, 458-459  
   self, 407  
   of solenoid, 408  
   of square loop, 343  
   of toroid, 409  
   per unit length on transmission line, 570, 572  
 Induction, electromagnetic, 394-395  
   electrostatic, 51-54, 224-230  
   machine, 446-450  
 Inertial coordinate system, 417  
 Internal inductance, 457-458  
 International system of units, 55  
 Ionic crystal energy, 205-206  
 Ionic polarization, 136-137

- Ionosphere plane wave propagation, 511-512, 557  
 Isotopes, 318-319  
 Kelvin's dynamo, 227  
 Kerr effect, 520, 558  
 Kinetic energy, 199  
 Kirchoff's current law, 154, 490  
 Kirchoff's laws on transmission lines, 569-570  
 Kirchoff's voltage law, 86, 490  
  
 Laminations, 401-402, 470-471  
 Lange's *Handbook of Chemistry*, 147  
 Langevin equation, 251  
     for magnetic dipoles, 355  
 Langmuir-Child law, 200  
 Laplace's equation, 93, 258  
     Cartesian (rectangular) coordinates, 260  
     cylindrical coordinates, 271  
     and magnetic scalar potential, 365  
     spherical coordinates, 284  
 Laplacian of reciprocal distance, 73-74  
 Larmor angular velocity, 316  
 Laser, 517  
 Law of sines and cosines, 41  
 Leakage flux, 415  
 Left circular polarization, 516  
 Legendre's equation, 287  
 Legendre's polynomials, 287-288  
 Lenz's law, 395-397  
     and betatron, 403  
 Leyden jar, 227  
 L'Hôpital's rule, 589  
 Lightning producing atmospheric charge, 197  
 Light pipe, 550-552, 565  
 Light velocity, 56, 497  
 Linear dielectrics, 143-147  
 Linear induction machine, 446-450  
 Linear magnetic material, 352, 356  
 Linear polarization, 515  
 Line charge:  
     distributions, 60  
     finite length, 88-89  
     hoop, 69  
     infinitely long, 64-65  
     method of images, 96-103  
     near conducting plane, 96-97  
     near cylinder, 97-99  
     two parallel, 93-96  
     two wire line, 99-103  
 Line current, 324  
 Line integral, 18-21  
     of electric field, 85  
     of gradient, 19-20  
     and Stokes' theorem, 36  
     and work, 18-19  
 Local electric field, 145-146  
 Lord Kelvin's dynamo, 227  
 Lorentz field, 238  
 Lorentz force law, 314-316  
 Lorentz gauge, 665  
 Lorentz transformation, 417, 505  
 Lossy capacitor, 184-189  
  
 Madelung, electrostatic energy, 205  
 Magnesium isotopes, 319  
 Magnetic charge, 489  
 Magnetic circuits, 405-407  
 Magnetic diffusion, 435  
     with convection, 444-446  
     equation, 437  
     Reynold's number, 446  
     skin depth, 442-443  
     transient, 438-441  
 Magnetic dipole, 344  
     field of, 346  
     radiation from, 679-681  
     vector potential, 345, 680  
 Magnetic energy:  
     density, 455  
     and electrical work, 452  
     and forces, 460-461  
     and inductance, 454  
     and mechanical work, 453, 460-461  
     stored in current distribution, 454  
 Magnetic field, 314, 322-323  
     and Ampere's circuital law, 333-334  
     boundary conditions, 359-360  
     due to cylinder of volume current, 336  
     due to finite length line current, 341  
     due to finite width surface current, 342  
     due to hollow cylinder of surface current, 332, 336  
     due to hoop of line current, 330  
     due to infinitely long line current, 324-325  
     due to magnetization, 348-349  
     due to single current sheet, 327  
     due to slab of volume current, 327  
     due to two hoops of line current (Helmholtz coil), 331  
     due to two parallel current sheets, 328  
     in Helmholtz coil, 331  
     and Gauss's law, 332-333  
     of line current above perfect conductor or infinitely permeable medium, 363

- of line current in permeable cylinder, 358
- in magnetic circuits, 405-407, 411
- of magnetic dipole, 346
- in magnetic slab within uniform field, 361
- of radiating electric dipole, 670
- of radiating magnetic dipole, 681
- in solenoid, 408
- of sphere in uniform field, 364-367
- in toroid, 409
- and vector potential, 336-338
- Magnetic field lines, 342, 366-367
- Magnetic flux, 333, 343
  - in magnetic circuits, 406-411
- Magnetic flux density, 349
- Magnetic scalar potential, 365
- Magnetic susceptibility, 350, 352
- Magnetite, 343
- Magnetization, 343
  - currents, 346-348
- Magnetohydrodynamics (MHD), 430
- Magnetomotive force (mmf), 409
- Magnetron, 375-376
- Mahajan, S., 206
- Malus, law of, 518
- Mass spectrograph, 318-319
- Matched transmission line, 582, 584
- Maxwell's equations, 489, 664
- Meissner effect, 451
- Melcher, J. R., 227, 264, 420, 435
- Method of images, 96
  - line charge near conducting plane, 96-97
  - line charge near cylinder, 97-99
  - line charge near dielectric cylinder, 238-239
  - line current above perfect conductor or infinitely permeable material, 361-363
  - point charge near grounded plane, 106-107
  - point charge near grounded sphere, 103-106
  - point charge near sphere of constant charge, 109
  - point charge near sphere of constant potential, 110
  - two contacting spheres, 178-181
  - two parallel line charges, 93-96
  - two wire line, 99-103
- M field, 343
- MHD, 430
- Michelson-Morley experiment, 503
- Millikan oil drop experiment, 110-111
- Mirror, 547
- MKSA System of units, 55
- Mobility, 156, 201, 293
- Modulus of elasticity, 252
- Momentum, angular, 350
- Motors, 427-429
- Mutual inductance, 398
- Near radiation field, 671
- Newton's force law, 155
- Nondispersive waves, 503
- Nonuniform plane waves, 529, 532-533
  - and critical angle, 542
- Normal component boundary conditions:
  - current density, 168
  - displacement field, 163-164
  - magnetic field, 360
  - polarization and  $\epsilon_0 E$ , 165-166
- Normal vector:
  - and boundary condition on displacement field, 163-164
  - and contour (line) integral, 29
  - and divergence theorem, 27
  - and flux, 22
  - integrated over closed surface, 44
  - and surface integral, 22
- Numerical method of solution to Poisson's equation, 297-301
- Oblique incidence of plane waves, onto dielectric, 538-543
  - onto perfect conductor, 534-537
- Oersted, 314
- Ohmic losses, of plane waves, 508-511
  - in transmission lines, 602-606
  - in waveguides, 643-644
- Ohm's law, 159-160
  - with convection currents, 182
  - in moving conductors, 418
- Open circuited transmission lines, 585, 589-590, 599-600
- Optical fibers, 550-552
- Orientational polarization, 136-137
- Orthogonal vectors and cross product, 14
- Orthogonal vectors and dot product, 11-12
- Paddle wheel model for circulation, 30-31
- Parallelogram, and cross (vector) product, 13
  - rule for vector addition and subtraction, 9-10
- Parallelepiped volume and scalar triple product, 42
- Paramagnetism, 352-356

- Perfect conductor, 159-160  
 Period, 506  
 Permeability, of free space, 322  
   magnetic, 352, 356  
 Permeance, 411  
 Permittivity:  
   complex, 509, 524  
   dielectric, 146-147  
   of free space, 56  
   frequency dependent, 511  
 P field, 140, 165-166. *See also* Polarization  
 Phase velocity, 513  
   on distortionless transmission line, 603  
   in waveguide, 641  
 Photoelastic stress, 520  
 Piezoelectricity, 151  
 Planck's constant, 350  
 Plane waves, 496-497  
   losses, 508-511  
   non-uniform, 530-533  
   normal incidence onto lossless dielectric, 522-523  
   normal incidence onto lossy dielectric, 524-525  
   normal incidence onto perfect conductor, 520-522  
   oblique incidence onto dielectrics, 538-544  
   oblique incidence onto perfect conductors, 534-537  
   power flow, 498, 532  
   uniform, 529-530  
 Plasma, conduction model, 154-155  
   frequency, 161, 511  
   wave propagation, 511-512  
 Pleines, J., 206  
 Point charge:  
   above dielectric boundary, 164-165  
   within dielectric sphere, 147-149  
   force on, 55-58  
   near plane, 106-108  
   in plasma, 158-159  
   radiation from, 666-667  
   near sphere, 103-110  
 Poisson equation, 93, 258  
   and Helmholtz theorem, 338  
   and radiating waves, 665-666  
   within vacuum tube diode, 199  
 Poisson-Boltzmann equation, 157  
 Polariscopes, 518-520  
 Polarizability, 143-144  
   and dielectric constant, 147  
 Polarization:  
   boundary conditions, 165-166  
   charge, 140-142, 149  
   cylinder, 166-168  
   and displacement field, 146-147  
   electronic, 136  
   force density, 215-219  
   ionic, 136  
   orientational, 136  
   in parallel plate capacitor, 176-177  
   by reflection, 546-547  
   spontaneous, 149-151  
   of waves, 514-516  
 Polarizers, 517-520  
 Polarizing angle, 547  
 Polar molecule, 136-137  
 Polar solutions to Laplace's equation, 271-272  
 Potential:  
   energy, 199  
   retarded, 664-667  
   scalar electric, 86-93, 664-667  
   scalar magnetic, 365-367  
   vector, 336, 664-667  
   *see also* Electric potential; Vector potential  
 Power:  
   in capacitor, 220  
   on distributed transmission line, 576-578  
   in electric circuits, 493-494  
   electromagnetic, 491  
   flow into dielectric by plane waves, 524  
   in ideal transformer, 415  
   in inductor, 461  
   from long dipole antenna, 692  
   in lossy capacitor, 492  
   from radiating electric dipole, 675-676  
   time average, 495  
   in waveguide, 641  
 Poynting's theorem, 490-491  
   complex, 494-496  
   for high frequency wave propagation, 512  
   and hysteresis, 553  
 Poynting's vector, 491  
   complex, 495  
   and complex propagation constant, 532  
   through dielectric coating, 528  
   due to current sheet, 503  
   of long dipole antenna, 691  
   for oblique incidence onto perfect conductor, 536-537  
   through polarizer, 518  
   and radiation resistance, 674  
   in rectangular waveguide, 641-642

- reflected and transmitted through lossless dielectric, 524
- time average, 495
- of two element array, 683
- and vector wavenumber, 530
- Precipitator, electrostatic, 293-297, 307
- Pressure, 154
  - force due to, 155
  - radiation, 522
- Primary transformer winding, 415
- Prisms, 549-550
- Product, cross, 13-16
  - dot, 11-13
  - vector, 13-16
- Product solutions:
  - to Helmholtz equation, 632
  - to Laplace's equation:
    - Cartesian (rectangular) coordinates, 260
    - cylindrical coordinates, 271-272
    - spherical coordinates, 284-288
- Pyroelectricity, 151
- Q of resonator, 660
- Quadrupole, 233
- Quarter wave long dielectric coating, 528
- Quarter wave long transmission line, 608-610
- Quarter wave plate, 520
- Quasi-static circuit theory approximation, 490
- Quasi-static inductors and capacitors as approximation to transmission lines, 589-592
- Quasi-static power, 493-494
- Radiation:
  - from electric dipole, 667-677
    - field, 671
  - from magnetic dipole, 679-681
  - pressure, 522
  - resistance, 674-677, 691-694
- Radius of electron, 207
- Rationalized units, 55
- Rayleigh scattering, 677-679
- Reactive circuit elements as short transmission line approximation, 601-602
- Reciprocal distance, 72
  - and Gauss's law, 74-75
  - gradient of, 73
  - laplacian of, 73-74
- Reciprocity theorem, 124
- Rectangular (Cartesian) coordinate system, 2-4
  - curl, 29-30
  - divergence, 23-24
  - gradient, 16-17
- Rectangular waveguide, 629-644. *See also* Waveguide
- Reference potential, 86-87
- Reflected wave, plane waves, 520, 522, 535-536, 538, 542
  - transmission line, 581-582, 586-587, 592-595
- Reflection, from mirror, 545
  - polarization by, 546-548
- Reflection coefficient:
  - arbitrary terminations, 592-593
  - generalized, 607-608
  - of plane waves, 523
  - of resistive transmission line terminations, 581-582
- Refractive index, 540
- Relative dielectric constant, 146
- Relative magnetic permeability, 356
- Relativity, 503-505
- Relaxation, numerical method, 297-301
- Relaxation time, 182
  - of lossy cylinder in uniform electric field, 275
  - of two series lossy dielectrics, 186-187
- Reluctance, 409
  - motor, 482-483
  - in parallel, 411
  - in series, 410
- Resistance:
  - between electrodes, 169-170
  - between coaxial cylindrical electrodes, 172
  - in open box, 262-264
  - between parallel plate electrodes, 170-171
  - in series and parallel, 186-187
  - between spherical electrodes, 173
- Resistivity, 159
- Remanent magnetization, 356-357
- Remanent polarization, 151
- Resonator, 660
- Retarded potentials, 664-667
- Reynold's number, magnetic, 446
- Right circular polarization, 516
- Right handed coordinates, 3-5
- Right hand rule:
  - and circulation, 29-30
  - and cross products, 13-14
  - and Faraday's law, 395
  - and induced current on perfectly conducting sphere, 367
  - and line integral, 29

- and magnetic dipole moment, 344-345
- and magnetic field, 324
- Saturation, magnetic, 356-357
  - polarization, 150-151
- Saturation charge, 295
- Scalar electric potential, 86-87
- Scalar magnetic potential, 365
- Scalar potential and radiating waves, 664-667, 669-670
- Scalar (dot) product, 11-13
- Scalars, 7-8
- Scalar triple product, 42
- Schneider, J. M., 201
- Seawater skin depth, 443
- Secondary transformer winding, 415
- Self-excited machines, electrostatic, 224-230
  - homopolar generator, 422-427
- Self-inductance, *see* Inductance
- Separation constants, to Helmholtz equation, 632
  - to Laplace's equation, 260-261, 271, 278-280, 286-287
- Separation of variables:
  - in Helmholtz equation, 632
  - in Laplace's equation:
    - Cartesian, 260-261, 264-265, 270
    - cylindrical, 271, 277-282
    - spherical, 284-288
- Short circuited transmission line, 585, 590, 596-599
- Sidelobes, 688
- Sine integral, 691, 694
- SI units, 55-56, 322
  - capacitance, 175
  - resistance, 171
- Skin depth, 442-443
  - with plane waves, 511, 525
  - and surface resistivity, 604-606, 643
- Slip, 448
- Single stub tuning, 623-625
- Sinusoidal steady state:
  - and complex Poynting's theorem, 494-495
  - and linear induction machine, 446-450
  - and magnetic diffusion, 442-444
  - and Maxwell's equations, 530-532
  - and radiating waves, 667-671
  - and series lossy capacitor, 188-189
  - and TEM waves, 505-507
- Slot in waveguide, 635
- Smith chart, 611-615
  - admittance calculations, 620-621
  - stub tuning, 623-629
- Snell's law, 540
- Sohon, H., 431
- Solenoid self-inductance, 407-408
- Space charge limited conduction, in dielectrics, 201-203
  - in vacuum tube diode, 198-201
- Speed coefficient, 421
- Sphere:
  - capacitance of isolated, 178
  - of charge, 61-63, 76-80, 91
  - charge relaxation in, 183-184
  - earth as leaky capacitor, 195-197
  - as electrostatic precipitator, 293-297
  - lossy in uniform electric field, 288-293
  - method of images with point charge, 103-110
  - point charge within dielectric, 147-149
  - two charged, 92
  - two contacting, 178-181
  - in uniform magnetic field, 363-368
- Spherical coordinates, 4-6
  - curl, 33-37
  - divergence, 26
  - gradient, 17
- Spherical waves, 671
- Spin, electron and nucleus, 344
- Standing wave, 521-522
- Standing wave parameters, 616-620
- Stark, K. H., 252
- Stewart, T. D., 237
- Stokes' theorem, 35-38
  - and Ampere's law, 349
  - and electric field, 85-86
  - and identity of curl of gradient, 38-39
  - and magnetic flux, 338
- Stream function:
  - of charged particle precipitation onto sphere, 297
  - cylindrical coordinates, 276-277
  - of radiating electric dipole, 672
  - spherical coordinates, 290-291
- Stub tuning, 620-629
- Successive relaxation numerical method, 297-301
- Superconductors, 160-161
  - and magnetic fields, 450-451
- Surface charge distribution, 60
  - and boundary condition on current density, 168
  - and boundary condition on displacement field, 163-164
  - and boundary condition on  $\epsilon_0 E$ , 83, 166
  - on cylinder in uniform electric field, 273-275

- of differential sheets, 68-69
- disk, 69-71
- electric field due to, 65-67
- force on, 213-215
- hollow cylinder, 71
- induced by line charge near plane, 97
- induced by point charge near plane, 107-108
- induced by point charge near sphere, 106
- and parallel plate capacitor, 175
- on slanted conducting planes, 273
- on spatially periodic potential sheet, 266
- on sphere in uniform electric field, 289
- between two lossy dielectrics, 186-187
- two parallel opposite polarity sheets, 67-68
- Surface conductivity, 435, 601
- Susceptibility, electric, 146
- magnetic, 350, 352
- Tangential component boundary conditions, electric field, 162-163
- magnetic field, 359-360
- Taylor, G. I., 264
- Taylor series expansion, 298
- of logarithm, 205
- Temperature, ideal gas law, 154-155
- TEM waves, *see* Transverse electromagnetic waves
- TE waves, *see* Transverse electric waves
- Tesla, 314
- Test charge, 57
- Thermal voltage, 156, 158
- Thermionic emission, 108-109
- in vacuum tube diode, 198
- Thomson, J. J., 377
- Till, H. R., 201
- Time constant:
  - charged particle precipitation onto sphere, 296
  - charging of lossy cylinder, 273
  - discharge of earth's atmosphere, 197
  - distributed lossy cable, 192-194
  - magnetic diffusion, 440
  - ohmic charge relaxation, 182-184
  - resistor-inductor, 436
  - for self-excited electrostatic induction machine, 226
  - series lossy capacitor, 186-188
- Time dilation, 505
- TM waves, *see* Transverse magnetic waves
- Tolman, R. C., 237
- Torque, on electric dipole, 215
- on homopolar machine, 422
- on magnetic dipole, 353
- Toroid, 408-409
- Tourmaline, 517
- Transformer:
  - action, 411
  - autotransformer, 474
  - ideal, 413-416
  - impedance, 415-416
  - real, 416-417
  - twisted, 473-474
- Transient charge relaxation, *see* Charge relaxation
- Transmission coefficient, 523
- Transmission line:
  - approach to dc steady state, 585-589
  - equations, 568-576
  - losses, 602-603
  - sinusoidal steady state, 595-596
  - transient waves, 579-595
- Transverse electric (TE) waves, in dielectric waveguide, 647-648
- in rectangular waveguide, 635-638
- power flow, 642-643
- Transverse electromagnetic (TEM) waves, 496-497
- power flow, 532
- transmission lines, 569-574
- Transverse magnetic (TM) waves: in dielectric waveguide, 644-647
- power flow, 641-642
- in rectangular waveguide, 631-635
- Traveling waves, 497-500
- Triple product, scalar, 42
- vector, 42
- Two wire line, 99-103
- Uman, M. A., 195
- Uniform plane waves, 529-530
- Uniqueness, theorem, 258-259
- of vector potential, 336-338
- Unit:
  - capacitance, 175
  - rationalized MKSA, 55-56
  - resistance, 171
  - SI, 55-56
- Unit vectors, 3-5
- divergence and curl of, 45
- Unpolarized waves, 546-547
- Vacuum tube diode, 198-201
- Van de Graaff generator, 223-224
- Vector, 8-16
- addition and subtraction, 9-11
- cross(vector) product, 13-16

- distance between two points, 72
- dot(scalar) product, 11-13
- identities, 46-47
  - curl of gradient, 38-39
  - divergence of curl, 39
  - triple product, 42
- magnitude, 8
- multiplication by scalar, 8-9
- product, 11-16
- scalar (dot) product, 11-13
- Vector potential, 336
  - of current distribution, 338
  - of finite length line current, 339
  - of finite width surface current, 341
  - of line current above perfect conductor
    - or infinitely permeable medium, 363
  - of magnetic dipole, 345
  - and magnetic field lines, 342
  - and magnetic flux, 338
  - of radiating electric dipole, 668-669
  - of radiating waves, 667
  - uniqueness, 336-338
- Velocity:
  - conduction charge, 156
  - electromagnetic waves, 500
  - group, 513
  - light, 56, 500
  - phase, 513
- Virtual work, 460-461
- VSWR, 616-620
- Voltage, 86
  - nonuniqueness, 412
  - standing wave ratio, 616-620
- Volume charge distributions, 60
  - cylinder, 72-82
  - slab, 68-69
  - sphere, 79-80
- Von Hippel, A. R., 147
- Water, light propagation in, 548-549
- Watson, P. K., 201
- Wave:
  - backward, 651
  - dispersive, 512-514
  - equation, 496-497
  - high frequency, 511-512
  - nondispersive, 503
  - plane, 496-497
  - properties, 499-500
  - radiating, 666-667
  - solutions, 497-499
  - sources, 500-503
  - standing, 521-522
  - transmission line, 578-579
  - traveling, 499-500
- Waveguide:
  - dielectric, 644-648
  - equations, 630
  - power flow, 641-644
  - rectangular, 629-644
  - TE modes, 635-638
  - TM modes, 631-635
  - wall losses, 643-644
- Wave impedance, 498
- Wavelength, 506
- Wavenumber, 505-506
  - on lossy transmission line, 604
  - as vector, 530
- Wheelon, A. D., 181
- Whipple, F. J. W., 293
- White, H. J., 293
- White light, 563
- Wimshurst machine, 227
- Woodson, H. H., 420, 435
- Work:
  - to assemble charge distribution, 204-208
  - and dot product, 11
  - mechanical, 453
  - to move point charge, 84-85
  - to overcome electromagnetic forces, 452
- Zeeman effect, 378
- Zero potential reference, 87

## VECTOR IDENTITIES

$$(\mathbf{A} \times \mathbf{B}) \cdot \mathbf{C} = \mathbf{A} \cdot (\mathbf{B} \times \mathbf{C}) = (\mathbf{C} \times \mathbf{A}) \cdot \mathbf{B}$$

$$\mathbf{A} \times (\mathbf{B} \times \mathbf{C}) = \mathbf{B}(\mathbf{A} \cdot \mathbf{C}) - \mathbf{C}(\mathbf{A} \cdot \mathbf{B})$$

$$\nabla \cdot (\nabla \times \mathbf{A}) = 0$$

$$\nabla \times (\nabla f) = 0$$

$$\nabla(fg) = f\nabla g + g\nabla f$$

$$\begin{aligned} \nabla(\mathbf{A} \cdot \mathbf{B}) &= (\mathbf{A} \cdot \nabla)\mathbf{B} + (\mathbf{B} \cdot \nabla)\mathbf{A} \\ &\quad + \mathbf{A} \times (\nabla \times \mathbf{B}) + \mathbf{B} \times (\nabla \times \mathbf{A}) \end{aligned}$$

$$\nabla \cdot (f\mathbf{A}) = f\nabla \cdot \mathbf{A} + (\mathbf{A} \cdot \nabla)f$$

$$\nabla \cdot (\mathbf{A} \times \mathbf{B}) = \mathbf{B} \cdot (\nabla \times \mathbf{A}) - \mathbf{A} \cdot (\nabla \times \mathbf{B})$$

$$\begin{aligned} \nabla \times (\mathbf{A} \times \mathbf{B}) &= \mathbf{A}(\nabla \cdot \mathbf{B}) - \mathbf{B}(\nabla \cdot \mathbf{A}) \\ &\quad + (\mathbf{B} \cdot \nabla)\mathbf{A} - (\mathbf{A} \cdot \nabla)\mathbf{B} \end{aligned}$$

$$\nabla \times (f\mathbf{A}) = \nabla f \times \mathbf{A} + f\nabla \times \mathbf{A}$$

$$(\nabla \times \mathbf{A}) \times \mathbf{A} = (\mathbf{A} \cdot \nabla)\mathbf{A} - \frac{1}{2}\nabla(\mathbf{A} \cdot \mathbf{A})$$

$$\nabla \times (\nabla \times \mathbf{A}) = \nabla(\nabla \cdot \mathbf{A}) - \nabla^2 \mathbf{A}$$

## INTEGRAL THEOREMS

*Line Integral of a Gradient*

$$\int_a^b \nabla f \cdot d\mathbf{l} = f(b) - f(a)$$

*Divergence Theorem:*

$$\int_V \nabla \cdot \mathbf{A} dV = \oint_S \mathbf{A} \cdot d\mathbf{S}$$

Corollaries

$$\int_V \nabla f dV = \oint_S f d\mathbf{S}$$

$$\int_V \nabla \times \mathbf{A} dV = -\oint_S \mathbf{A} \times d\mathbf{S}$$

*Stokes' Theorem:*

$$\oint_L \mathbf{A} \cdot d\mathbf{l} = \int_S (\nabla \times \mathbf{A}) \cdot d\mathbf{S}$$

Corollary

$$\oint_L f d\mathbf{l} = -\int_S \nabla f \times d\mathbf{S}$$

Resource: [Ò^&d\[ { æ } ^æÁ@|áÁ@|^kÁÚ:\[ à|^{ Á\[|çã \\* Á\] \]:\[ æ&@](#)  
T æ\^•Áæ@

The following may not correspond to a particular course on MIT OpenCourseWare, but has been provided by the author as an individual learning resource.

For information about citing these materials or our Terms of Use, visit: <http://ocw.mit.edu/terms>.